Synthesis and Characterization of Novel Self-Delivering Amino Acid-RNA Conjugates for the Development of Potent siRNA Prodrugs

Jovanka J. Bogojeski

Department of Chemistry, McGill University

Montreal, QC, Canada

October, 2016

A thesis submitted to McGill University in partial fulfilment of the requirements of the degree of Doctor of Philosophy

For my first teacher, Mira Đorđeska.

Copyright Statement

A license number for the use of the image in Figure 1.2 was obtained from Elsevier and Copyright Clearance Center: 4082700885826.

Permission to reprint the images used in Figure 1.4 was obtained directly *via* email communication from RSC Publishing.

A license number for the reprint the images used in Figures 1.5 and 1.6 was obtained from Nature Publishing Group and Copyright Clearance Center: 4082650556813.

A license number for the reprint of the images used in Figures 1.13 and 1.16 was obtained from Nature Publishing Group and Copyright Clearance Center: 4082660445787.

Permission for the reprint of the image used in Figure 1.14 was obtained from ACS Publications and Copyright Clearance Center.

The image reprinted in Figure 1.15 is free to redistribute under a Creative Commons License: https://creativecommons.org/licenses/by/4.0/.

Some content in Chapter 2 has been adapted from Johnsson, R.; Lackey, J. G.; Bogojeski, J. J.; Damha, M. J., New light labile linker for solid phase synthesis of 2′-O-acetalester oligonucleotides and applications to siRNA prodrug development. *Bioorganic & Medicinal Chemistry Letters* **2011,** *21* (12), 3721-3725. © 2011 Elsevier Ltd. Elsevier grants authors publishing in Elsevier journals rights to use their works for scholarly purposes according to the following URL: https://www.elsevier.com/__data/assets/pdf_file/0007/55654/AuthorUserRights.pdf. A license number for the reprint of data in Figure 2.3 was obtained from Elsevier and Copyright Clearance Center: 4085410520073.

Abstract

Small interfering RNA (siRNA) has the ability to silence virtually any gene of interest. The canonical structure, however, is negatively charged and hydrophilic. It is thus repulsed by the negatively charged phosphodiesters of the cellular membrane and prevented from penetrating the lipophilic membrane core. The main goal of this thesis is to synthesize siRNA conjugates containing 2'-sugar modifications that reduce the overall negative charge of the molecule and cause its unassisted cellular uptake, and to utilize these modifications to synthesize a biolabile analogue (a promoiety) in a prodrug siRNA (proRNA) construct.

To this end, RNA conjugates were synthesized containing various 2'-*O*-amino acid acetal ester (2'-*O*-AAE) promoieties. The 2'-*O*-phenylalanine (2'-*O*-Phe) AAE was most stable in the aqueous and alcoholic RNA purification and handling conditions to which the 2'-*O*-AAEs investigated were exposed. A comparison of hydrolysis rates between the 2'-*O*-Phe AAE and a 2'-*O*-hydrocinnamic acetal ester suggested that 2'-*O*-Phe AAE hydrolysis occurs in aqueous buffer due to the alpha amino group acting as a general acid catalyst. Anhydrous and aprotic deprotection and handling solutions were employed, including FMOC and cyanoethyl elimination with dry triethylamine/acetonitrile, to yield a poly-thymidine oligonucleotide containing a 2'-*O*-Phe AAE insert, with minimal evidence of premature cleavage.

In order to validate the incorporation of the 2'-*O*-Phe AAE modification in a self-delivering proRNA construct, the analogous 2'-*N*-acyl-L-phenylalanine modification was assessed for its ability to cause RNA conjugates to penetrate cellular membranes. Using flow cytometric fluorescence resonance energy transfer (FCET), naked cyanine-3/5 labeled RNA conjugates containing 2'-*N*-acyl-L-phenylalanine modifications were found to penetrate human glial cells to a much greater extent than the unmodified counterpart. This work suggests that the analogous 2'-*O*-Phe AAE modification could also cause increased cellular uptake of RNA conjugates.

2'-*N*-acyl-L-phenylalanine modification was incorporated into internal positions of siRNAs targeting endogenous genes B-cell lymphoma-2 (*bcl-2*) and downregulated in renal cell carcinoma (*drr*), and the siRNAs were transfected into human colonic cells and human glial cells, respectively. Downregulation was dependent on the placement of these inserts; insertion of biolabile 2'-*O*-Phe AAEs at positions particularly vulnerable to modification may improve potencies. A self-delivering siRNA construct comprised of a phosphorothioate tail and thirteen

2'-*N*-acyl-L-phenylalanine inserts achieved potent DRR downregulation in comparison to the unmodified siRNA containing only a phosphorothioate tail. Delayed onset of silencing by our highly modified asymmetric siRNA suggests that the construct's silencing kinetics diverges from that of canonical siRNA, and thus selective insertion of 2'-*O*-Phe AAEs may extend the duration of action of the self-delivering tailed siRNA.

Finally, high-purity RNA was synthesized using a solid support linker and protecting groups that are orthogonal to the 2'-*O*-Phe AAE modification in preparation for the synthesis of proRNA. This work lays the foundation for the rational design of self-delivering and potent asymmetric proRNA.

Résumé

Les petits ARN interférents (siARN) ont la possibilité d'inhiber l'expression de pratiquement n'importe quel gène d'intérêt. Un siARN étant hydrophile et chargé négativement, il est soumis à une répulsion électrostatique avec les phosphodiesters de la membrane cellulaire chargés négativement et, ainsi, n'est pas à même de traverser la membrane lipophile. L'objectif principal de cette thèse est de synthétiser des conjugués de siARNs comportant des modifications chimiques sur la position 2′ du sucre réduisant sa charge globale négative et susceptibles d'entraîner une pénétration cellulaire sans assistance afin, à terme, de fabriquer des analogues biolabiles (progroupes) dans une approche de synthèse de prodrogues de siARN (proARN).

Pour ce faire, des brins d'ARN contenant des progroupes d'acétalesters d'acides aminés en position 2′ ont été synthétisés (2′-*O*-AAE). L'acétalester de la phénylalanine en position 2′ (2′-*O*-Phe AAE) était la plus stable des modifications étudiées, en milieu aqueux et alcoolique nécessaires à la purification d'ARN et face aux conditions expérimentales de manipulation. En comparant les taux d'hydrolyse des AAE 2′-*O*-Phe et d'acide hydrocinnamique, nous avons estimé que l'hydrolyse des 2′-*O*-Phe AAE en milieu aqueux s'effectue à l'aide de la fonction α-amine jouant le rôle d'un catalyseur acide. Sous des conditions de déprotection et de manipulation anhydres et aprotiques, et ce pendant la déprotection des groupements Fmoc et cyanoéthyles requérant l'utilisation de triéthylamine/acétonitrile secs, nous avons pu isoler un polythymidylate contenant une modification 2′-*O*-Phe AAE en minimisant son hydrolyse prématurée.

Afin de valider l'intérêt de l'incorporation d'une modification 2′-*O*-Phe AAE dans un siARN capable de s'auto-administrer dans une cellule, nous avons testé la capacité d'une modification analogue, la 2′-*N*-acyl-L-phénylalanine, à induire la pénétration cellulaire d'un conjugué d'ARN. En utilisant la technique de transfert d'énergie entre molécules fluorescentes suivi par cytométrie en flux (FCET « *flow cytometric fluorescence resonance energy transfer* »), il a été possible de voir que des conjugués « nus » d'ARN, possédant un marqueur fluorescent cyanine3 ou 5 ainsi que des modifications 2′-*N*-acyl-L-phénylalanine étaient capables de pénétrer des cellules gliales humaines en plus grande proportion que les versions d'ARN non-modifié. Cette étude suggère que la modification analogue 2′-*O*-Phe AAE aurait un effet similaire sur la pénétration cellulaire de conjugués d'ARN.

La modification 2′-*N*-acyl-L-phénylalanine fut ensuite intégrée à des siARNs ciblant les gènes des lymphomes à cellule B (*B-cell lymphoma 2*, *bcl-2*) de cellules humaines du côlon et les oncogènes de carcinomes à cellules rénales (*downregulated in renal cell*, *drr*) dans des cellules gliales humaines. La régulation négative s'est révélée dépendante du positionnement de ces insertions et la présence de groupements biolabiles 2′-*O*-Phe AAE à des positions particulièrement sensibles aux modifications pourrait améliorer l'efficacité des siARNs. Un siARNs modifié avec treize incorporations de 2′-*N*-acyl-L-phénylalanine ainsi que des liens phosphorothioate sur la partie terminale de la chaîne oligonucléotidique (queue) s'est montré capable de régulation négative de *drr* en l'absence d'agent de transfection, contrairement à des siARNs ne contenant que des liens phosphorothioate en queue de chaîne. L'action retardée de silençage de l'expression génétique induite par nos siARN largement modifiés suggère que la cinétique du silençage diffère de celle des siARNs non-modifiés, et laisse ainsi entrevoir la possibilité que l'insertion sélective de 2′-*O*-Phe AAEs puisse accroître la durée d'action de siARNs auto-délivrants.

Enfin, la synthèse d'ARN de grande pureté s'est effectuée à l'aide d'un lien sur support solide et de groupements protecteurs orthogonaux à la modification 2′-*O*-Phe AAE, et ce en préparation de la synthèse de prodrogues de siARN. Le travail de cette thèse représente ainsi un dévelopement important vers la conception méthodique et la préparation de prodrogues auto-délivrantes et efficaces de siARN.

Acknowledgements

I want to first express my appreciation to Dr. Masad Damha for his guidance, enthusiasm, and trust in me. I will always be in debt to him for this unique and rich experience. I am grateful for the many opportunities to convene with diverse and talented individuals and to expand my knowledge, which were made possible to me through the Damha lab. Indeed, a large part of this thesis would not have been possible without the graciousness of Dr. Kevin Petrecca in making his laboratory space at the Montreal Neurological Institute available to me. I thank Dr. Phuong Le for showing me the ropes there and for testing 'one last compound' several times over. Elena Moroz in the lab of Dr. Jean-Christophe Leroux, as well as Dr. Johans Fakhoury of the Dr. Hanadi Sleiman lab, kindly performed additional tests with high quality. I was also very fortunate to have worked with Dr. Ken Yamada on expanding our catalogue of testable compounds. His attention to detail improved the quality of my work a great deal. I am also grateful for the lending hand I received from Erika Steels in making more material needed for the dimer studies carried out in Chapter 2. Dr. Alexander Wahba and Nadim Saadeh were also invaluable in providing mass spectrometry data to support my research over the years.

Many past and present members of the Damha lab provided assistance in editing parts of this thesis. I thank Dr. Jory Liétard and Dr. Adam Katolik for taking time out of their post-doctoral research to share their thoughts, and Brandon Payliss for making suggestions that were very helpful to clarifying my introductory comments. Current members Danielle Vlaho and Dan O'Reilly were gracious in offering their advice at a time that was convenient to me. I will miss Danielle's enthusiasm and Dan's wise advice. I must also thank other current members that will also be missed – Maryam Habibian's funny stories, Hala Abou Assi's calming morning talks, and Elise Malek-Adamian's generous smiles and laughs. I am also thankful for the time I was able to spend with past members Dr. Jeremy Lackey (and his enthusiasm and guidance on proRNA), Fereshteh Azizi, Pascal Gallant, Dr. Robert Donga, Dr. Richard Johnsson, Dr. Dilip Dixit, Dr. Mathew Hassler, Dr. Glen Deleavey, Dr. Maryam Yahyaee-Anazahaee, and Dr. Saúl Martinez-Montero who all made the lab a fun and enlightening experience when I joined. I thank Chantal Marotte for having all the administrative answers and being available at any time.

There is so much I could say about the influence of my family, but I will sum it up by acknowledging the fact that they taught me to believe in myself and to pursue anything my heart

desires. Without my first teacher, Mom, I am nothing. With my best friend and sister, Nancy, I always have the feeling of a supporter in my corner. Thank you to my brother-in-law Radoslav for being a good friend and to my sweet nephews Miloš and Milan for lighting up my world.

Contribution of Authors

Several researchers made contributions to the projects described in this thesis. Undergraduate student Erika Steels synthesized a batch of uridine 3'-*O*-phosphoramidite containing the 2'-*O*-phenylalanine acetal ester modification. I employed these phosphoramidites to synthesize dimers that were monitored for chemical stability under various conditions in Chapter 2.

Photocleavable solid support linker and the dimer phosphoramidite used to derivatize the solid support were synthesized and appended to the support by Dr. Richard Johnsson. This support was employed in the synthesis of 2'-*O*-acetal ester-containing oligonucleotides in Chapter 2. In Chapter 5, I utilized the solid support derivatized with photocleavable linker to couple it to dimer phosphoramidites.

Dr. Ken Yamada synthesized cytidine 3'-*O*-phosphoramidite containing 2'-*N*-acyl-L-phenylalanine modification and used it to synthesize a sense strand containing six 2'-*N*-acyl-L-phenylalanine modifications, employed in Chapter 3. He also utilized the phorphoramidite to synthesize *drr*-targeting sense strands containing four, five, and six 2'-*N*-acyl-L-phenylalanine modifications, as well as a strand containing three cytidine 2'-*N*-acyl-L-phenylalanine modifications. These strands were utilized in Chapter 4. Dr. Yamada measured the thermal melting temperatures reported in Chapter 4 and tabulated the RP-HPLC retention times in Figure 4.17. Dr. Yamada also synthesized uridine phosphoramidite containing 2'-*N*-acyl-glycine modification for the synthesis of a sense strand in Chapter 3.

Dr. Phuong Le performed the immunofluorescent stains on the cells pictured in Figures 3.4, 3.8, 3.14, 3.15, 4.19. Dr. Le also carried out the Western blots shown in Figures 4.2, 4.3, 4.18, and 4.20, and the invasion assays of Figures 4.8 and 4.9.

Elena Moroz carried out the experiments to produce the qPCR results in Figure 4.12, as well as the cell viability assays of Figure 4.13, the polyacrylamide gel shown in Figure 4.16, and the flow cytometry required to compare the cellular uptake of human colonic cells with that of HeLa cells in Chapter 3.

Table of Contents

List of Tables

List of Figures

List of Schemes

List of Abbreviations and Acronyms

λ_{max}	maximum wavelength
ΔT_m	change in T_m
Å	angstrom
2'-F-ANA	2'-deoxy-2'-fluoro-β-D-arabino nucleic acid
2'-F-RNA	2'-deoxy-2'-fluororibonucleic acid
2'-*O*-MOE	2'-*O*-(2-methoxyethyl)
AAE	amino acetal ester
Ac	acetyl
Ac_2O	acetic anhydride
AcOH	acetic acid
Ade	adenine
AGO	Argonaute protein
Ala	L-alanine
ALE	acetal levulinyl ester
AMO	anti-miRNA oligonucleotide
amu	atomic mass units
AON	antisense oligonucleotide
asiRNA	asymmetric shorter-duplex siRNA
aq.	aqueous
bcl-2	B-cell lymphoma gene
Bn	benzyl
bp	base pair
Bu	butyl
Bz	benzoyl
CH_2Cl_2	dichloromethane
COSY	correlation spectroscopy, homonuclear (NMR)
CPG	controlled pore glass
CPP	cell penetrating peptide
CSO	(1*S*)-(+)-(10-camphorsulfonyl)-oxaziridine
Cy3	cyanine-3

Cy5	cyanine-5
Cyt	cytosine
d	doublet
dA	2'-deoxyriboadenosine
DBU	1,8-diazabicyclo[5.4.0]undec-7-ene
dC	2'-deoxyribocytidine
DCC	*N*,*N'*-dicyclohexylcarbodiimide
DCI	4,5-dicyanoimidazole
dd	doublet of doublets
dG	2'-deoxyriboguanosine
ddT	dideoxythymidine
DDTT	((dimethylamino-methylidene)amino)-3*H*-1,2,4-dithiazaoline-3-thione
DEPC	diethylpyrocarbonate
DIPEA	*N*,*N*-diisopropylethylamine
DMAP	4-(dimethylamino)pyridine
DMEM	Dulbecco's modified eagle medium
dmf	*N*,*N*-dimethylformamidine
DMF	*N*,*N*-dimethylformamide
DMSO	dimethylsulfoxide
DMTr	4,4'-dimethoxytrityl
DNA	2'-deoxyribonucleic acid
DRR	downregulated in renal cell carcinoma protein
drr	downregulated in renal cell carcinoma gene
ds	double-stranded
dt	doublet of triplets
EDTA	ethylenediaminetetraacetic acid
EEDQ	2-ethoxy-1-ethoxycarbonyl-1,2-dihydroquinoline
ESI	electrospray ionization
Et	ethyl
EtOAc	ethyl acetate
EtOH	ethanol

ETT	5-ethylthio-1*H*-tetrazole
FA	focal adhesion
FBS	fetal bovine serum
FCET	flow cytometric fluorescence resonance energy transfer
FMOC	9-fluorenylmethoxycarbonyl
FRET	Förster resonance energy transfer
GalNAc	*N*-acetylgalactosamine
Gua	guanine
hυ	the energy of light (h = Planck's constant; υ = frequency)
HCA	hydrocinnamic acid
HEPES	2-[4-(2-hydroxyethyl)piperazin-1-yl]ethanesulfonic acid
HFIP	hexafluoroisopropanol
HPLC	high performance liquid chromatography
hr	hour
hsiRNA	hydrophobic siRNA
*i*Bu	isobutyryl
IE	ion exchange
*i*Pr	isopropyl
J	scalar coupling contstant (Hz)
LC	liquid chromatography
Lev	levulinyl
LNA	locked nucleic acid
Lys	L-lysine
m	multiplet
Me	methyl
MeCN	acetonitrile
$MeNH_2$	methylamine
MeOH	methanol
-mer	suffix to indicate polymer (oligonucleotide) of indicated length
min	minute(s)
miRNA	microRNA

mod	modification
mRNA	messenger RNA
MS	mass spectrometry
MTM	methylthiomethylene
NBS	*N*-bromosuccinamide
NEt_3	triethylamine
NH_2NH_2-H_2O	hydrazine hydrate
NMI	*N*-methylimidazole
NMP	*N*-methylpyrrolidinone
NMR	nuclear magnetic resonance
NH_4OH	aqueous ammonia
-nt	nucleotide
OD	optical density units (the absorbance at 260 nm of oligonucleotide dissolved in 1 mL of water in a cuvette of 1-cm path length)
oligo	oligonucleotide
ON	oligonucleotide
PAC	phenoxyacetyl
PACE	phosphoroacetate
PAC_2O	phenoxyacetic anhydride
PAGE	polyacrylamide gel electrophoresis
PBS	phosphate-buffered saline
PEG	poly(ethyleneglycol)
PEI	polyethylenimine
Phe	L-phenylalanine
piRNA	PIWI-interacting RNA
pivOM	pivaloyloxymethyl
PIWI	P-element Induced Wimpy testis
PLL	poly-L-lysine
PNA	peptide nucleic acid
pri-miRNA	primary miRNA
Pro	L-proline

pro-ON	oligonucleotide prodrug
proRNA	siRNA prodrug
PS	phosphorothioate or polystyrene
PTD	protein transduction domain
py	pyridine
qPCR	quantitative polymerase chain reaction
QTOF	quadrupole time-of-flight
rA	riboadenosine
rC	ribocytidine
R_f	retention factor (the ratio of the distance traveled from the baseline by a spot on TLC to the solvent front)
rG	riboguanosine
rN	ribonucleotide
RP	reversed-phase
RISC	RNA-induced silencing complex
RNA	ribonucleic acid
RNAi	RNA interference
rRNA	ribosomal RNA
r.t.	room temperature
RVG	rabies virus glycoprotein
s	singlet
SATE	S-acetyl-2-thioethyl
scr	scramble
sec	second(s)
shRNA	short hairpin RNA
siRNA	small interfering RNA
SMoC	small molecule carrier
SNALP	stable nucleic acid lipid particle
SO_2Cl_2	sulfuryl chloride
ss	single-stranded
$t_{1/2}$	half-life

t	triplet or thymidine or time
T	2'-deoxyribothymidine
TAT	trans-activating transcriptional activator
TBDMS	*tert*-butyldimethylsilyl
TCA	trichloroacetic acid
TEAA	triethylammonium acetate
THF	tetrahydrofuran
Thy	thymine
T*i*PDSiCl_2	1,3-dichloro-1,1,3,3-tetraisopropyldisiloxane
TLC	thin-layer chromatography
TLR	toll-like receptor
T_m	thermal melting temperature (^oC) (the temperature at which the mole fraction is 0.5 for both the duplex and the single strands (for a simple two-state transition))
tRNA	transfer RNA
U	uridine
UNA	unlocked nucleic acid
Ura	uracil

Chapter 1: Introduction

1.1. A Contemporary Understanding of the Diverse Biological Uses of Nucleic Acids

The central dogma of molecular biology involves the residue-by-residue transfer of the information stored in deoxyribonucleic acid (DNA) and ribonucleic acid (RNA).[1,2] It was simply stated in 1956 by Francis Crick as a sequential information transfer that disallowed backward transfer from protein to DNA or RNA, or from protein to protein. It was also understood to mean that DNA produces RNA and RNA produces protein. While this is indeed true, it has been established that RNA can be used to produce other RNA (ribozymes)[3] as well as DNA (reverse transcription), and that DNA can be used to produce other DNA (DNA polymerases).[4] Adding to the portfolio of RNA molecules that act as scaffolds for building nucleic acids, we are learning of the diverse groups of RNA molecules that act as templates for breaking nucleic acids down. This breakdown of RNA molecules can prevent the production of proteins and is further discussed in section 1.3, as well as gene expression modulation done by DNA (antisense molecules). The research carried out as a part of this thesis focuses on the synthesis, characterization, and biological use of small interfering RNA (siRNA) as part of the search for and development of cell-penetrating and efficient therapeutic RNA conjugates capable of mRNA breakdown. Before discussing the complex world of gene expression modulation, the framework for this phenomenon (the structure and function of nucleic acid) must be discussed.

1.2. Nucleic Acid Structure and Function

1.2.1. Nucleoside and Nucleotide Structure and Conformation

The nucleotide (nt) monomers that make up nucleic acids are comprised of a nucleobase, a ribose sugar or 2'-deoxyribose sugar in five-membered ring formation, and a 5'-phosphate group (Figure 1.1). A nucleoside is composed of the sugar with a nucleobase (without the phosphate group as the point of condensation into a nucleic acid polymer). While the six-membered pyranose form of the ribose sugar predominates in aqueous solution, it is the five-membered furanose form that is found in RNA. These furanose rings are numbered 1' to 5', starting from the glycosidic bond that is connected to the nucleobase. The nucleobase can be adenine (Ade), guanine (Gua), or cytosine (Cyt) for both RNA and DNA, while the fourth nucleobase is uracil (Ura) in RNA and thymine (Thy) in DNA. The purines adenine and guanine

are larger bicyclic molecules bonded to C1' of the sugar *via* their N9 atoms, while the pyrimidines cytosine, uracil, and thymine are monocyclic molecules bonded to the sugar *via* their N1 atoms.

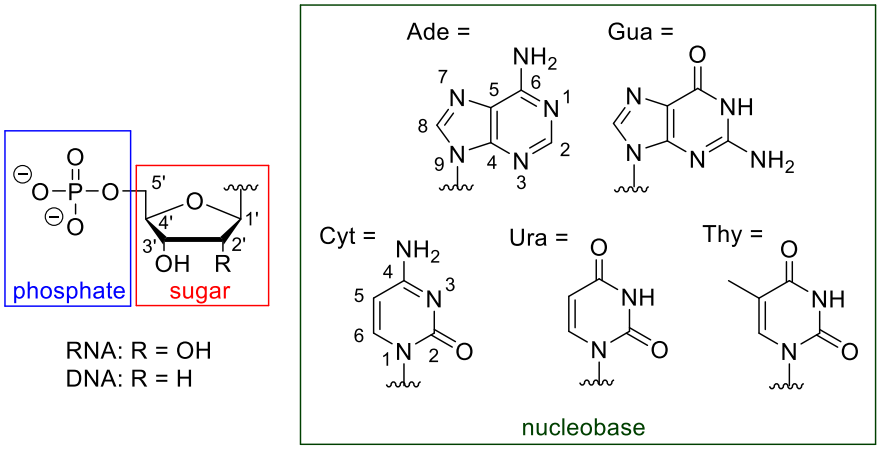

Figure 1.1. The nucleotide structures of monomers that comprise canonical RNA and DNA include purines adenosine and guanosine and pyrimidines cytidine, uracil, and thymidine.

The furanose ring can adopt different conformations in space. The *syn-anti* orientation of the nucleobases, the orbital geometry of the sugar, and other factors influence the conformation. Using the torsion angles of the bonds, a phase angle *P* can be calculated and found on a pseudorotational wheel that includes the possible conformations (Figure 1.2).[5,6] Two reference conformations, North and South, describe the sugar pucker of the ribose and 2'-deoxyribose sugar, respectively. The North pucker displaces the C3' atom on the same side of the C1'-O4'-C4' median plane as the nucleobase and the C5' atom, and the C2' atom is displaced to the opposite side. Thus it is also called the C3'-*endo* conformation. The South pucker displaces the C2' atom above the plane and the C3' atom below, and thus is described as C2'-*endo*. Other conformational reference points exist such as the East conformation in which the O4' atom is on the same side of the C5' atom and the nucleobase, and thus described as O4'-*endo*. Nucleosides and nucleotides can, and generally do, exist in equilibrium between two conformations. For example, canonical ribonucleosides are actually about 51% North and 49% South, while canonical 2'-deoxyribonucleosides are about 65% South.[7] This distribution can be calculated for novel nucleoside structures based on the coupling constants of the sugar ring protons.[8]

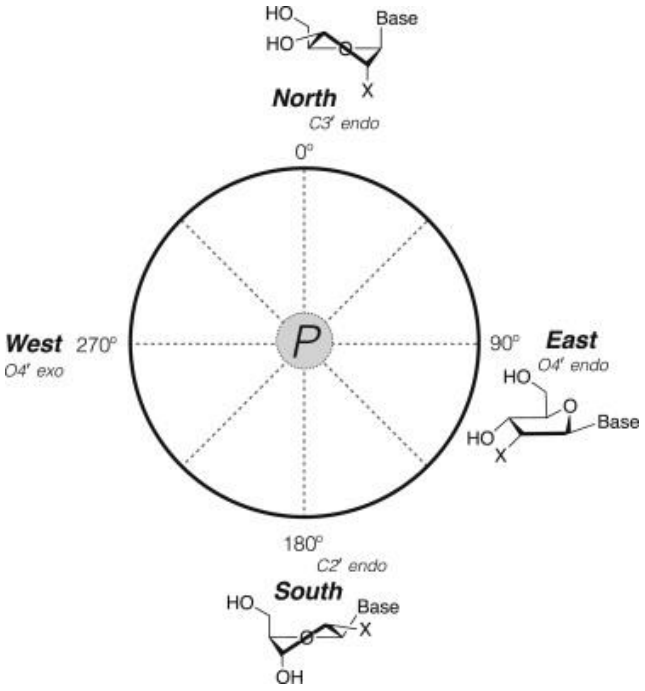

Figure 1.2. The sugar puckers correspond to phase angles on the pseudorotational wheel. Reprinted with permission from reference 6. Copyright 2012 Elsevier.

1.2.2. Common Nucleic Acid Structures

Nucleic acids are polymers made up of nucleotide subunits connected by a negatively charged (at physiological pH) internucleotide phosphodiester (Figure 1.3). Nucleotides are connected to each other at their 3'- and 5'-ends, thus the linkages are termed 3'-5' linkages. Their linear nucleobase sequence is written in the 5' to 3' direction with the letters dA, dG, dC, and T representing the 2'-deoxyribose nucleotides adenosine, guanosine, cytidine, and thymidine, while the letters rA, rG, rC, and U represent the corresponding ribose nucleotides. The sequence of these letters constitutes nucleic acid primary structure.

Secondary structure allows nucleic acid strands to base pair and form helices with other nucleic acid strands. Watson-Crick base pairing dictates that A and T/U base pair to each other while C and G base pair to each other. The strands pair to each other in an antiparallel fashion where the 3'-terminal end of one strand terminates its base pairing to the 5'-terminal end of the other. Double stranded RNA is almost entirely configured in an A-form right-handed helix,

while DNA is polymorphic and can be found in many right-handed configurations, including the B-form (Figure 1.4).[9,10] The A-from duplex is more tightly wound than the B-form duplex; there are 11 nucleotides per turn in an A-form duplex as opposed to 10 in a B-form duplex.[11] The greater South nature of the nucleotides that make up a B-form duplex prevents RNA from conforming into this secondary structure due to steric interactions of the 2'-OH group.[10]

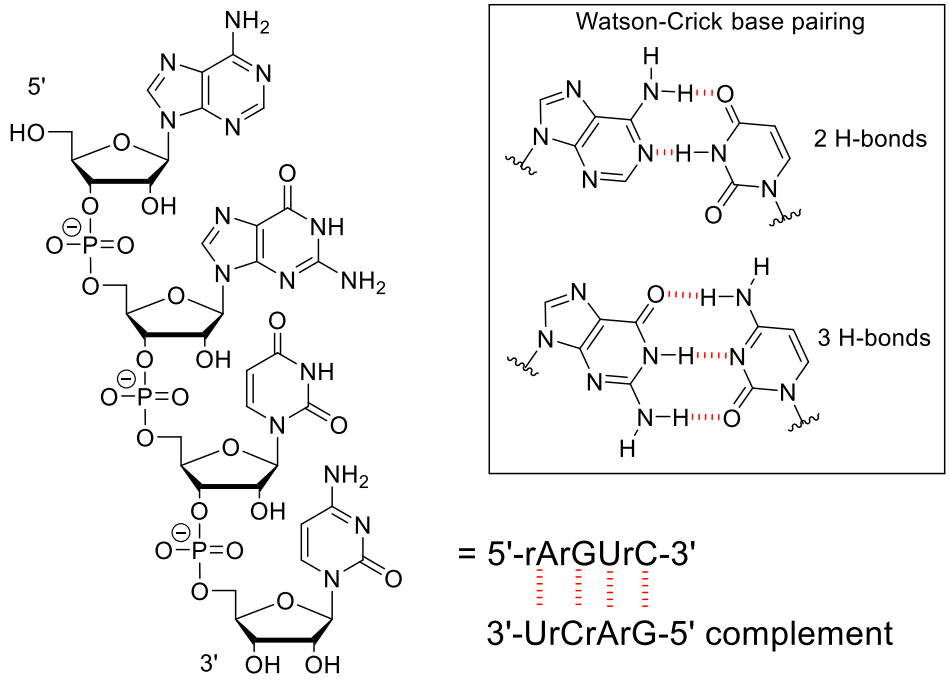

Figure 1.3. Nucleic acids join nucleotides by 5'-3' internucleotide bonds. The antiparallel complements of nucleic acid strands are hydrogen bonded by Watson-Crick base-pairs.

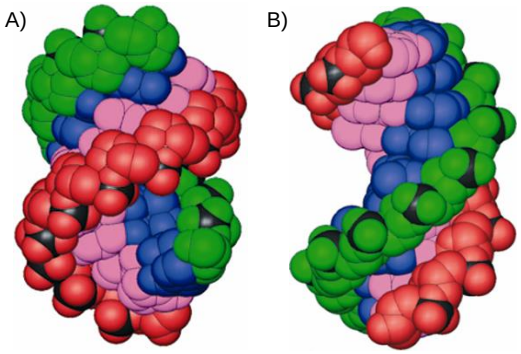

Figure 1.4. The A) A-form DNA helix and B) B-form DNA helix have different geometries. The sugar-phosphate backbones of the two strands are in green and red. Reproduced from reference 11 (http://dx.doi.org/10.1039/9781847555380) by permssion of The Royal Society of Chemistry.

1.2.3. Conventional Functions of Nucleic Acids

The extraction of DNA-containing "nuclein" occurred in 1869,[12] leading to a series of discoveries of nucleic acid components and proposed structures of the fascinating macromolecule with the apparent role in transmitting genetic information. Many contributors performed seminal work leading up to the double-helix model of Watson and Crick being published.[9] For example, DNA's role in heredity was already confirmed by Hershey and Chase in 1952, who discovered that most of the encapsulating protein of bacteriophage T2 was not absorbed into the *Escherichia coli* bacteria, while most of the DNA was in fact absorbed and thus had "some function" in the growth of T2 phage intracellularly.[13] Illustration of the DNA-to-RNA-to-protein flow of information was also done by various researchers. In 1960, Brachet affirmed that the cell nucleus is the primary site of nucleic acid synthesis, while proteins are synthesized in the cytoplasm through information transfer from RNA.[14] Brenner, Jacob and Meselson discovered unstable messenger (mRNA) intermediates in 1961, proposed by Jacob and Monod,[15] that act as carriers of bacteriophage genetic information for protein production using host ribosome enzymes.[16] The final pieces of the DNA-to-RNA-to-protein puzzle were finally laid when the first structure of a transfer RNA (tRNA) molecule was reported in 1965,[17] and when Altman and Cech's 1989 Nobel prize-winning work on the catalytic capacity of RNA confirmed that the RNA component of the ribosome (ribosomal RNA (rRNA)), rather than the protein component, catalyzes the production of protein from RNA.[3]

A simplistic summary of the conventional functional understanding of nucleic acids begins with transcription of single-stranded (ss) pre-mRNA by RNA polymerase II in the nucleus using ssDNA as a template.[18] It is complementary to the region of DNA from which it is copied (the antisense strand), and is therefore termed sense. It can be further processed when its intronic regions not coding for amino acids are spliced out of the molecule, leaving behind the ligated exon regions to produce a single mature mRNA.[18] In the cytoplasm, the ribosome brings together the mRNA strand and tRNA molecules in order to translate the mRNA sequence information into a peptide chain. Each tRNA has a region to detect the nucleobase sequence of the mRNA three sequential nucleotides at a time. This 3-nt-long block on the mRNA strand is termed a codon, while its corresponding region on the tRNA is termed an anticodon. There is also a region on the tRNA that carries the amino acid that corresponds to its anticodon. As the

amino acids are condensed to form a growing peptide chain, the sequence of the transcribed genomic DNA is translated into a polypeptide. Polypeptides with more than 50 amino acid residues make up a protein.

Less historically understood natural RNA function includes regulation, done with micro RNA (miRNA), PIWI-interacting RNA (piRNA), and small nuclear RNA (snRNA) to name a few, which is discussed in section 1.3.[19,20]

1.3. Gene Knockdown by Nucleic Acids

Complete knockout of a gene or alteration of the genetic code entails either addition or removal of genetic code from an organism, which can be accomplished by TAL (transcription activator-like) effectors[21] or the CRISPR/Cas9 system.[22] Changing gene expression without editing genomic DNA, on the other hand, is caused by an oligonucleotide temporarily binding to a component involved in gene expression or the gene itself. There are various transient mechanisms such as RNA interference (RNAi) mechanisms[23] and the RNase-H-dependent[24] and -independent antisense mechanisms.[25] The antisense mechanism was first demonstrated by Zamecnik *et al.*[26,27] It involves the introduction of a single-stranded antisense oligonucleotide (AON) that is complementary to a target mRNA. Multiple reviews have been written that distinguish RNase-H-dependent and RNase-H-independent antisense mechanisms.[28,29] RNase-H mediates cleavage of mRNA, while RNase-H-independent silencing can be accomplished by the AON sterically blocking the translation machinery. The research performed in this thesis will be concerned with the RNA interference mechanism of small interfering RNA. Therefore, the mechanisms of RNA interference will be discussed at greater length in sections 1.3.1 and 1.3.2.

1.3.1. RNA Interference in Mammals

RNA interference (RNAi) phenomena in particular have been and continue to be discovered in many eukaryotes as the ability of small non-coding RNA to inhibit gene expression at the post-transcriptional level. The understanding that the three-billion-base-pair genomic DNA contained in the nucleus of human cells not only contains genes, but many other sequences transcribed into RNA molecules dedicated to various cellular processes, including regulation, makes this possible. The two main RNAi mechanisms involving transient RNA duplexes are

miRNA (microRNA) and siRNA (small interfering RNA) and have been more commonly studied as performing interference in the cytoplasm of cells.

In the miRNA mechanism illustrated in Figure 1.5, a primary miRNA (pri-miRNA) hairpin of about 65-70-nt is generated from the genome, which is processed by the RNase III endonuclease Drosha into pre-miRNA with a 3'-overhang on one end and a stem-loop on the other.[23] That construct can be transported into the cytosol and cleaved by Dicer, another RNase III enzyme, producing a duplex of about 21-25-nt with 3'-overhangs and 5'-phosphates.[23] The duplex has some degree of mismatch, but if the strand loaded into the RNA-induced Silencing Complex (RISC), denoted by an asterisk, is perfectly complementary to an mRNA, it will cause the cleavage of the mRNA.[23] If there is some mismatch of the miRNA* strand to the mRNA, translation will be blocked or the mRNA will be destabilized by the shortening of its poly-A tail and then degraded.[23] For example, full complements to the seed region, which includes bases 2-8 of the miRNA* strand, can trigger silencing of multiple genes involved in an inflammatory response due to the common seed region sequences in many inflammatory genes. In that case, full complements to the mRNA from base 9 onward is not necessary. With knowledge of these details regarding the miRNA mechanism, a synthetic mimic of the miRNA* strand hybridized to an RNA complement can be introduced into the cell in order to hijack this natural process of regulating endogenous genes.

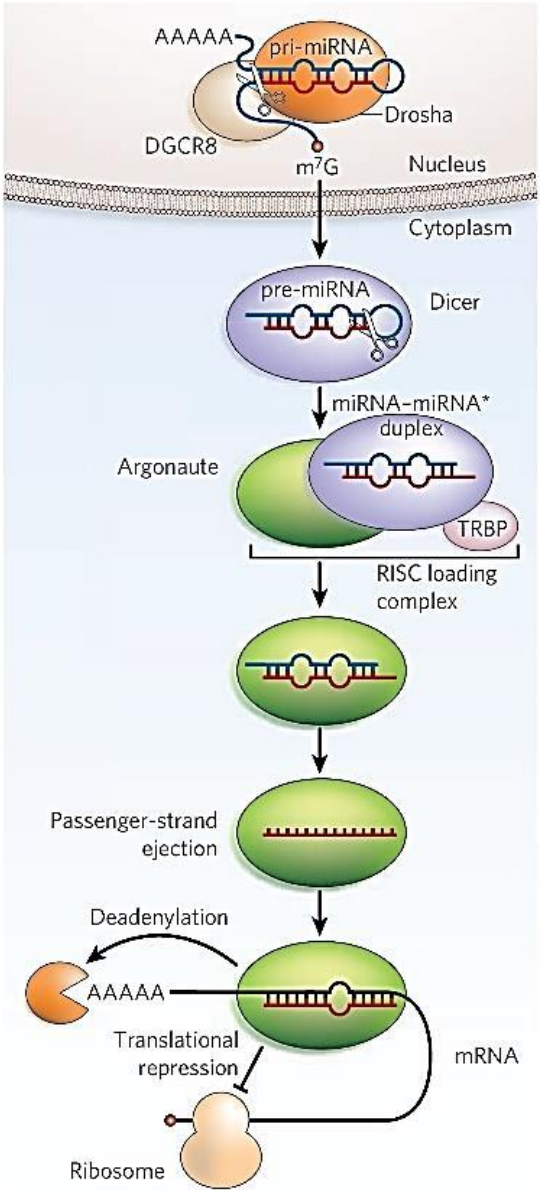

Figure 1.5. The miRNA mechanism in humans begins with pri-miRNA in the nucleus and either destabilization of mRNA or translational arrest. Reprinted with permission from reference 23. Copyright 2009 Nature Publishing Group.

Initial work in the 1990s on exogenously-introduced RNA causing potent silencing of plant genes[30,31,32,33] was followed by the Nobel prize-winning work of Fire and Mello in which siRNA was introduced into a species of nematode to reduce expression of the gene *unc*-22, by which a severe twitching phenotype was observed.[34] The work of Fire and Mello stimulated the interest in using synthetic RNA to exploit its therapeutic potential in humans. In 2001, Tuschl and coworkers extended the application of the siRNA mechanism to different mammalian cell lines and restricted the trigger's molecular structure to a 19-nt RNA duplex with 2-nt overhangs at the 3'-ends.[35] In the cytoplasm, the duplex is loaded into RISC (Figure 1.6). The strand that is analogous to the miRNA* strand, called the guide strand, remains in the silencing machinery while the other (passenger) strand is cleaved by an Argonaute (AGO) protein (AGO2 in humans) and discarded (Figure 1.6).[23] The strands are differentiated by the bias in stability between each end; the strand with the 5'-end that has weaker hybridization to the complement becomes the guide strand.[36] They are also differentiated by the presence of a 5'-end phosphate[37] on the guide strand and desirable uridine and adenosine nucleotides at the 5'-end as opposed to guanosine and cytidine.[38] When the guide strand is perfectly complementary to an mRNA it facilitates the cleavage of the mRNA between bases 10 and 11 of the guide strand (in reference to its 5'-end).[36] The guide strand remains loaded in RISC for more catalytic rounds of mRNA

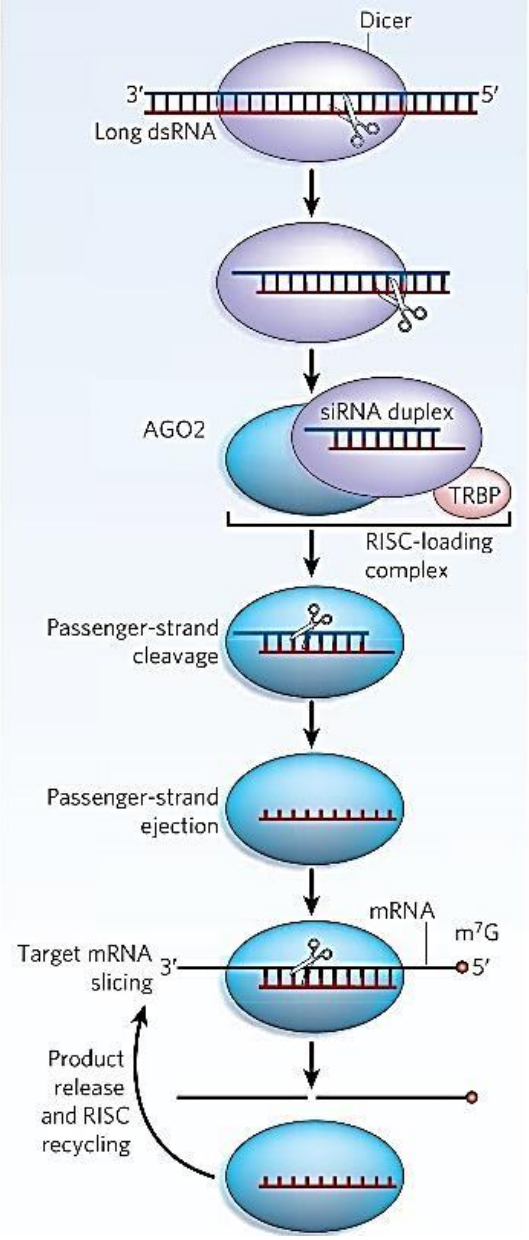

Figure 1.6. The exogenously-triggered siRNA mechanism in humans begins with 21-nt-long duplexes loaded into RISC or longer substrates of Dicer cut into siRNA. Reprinted with permission from reference 23. Copyright 2009 Nature Publishing Group.

cleavage. Given the well-established mechanism of siRNA silencing and the simple requirement of Watson-Crick base pairing to mRNA, siRNA therapy in humans could potentially treat a multitude of diseases with a genetic component simply by a change in siRNA nucleobase sequence.

1.3.2. Issues with Hijacking the miRNA Mechanism with siRNA

The relative ease of rationally designing a sequence-specific siRNA in an age of complete disclosure of the human genome is antagonized by the hurdles presented by siRNA structure in safely delivering the molecule into cells. Naked, meaning non-encapsulated in this thesis, and unmodified siRNA molecules are extremely susceptible to serum nuclease digestion. They are also hydrophilic and negatively charged (Figure 1.3), experiencing cellular membrane repulsion, poor circulation, and thus rapid renal clearance after being introduced into systemic circulation. Naked oligonucleotides can also stimulate the innate immune system to induce proinflammatory cytokines (signalling molecules), depending on their site and route of delivery as well as sequence,[39] since they resemble viral and bacterial components,[40] also causing their rapid removal from circulation by cytokine-stimulated phagocytotic cells.[41] Depending on the type of oligonucleotide, the delivery complex, and the mechanism of internalization, different cellular receptors can be stimulated. For example, double-stranded (ds) RNA stimulates TLR3 (Toll-Like Receptor 3) in endosomes[42] and on certain cell surfaces,[41] while Protein Kinase R (PKR) and RNA helicase enzymes Melanoma Differentiation-Associated protein 5 (MDA5) and Retinoic acid Inducible Gene 1 (RIG-1) are stimulated in the cytoplasm.[43] TLR7 and TLR8 are stimulated by ssRNA exclusively in endosomes.[42,41] ssDNA sequences with unmodified 5'-CpG can be recognized by TLR9 in endosomes.[42] These immunostimulatory effects as well as cellular delivery issues are the most restrictive obstacles that are being researched to date.

Of the more manageable issues, sequence-specific off-target effects can be avoided by screening potential siRNA molecules for any significant complementarity to an endogenous off-target. This can be done by inserting the sequence in the National Center for Biotechnology Information's online Basic Local Alignment Search Tool (BLAST). An unintended immune response due to off-target siRNA binding can be avoided by using a sequence that is not complementary to the seed region (Figure 1.7) of genes of the immune system. The loading of the intended passenger strand in the RISC machinery must be avoided; otherwise the wrong

mRNA strand will be targeted. Fortunately, there are chemical modifications that can be used to introduce thermodynamic bias between the ends of the duplex to cause preferential RISC loading of the intended guide strand.[44] Any secondary structure in a proposed siRNA that could prevent its binding to mRNA and/or its binding to the enzymatic machinery can also be screened out with online predictive tools such as the mfold web server.[45]

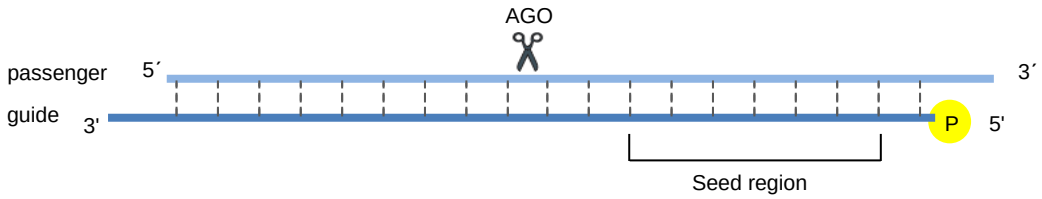

Figure 1.7. An siRNA duplex has two 3'-overhangs, a seed region at bases 2-8 of the guide strand, and directs cleavage of the complementary passenger and mRNA strands between bases 10 and 11 with respect to the guide strand.

1.3.3. Alternative Mechanisms of Nucleic Acid Mediated Control of Gene Expression

Some silencing methods are listed in Table 1.1. One of those methods, the short hairpin RNA (shRNA) interference mechanism, generates siRNAs. It begins, however, with the exogenous delivery and integration of a plasmid vector in the host genome.[46] The integrated DNA can produce a hairpin RNA resembling a pri-miRNA in the nucleus, but with full duplex complementarity reminiscent of siRNA, for processing by Drosha and Dicer into siRNA capable of RNA interference.[46]

Exogenously introduced oligonucleotides with many of the chemical modifications discussed in sections 1.3.4 can also be made to sterically block the work of an aberrant miRNA by hybridizing to it, preventing its hybridization to its target mRNA. These miRNA-targeting oligonucleotides are called anti-miRNA oligonucleotides (AMOs), or antagomirs by Krutzfeldt *et al*. in their pioneering *in vivo* work.[47] An exact complement to the aberrant miRNA is typical of anti-miRNAs studied, however RNase-H-mediated cleavage of the mRNA is rare.[48] Single strands of oligonucleotide mimics such as morpholino oligonucleotides can also be synthesized as site-selective binders to pre-mRNA to modulate the splicing of the mRNA.[49]

Knowledge on gene knockdown mechanisms continues to expand and teach us that one type of RNA molecule can regulate genes in different ways and in different parts of the cell. The fact that endogenous human AGO2-small RNA complexes are mainly loaded in the cytoplasm but can be shuttled to the nucleus allows for this kind of versatility.[50] For example, nuclear miRNAs and siRNAs can cause cleavage of RNAs such as 7SK small nuclear RNA, which plays an integral role in the association of positive transcription elongation factor (P-TEFb) with RNA polymerase II in eukaryotes.[51] Plants use endogenously generated siRNA to cause RNA-directed DNA methylation (RdDM) as well by guiding *de novo* methyltransferases to DNA.[52,53]

Table 1.1. Some of the functions of gene silencing molecules operating in animals are summarized below.

	Molecule	2^o structure	Nucleic acid	Effect	Genesis
'antisense'	AON, AMO	ss	DNA and DNA-like	• AON: Steric block of translational machinery • AON: RNase-H-mediated mRNA cleavage • AON: Post transcriptional splice-switching • AMO: Steric block of AGO	exogenous
RNA interference	miRNA	ds	RNA	AGO-mediated mRNA and small nuclear RNA cleavage	endogenous
	siRNA	ds	RNA and RNA-like	AGO-mediated mRNA cleavage	exogenous
	shRNA	ds (hairpin)	DNA		exogenous
	piRNA	ss	RNA	DNA methylation	endogenous

There is a great variety in the type of trigger RNA molecules capable of gene regulation. PIWI-interacting RNAs (piRNAs) in animal germlines are also small RNAs that bind to the domain of AGO encoded by the P-element Induced Wimpy testis (PIWI) class of genes to direct it to transposons and repeat sequences in the genome.[20] piRNAs are endogenously generated but do not require Dicer for biogenesis, as in the case of miRNAs, even though their exact method of generation is unknown.[54] These are about 24-31-nt-long single strands[23] with 2'-*O*-methylation

at the 3'-termini.[55] In an epigenetic twist, they can interact with complementary chromatin-associated or nascent RNA to methylate DNA.[56]

AONs, siRNAs, shRNAs, and anti-miRNAs have all progressed to clinical trials using various delivery methods outlined in section 1.4.1 as well as many of the chemical modifications outlined in section 1.3.4. AONs have had therapeutic success with three FDA approved drugs – fomivirsen (Vitravene^{TM}), mipomersen (Kynamro^{TM}), and eteplirsen (Exondys 51^{TM}).

1.3.4. Available Chemistries for Oligonucleotides

Chemical modification to oligonucleotides can confer desirable traits such as reducing immunostimulation and other off-target effects, modifying binding affinity, tuning conformation in predictable directions, and improving resistance against nuclease-mediated degradation of the sugar phosphate backbone. Modification can be made to the internucleotide linkage, the sugar, and/or the nucleobase.

1.3.4.1. Internucleotide Modifications

One of the most common internucleotide linkages in oligonucleotide gene expression regulators is the phosphorothioate (PS) linkage.[57,58] It comprises the entire backbone of almost all of the AON drugs that have entered clinic trials. The FDA approved drugs fomivirsen (Figure 1.8) and mipomersen are comprised entirely of PS linkages. The established solid-supported synthetic protocol introduces sulfur at the non-bridging position of the internucleotide linkage (see section 1.5.1), thus producing 2^n diastereomeric oligonucleotides (n = number of epimeric PS linkages). Methods for diastereoselective synthesis have been established[59] since different combinations of S_p and R_p phosphorothioate insertions confer different stabilities and activities. A single S_p linkage confers greater plasma 3'-exonuclease stability than an R_p linkage, while full R_p modification causes greater mRNA cleavage by RNase-H on account of greater binding affinity to the target as compared to that of the oligonucleotide with full S_p modification.[60] The diastereoisomers can also have different immunostimulatory properties.[61] Regardless, PS-AONs are synthesized and used as diastereometric mixtures since the multiple PS bonds confer an overall improvement to stability and pharmacokinetics. PS linkages bind better to serum albumin than phosphate linkages, thus increasing the systemic circulation time of the AON. They are also compatible with the RNase-H machinery to cause mRNA cleavage[60]

and they increase cellular uptake during gymnosis.[62] Even though they can negatively impact AON binding affinity to RNA targets and some toxicity has been observed,[63,64,65,66] the advantages greatly outweigh the disadvantages.

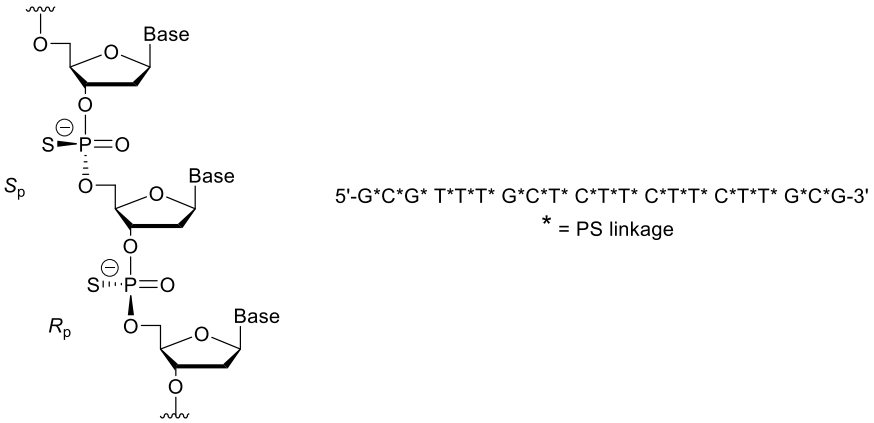

Figure 1.8. The diastereomeric phosphorothioate linkages shown are found in fomivirsen.

PS-modified ssON co-incubated with unmodified siRNA actually increases the cellular uptake of siRNA, presumably through PS-stimulated receptor-mediated uptake.[67] Their potency, however, is inferior to unmodified siRNA delivered *via* standard cationic liposomal transfection reagent Lipofectamine™ 2000, presumably due to retention of the siRNA in cellular vesicles.[67] Complete PS modification in siRNA has been avoided because while a few terminal inserts have caused minimal reduction in activity,[68] heavy or full modification severely reduces activity.[69] An achiral phosphorodithioate (PS2) linkage shown in Figure 1.9A has been combined with 2'-*O*-methyl modification (common in RNA mimics) on the same two nucleotides in the seed region of the sense strand to synergistically produce enhanced-potency siRNA.[70] The A-form of the duplex was retained with this minimal modification.[70]

Other studied internucleotide modifications include phosphonoacetate (PACE) linkages with both non-bridging oxygen and non-bridging sulfur (Figure 1.9B). They retain the negative charge of the backbone, predictably increase nuclease resistance, and stimulate RNase-H activity.[71,72] The PACE and thio-PACE modifications were combined, on the same nucleotide, with 2'-*O*-methyl modifications in siRNA with up to four modifications on each terminal end.[73] The siRNAs achieved some gene silencing without transfection agent due to their relatively strong activity but meagre cellular uptake.[73] Ester derivatives of the PACE modification are

reminiscent of thioesters incorporated into nucleoside prodrugs, and later siRNA prodrugs, such as S-acetyl-2-thioethyl (SATE), which are discussed in section 1.6.2.1. Amide-linked (Figure 1.9C) and peptide nucleic acids (Figure 1.9D) are both uncharged and do not contain phosphorus. Up to eight amide linkages have been used in siRNA at the 5'-end of the antisense strand to increase activity.[74] Peptide nucleic acid (PNA), in particular, has been used as an inhibitor of mRNA translation[75] and it has been incorporated at the 3'-termini of siRNA to increase nuclease stability and effect translational inhibition.[76] The FDA approved drug eteplirsen is a morpholino oligonucleotide – that is, it is comprised entirely of a morpholino backbone.

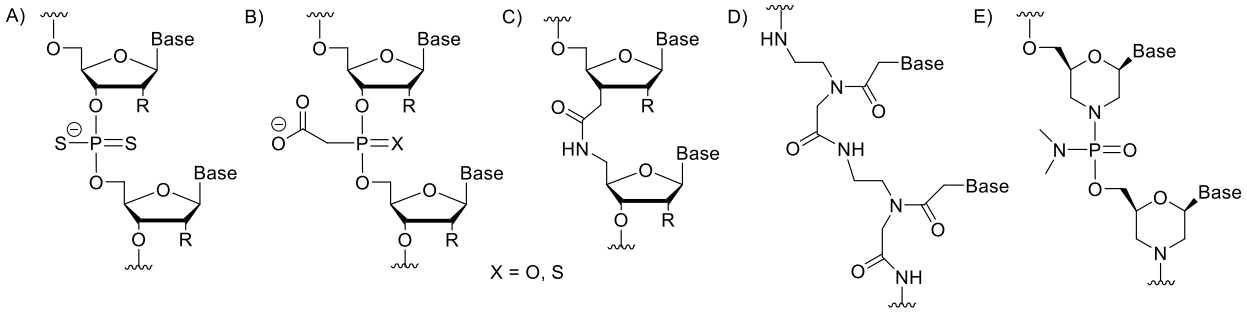

Figure 1.9. Backbone modifications that have been studied in siRNA include A) phosphorodithioate (PS2), B) phosphonoacetate and thiophosphonoacetate, C) amide-linked RNA and DNA, D) peptide nucleic acid, and E) morpholino. RNA: R = OH; DNA: R= H.

1.3.4.2. Sugar Modifications

Sugar modifications such as those shown in Figure 1.10 can be used alone or combined with other sugar and/or backbone modifications for a desired oligonucleotide function. Sugar modifications can impart great influence in binding affinity to target RNA, furanose conformation, and thus duplex structure, RNase-H and/or AGO compatibility, nuclease resistance, immunostimulation, and off-target effects. The 2'-position on the furanose ring in particular is easily accessible to chemical modification and can cause enhanced binding affinity to RNA (first 4 entries in Table 1.2). For example, a significant increase in thermal melting temperature (ΔT_m) per insert is observed for the 2'-*O*-(2-methoxyethyl) (2'-*O*-MOE),[77] 2'-fluoro-ribo nucleic acid (2'-F-RNA),[78] and 2'-deoxy-2'-fluoro-β-D-arabino nucleic acid (2'-F-ANA) modifications.[79]

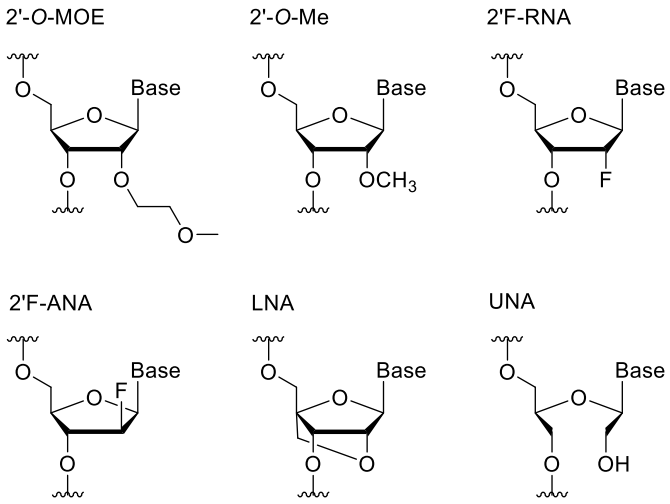

Figure 1.10. Several sugar modifications have been studied in siRNA.

The enhanced binding affinity of the modified strands to RNA is tantamount to being a good candidate for transient knockdown molecules since the targets are RNA molecules – i.e. mRNA, miRNA, or pre-mRNA. The 2'-*O*-MOE,[77] 2'-*O*-Me,[80] and 2'-F-RNA furanoses adopt North sugar puckers, [81] making them excellent inserts in RNA-based oligonucleotides like siRNA. They have been used in siRNA to effect AGO-mediated target cleavage in mammalian cells.[82] Three 2'-F-RNA inserts are well-tolerated in the antisense (guide) strand, regardless of whether the inserts are placed near the 3'-end, the middle of the strand, or near the 5'-end.[82] Three 2'-*O*-MOE inserts, however, diminish activity regardless of where they are placed in the antisense strand.[82] Three 2'-*O*-Me inserts are well-tolerated further away from the 5'-end of in the antisense strand.[82] By contrast, active siRNAs tolerate all of these inserts in the sense strand very well.[82] The 2'-*O*-MOE and 2'-*O*-Me modifications can also be combined with DNA residues in the so called 'gapmer' design to effect RNase-H cleavage of mRNA. The DNA gap when hybridized to the RNA target provides the required DNA/RNA 'hybrid' substrate for RNase-H, which cleaves the RNA to release the modified oligomer for further RNA binding.[77] Mipomersen contains 2'-*O*-MOE modifications in a gapmer design (Figure 1.11). Despite the issue of liver toxicity observed with this drug, it has been used for management of cholesterol. While 2'-*O*-MOE and 2'-*O*-Me modifications cause significant increase in serum stability,[77,83] the 2'-F-RNA modification does not.[84] Despite having South East sugar pucker,[81] its stereoisomeric form, 2'-F-ANA, can be used in siRNA to improve serum stability and potency.[85,86]

Table 1.2. Selected sugar modifications have been investigated for their use as RNA binding agents.

	Binding to RNA relative to DNA	ΔT_m /insert (^oC)	Sugar pucker / duplex form	RNase-H or AGO?	Stability to nucleases	Immuno-stimulation when in siRNA	FDA-approved ON therapy
5-membered							
2'-*O*-MOE	Enhanced	+ ~2	North / A-form	Both	Increase		mipomersen (AON)
2'-*O*-Me	Enhanced		North / A-form	Both	Increase	Reduced	pegaptanib (aptamer)
2'-F-RNA	Enhanced	+ ~2 – 3	North / A-form	AGO	Minor increase	Reduced	pegaptanib (aptamer)
2'-F-ANA	Enhanced	+ ~1 – 2	South East / B-form	Both	Increase	Reduced if with LNA and 2'-F-RNA	-
4'-*S*-DNA			A-form[87]	Both	Increase		-
Bicyclic							
LNA	Enhanced	+ ~5	North / A-form	Both	Increase	Reduced	-
Acyclic							
UNA		- ~5 – 10	Flexible / no global change	Both	Increase	Reduced if off-target seed region binding avoided	-
6-membered							
ceNA	Enhanced			RNase-H	Increase		-

The bicyclic locked nucleic acid (LNA) and acyclic unlocked nucleic acid (UNA) have had utility in siRNA and AON constructs. While LNA is constrained in the North conformation due to the methylene bridge joining the 2'-OH and C4' positions,[88] the flexible UNA loses some entropy when conforming to an A-form helix. Thus, LNA is suitable in siRNAs and in the wings of gapmer AONs. UNA flexibility can be helpful in accommodating AON conjugates in RNase-H,[24] causing preferential loading of the antisense strand of siRNA when used at the 5'-terminus of the passenger strand, and minimizing off-target effects when used in the guide strand seed region.[89]

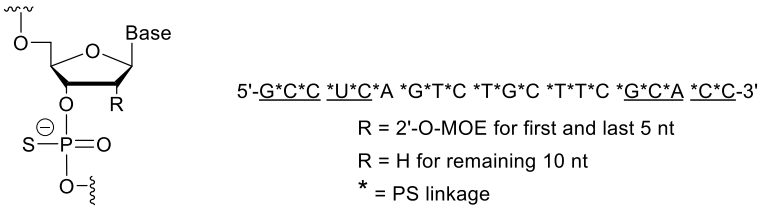

Figure 1.11. Antisense oligonucleotide mipomersen contains nineteen phosphorothioate and ten 2'-*O*-MOE sugar modifications.

1.4. Cellular Delivery of Nucleic Acids

1.4.1. Delivery Methods for Chemically Inert Nucleic Acids

Delivering unmodified nucleic acids to cells is a major hurdle in the development of ON based therapeutics. The challenge arises from the chemical structure of ONs (negatively charged, hydrophilic, and large), which is incompatible with the negatively charged lipophilic membrane core. In the absence of a delivery vehicle or 'conjugate' moiety, nucleic acids (AON, siRNA) can undergo rapid renal clearance, degradation by blood serum exo- and endonucleases, and trigger an immune response. Many delivery methods have been pursued, with some examples of systemic administration resulting in gene silencing.

1.4.1.1. Terminal Conjugation of Large Structures

The common theme among conjugates utilized for systemic delivery is covalent attachment of a large molecule to the 5'- or 3'-terminus of a chemically modified oligonucleotide. Cholesterol (Figure 1.12B) remains in circulation *via* binding to lipoprotein particles.[90] It can be covalently linked to hydrophobic siRNA (hsiRNA) with extensive PS, 2'-*O*-Me, and 2'-F-RNA modifications to self-deliver to hepatocytes *via* intravitreal injection (through the eye).[91,92] Another lipophilic moiety, α-tocopherol (vitamin E), which binds to serum albumin to keep it in circulation, has been conjugated to siRNA injected intracerebroventribularly in mice with high-density lipoprotein (HDL) carrier. The vitamin moiety binds to the HDL that is able to trigger lipoprotein receptor-mediated endocytosis.[93] One highly successful example is *N*-acetylgalactosamine (GalNAc) conjugation to siRNA (Figure 1.12D), which delivers it *in vivo via* subcutaneous injection to hepatocytes using asialoglycoprotein receptor (ASGPR)-mediated endocytosis.[94]

Oligonucleotide aptamers also act as ligands to cell surface receptors to guide endocytosis of aptamer-siRNA conjugates (Figure 1.12A) to target tissue. Prostate-specific membrane antigen (PSMA), overexpressed in prostate cancer cells and tumor vascular endothelium, can be bound by aptamer conjugated to siRNA targeting tumor growth. PSMA-binding aptamer-conjugated siRNA has been injected intratumorally into mice and tumor growth has been inhibited.[95]

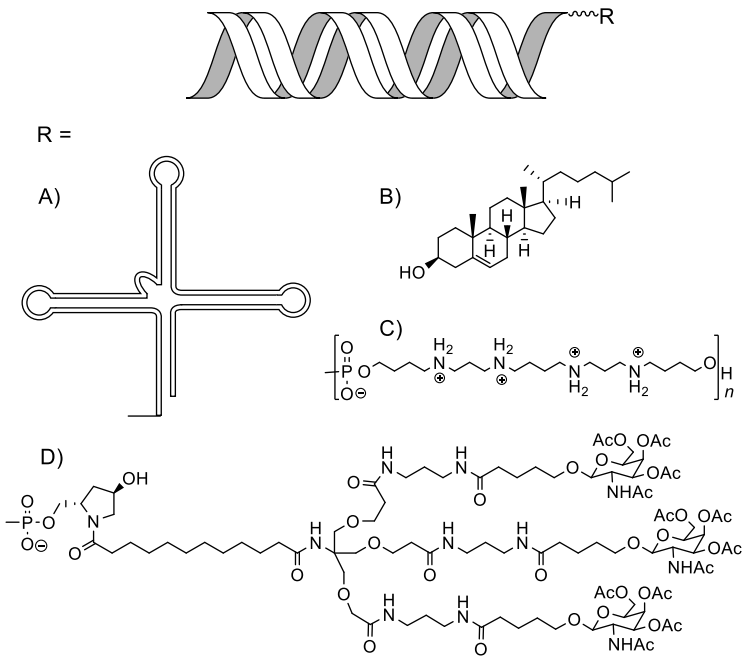

Figure 1.12. siRNA conjugates can be terminated with A) aptamers, B) cholesterol and other lipids, C) spermine and other polycationic polymers, and D) GalNAc.

Cationic polymers such as spermine have been conjugated to siRNA to mediate uptake (Figure 1.12C). At or above a ratio of amines (positive charges) to phosphates (negative charges) of 1.5, the pK_as of the excess amines are gradually lowered due to the nearby positive charges, allowing them to act as proton sponges once inside the acidic endosome. This allows for a release of the siRNA cargo into the cytoplasm and RNAi to occur.[96] While cationic polymers have traditionally been understood to bind anionic heparin sulfate proteoglycans (HSPG) on the cell surface to trigger endocytosis, another class of cationic polymers called cell penetrating peptides (CPPs) employ other mechanisms of internalization based on the peptide

structure.[97] siRNA-delivering CPPs include trans-activating transcriptional activator (TAT),[98] penetratin, and transportan.[99]

1.4.1.2. Encapsulation

Encapsulating structures can deliver nucleic acids quite efficiently. Biological vectors are prime examples of innovative and promising carriers that can be exploited for their protective encapsulation and release of nucleic acids in a variety of tissues. These encapsulating structures take a variety of forms: Organisms such as strains of *Escherichia coli* are well-tolerated in gastrointestinal organs, cell-derived particles such as exosomes are tolerated by neurons, and adeno-associated virus is tolerated by organs of the circulatory system.[100]

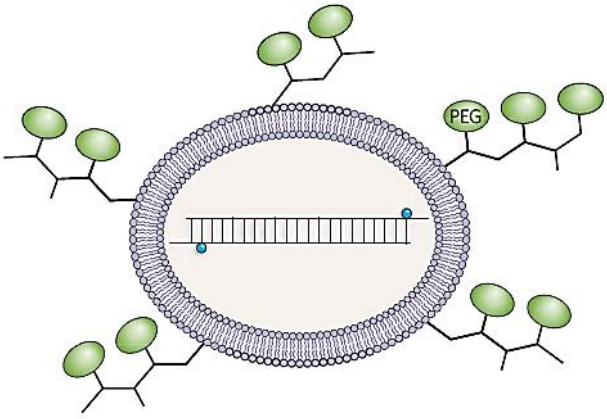

Figure 1.13. A PEGylated SNALP distributes in systemic circulation and delivers a positively charged lipoplex to cells. Reprinted with permission from reference 44. Copyright 2009 Nature Publishing Group.

Cationic liposomes internalize oligonucleotides *via* endocytosis as well as through direct fusion with the cellular membrane. A minority population of administered lipoplexes directly fuse with the membrane to deliver the siRNA that will cause RNAi, while the rest is degraded in lysosomes.[101] Consequently, a stable nucleic acid lipid particle (SNALP) such as that shown in

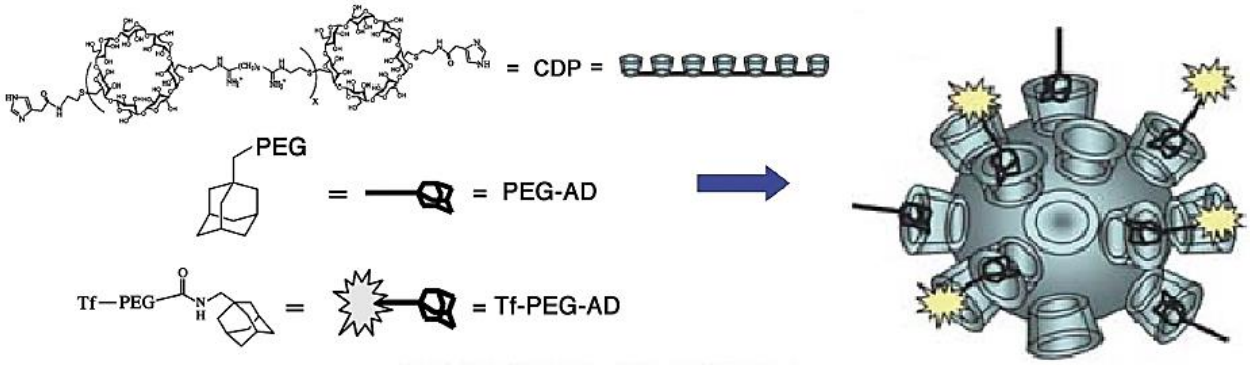

Figure 1.14. The cyclodextrin-based nanoparticle pictured was used to encapsulate and deliver siRNA in humans. Reprinted with permission from reference 105. Copyright 2009 American Chemical Society.

Figure 1.13 was developed with conjugation of the cationic lipid (such as 1,2-dilinoleyloxy-N,N-dimethyl-3-aminopropane (DLinDMA) or other more fusogenic lipids) to hydrophilic poly(ethyleneglycol) (PEG) to increase residence time in blood.[102] MacLachlan and colleagues were first to evidence systemically-administered RNAi in non-human primates by targeting apolipoprotein B (ApoB) for cholesterol management with a SNALP that was intravenously administered to monkeys.[103]

RNAi was first evidenced in humans after intravenous administration of a transferrin-carrying nanoparticle targeting transferrin receptors on cancer cells (Figure 1.14).[104] The nanoparticle scaffold was made up of a linear polymer of cyclodextrin interspaced with positively charged as well as pH-buffering amines that electrostatically associated with siRNA and assisted in the release of nanoparticles from endosomes, respectively.[105] The heavily-decorated outer surface contained PEG solubilizers and transferrin (Tf), which completely encapsulated and protected the siRNA from nuclease degradation.[105]

Other nanoparticles have been synthesized to deliver siRNA to cells, including non-encapsulated Dicer-substrate siRNA with strategic sugar modifications.[106] Some of the other encapsulating varieties of nanocarriers include siRNA encapsulated in nanoliposomes loaded onto porous silicon nanoparticles,[107] and single siRNA nanocapsules that must not only undergo a physical breakdown for cargo release, but also a chemical breakdown of the positively charged, degradable under pH 6, and hydrophilic portions of the capsule that were polymerized around a single siRNA molecule.[108]

1.4.1.3. Non-Encapsulation and Non-Conjugation

Transfer of non-encapsulated and non-conjugated nucleic acid across cellular membranes has also been achieved. It can be done without vectors using physical methods that increase cell membrane permeability such as electroporation (short bursts of strong electric field) and sonoporation (intense ultrasound exposure). In a similarly simple, but slow, method of delivery without a delivery vector, Stein and coworkers found that naked phosphorothioated AONs (i.e. PS-DNA, LNA, and 2'-F-ANA) can be taken up by cells in culture at a very slow rate in uniform and low levels by a processes coined gymnosis, causing maximal transient knockdown after 6-10 days.[62,109] The hydrodynamic method is a physical method in which murine specimen can be

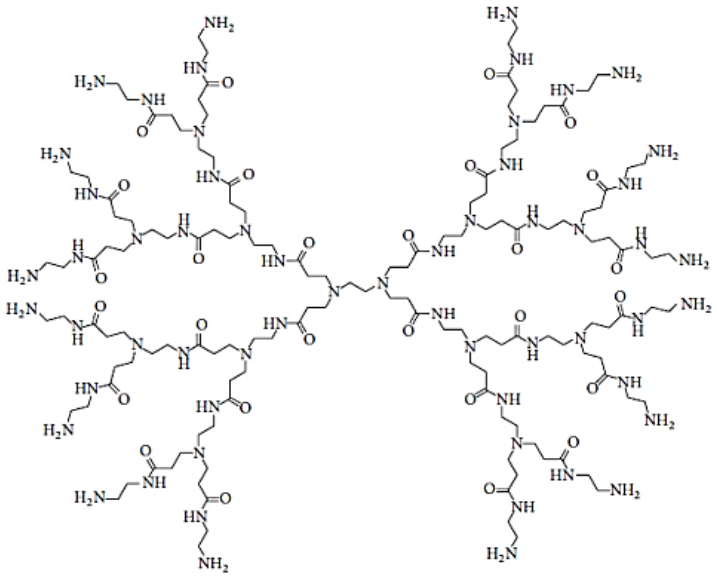

Figure 1.15. A PAMAM dendrimer with an ethylenediamine (EDA) core can be used as an siRNA delivery vector. Reprinted from reference 113 under a Creative Commons License.

rapidly injected through the tail with large volumes of dissolved nucleic acids to cause enough high-pressure liver membrane disruption for internalization.[110,111]

Cationic polymers have been used as delivery vectors by electrostatically complexing to oligonucleotides and conferring the cell penetrating properties of the polymers to the oligonucleotide-polymer complex. Dendritic poly-L-lysine has been used to deliver siRNA to cells *in vitro*,[112] while the most common type of dendrimer used is the poly(amidoamine) (PAMAM) variety (Figure 1.15).[113] A large enough dendrimer radius and a large ratio of primary amines (positive charges) to phosphate groups (negative charges) improves transfection efficiency on account of the proton sponge effect.[114,115] CPPs have also found use as non-covalent carriers. The synthetic amphipathic MPG peptide vector has allowed for *in vitro* delivery of siRNA.[116] The nucleic acid-binding protamine, found in nature complexed with DNA in sperm, has been fused with an antibody Fab fragment directed against the HIV-1 envelope (Figure 1.16). It was complexed to siRNA *via* the electrostatic interactions of the siRNA backbone and protamine portion, and the antibody portion directed the complex to HIV-infected T lymphocytes and other primary cells, which are difficult to transfect with lipoplexes.[117] Intratumoral and intravenous injections in mice successfully treated target cells without affecting non-infected cells.[117]

Gooding *et al* demonstrated that biphenyl polyguanidinium carriers of siRNA, small molecule carriers (SMoCs) based on amphipathic CPPs that combine both cationic and lipophilic residues, internalize siRNA when co-administered to cultured fibroblasts.[97] SMoCs do not have to be cationic; Retro-1 is a SMoC of AONs. Intraperitoneal administration (in mice) of the AON

immediately followed by intravenous administration of Retro-1, improved silencing to a lesser degree than what can be accomplished with cationic liposomes, but nonetheless demonstrated an improvement *via* its own mechanism.[118]

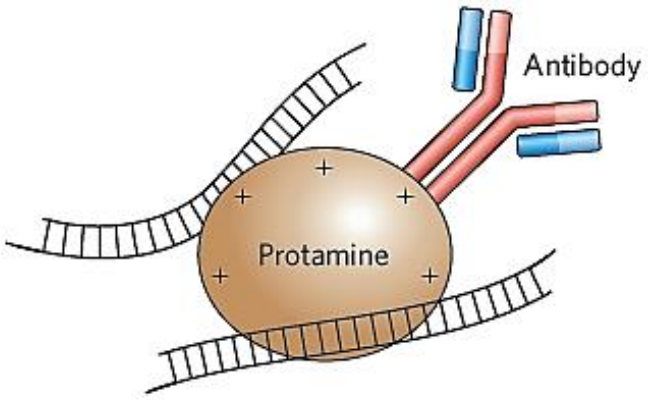

Figure 1.16. A fusion protein has been used to complex siRNA and direct it to target cells. Reprinted with permission from reference 44. Copyright 2009 Nature Publishing Group.

1.4.2. Obstacles Encountered with Delivery Methods

The safe delivery of siRNAs to target cells and only target cells is paramount in siRNA therapeutics; unintended side effects, from the immune system and from other sources, are bound to accumulate from the high doses of siRNA and vectors administered to animals. Efficient systemic delivery and knockdown are thus requirements. Fortunately, a relatively low number of siRNA molecules loaded into RISC (500) are needed in the cytoplasm to elicit the desired silencing effect regardless of the millions of siRNA molecules that can be delivered into the cells.[91]

1.4.2.1. Non-Encapsulated Oligonucleotides

Naked chemically modified nucleic acids have been evaluated in the literature for their unassisted cellular uptake. Many of those attempts use a very large concentration of oligonucleotide to achieve cellular internalization in cell culture, which is not practical for systemic human use.[119] Naked chemically modified nucleic acids have, nonetheless, been evaluated in clinical trials without the aid of delivery vehicles. Pulmonary epithelial cells, for example, are unique in their affinity for carrier-free siRNA; respiratory syncytial virus infection can be treated in mice by nasal administration.[120] However, in moving away from more easily

accessible tissue, which can also receive intralesional administration or mediums such as aerosols and ophthalmic drops, and towards less accessible targets, current drug candidates face the serious drawback of invasive administration and the associated unwanted side effects. Irritation at the site of injection and high local concentration of oligonucleotide causing immunostimulation are common side effects. Systemic delivery of naked oligonucleotides is not better; the lack of organ-specific distribution and rapid renal clearance causes low cellular uptake efficiency. In fact, the recently FDA approved drug eteplirsen was administrated intravenously once a week at doses of 30 mg/kg and 50 mg/kg in clinical trials, resulting in 64% and 69%, respectively, of the drug being excreted in the urine after 24 hours.[121] Nonclinical results predicted these results as the drug was found in high concentrations in the kidneys and was predominantly excreted in the urine.[121] A forceful method such as hydrodynamic injection actually causes right-sided heart failure.[117] Two of the three FDA-approved nucleic acid drugs to-date, fomivirsen, a phosphorothioated DNA antisense molecule, and pegaptanib (Macugen™), a pegylated RNA aptamer with 2'-*O*-methyl and 2'-fluoro modifications, are injected directly into the eye. Pegaptanib works extracellularly by binding to a membrane protein, which does not require cellular membrane penetration, and its sales have severely declined due to the development of a more effective antibody treatment. Mipomersen, one of the other FDA-approved AONs, is injected subcutaneously once a week as 200 mg of sodium mipomersen in 1 mL of liquid.[122] It accumulates in the liver to treat hypercholesterolemia by targeting the mRNA for apolipoprotein B.

The use of cationic polymers complexed to nucleic acids, for example, is most severely impeded by their polydispersity and inefficiency, as it is difficult to produce them in a defined and uniform drug formulation.[123] In addition to the immune response that can be initiated by CPPs, there is much uncertainty with these delivery systems. The mechanism of internalization (e.g. receptor-mediated endocytosis) in relation to their sequence is still unclear as well as whether they are able to cause endosome or membrane destabilization to release the cargo. Ligands to cell surface receptors, including antibodies, can be used in conjugates to ensure receptor-mediated endocytosis but also cause receptor saturation after repeated use and the subsequent decrease in receptor expression by the cell.

1.4.2.2. Encapsulated Oligonucleotides

The modification, assembly, purification, and administration of biological vectors that are capable of evading the immune system through the engineered removal of their natural surface markers and/or the concomitant use of immunosuppressive agents is a worthwhile task, but will undoubtedly require a considerable amount of time for their development and success in clinical trials. Bacteriophages, for example, must also be modified to evade rapid degradation by the reticuloendothelial system (RES). This has been accomplished with lambda phage variants carrying mutations in D and E capsid proteins,[124] but the mechanism of this evasion is not understood and they have not been tested in humans.[100]

The use of positively charged lipids for the delivery of nucleic acids in lipoplexes has been limited to *in vitro* applications due to strong toxicity in different cell types (causing cell death, for example) as well as colloidal instability upon systemic administration. The positively charged lipids aggregate with negatively charged serum proteins and accumulate mostly in the liver, lungs, and spleen.[102] Their use *in vitro*, however, is commonplace on account of their high transfection efficiency.[123] PEG-derivatized lipids have been tested *in vivo* with expectations that circulation would increase through binding to serum albumin and that their hydrophilicity would form an aqueous shield to prevent labelling and recognition by the immune system.[102] However, repeated administrations caused a strong immune response that cleared the carrier rapidly from the body. Work has been done to formulate more stabilized versions (e.g. SNALPs) with different linker lengths to cause less immunogenicity, but the most successful candidates thus far take advantage of the fact that foreign bodies accumulate in the liver, and thus target liver-associated diseases. Unfortunately, the targeting of non-hepatic cells in late-stage clinical trials has been rare. Newer versions of SNALPs use ligands such as antibodies and CPPs instead of PEG to target specific tissues and to remove the impediment in cellular uptake that PEG causes. Immune response can occur with CPP use, as it does with complexed CPPs. Receptor saturation also occurs with the use of antibodies, and is thus an issue if CPPs are replaced with them.

1.4.3. A Prodrug Approach

An inactive, cell-penetrating form of a prodrug undergoes an enzymatically, chemically, or thermally triggered transformation into an active form before it elicits its pharmacological

effect. There is a multitude of small molecule prodrugs in use today. Tenofovir diisoproxyl is an antiretroviral nucleotide analogue that is first chemically cleaved or enzymatically cut by liver carboxylesterases into a metabolite that undergoes spontaneous decarboxylation and formaldehyde release before a final cleavage by a phosphodiesterase (Scheme 1.1A). Demasking is also not limited to hydrolysis of lipophilic groups; fospropofol is dephosphorylated ubiquitously throughout the body by alkaline phosphatases to release the general anesthetic propofol (Scheme 1.1B). Prodrug transformation is also not limited to demasking; prednisone is reduced in hepatocytes into prednisolone for its immunosuppressive properties (Scheme1.1C).

Given that dozens of potential siRNA therapeutics have failed and that there is no approved siRNA drug to date, basic research is needed to improve their cellular uptake for systemic delivery. Like the successfully applied AON mechanism, the siRNA mechanism is very well understood and has the potential to treat a multitude of diseases very efficiently. In fact, occasional vascular injury is observed with AONs in preclinical studies, but much less is seen with other types of therapeutic oligonucleotides such as siRNAs.[66] This in part due to the high doses administered for AON drugs. An siRNA prodrug (proRNA) would require a suitable biocleavable 'tag' that increases cellular delivery of the inactive siRNA prodrug. The proRNA would reveal canonical siRNA after its transformation inside the cell (Scheme 1.2). Biocleavable modifications are also attractive for the fact that, like many of the modifications outlined in section 1.3.4, they

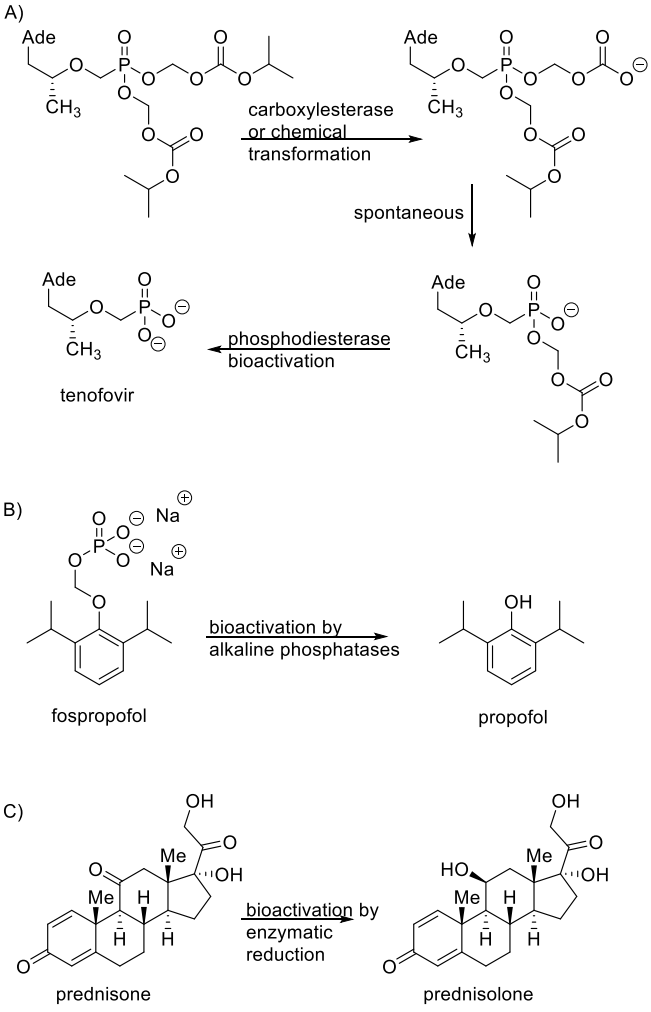

Scheme 1.1. There many examples of small molecule prodrugs in use today.

increase nuclease resistance, but unlike the previously mentioned modifications, their transient nature would allow siRNA modified even at the 5'-end of the antisense strand to possess high potency once inside the target cell.

Promoieties have been utilized on the phosphate groups and the 2'-hydroxyl groups of nucleic acids. However, the potential for undesirable side reactions, including their premature cleavage, during standard solid-phase synthesis conditions creates a need for careful planning of orthogonal protecting groups and reagents during oligonucleotide extension. Due to these complications, examples of pharmacologically significant mixed base prooligonucleotides are sparse.[125,126] The idea, however, is not new. Prior to the development of nucleic acid prodrugs, pronucleotides (protides) were developed as nucleotide 5'-phosphate prodrugs. These developments inspired researchers developing methods for the synthesis of the first oligonucleotide prodrugs ("prooligonucleotides") or "pro-ONs".[127]

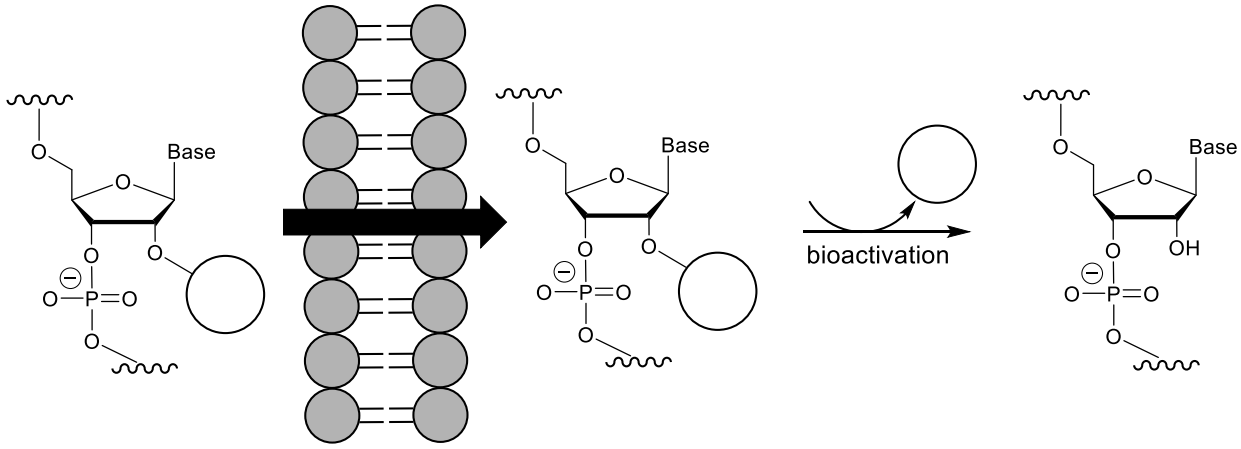

Scheme 1.2. The transformation of proRNA with 2'-promoiety modification occurs in the body after cellular entry takes place.

1.4.3.1. Biocleavable Internucleotide Tags ('Promoieties') for Nucleic Acid

In 1995, researchers developed an α-hydroxybenzylphosphonate triester that rearranged in basic buffer to a hydrolyzable benzylphosphotriester (Scheme 1.3).[128,129] This modification was inserted in thymidine dimers and poly-thymidine oligonucleotides using separate dimer building blocks for 3'-end insertion and for 5'-end insertion, which is a lengthy and tedious

methodology.[130,131] The modification exhibited 3'-exonuclease stability *in vitro*, however its use in a biologically significant pro-ON has not been demonstrated.

Agrawal and coworkers then synthesized oligodeoxynucleotides with S-acyloxyaryl phosphorothioates in 1997. The more hindered 2,6-dimethylphenylacyl substituent, compared to a *tert*-butyl one, evaded premature cleavage during nucleobase deprotection and support linker cleavage with mild potassium carbonate in methanol. The mixed-nucleobase pro-ON was then a substrate of pig liver esterase and chymotrypsin,[132] but no demonstration of gene regulation has thus far been demonstrated. Concurrently, a solid-phase synthetic protocol for incorporating a variation of the S-acyloxyaryl promoiety, the S-acetyl-2-thioethyl (SATE) modification (Scheme 1.4) developed by Imbach,[133] was used.[134] Poly-thymidine thioesters were shown to have stability in the presence of phosphodiesterases and in serum and gastric juice, while they were transformed to phosphorothioates in cell extracts.

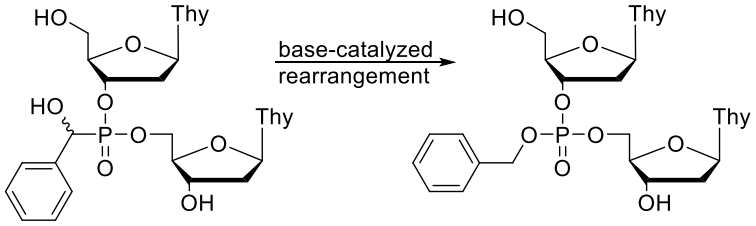

Scheme 1.3. An α-hydroxybenzylphosphonate triester rearranges into a hydrolysable benzylphosphotriester promoiety. Adapted from reference 128.

Other reversible internucleotide modifications to poly-thymidine oligonucleotides such as the 2-(*N*-formyl-*N*-methyl) aminoethyl phosphate protecting group and the phosphonoacetate protecting group have been characterized as possible pro-ON candidates based on their thermal activation in buffered water or projected susceptibility to esterases while showing stability to exonucleases, respectively.[135,71] However, their application to pro-ONs was not made.

Quite recently, Dowdy and coworkers implemented mild deprotection conditions for mixed-base short interfering siRNAs with up to nineteen SATE-modified phosphotriesters and either a GalNAc molecule at the 5'-terminal or up to four Tat peptides conjugated to the SATE phosphotriesters.[126] These conjugates acted as functional siRNA after intracellular cleavage of the triester linkers. This represents the first complete example of a pro-ON exhibiting unassisted

uptake (i.e. no lipids added) and causing gene downregulation. This 'autotransfection', however, was only achieved after promoiety conjugation to GalNAc or Tat; i.e. the phosphate promoieties alone were not sufficient to promote uptake.

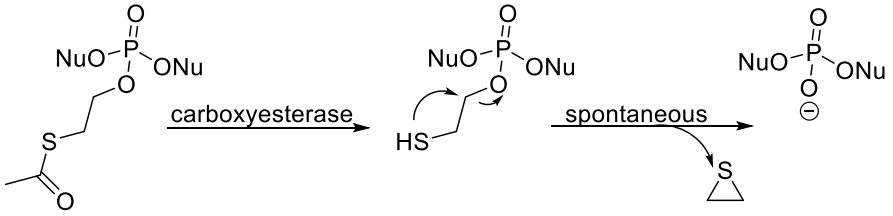

Scheme 1.4. The SATE modification decomposes into the active phosphodiester after enzymatic transformation. Adapted from reference 133.

1.4.3.2. Promoieties in the Sugars of Nucleic Acids

Promoieties on the sugar of nucleic acids have been explored heavily by the Debart group in the form of 2'-*O*-acetalesters.[136,137,125] Independently, the Damha lab published on 2'-*O*-acetal levulinyl esters as a potential biocleavable promoiety.[138] The 2'-*O*-pivaloyloxymethyl ester in particular (Figure 1.17A) has been exploited for its resistance against nucleases, its susceptibility to esterases, and its relative ease of incorporation into the established solid phase synthetic cycle. As such, a method for its incorporation in proRNA of mixed base composition was developed using phosphoramidites. Synthesis of these building blocks were laborious requiring tboc protection on adenine and cytosine nucleobases and 4,4'-dimethoxytrityl (DMTr) protection on guanine. Each monomer had either *tert*-butyl-dimethoxysilyl (TBDMS) protection or pivaloyloxymethyl ester protection at the 2'-hydroxyl position. The RNA was grown on hydroquinone-*O*,*O*'-diacetic acid (Q-linker) solid support that was cleaved in tandem with the nucleobase protecting groups, providing proRNA.[125] That work in 2011 described the first synthesis of proRNA heteropolymers capable of gene silencing. However, these proRNA required either a standard transfecting agent (Lipofectamine^{TM}) or the application of an external field (electroporation).

Our lab independently published on the synthesis of poly-T strands containing up to three 2'-*O*-amino acid acetal ester moieties (AAEs). The three amino acids studied were lysine, alanine, and phenylalanine. The latter appeared to be the most compatible during isolation and

purification of the desired pro-ONs (Figure 1.17B).[139] The positive charge of the amino acid was expected to enhance both RNA target affinity (by neutralizing phosphate/phosphate interactions) and cellular uptake.

The Debart group built upon our work by synthesizing pro-ONs containing AAEs based on basic amines (e.g. guanidine). For instance, the 2'-*O*-(2-amino-methyl-2-ethyl)butyryloxymethyl modification (Figure 1.17C) when incorporated into 12-nt oligomers was shown to confer moderate nuclease resistance and cellular uptake at the expense of duplex destabilization.[140]

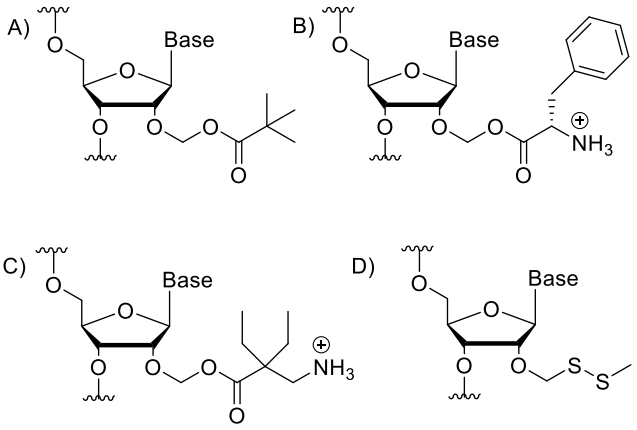

Figure 1.17. There are several 2'-promoiety modifications explored in the literature for use in oligonucleotides.

The Urata group designed the 2'-*O*-methyldithiomethyl (MDTM) modification in 2013 (Figure 1.17D) and assessed its gene silencing potential in siRNA containing 2'-*O*-MDTM-uridine in 2016.[141] The 2'-*O*-MDTM modification was introduced post-synthetically in one to four positions to allow for the synthesis of the RNA skeleton using phosphoramidites with standard protecting groups. siRNA with 2'-*O*-MDTM modifications was fully reduced by 10 mM glutathione, which mimics an intracellular reducing environment. Cellular transfection of the proRNA in a lipoplex resulted in siRNAs that had greater or equal potentcy than the unmodified siRNA, regardless of the modification position.[141] In 2016, the Debart group built upon the post-synthetic instalment of 2'-*O*-alkyldithiomethyl (RSSM) modifications by expanding the alkyl group to aromatic, aliphatic, negatively charged, positively charged, and hydroxylated moieties. Four of each modification was inserted into the sense strand of an siRNA

and evaluated for thermal stability, 3'-exonuclease stability, helix conformation, and RNA purity. They were also successfully reduced to unmodified strands with glutathione in buffer, displayed with retention time shifts in HPLC that correspond to the unmodified sense strand.[142]

1.5. Solid-Supported Synthesis of RNA

A proRNA approach is an attractive avenue for conferring targeted cellular delivery and cytoplasmic accumulation; however, it first requires a development of prodrug moieties that are amenable to solid-supported synthesis of nucleic acids.

1.5.1. Conventional Synthesis and Preparation of Oligonucleotides

The synthesis of oligonucleotides on functionalized controlled pore glass (CPG) solid support for their release under basic conditions has become standard protocol. The iterative cycle begins with removal of the DMTr protecting group from the support to reveal a hydroxyl group available for coupling to the first nucleotide. Standard exocyclic nucleobase protecting groups (PGs) are benzoyl (Bz) for adenosine (and sometimes cytosine), isobutyryl (iBu) for guanosine, and acetyl (Ac) for cytosine.

The cycle shown in Scheme 1.5 starts with the detritylation of the first nucleotide bound to the solid support. This is accomplished with 3% trichloroacetic acid (TCA) in dichloromethane (CH_2Cl_2) and washing of the support with acetonitrile. The free 5'-OH group is then coupled with a nucleoside 3'-*O*-phosphoramidite in the presence of a weak organic acid (e.g. 1*H*-tetrazole or 4,5-dicyanoimidazole) to produce the first phosphite triester internucleotide linkage (step 2). After washing the support with more acetonitrile, any unreacted 5'-hydroxyls are capped with acetic anhydride/*N*-methyl-imidazole (NMI) to prevent the growth of shorter (failure) sequences (step 3). The P(III) species of the newly-formed phosphite triester is then oxidized to a P(V) phosphate triester with the common oxidizing solution of iodine (I_2) in tetrahydrofuran (THF)/pyridine (py)/H_2O (step 4). Sulfurization of the phosphite to a phosphorothioate can be done by replacing the oxidation solution with a sulfurization solution such as 3*H*-1,2-benzodithiol-3-one 1,1-dioxide (Beaucage's Reagent) in acetonitrile (MeCN), xanthane hydride in py/MeCN, or ((dimethylamino-methylidene)amino)-3*H*-1,2,4-dithiazaoline-3-thione (DDTT) in MeCN.

The cycle is repeated until the desired number of nucleotides is coupled. The cyanoethyl group is commonly used to protect the phosphate moieties, whereas the nucleobases are protected with acyl or aryl protecting groups. This cycle has been used to make oligonucleotides of up to 200 units. Synthesis of longer chains is limited by the accumulation of side reactions (e.g. depurination) and failure sequences as stepwise coupling yields are rarely quantitative (typically 98-99% for DNA monomers and 96-98% for RNA monomers).

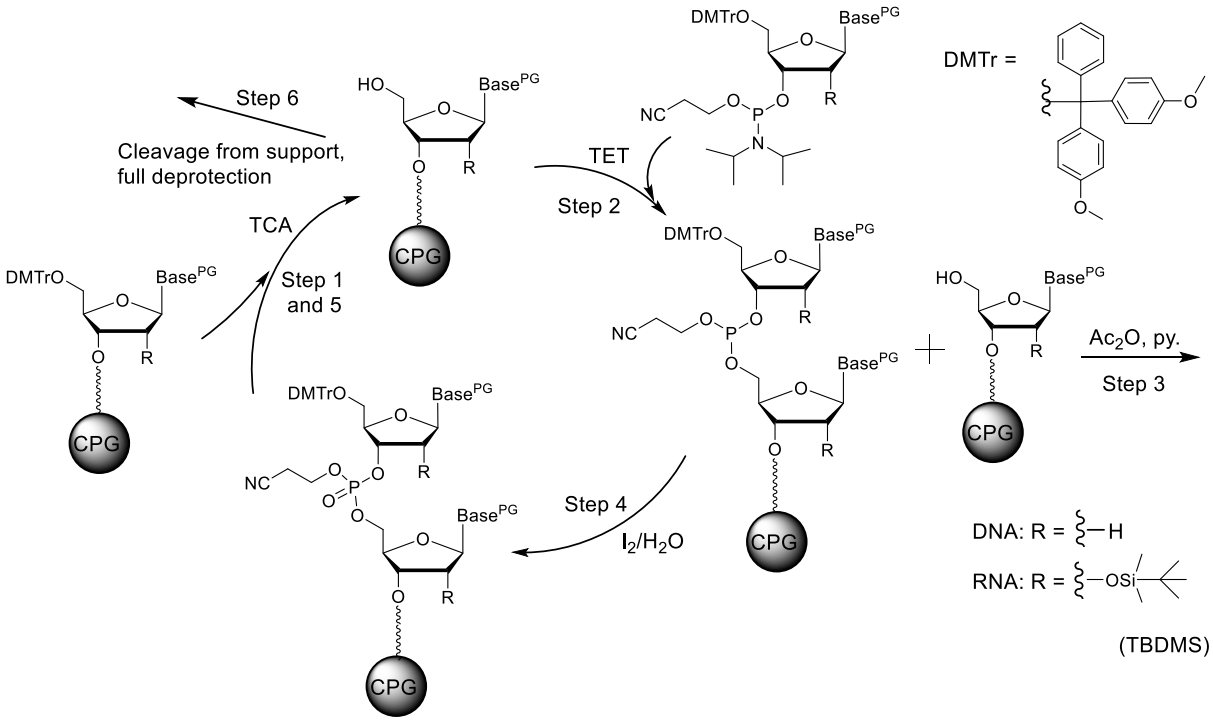

Scheme 1.5. The solid-phase DNA and RNA synthesis cycle is multi-step. In the case of RNA, the 2'-OH group is commonly protected with the *tert*-butyldimethysilyl group (TBDMS), requiring an extra step (fluoride treatment) during deprotection of the RNA chain.

To obtain the desired oligonucleotide, solid support is treated with an aqueous amine (step 6). This step serves several purposes. First, it cleaves the oligomer from the support, which is commonly attached *via* a 'universal' UnyLinker^{TM} as shown in Scheme 1.6.[143] The key feature of this linker is an acetyl ester that is *syn*-planar to the 3'-terminal phosphate. Upon treatment with 40% ammonia in water/ethanol (65^{o}C, 10 min.), the unmasked hydroxyl group attacks the phosphorous center cleaving the oligonucleotide from the solid support.[143] This step also cleaves the phosphate cyanoethyl groups and the nucleobase acyl groups. The use of

methylamine ($MeNH_2$) must be avoided when cytosine is protected with a benzoyl (Bz) group to avoid transamination.[144] Normally, deprotection of *N*-isobutyryl guanine is the rate limiting step to fully deprotect the oligonucleotide chains.[144] With the cleaved oligonucleotide now dissolved in aqueous basic solution, it can be separated from the support and lyophilized to a dry pellet. Deprotection of RNA requires two extra steps, namely fluoride treatment to cleave the 2'-silyl ethers (TBDMS) and precipitating out the oligomer in a solution of 3 M sodium acetate.

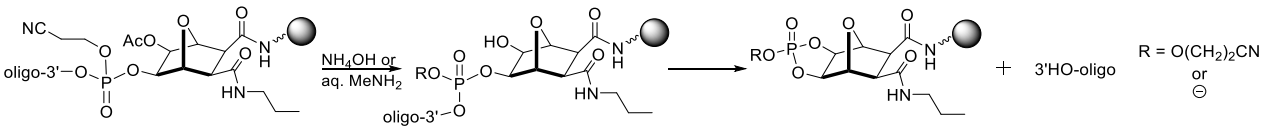

Scheme 1.6. Release of oligonucleotides from the universal UnyLinker™ under basic conditions. Adapted from reference 143.

1.5.2. Nucleobase Protecting Groups for Base-Sensitive Oligonucleotides

Under acidic conditions, ribonucleosides are more resistant to glyosidic bond cleavage relative to deoxynucleosides, owing to the destabilization of the oxycarbenium intermediate. As such, the oxycarbenium intermediate of deoxyadenosine shown in Scheme 1.7 is more stable than that of riboadenosine. The purine nucleobases (adenine and guanine) are particularly vulnerable to *N*-glycosidic bond cleavage.[145] For example, *N*6-acyl-2'-deoxyadenosine bound to solid support undergoes depurination readily in 3% trichloroacetic acid in dichloromethane after 1 hour.[146] While protonation at either N1 or N7 is possible, protonation at N7 is favoured for N6-acyl adenine derivatives as the acyl group decreases the basicity of the N6-C6=N1 amidine group.[145]

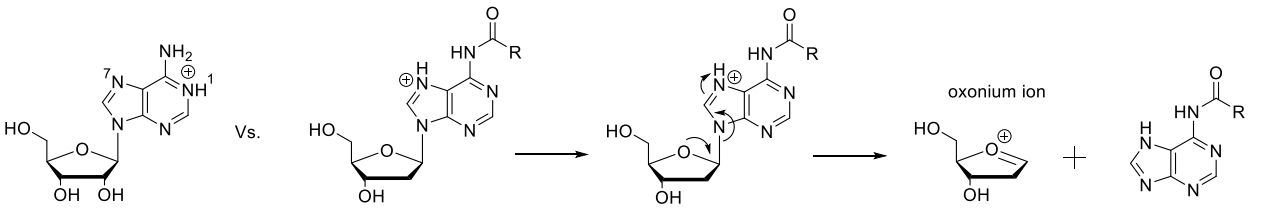

Scheme 1.7. The depurination of 2'-deoxyadenosine (dA) through an oxonium ion is encouraged by the N-acylation of the exocyclic amine at C6 of the purine ring.

The multiple exposures to acidic conditions during oligonucleotide synthesis fuelled interest in the development of alternative protecting groups for the nucleobases. There now exists a vast repertoire of protecting groups that are cleaved quickly under milder conditions (reviewed by Beaucage *et al.*),[145] many of which have found utility in the deprotection of oligonucleotides containing sensitive functionalities such as those used in the development of nucleic acid prodrugs.

Amidine-protected dA (Figure 1.18A) is more resistant to depurination (e.g. relative to N^6-benzoyl dA), as N1 protonation is favoured over N7 protonation.[147] This type of protecting group is suitable for guanine[148,149,138] and cytosine[148] nucleosides and is cleavable by NH_4OH[148,149,150] as well as hydrazine hydrate ($NH_2NH_2{\cdot}H_2O$) in py/acetic acid (AcOH) buffer.[151,138]

The 4,4',4"-tris-(benzoyloxy)trityl (TBTr) group (Figure 1.18B) has been used for protection of the exocyclic amine of all three canonical nucleobases as it also decreases the rate of glycosidic bond cleavage relative to N^6-Bz dA.[152] It is removed with 2 M sodium hydroxide or N^1,N^1,N^3,N^3-tetramethylguanidinium 2-pyridinecarboxaldoximate.[152] However, *N*-TBTr protected purines (dG) couple poorly during solid-phase synthesis, likely due to steric hindrance.[145]

Fluoroenylmethoxycarbonyl (FMOC) protection (Figure 1.18C) affords protected nucleosides that are more resistant to depurination relative to N6-Bz dA.[145] It is removed from the nucleobase with NH_4OH/py,[153] non-nucleophilic triethylamine (NEt_3),[153] or oximate ions.[154,155] Another avenue for reducing the depurination rate of N6-acylated deoxyadenosine is replacing the 5'-hydroxyl protecting group DMTr with the base sensitive FMOC group and thus entirely eliminating the need for acid mediated deprotection steps.[156] Non-nucleophilic bases such as NEt_3 or 1,8-diazabicyclo[5.4.0]undec-7-ene (DBU) can be used to deblock the FMOC in this case,[157] but larger oligonucleotides result in truncated sequences and/or side products that are most likely due to reactive dibenzofulvene generated during deprotection.[158] Morpholine and piperidine, on the other hand, reversibly added to this byproduct to significantly improve yield.[159]

While it only mildly slows down depurination rates, the phenoxyacetyl group (Figure 1.18D) has become widely used given its fast deprotection rates at room temperature (NH_4OH, 1 min, or potassium carbonate in methanol, 44 min).[144] This is particularly important when deprotecting RNA oligomers as prolonged ammonia treatment can lead to premature cleavage of the 2'-TBDMS groups followed by fragmentation of the RNA chain.[145]

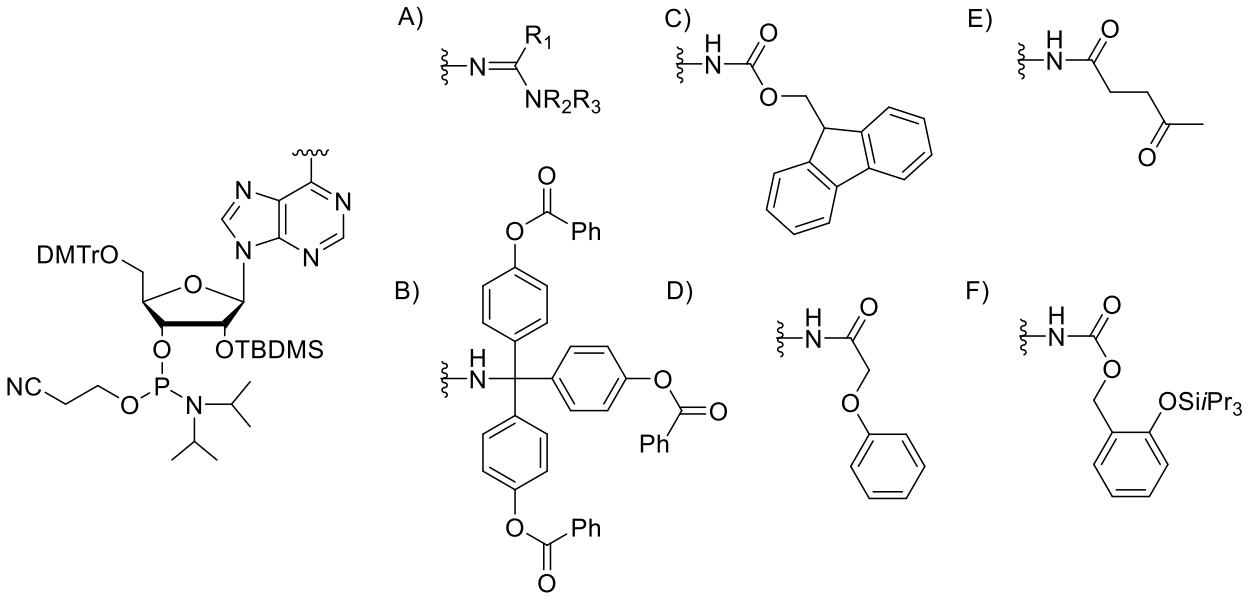

Figure 1.18. Structure of protecting groups used on the exocyclic amine of nucleoside phosphoramidites for the synthesis of base sensitive oligonucleotides (a dA monomer is shown as an example).

Some other alternative protecting groups for the exocyclic amines are levulinyl (Figure 1.18E) and silicon-containing groups (Figure1.18F). The levulinyl group can be cleaved with $NH_2NH_2{\cdot}H_2O$ in py/AcOH – conditions that do not cleave the oligonucleotide from the solid support.[160] The Damha lab has used the group for nucleobase and 2'-protection of riboadenosine and ribocytidine nucleotides to prepare oligonucleotides and achieve full deprotection by hydrazinolysis at room temperature.[161] The 2-(*tert*-butyldiphenylsilyloxymethyl)benzoyl (SiOMB)[162,163] and 2-(triisopropylsilyloxy)benzyloxycarbonyl (tboc)[125] groups are both cleaved from oligonucleotides by fluoride ions. The protecting groups discussed in this section are all worthy candidates for proRNA synthesis, a topic discussed in Chapter 5 of this thesis.

1.6. Thesis Objectives

Cellular delivery of therapeutic ONs remains a pivotal issue that must be overcome. Unmodified siRNA in particular is highly hydrophilic and susceptible to nuclease degradation. The hydrophobicity, negative charge, and susceptibility to nuclease degradation of unmodified siRNA pose challenges for their delivery and uptake into cells, particularly following systemic administration. All chapters of this thesis concern the synthesis, evaluation, and/or characterization of siRNA modified with novel moieties selected for improving cellular uptake. We will focus our work on the derivatization of the 2'-hydroxyl group of the ribose sugar in an attempt to enhance delivery of siRNA into cells. More specifically, we will append amino acids *via* 2'-*O*-acetal ester (AAE) moieties designed to be positively charged under physiological conditions.

1.6.1. Chapter 2: Development of Amino Acid Acetal Esters as Promoieties of RNA Prodrugs

Nucleosides containing L-alanine, L-lysine, L-proline, and L-phenylalanine acetal esters will be synthesized and incorporated into poly-thymidine ONs. The ONs will be synthesized on photocleavable solid support recently developed in our laboratory.[164] These studies will expand previous work conducted on ONs containing the 2'-*O*-acetal levulinyl ester (ALE) promoieties.[138] These studies demonstrated that 2'-*O*-ALE groups are prematurely removed during synthesis and purification of the ONs. Thus, the first objective will be to assess the chemical stability of the 2'-*O*-AAE moieties to ON solid-phase synthesis, purification, and conditions that mimic the physiological state. The chemical reactivity and physical properties of 2'-*O*-AAE ONs will be useful for designing potent siRNA prodrugs (proRNA). Thus another objective is the development of a protocol for the synthesis of poly-thymidine ONs with completely intact 2'-*O*-AAEs.

1.6.2. Chapter 3: Fluorometric Assay for Cellular Uptake of Amino Acid-siRNA Conjugates

Chapter 3 examines proRNAs containing 2'-*N*-acyl-amino acid modifications [2'-$NHCOCH(R)NH_3(+)$], which are expected to be significantly more stable than 2'-*O*-AAEs. This requires the synthesis of nucleoside amino acid conjugates and their incorporation into siRNAs.

The conjugates (containing fluorophores attached at the 5'/3'-termini) will be assessed for their ability to increase the cellular uptake of the siRNA *via* flow cytometric fluorescence resonance energy transfer (FCET). Uptake will be assessed in human glial cells and other cell lines. Another objective is the design of siRNA conjugates that are taken up by cells without transfection.

1.6.3. Chapter 4: Gene Silencing Properties of Amino Acid-siRNA Conjugates

Chapter 4 examines the ability of siRNA containing 2'-*N*-acyl-amino acid modifications to knockdown two endogenous genes; namely, downregulated in renal cell carcinoma (*drr*) and B-cell lymphoma 2 (*bcl-2*). The effect of 2'-*N*-acyl-amino acid moieties on the thermal melting temperature, uptake, lipophilicity, and nuclease stability of the siRNAs will also be assessed.

1.6.4. Chapter 5: Towards a Method for the Synthesis of proRNA

Chapter 5 describes preliminary studies aimed at the solid phase synthesis of 2'-*O*-AAE modified proRNAs of mixed base composition. Such syntheses are a tall order as they require orthogonal deprotection of the phosphate linkages and nucleobases, and release of the RNA from the solid support under conditions that do not cleave the 2'-*O*-AAE moieties. Towards this goal, we assess *N*-FMOC protection of the nucleobases and a photocleavable solid support. In principle, the *N*-FMOC groups can be cleaved with mild base under anhydrous conditions, while the RNA can be photocleaved from the solid support under conditions that minimizes cleavage of the 2'-*O*-AAE moieties.

1.7. References

1. Crick, F. H. C., On Protein Synthesis. *Symp. Soc. Exp. Biol.* **1956,** *XII*, 139-163.

2. Crick, F., Central dogma of molecular biology. *Nature* **1970,** *227* (5258), 561-563.

3. Cech, T. R., The Ribosome Is a Ribozyme. *Science* **2000,** *289* (5481), 878-879.

4. Temin, H., The DNA provirus hypothesis. *Science* **1976,** *192* (4244), 1075-1080.

5. Altona, C.; Sundaralingam, M., Conformational analysis of the sugar ring in nucleosides and nucleotides. New description using the concept of pseudorotation. *J. Am. Chem. Soc.* **1972,** *94* (23), 8205-8212.

6. Deleavey, G. F.; Damha, M. J., Designing chemically modified oligonucleotides for targeted gene silencing. *Chem. Biol.* **2012,** *19* (8), 937-954.

7. Davies, D. B., Conformations of nucleosides and nucleotides. *Prog. Nucl. Magn. Reson. Spectrosc.* **1978,** *12* (3), 135-225.

8. Altona, C.; Sundaralingam, M., Conformational analysis of the sugar ring in nucleosides and nucleotides. Improved method for the interpretation of proton magnetic resonance coupling constants. *J. Am. Chem. Soc.* **1973,** *95* (7), 2333-2344.

9. Watson, J. D.; Crick, F. H., Molecular structure of nucleic acids; a structure for deoxyribose nucleic acid. *Nature* **1953,** *171* (4356), 737-738.

10. Milman, G.; Langridge, R.; Chamberlin, M. J., The structure of a DNA-RNA hybrid. *Proc. Natl. Acad. Sci. U.S.A.* **1967,** *57* (6), 1804-1810.

11. Blackburn, M. G.; Gait, M. J.; Loakes, D.; Williams, D. M., *Nucleic Acids in Chemistry and Biology*. 3 ed.; RSC Publishing: Cambridge, UK, 2006.

12. Dahm, R., Discovering DNA: Friedrich Miescher and the early years of nucleic acid research. *Human Genetics* **2008,** *122* (6), 565-581.

13. Hershey, A. D.; Chase, M., Independent functions of viral protein and nucleic acid in growth of bacteriophage. *J. Gen. Physiol.* **1952,** *36* (1), 39-56.

14. Brachet, J., Ribonucleic Acids and the Synthesis of Cellular Proteins. *Nature* **1960,** *186* (4720), 194-199.

15. Jacob, F.; Monod, J., Genetic regulatory mechanisms in the synthesis of proteins. *J. Mol. Biol.* **1961,** *3*, 318-356.

16. Brenner, S.; Jacob, F.; Meselson, M., An Unstable Intermediate Carrying Information from Genes to Ribosomes for Protein Synthesis. *Nature* **1961,** *190* (4776), 576-581.

17. Holley, R. W.; Apgar, J.; Everett, G. A.; Madison, J. T.; Marquisee, M.; Merrill, S. H.; Penswick, J. R.; Zamir, A., Structure of a Ribonucleic Acid. *Science* **1965,** *147* (3664), 1462-1465.

18. Nelson, D. L. C., M. M., *Lehninger Principles of Biochemistry*. 4th ed.; W.H. Freeman and Company: New York, NY, 2005.

19. Huang, Y.; Zhang, J. L.; Yu, X. L.; Xu, T. S.; Wang, Z. B.; Cheng, X. C., Molecular functions of small regulatory noncoding RNA. *Biochemistry (Moscow)* **2013,** *78* (3), 221-230.

20. Gagnon, K. T.; Corey, D. R., Argonaute and the nuclear RNAs: new pathways for RNA-mediated control of gene expression. *Nucleic Acid Ther.* **2012,** *22* (1), 3-16.

21. Bogdanove, A. J.; Voytas, D. F., TAL Effectors: Customizable Proteins for DNA Targeting. *Science* **2011,** *333* (6051), 1843-1846.

22. Jinek, M.; Chylinski, K.; Fonfara, I.; Hauer, M.; Doudna, J. A.; Charpentier, E., A Programmable Dual-RNA–Guided DNA Endonuclease in Adaptive Bacterial Immunity. *Science* **2012,** *337* (6096), 816-821.

23. Jinek, M.; Doudna, J. A., A three-dimensional view of the molecular machinery of RNA interference. *Nature* **2009,** *457* (7228), 405-412.

24. Mangos, M. M.; Min, K. L.; Viazovkina, E.; Galarneau, A.; Elzagheid, M. I.; Parniak, M. A.; Damha, M. J., Efficient RNase H-directed cleavage of RNA promoted by antisense DNA or 2'F-ANA constructs containing acyclic nucleotide inserts. *J. Am. Chem. Soc.* **2003,** *125* (3), 654-661.

25. Summerton, J., Morpholino antisense oligomers: the case for an RNase H-independent structural type. *Biochim. Biophys. Acta, Gene Struct. Express.* **1999,** *1489* (1), 141-158.

26. Zamecnik, P. C.; Stephenson, M. L., Inhibition of Rous sarcoma virus replication and cell transformation by a specific oligodeoxynucleotide. *Proc. Natl. Acad. Sci. U.S.A.* **1978,** *75* (1), 280-284.

27. Stephenson, M. L.; Zamecnik, P. C., Inhibition of Rous sarcoma viral RNA translation by a specific oligodeoxyribonucleotide. *Proc. Natl. Acad. Sci.* **1978,** *75* (1), 285-288.

28. Summerton, J. E., Morpholino, siRNA, and S-DNA Compared: Impact of Structure and Mechanism of Action on Off-Target Effects and Sequence Specificity. *Curr. Top. Med. Chem.* **2007,** *7* (7), 651-660.

29. Bennett, C. F.; Swayze, E. E., RNA targeting therapeutics: molecular mechanisms of antisense oligonucleotides as a therapeutic platform. *Annu. Rev. Pharmacol. Toxicol.* **2010,** *50*, 259-293.

30. van der Krol, A. R.; Mur, L. A.; Beld, M.; Mol, J. N.; Stuitje, A. R., Flavonoid genes in petunia: addition of a limited number of gene copies may lead to a suppression of gene expression. *Plant Cell* **1990,** *2* (4), 291-299.

31. Baulcombe, D. C., RNA as a target and an initiator of post-transcriptional gene silencing in transgenic plants. *Plant Mol. Biol.* **1996,** *32* (1-2), 79-88.

32. Metzlaff, M.; O'Dell, M.; Cluster, P. D.; Flavell, R. B., RNA-Mediated RNA Degradation and Chalcone Synthase A Silencing in Petunia. *Cell* **1997,** *88* (6), 845-854.

33. Voinnet, O.; Baulcombe, D. C., Systemic signalling in gene silencing. *Nature* **1997,** *389* (6651), 553.

34. Fire, A.; Xu, S.; Montgomery, M. K.; Kostas, S. A.; Driver, S. E.; Mello, C. C., Potent and specific genetic interference by double-stranded RNA in Caenorhabditis elegans. *Nature* **1998,** *391* (6669), 806-811.

35. Elbashir, S. M.; Harborth, J.; Lendeckel, W.; Yalcin, A.; Weber, K.; Tuschl, T., Duplexes of 21-nucleotide RNAs mediate RNA interference in cultured mammalian cells. *Nature* **2001,** *411* (6836), 494-498.

36. Engels, J. W., Gene silencing by chemically modified siRNAs. *New Biotechnol.* **2013,** *30* (3), 302-307.

37. Schwarz, D. S.; Hutvágner, G.; Haley, B.; Zamore, P. D., Evidence that siRNAs Function as Guides, Not Primers, in the Drosophila and Human RNAi Pathways. *Mol. Cell* **2002,** *10* (3), 537-548.

38. Frank, F.; Sonenberg, N.; Nagar, B., Structural basis for 5'-nucleotide base-specific recognition of guide RNA by human AGO2. *Nature* **2010,** *465* (7299), 818-822.

39. Heidel, J. D.; Hu, S.; Liu, X. F.; Triche, T. J.; Davis, M. E., Lack of interferon response in animals to naked siRNAs. *Nat. Biotechnol.* **2004,** *22* (12), 1579-1582.

40. Torrence, P. F.; De Clercq, E., Inducers and induction of interferons. *Pharmacol. Ther. Part A* **1977,** *2* (1), 1-88.

41. Whitehead, K. A.; Dahlman, J. E.; Langer, R. S.; Anderson, D. G., Silencing or stimulation? siRNA delivery and the immune system. *Annu. Rev. Chem. Biomol. Eng.* **2011,** *2*, 77-96.

42. Takeda, K.; Akira, S., Toll-like receptors in innate immunity. *Int. Immunol.* **2005,** *17* (1), 1-14.

43. Judge, A.; MacLachlan, I., Overcoming the Innate Immune Response to Small Interfering RNA. *Hum. Gene Ther.* **2008,** *19* (2), 111-124.

44. Castanotto, D.; Rossi, J. J., The promises and pitfalls of RNA-interference-based therapeutics. *Nature* **2009,** *457* (7228), 426-433.

45. Zuker, M., Mfold web server for nucleic acid folding and hybridization prediction. *Nucleic Acids Res.* **2003,** *31* (13), 3406-3415.

46. Mittal, V., Improving the efficiency of RNA interference in mammals. *Nat. Rev. Genet.* **2004,** *5* (5), 355-365.

47. Krutzfeldt, J.; Rajewsky, N.; Braich, R.; Rajeev, K. G.; Tuschl, T.; Manoharan, M.; Stoffel, M., Silencing of microRNAs in vivo with 'antagomirs'. *Nature* **2005,** *438* (7068), 685-689.

48. Lennox, K. A.; Behlke, M. A., Chemical modification and design of anti-miRNA oligonucleotides. *Gene Ther.* **2011,** *18* (12), 1111-1120.

49. Heasman, J.; Kofron, M.; Wylie, C., βCatenin Signaling Activity Dissected in the Early Xenopus Embryo: A Novel Antisense Approach. *Dev. Biol.* **2000,** *222* (1), 124-134.

50. Ohrt, T.; Mutze, J.; Staroske, W.; Weinmann, L.; Hock, J.; Crell, K.; Meister, G.; Schwille, P., Fluorescence correlation spectroscopy and fluorescence cross-correlation spectroscopy reveal the cytoplasmic origination of loaded nuclear RISC in vivo in human cells. *Nucleic Acids Res.* **2008,** *36* (20), 6439-6449.

51. Robb, G. B.; Brown, K. M.; Khurana, J.; Rana, T. M., Specific and potent RNAi in the nucleus of human cells. *Nat. Struct. Mol. Biol.* **2005,** *12* (2), 133-137.

52. Onodera, Y.; Haag, J. R.; Ream, T.; Nunes, P. C.; Pontes, O.; Pikaard, C. S., Plant Nuclear RNA Polymerase IV Mediates siRNA and DNA Methylation-Dependent Heterochromatin Formation. *Cell* **2005,** *120* (5), 613-622.

53. Yoshikawa, M.; Peragine, A.; Park, M. Y.; Poethig, R. S., A pathway for the biogenesis of trans-acting siRNAs in Arabidopsis. *Genes Dev.* **2005,** *19* (18), 2164-2175.

54. Klattenhoff, C.; Theurkauf, W., Biogenesis and germline functions of piRNAs. *Development (Cambridge, England)* **2008,** *135* (1), 3-9.

55. Kirino, Y.; Mourelatos, Z., Mouse Piwi-interacting RNAs are 2[prime]-O-methylated at their 3[prime] termini. *Nat. Struct. Mol. Biol.* **2007,** *14* (4), 347-348.

56. Aravin, A. A.; Sachidanandam, R.; Bourc'his, D.; Schaefer, C.; Pezic, D.; Toth, K. F.; Bestor, T.; Hannon, G. J., A piRNA Pathway Primed by Individual Transposons Is Linked to De Novo DNA Methylation in Mice. *Mol. Cell* **2008,** *31* (6), 785-799.

57. Eckstein, F., Nucleoside Phosphorothioates. *J. Am. Chem. Soc.* **1966,** *88* (18), 4292-4294.

58. Eckstein, F., Phosphorothioates, essential components of therapeutic oligonucleotides. *Nucleic Acid Ther.* **2014,** *24* (6), 374-387.

59. Stec, W. J.; Grajkowski, A.; Koziolkiewicz, M.; Uznanski, B., Novel route to oligo(deoxyribonucleoside phosphorothioates). Stereocontrolled synthesis of P-chiral oligo(deoxyribonucleoside phosphorothioates). *Nucleic Acids Res.* **1991,** *19* (21), 5883-5888.

60. Koziolkiewicz, M.; Krakowiak, A.; Kwinkowski, M.; Boczkowska, M.; Stec, W. J., Stereodifferentiation--the effect of P chirality of oligo(nucleoside phosphorothioates) on the activity of bacterial RNase H. *Nucleic Acids Res.* **1995,** *23* (24), 5000-5005.

61. Krieg, A. M.; Guga, P.; Stec, W., P-Chirality-Dependent Immune Activation by Phosphorothioate CpG Oligodeoxynucleotides. *Oligonucleotides* **2003,** *13* (6), 491-499.

62. Stein, C. A.; Hansen, J. B.; Lai, J.; Wu, S.; Voskresenskiy, A.; Høg, A.; Worm, J.; Hedtjärn, M.; Souleimanian, N.; Miller, P.; Soifer, H. S.; Castanotto, D.; Benimetskaya, L.; Ørum, H.; Koch, T., Efficient gene silencing by delivery of locked nucleic acid antisense oligonucleotides, unassisted by transfection reagents. *Nucleic Acids Res.* **2010,** *38* (1), e3-e3.

63. Monteith, D. K.; Horner, M. J.; Gillett, N. A.; Butler, M.; Geary, R.; Burckin, T.; Ushiro-Watanabe, T.; Levin, A. A., Evaluation of the renal effects of an antisense phosphorothioate oligodeoxynucleotide in monkeys. *Toxicol. Pathol.* **1999,** *27* (3), 307-317.

64. Frazier, K. S.; Sobry, C.; Derr, V.; Adams, M. J.; Besten, C. D.; De Kimpe, S.; Francis, I.; Gales, T. L.; Haworth, R.; Maguire, S. R.; Mirabile, R. C.; Mullins, D.; Palate, B.; Doorten, Y. P.; Ridings, J. E.; Scicchitano, M. S.; Silvano, J.; Woodfine, J., Species-specific inflammatory responses as a primary component for the development of glomerular lesions in mice and monkeys following chronic administration of a second-generation antisense oligonucleotide. *Toxicol. Pathol.* **2014,** *42* (5), 923-935.

65. Frazier, K. S., Antisense oligonucleotide therapies: the promise and the challenges from a toxicologic pathologist's perspective. *Toxicol. Pathol.* **2015,** *43* (1), 78-89.

66. Engelhardt, J. A.; Fant, P.; Guionaud, S.; Henry, S. P.; Leach, M. W.; Louden, C.; Scicchitano, M. S.; Weaver, J. L.; Zabka, T. S.; Frazier, K. S., Scientific and Regulatory Policy Committee Points-to-consider Paper*: Drug-induced Vascular Injury Associated with Nonsmall Molecule Therapeutics in Preclinical Development: Part 2. Antisense Oligonucleotides. *Toxicol. Pathol.* **2015,** *43* (7), 935-944.

67. Detzer, A.; Overhoff, M.; Mescalchin, A.; Rompf, M.; Sczakiel, G., Phosphorothioate-stimulated cellular uptake of siRNA: a cell culture model for mechanistic studies. *Curr. Pharm. Des.* **2008,** *14* (34), 3666-3673.

68. Amarzguioui, M.; Holen, T.; Babaie, E.; Prydz, H., Tolerance for mutations and chemical modifications in a siRNA. *Nucleic Acids Res.* **2003,** *31* (2), 589-595.

69. Braasch, D. A.; Jensen, S.; Liu, Y.; Kaur, K.; Arar, K.; White, M. A.; Corey, D. R., RNA Interference in Mammalian Cells by Chemically-Modified RNA. *Biochemistry* **2003,** *42* (26), 7967-7975.

70. Wu, S. Y.; Yang, X.; Gharpure, K. M.; Hatakeyama, H.; Egli, M.; McGuire, M. H.; Nagaraja, A. S.; Miyake, T. M.; Rupaimoole, R.; Pecot, C. V.; Taylor, M.; Pradeep, S.; Sierant, M.; Rodriguez-Aguayo, C.; Choi, H. J.; Previs, R. A.; Armaiz-Pena, G. N.; Huang, L.; Martinez,

C.; Hassell, T.; Ivan, C.; Sehgal, V.; Singhania, R.; Han, H.-D.; Su, C.; Kim, J. H.; Dalton, H. J.; Kovvali, C.; Keyomarsi, K.; McMillan, N. A. J.; Overwijk, W. W.; Liu, J.; Lee, J.-S.; Baggerly, K. A.; Lopez-Berestein, G.; Ram, P. T.; Nawrot, B.; Sood, A. K., 2′-OMe-phosphorodithioate-modified siRNAs show increased loading into the RISC complex and enhanced anti-tumour activity. *Nat. Commun.* **2014,** *5*.

71. Dellinger, D. J.; Sheehan, D. M.; Christensen, N. K.; Lindberg, J. G.; Caruthers, M. H., Solid-phase chemical synthesis of phosphonoacetate and thiophosphonoacetate oligodeoxynucleotides. *J. Am. Chem. Soc.* **2003,** *125* (4), 940-950.

72. Sheehan, D.; Lunstad, B.; Yamada, C. M.; Stell, B. G.; Caruthers, M. H.; Dellinger, D. J., Biochemical properties of phosphonoacetate and thiophosphonoacetate oligodeoxyribonucleotides. *Nucleic Acids Res.* **2003,** *31* (14), 4109-4118.

73. Threlfall, R. N.; Torres, A. G.; Krivenko, A.; Gait, M. J.; Caruthers, M. H., Synthesis and biological activity of phosphonoacetate- and thiophosphonoacetate-modified 2[prime or minute]-O-methyl oligoribonucleotides. *Org. Biomol. Chem.* **2012,** *10* (4), 746-754.

74. Mutisya, D.; Selvam, C.; Lunstad, B. D.; Pallan, P. S.; Haas, A.; Leake, D.; Egli, M.; Rozners, E., Amides are excellent mimics of phosphate internucleoside linkages and are well tolerated in short interfering RNAs. *Nucleic Acids Res.* **2014,** *42* (10), 6542-6551.

75. Bennett, C. F.; Swayze, E. E., RNA Targeting Therapeutics: Molecular Mechanisms of Antisense Oligonucleotides as a Therapeutic Platform. *Annu. Rev.Pharmacol. Toxicol.* **2010,** *50* (1), 259-293.

76. Potenza, N.; Moggio, L.; Milano, G.; Salvatore, V.; Di Blasio, B.; Russo, A.; Messere, A., RNA Interference in Mammalia Cells by RNA-3'-PNA Chimeras. *Int. J. Mol. Sci.* **2008,** *9* (3), 299-315.

77. Manoharan, M., 2'-carbohydrate modifications in antisense oligonucleotide therapy: importance of conformation, configuration and conjugation. *Biochim. Biophys. Acta* **1999,** *1489* (1), 117-130.

78. Kawasaki, A. M.; Casper, M. D.; Freier, S. M.; Lesnik, E. A.; Zounes, M. C.; Cummins, L. L.; Gonzalez, C.; Cook, P. D., Uniformly modified 2'-deoxy-2'-fluoro-phosphorothioate oligonucleotides as nuclease-resistant antisense compounds with high affinity and specificity for RNA targets. *J. Med. Chem.* **1993,** *36* (7), 831-841.

79. Wilds, C. J.; Damha, M. J., 2′-Deoxy-2′-fluoro-β-d-arabinonucleosides and oligonucleotides (2′F-ANA): synthesis and physicochemical studies. *Nucleic Acids Res.* **2000,** *28* (18), 3625-3635.

80. Kawai, G.; Yamamoto, Y.; Kamimura, T.; Masegi, T.; Sekine, M.; Hata, T.; Iimori, T.; Watanabe, T.; Miyazawa, T.; Yokoyama, S., Conformational rigidity of specific pyrimidine

residues in tRNA arises from posttranscriptional modifications that enhance steric interaction between the base and the 2'-hydroxyl group. *Biochemistry* **1992,** *31* (4), 1040-1046.

81. Ikeda, H.; Fernandez, R.; Barchi, J. J.; Huang, X.; Marquez, V. E.; Wilk, A., The effect of two antipodal fluorine-induced sugar puckers on the conformation and stability of the Dickerson-Drew dodecamer duplex [d(CGCGAATTCGCG)]2. *Nucleic Acids Res.* **1998,** *26* (9), 2237-2244.

82. Prakash, T. P.; Allerson, C. R.; Dande, P.; Vickers, T. A.; Sioufi, N.; Jarres, R.; Baker, B. F.; Swayze, E. E.; Griffey, R. H.; Bhat, B., Positional effect of chemical modifications on short interference RNA activity in mammalian cells. *J. Med. Chem.* **2005,** *48* (13), 4247-4253.

83. Czauderna, F.; Fechtner, M.; Dames, S.; Aygün, H.; Klippel, A.; Pronk, G. J.; Giese, K.; Kaufmann, J., Structural variations and stabilising modifications of synthetic siRNAs in mammalian cells. *Nucleic Acids Res.* **2003,** *31* (11), 2705-2716.

84. Kawasaki, A. M.; Casper, M. D.; Freier, S. M.; Lesnik, E. A.; Zounes, M. C.; Cummins, L. L.; Gonzalez, C.; Cook, P. D., Uniformly modified 2'-deoxy-2'-fluoro phosphorothioate oligonucleotides as nuclease-resistant antisense compounds with high affinity and specificity for RNA targets. *J. Med. Chem.* **1993,** *36* (7), 831-841.

85. Dowler, T.; Bergeron, D.; Tedeschi, A.-L.; Paquet, L.; Ferrari, N.; Damha, M. J., Improvements in siRNA properties mediated by 2′-deoxy-2′-fluoro-β-d-arabinonucleic acid (FANA). *Nucleic Acids Res.* **2006,** *34* (6), 1669-1675.

86. Deleavey, G. F.; Watts, J. K.; Alain, T.; Robert, F.; Kalota, A.; Aishwarya, V.; Pelletier, J.; Gewirtz, A. M.; Sonenberg, N.; Damha, M. J., Synergistic effects between analogs of DNA and RNA improve the potency of siRNA-mediated gene silencing. *Nucleic Acids Res.* **2010,** *38* (13), 4547-4557.

87. Matsugami, A.; Ohyama, T.; Inada, M.; Inoue, N.; Minakawa, N.; Matsuda, A.; Katahira, M., Unexpected A-form formation of 4'-thioDNA in solution, revealed by NMR, and the implications as to the mechanism of nuclease resistance. *Nucleic Acids Res.* **2008,** *36* (6), 1805-1812.

88. Koshkin, A. A.; Singh, S. K.; Nielsen, P.; Rajwanshi, V. K.; Kumar, R.; Meldgaard, M.; Olsen, C. E.; Wengel, J., LNA (Locked Nucleic Acids): Synthesis of the adenine, cytosine, guanine, 5-methylcytosine, thymine and uracil bicyclonucleoside monomers, oligomerisation, and unprecedented nucleic acid recognition. *Tetrahedron* **1998,** *54* (14), 3607-3630.

89. Vaish, N.; Chen, F.; Seth, S.; Fosnaugh, K.; Liu, Y.; Adami, R.; Brown, T.; Chen, Y.; Harvie, P.; Johns, R.; Severson, G.; Granger, B.; Charmley, P.; Houston, M.; Templin, M. V.; Polisky, B., Improved specificity of gene silencing by siRNAs containing unlocked nucleobase analogs. *Nucleic Acids Res.* **2011,** *39* (5), 1823-1832.

90. Wolfrum, C.; Shi, S.; Jayaprakash, K. N.; Jayaraman, M.; Wang, G.; Pandey, R. K.; Rajeev, K. G.; Nakayama, T.; Charrise, K.; Ndungo, E. M.; Zimmermann, T.; Koteliansky, V.; Manoharan, M.; Stoffel, M., Mechanisms and optimization of in vivo delivery of lipophilic siRNAs. *Nat. Biotechnol.* **2007,** *25* (10), 1149-1157.

91. Osborn, M. F.; Alterman, J. F.; Nikan, M.; Cao, H.; Didiot, M. C.; Hassler, M. R.; Coles, A. H.; Khvorova, A., Guanabenz (Wytensin™) selectively enhances uptake and efficacy of hydrophobically modified siRNAs. *Nucleic Acids Res.* **2015,** *43* (18), 8664-8672.

92. Byrne, M.; Tzekov, R.; Wang, Y.; Rodgers, A.; Cardia, J.; Ford, G.; Holton, K.; Pandarinathan, L.; Lapierre, J.; Stanney, W.; Bulock, K.; Shaw, S.; Libertine, L.; Fettes, K.; Khvorova, A.; Kaushal, S.; Pavco, P., Novel hydrophobically modified asymmetric RNAi compounds (sd-rxRNA) demonstrate robust efficacy in the eye. *J. Ocul. Pharm. Ther.* **2013,** *29* (10), 855-864.

93. Uno, Y.; Piao, W.; Miyata, K.; Nishina, K.; Mizusawa, H.; Yokota, T., High-Density Lipoprotein Facilitates In Vivo Delivery of α-Tocopherol–Conjugated Short-Interfering RNA to the Brain. *Hum. Gene Ther.* **2011,** *22* (6), 711-719.

94. Nair, J. K.; Willoughby, J. L. S.; Chan, A.; Charisse, K.; Alam, M. R.; Wang, Q.; Hoekstra, M.; Kandasamy, P.; Kel'in, A. V.; Milstein, S.; Taneja, N.; O'Shea, J.; Shaikh, S.; Zhang, L.; van der Sluis, R. J.; Jung, M. E.; Akinc, A.; Hutabarat, R.; Kuchimanchi, S.; Fitzgerald, K.; Zimmermann, T.; van Berkel, T. J. C.; Maier, M. A.; Rajeev, K. G.; Manoharan, M., Multivalent N-Acetylgalactosamine-Conjugated siRNA Localizes in Hepatocytes and Elicits Robust RNAi-Mediated Gene Silencing. *J. Am. Chem. Soc.* **2014,** *136* (49), 16958-16961.

95. McNamara, J. O.; Andrechek, E. R.; Wang, Y.; Viles, K. D.; Rempel, R. E.; Gilboa, E.; Sullenger, B. A.; Giangrande, P. H., Cell type-specific delivery of siRNAs with aptamer-siRNA chimeras. *Nat. Biotechnol.* **2006,** *24* (8), 1005-1015.

96. Nothisen, M.; Kotera, M.; Voirin, E.; Remy, J.-S.; Behr, J.-P., Cationic siRNAs Provide Carrier-Free Gene Silencing in Animal Cells. *J. Am. Chem. Soc.* **2009,** *131* (49), 17730-17731.

97. Gooding, M.; Tudzarova, S.; Worthington, R. J.; Kingsbury, S. R.; Rebstock, A. S.; Dube, H.; Simone, M. I.; Visintin, C.; Lagos, D.; Quesada, J. M.; Laman, H.; Boshoff, C.; Williams, G. H.; Stoeber, K.; Selwood, D. L., Exploring the interaction between siRNA and the SMoC biomolecule transporters: implications for small molecule-mediated delivery of siRNA. *Chem. Biol. Drug Des.* **2012,** *79* (1), 9-21.

98. Chiu, Y. L.; Ali, A.; Chu, C. Y.; Cao, H.; Rana, T. M., Visualizing a correlation between siRNA localization, cellular uptake, and RNAi in living cells. *Chem. Biol.* **2004,** *11* (8), 1165-1175.

99. Muratovska, A.; Eccles, M. R., Conjugate for efficient delivery of short interfering RNA (siRNA) into mammalian cells. *FEBS Lett.* **2004,** *558* (1-3), 63-68.

100. Seow, Y.; Wood, M. J., Biological Gene Delivery Vehicles: Beyond Viral Vectors. *Mol. Ther., J. Am. Soc. Gene Ther.* **2009,** *17* (5), 767-777.

101. Lu, J. J.; Langer, R.; Chen, J., A Novel Mechanism Is Involved in Cationic Lipid-Mediated Functional siRNA Delivery. *Mol. Pharmaceutics* **2009,** *6* (3), 763-771.

102. Gomes-da-Silva, L. C.; Fonseca, N. A.; Moura, V.; Pedroso de Lima, M. C.; Simões, S.; Moreira, J. N., Lipid-Based Nanoparticles for siRNA Delivery in Cancer Therapy: Paradigms and Challenges. *Acc. Chem. Res.* **2012,** *45* (7), 1163-1171.

103. Zimmermann, T. S.; Lee, A. C. H.; Akinc, A.; Bramlage, B.; Bumcrot, D.; Fedoruk, M. N.; Harborth, J.; Heyes, J. A.; Jeffs, L. B.; John, M.; Judge, A. D.; Lam, K.; McClintock, K.; Nechev, L. V.; Palmer, L. R.; Racie, T.; Röhl, I.; Seiffert, S.; Shanmugam, S.; Sood, V.; Soutschek, J.; Toudjarska, I.; Wheat, A. J.; Yaworski, E.; Zedalis, W.; Koteliansky, V.; Manoharan, M.; Vornlocher, H.-P.; MacLachlan, I., RNAi-mediated gene silencing in non-human primates. *Nature* **2006,** *441* (7089), 111-114.

104. Davis, M. E.; Zuckerman, J. E.; Choi, C. H. J.; Seligson, D.; Tolcher, A.; Alabi, C. A.; Yen, Y.; Heidel, J. D.; Ribas, A., Evidence of RNAi in humans from systemically administered siRNA via targeted nanoparticles. *Nature* **2010,** *464* (7291), 1067-1070.

105. Davis, M. E., The First Targeted Delivery of siRNA in Humans via a Self-Assembling, Cyclodextrin Polymer-Based Nanoparticle: From Concept to Clinic. *Mol. Pharmaceutics* **2009,** *6* (3), 659-668.

106. Chan, D. P. Y.; Deleavey, G. F.; Owen, S. C.; Damha, M. J.; Shoichet, M. S., Click conjugated polymeric immuno-nanoparticles for targeted siRNA and antisense oligonucleotide delivery. *Biomaterials* **2013,** *34* (33), 8408-8415.

107. Kafshgari, M. H.; Delalat, B.; Tong, W. Y.; Harding, F. J.; Kaasalainen, M.; Salonen, J.; Voelcker, N. H., Oligonucleotide delivery by chitosan-functionalized porous silicon nanoparticles. *Nano Res.* **2015,** *8* (6), 2033-2046.

108. Yan, M.; Liang, M.; Wen, J.; Liu, Y.; Lu, Y.; Chen, I. S. Y., Single siRNA Nanocapsules for Enhanced RNAi Delivery. *J. Am. Chem. Soc.* **2012,** *134* (33), 13542-13545.

109. Souleimanian, N.; Deleavey, G. F.; Soifer, H.; Wang, S.; Tiemann, K.; Damha, M. J.; Stein, C. A., Antisense 2'-Deoxy, 2'-Fluoroarabino Nucleic Acid (2'F-ANA) Oligonucleotides: In Vitro Gymnotic Silencers of Gene Expression Whose Potency Is Enhanced by Fatty Acids. *Mol. Ther. Nucleic Acids* **2012,** *1* (10), e43.

110. Zhang, G.; Budker, V.; Wolff, J. A., High Levels of Foreign Gene Expression in Hepatocytes after Tail Vein Injections of Naked Plasmid DNA. *Hum. Gene Ther.* **1999,** *10* (10), 1735-1737.

111. Bell, J. B.; Podetz-Pedersen, K. M.; Aronovich, E. L.; Belur, L. R.; McIvor, R. S.; Hackett, P. B., Preferential delivery of the Sleeping Beauty transposon system to livers of mice by hydrodynamic injection. *Nat. Protoc.* **2007,** *2* (12), 3153-3165.

112. Inoue, Y.; Kurihara, R.; Tsuchida, A.; Hasegawa, M.; Nagashima, T.; Mori, T.; Niidome, T.; Katayama, Y.; Okitsu, O., Efficient delivery of siRNA using dendritic poly(L-lysine) for loss-of-function analysis. *J. Controlled Release* **2008,** *126* (1), 59-66.

113. Wu, J.; Huang, W.; He, Z., Dendrimers as Carriers for siRNA Delivery and Gene Silencing: A Review. *Sci. World J.* **2013,** *2013*, 630654.

114. Haensler, J.; Szoka, F. C., Polyamidoamine cascade polymers mediate efficient transfection of cells in culture. *Bioconjugate Chem.* **1993,** *4* (5), 372-379.

115. Kukowska-Latallo, J. F.; Bielinska, A. U.; Johnson, J.; Spindler, R.; Tomalia, D. A.; Baker, J. R., Efficient transfer of genetic material into mammalian cells using Starburst polyamidoamine dendrimers. *Proc. Natl. Acad. Sci. U.S.A.* **1996,** *93* (10), 4897-4902.

116. Veldhoen, S.; Laufer, S. D.; Trampe, A.; Restle, T., Cellular delivery of small interfering RNA by a non-covalently attached cell-penetrating peptide: quantitative analysis of uptake and biological effect. *Nucleic Acids Res.* **2006,** *34* (22), 6561-6573.

117. Song, E.; Zhu, P.; Lee, S.-K.; Chowdhury, D.; Kussman, S.; Dykxhoorn, D. M.; Feng, Y.; Palliser, D.; Weiner, D. B.; Shankar, P.; Marasco, W. A.; Lieberman, J., Antibody mediated in vivo delivery of small interfering RNAs via cell-surface receptors. *Nat. Biotechnol.* **2005,** *23* (6), 709-717.

118. Ming, X.; Carver, K.; Fisher, M.; Noel, R.; Cintrat, J. C.; Gillet, D.; Barbier, J.; Cao, C.; Bauman, J.; Juliano, R. L., The small molecule Retro-1 enhances the pharmacological actions of antisense and splice switching oligonucleotides. *Nucleic Acids Res.* **2013,** *41* (6), 3673-3687.

119. Lietard, J.; Ittig, D.; Leumann, C. J., Synthesis, binding and cellular uptake properties of oligodeoxynucleotides containing cationic bicyclo-thymidine residues. *Bioorg. Med. Chem.* **2011,** *19* (19), 5869-5875.

120. Bitko, V.; Musiyenko, A.; Shulyayeva, O.; Barik, S., Inhibition of respiratory viruses by nasally administered siRNA. *Nat. Med.* **2005,** *11* (1), 50-55.

121. Sarepta Therapeutics. PCNSD Advisory Committee Meeting Briefing Document. http://www.fda.gov/downloads/AdvisoryCommittees/CommitteesMeetingMaterials/Drugs/PeripheralandCentralNervousSystemDrugsAdvisoryCommittee/UCM481912.pdf.

122. Kastle Therapeutics. Kynamro (mipomersen sodium) Injection 200 mg/mL. www.kynamro.com.

123. Pack, D. W.; Hoffman, A. S.; Pun, S.; Stayton, P. S., Design and development of polymers for gene delivery. *Nat. Rev. Drug Discov.* **2005,** *4* (7), 581-593.

124. Merril, C. R.; Biswas, B.; Carlton, R.; Jensen, N. C.; Creed, G. J.; Zullo, S.; Adhya, S., Long-circulating bacteriophage as antibacterial agents. *Proc. Natl. Acad. Sci. U. S. A.* **1996,** *93* (8), 3188-3192.

125. Lavergne, T.; Baraguey, C.; Dupouy, C.; Parey, N.; Wuensche, W.; Sczakiel, G.; Vasseur, J.-J.; Debart, F., Synthesis and Preliminary Evaluation of pro-RNA 2′-O-Masked with Biolabile Pivaloyloxymethyl Groups in an RNA Interference Assay. *J. Org. Chem.* **2011,** *76* (14), 5719-5731.

126. Meade, B. R.; Gogoi, K.; Hamil, A. S.; Palm-Apergi, C.; Berg, A. v. d.; Hagopian, J. C.; Springer, A. D.; Eguchi, A.; Kacsinta, A. D.; Dowdy, C. F.; Presente, A.; Lonn, P.; Kaulich, M.; Yoshioka, N.; Gros, E.; Cui, X.-S.; Dowdy, S. F., Efficient delivery of RNAi prodrugs containing reversible charge-neutralizing phosphotriester backbone modifications. *Nat. Biotechnol.* **2014,** *32* (12), 1256-1261.

127. Ducho, C., Enzymatically Cleavable siRNA Prodrugs: a New Paradigm for the Intracellular Delivery of RNA-Based Therapeutics. *ChemMedChem* **2015,** *10* (10), 1625-1627.

128. Meier, C.; Habel, L.; Laux, W.; Clercq, E. D.; Balzarini, J., Homo Dinucleoside-α-hydroxyphosphonate Diesters as Prodrugs of the Antiviral Nucleoside Analogues 2′,3′-Dideoxythymidine and 3′-Azido-2′,3′-dideoxythymidine. *Nucleosides Nucleotides* **1995,** *14* (3-5), 759-762.

129. Mauritz, R. P.; Schmelz, F. S.; Meier, C., Elucidation of the Hydrolytical Properties of α-Hydroxybenzylphosphonates as a New Potential Pro-Oligonucleotide Concept. *Nucleosides Nucleotides* **1999,** *18* (6-7), 1417-1418.

130. Mauritz, R. P.; Meier, C.; Uhlmann, E., Synthesis of 3′,5′-Dithymidylyl-α-hydroxyphosphonate Dimer Building Blocks for Oligonucleotide Synthesis—A New Pro-oliguncleotide. *Nucleosides Nucleotides* **1997,** *16* (7-9), 1209-1212.

131. Mauritz, R. P.; Meier, C., Fpmp-Protected α-Hydroxyphosphonate Diesters for The Synthesis of Pro-Oligonucleotides. *Nucleosides Nucleotides* **1997,** *16* (5-6), 675-678.

132. Iyer, R. P.; Ho, N.-h.; Yu, D.; Agrawal, S., Bioreversible oligonucleotide conjugates by site-specific derivatization. *Bioorg. Med. Chem. Lett.* **1997,** *7* (7), 871-876.

133. Périgaud, C.; Gosselin, G.; Lefebvre, I.; Girardet, J.-L.; Benzaria, S.; Barber, I.; Imbach, J.-L., Rational design for cytosolic delivery of nucleoside monphosphates : “SATE” and “DTE” as enzyme-labile transient phosphate protecting groups. *Bioorg. Med. Chem. Lett.* **1993,** *3* (12), 2521-2526.

134. Tosquellas, G.; Alvarez, K.; Dell'Aquila, C.; Morvan, F.; Vasseur, J.-J.; Imbach, J.-L.; Rayner, B., The pro-oligonucleotide approach: Solid phase synthesis and preliminary evaluation of model pro-dodecathymidylates. *Nucleic Acids Res.* **1998,** *26* (9), 2069-2074.

135. Grajkowski, A.; Wilk, A.; Chmielewski, M. K.; Phillips, L. R.; Beaucage, S. L., The 2-(N-formyl-N-methyl)aminoethyl group as a potential phosphate/thiophosphate protecting group in solid-phase oligodeoxyribonucleotide synthesis. *Org. Lett.* **2001,** *3* (9), 1287-1290.

136. Parey, N.; Baraguey, C.; Vasseur, J.-J.; Debart, F., First Evaluation of Acyloxymethyl or Acylthiomethyl Groups as Biolabile 2′-O-Protections of RNA. *Org. Lett.* **2006,** *8* (17), 3869-3872.

137. Martin, A. R.; Lavergne, T.; Vasseur, J. J.; Debart, F., Assessment of new 2'-O-acetalester protecting groups for regular RNA synthesis and original 2'-modified proRNA. *Bioorg. Med. Chem. Lett.* **2009,** *19* (15), 4046-4049.

138. Lackey, J. G.; Mitra, D.; Somoza, M. M.; Cerrina, F.; Damha, M. J., Acetal Levulinyl Ester (ALE) Groups for 2′-Hydroxyl Protection of Ribonucleosides in the Synthesis of Oligoribonucleotides on Glass and Microarrays. *J. Am. Chem. Soc.* **2009,** *131* (24), 8496-8502.

139. Johnsson, R.; Lackey, J. G.; Bogojeski, J. J.; Damha, M. J., New light labile linker for solid phase synthesis of 2′-O-acetalester oligonucleotides and applications to siRNA prodrug development. *Bioorg. Med. Chem. Lett.* **2011,** *21* (12), 3721-3725.

140. Biscans, A.; Rouanet, S.; Bertrand, J.-R.; Vasseur, J.-J.; Dupouy, C.; Debart, F., Synthesis, binding, nuclease resistance and cellular uptake properties of 2′-O-acetalester-modified oligonucleotides containing cationic groups. *Bioorg. Med. Chem.* **2015,** *23* (17), 5360-5368.

141. Ochi, Y.; Imai, M.; Nakagawa, O.; Hayashi, J.; Wada, S.; Urata, H., Gene silencing by 2'-O-methyldithiomethyl-modified siRNA, a prodrug-type siRNA responsive to reducing environment. *Bioorg. Med. Chem. Lett.* **2016,** *26* (3), 845-548.

142. Biscans, A.; Rouanet, S.; Vasseur, J. J.; Dupouy, C.; Debart, F., A versatile post-synthetic method on a solid support for the synthesis of RNA containing reduction-responsive modifications. *Org. Biomol. Chem.* **2016**, *14*, 7010-7017.

143. Guzaev, A. P.; Manoharan, M., A conformationally preorganized universal solid support for efficient oligonucleotide synthesis. *J. Am. Chem. Soc.* **2003,** *125* (9), 2380-2381.

144. Johnsson, R. A.; Bogojeski, J. J.; Damha, M. J., An evaluation of selective deprotection conditions for the synthesis of RNA on a light labile solid support. *Bioorg. Med. Chem. Lett.* **2014,** *24* (9), 2146-2149.

145. Beaucage, S. L.; Iyer, R. P., Advances in the Synthesis of Oligonucleotides by the Phosphoramidite Approach. *Tetrahedron* **1992,** *48* (12), 2223-2311.

146. Tanaka, T.; Letsinger, R. L., Syringe method for stepwise chemical synthesis of oligonucleotides. *Nucleic Acids Res.* **1982,** *10* (10), 3249-3259.

147. Remaud, G.; Zhou, X.-X.; Chattopadhyaya, J.; Oivanen, M.; Lönnberg, H., The effect of protecting groups of the nucleobase and the sugar moieties on the acidic hydrolysis of the glycosidic bond of 2′-deoxyadenosine: a kinet. *Tetrahedron* **1987,** *43* (19), 4453-4461.

148. Caruthers, M. H.; McBride, L. J.; Bracco, L. P.; Dubendorff, J. W., Studies on Nucleotide Chemistry 15. Synthesis of Oligodeoxynucleotides Using Amidine Protected Nucleosides. *Nucleosides Nucleotides* **1985,** *4* (1-2), 95-105.

149. Vinayak, R.; Anderson, P.; McCollum, C.; Hampel, A., Chemical synthesis of RNA using fast oligonucleotide deprotection chemistry. *Nucleic Acids Res.* **1992,** *20* (6), 1265-1269.

150. Lindström, U. M.; Kool, E. T., An orthogonal oligonucleotide protecting group strategy that enables assembly of repetitive or highly structured DNAs. *Nucleic Acids Res.* **2002,** *30* (19), e101-e101.

151. Froehler, B. C.; Matteucci, M. D., Dialkylformamldines: depurination resistant N6-protecting group for deoxyadenosine. *Nucleic Acids Res.* **1983,** *11* (22), 8031-8036.

152. Sekine, M.; Masuda, N.; Hata, T., Introduction of the 4,4′4′-tris(benzoyloxy)trityl group into the exo amino groups of deoxyribonucleosides and its properties. *Tetrahedron* **1985,** *41* (23), 5445-5453.

153. Heikkila, J. C., J., The 9-Fluorenylmethoxycarbonyl (Fmoc) Group for the Protection of Amino Functions of Cytidine, Adenosine, Guanosine and Their 2'-Deoxysugar Derivatives. *Acta Chem. Scand.* **1983,** *B37*, 263-265.

154. Scalfi-happ, C.; Happ, E.; Chladek, S., New Approach to the Synthesis of 2′(3′)-O-Aminoacyloligoribonucleotides Related to the 3′-Terminus of Aminoacyl Transfer Ribonucleic Acid. *Nucleosides Nucleotides* **1987,** *6* (1-2), 345-348.

155. Hagen, M. D.; Scalfi-Happ, C.; Happ, E.; Chladek, S., Aminoacyl derivatives of nucleosides, nucleotides, and polynucleotides. 45. Synthesis of 2'(3')-O-(aminoacyl) trinucleotides incorporating all four common bases. *J. Org. Chem.* **1988,** *53* (21), 5040-5045.

156. Balgobin, N.; Chattopadhyaya, J., Solid Phase Synthesis of DNA Under a Non-Depurinating Condition with a Base Labile 5′-Protecting Group (Fmoc) Using Phosphiteamidite Approach. *Nucleosides Nucleotides* **1987,** *6* (1-2), 461-463.

157. Gioeli, C.; Chattopadhyaya, J. B., The flouren-9-ylmethoxycarbonyl group for the protection of hydroxy-groups; its application in the synthesis of an octathymidylic acid fragment. *J. Chem. Soc., Chem. Commun.* **1982,** (12), 672-674.

158. Ma, Y.; Sonveaux, E., The 9-Fluorenylmethyloxycarbonyl (Fmoc) Group as a 5′-O Base Labile Protecting Group in Solid Supported Oligonucleotide Synthesis. *Nucleosides Nucleotides* **1987,** *6* (1-2), 491-493.

159. Ma, Y.; Sonveaux, E., The 9-fluorenylmethyloxycarbonyl group as a 5′-OH protection in oligonucleotide synthesis. *Biopolymers* **1989,** *28* (5), 965-973.

160. Ogilvie, K. K.; Nemer, M. J.; Hakimelahi, G. H.; Proba, Z. A.; Lucas, M., N-levulination of nucleosides. *Tetrahedron Lett.* **1982,** *23* (26), 2615-2618.

161. Lackey, J. G.; Sabatino, D.; Damha, M. J., Solid-Phase Synthesis and On-Column Deprotection of RNA from 2'- (and 3'-) O-Levulinated (Lv) Ribonucleoside Monomers. *Org. Lett.* **2007,** *9* (5), 789-792.

162. Dreef-Tromp, C. M.; Hoogerhout, P.; van der Marel, G. A.; van Boom, J. H., A new protected acyl protecting group for exocyclic amino functions of nucleobases. *Tetrahedron Lett.* **1990,** *31* (3), 427-430.

163. Dreef-Tromp, C. M.; van Dam, E. M. A.; van den Elst, H.; van der Marel, G. A.; van Boom, J. H., Solid-phase synthesis of H-Phe-Tyr-(pATAT)-NH_2: a nucleopeptide fragment from the nucleoprotein of bacteriophage øX174. *Nucleic Acids Res.* **1990,** *18* (22), 6491-6495.

164. Lackey, J. G. New methods for the synthesis of RNA, novel RNA pro-drugs and RNA microarrays. McGill University, Montreal, QC, 2010.

Chapter 2: Development of Amino Acid Acetal Esters as Promoieties of RNA Prodrugs

2.1. Amino Acid Promoieties in Prodrugs

2.1.1. Small Molecules

There are many examples of amino acid based prodrug moieties that have been conjugated to pharmacological compounds for their ability to improve the drug's solubility in serum, enhance bioavailability, increase cell permeability, target cellular membrane transporters in specific tissues, and overcome resistance, among other things.[1] Sustained release of active drug through the constant delivery and hydrolysis of a prodrug, as opposed to the abrupt release of a drug from a liposome, microsphere, or hydrogel formulation, reduces its *en route* susceptibility to changes in absorption.[1] For example, D-amphetamine (Scheme 2.1) is a psychostimulant for attention deficit/hyperactivity disorder (ADHD). It is delivered *via* its L-lysine amino acid amide prodrug lisdexamfetamine dimesylate (LDX)[2] in slow-release fashion, which also decreases abuse potential if inhaled or injected. Amino acid promoieties can be biotransformed in the intestines if administered orally, in systemic circulation if injected intraveneously, or in target cells once internalized.[3]

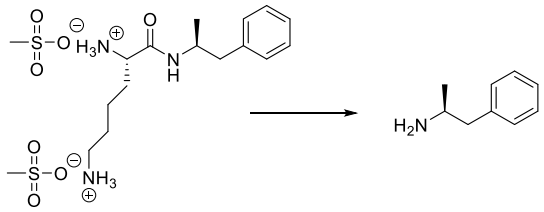

Scheme 2.1. The release of D-amphetamine from LDX occurs by amide hydrolysis in red blood cells.

2.1.2. Nucleosides

Many amino acid-conjugated nucleoside derivatives exist, far and beyond their use in nucleic acids.[4,5,6,7] Valacyclovir and valganciclovir (Scheme 2.2) are two of the more significant prodrug compounds that feature amino acid promoieties. While the charged L-valine-conjugated prodrugs have low membrane permeability, L-valine is exploited as a means for absorption by intestinal proton-coupled peptide transporter 1 (PepT1, *SLC15A1*) and intestinal Na^+-dependent neutral amino acid transporter ($ATB^{0,+}$, SLC6A14).[8,9] Once inside the cell, valacyclovir and

valganciclovir are hydrolyzed to acyclovir and ganciclovir, respectively. Next, thymidine kinase processes them to monophosphates and cellular kinases transform them to their respective triphosphates, enabling them to function as antiherpetic drugs.

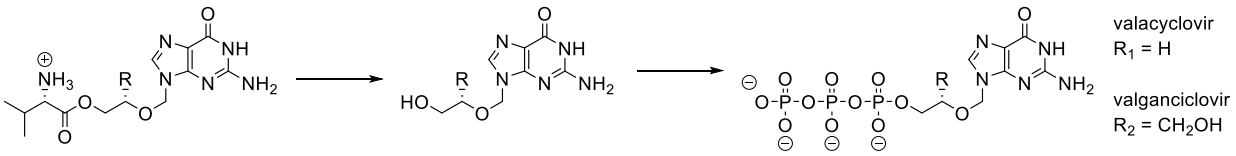

Scheme 2.2. The bioconversion of valacyclovir and valganciclovir proceeds first by valacyclovirase and then by kinases.

2-Bromo-5,6-dichloro-1-(β-D-ribofuranosyl)benzimidazole (BDCRB) is a potent and selective inhibitor of human cytomegalovirus. BDCRB faces the large hurdle of overcoming DNA glycosylase-mediated depurination *via* 8-oxoguanine and *N*-methylpurine intermediates by 8-oxoguanine DNA glycosylase (OGG1) and *N*-methylpurine DNA glycosylase (MPG), respectively.[10] An L-aspartic acid ester of the drug improves its *in vivo* metabolic stability, which increases its circulation time and bioavailability before it is enzymatically hydrolyzed into the active compound (Scheme 2.3A).[11] In a similar fashion, gemcitabine, an anticancer agent with poor membrane permeability and vulnerability to glycosidic bond breakage by cytosine deaminase, was esterified with L-isoleucine (Scheme 2.3B). The resulting prodrug was resistant to deactivation.[12]

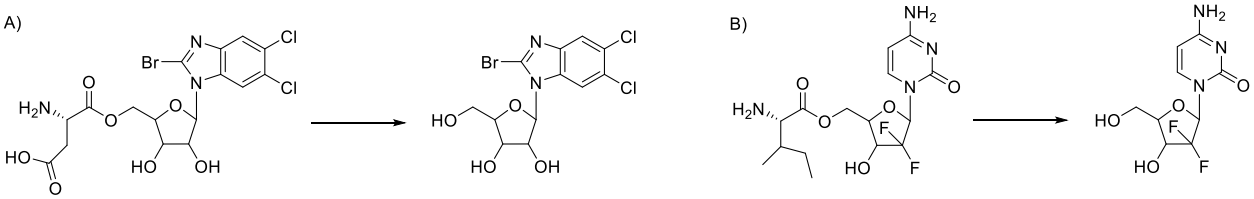

Scheme 2.3. The bioconversion of A) BDCRB and B) gemcitabine is achieved by hydrolases.

2.2. A Screening of Acetal Amino Esters (AAEs)

2.2.1. Advantages of 2'-O-AAEs

Amino acid esters are appealing promoieties because: 1) The amine is available for ionization; 2) there is a variety of chemically diverse R groups to choose from; and 3) they are

non-toxic when released into the body. The general structure of the amino acetal esters (AAEs) investigated is shown in Figure 2.1 and their structural features are summarized in Table 2.1. The ribose sugars are conjugated to their respective esters through acetal linkers. This is an artifact of monomer synthesis, necessary to prevent isomerization (without this linker, a 3'-hydroxyl is vulnerable to 2'/3' ester migration, as this is a vicinal diol system). Following the installation of the 2'-*O*-ester, the nearby 3'-hydroxyl must first be deprotected to enable 3'-*O*-phosphitylation in the presence of diisopropylethylamine (DIPEA).

Side chain variations were explored to investigate several potentially advantageous features – the additional positive charge of L-lysine, the aromatic group of L-phenylalanine, the small methyl group of L-alanine, and the strained cycle of L-proline. The additional positive charge of lysine (Lys) was expected to further counteract the repulsive effects of the phosphate group to the cellular membrane, thereby inducing the greatest cellular uptake of a hypothetical oligonucleotide; phenylalanine (Phe) was expected to cause the second greatest level of cellular uptake of an oligonucleotide conjugate on account of its non-polar side chain; and proline (Pro), second-to-last, was expected to cause cellular uptake of an oligonucleotide conjugate to a slightly greater extent than alanine (Ala) due to its additional methylene group.

Table 2.1. The purpose of the 2'-*O*-AAE modification in oligonucleotides.

Feature	Purpose
Linker	Prevents 2'/3' ester migration during phosphoramidite synthesis
Side chain	R = $-(CH_2)_4NH_3^+$ (Lys), additional positive charge, pK_a = 10.53
	R = $-(CH_2)_3NH_2^+-$ (Pro), positively charged aliphatic cycle, pK_a = 10.96
	R = -Bn (Phe), uncharged aromatic
	R = $-CH_3$ (Ala), uncharged aliphatic
Amine	Positive charge at physiological pH to counteract negative charge of phosphate group

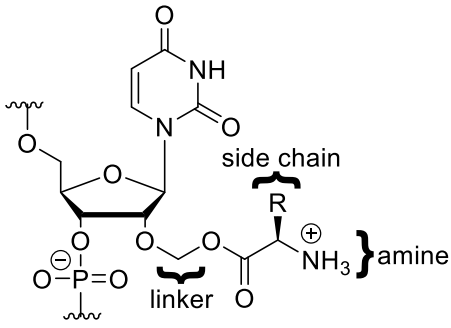

Figure 2.1. Features of the 2'-*O*-AAE modification.

A nucleophilic attack on the promoiety would release the amino acid and formaldehyde as shown in Scheme 2.4. Formaldehyde is an endogenous product of human metabolism, as well as an abundant dietary constituent in both food sources and the environment. The quantity of formaldehyde that would be released in the patient from a 2'-*O*-AAE siRNA is estimated to be

negligible relative to the body's basal level of formaldehyde. Thus, the introduction of small amounts of formaldehyde would be unlikely to cause toxicity.[13]

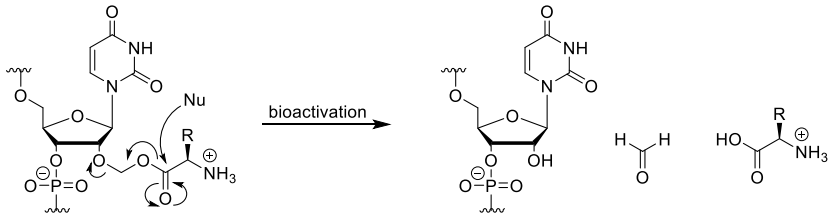

Scheme 2.4. The proposed bioactivation of a 2'-*O*-AAE releases an amino acid.

2.2.2. Synthesis of 2'-O-AAE Monomers

Uridine 2'-*O*-AAE monomers were comprised of protecting groups compatible with standard solid-supported synthesis (Scheme 2.5). First, the 3'- and 5'-hydroxyl groups of uridine nucleoside were simultaneously protected *via* the installation of a 1,1,3,3-tetraisopropyldisiloxane bridge (with Markiewicz reagent). Next, the 2'-hydroxyl function was subjected to a mixture of dimethylsulfoxide, acetic acid, and acetic anhydride (DMSO/AcOH/Ac_2O 1.5:1.5:1 v/v/v), resulting in a Pummerer-type reaction to form a 2-methylthiomethylene (MTM) ether (first reported by Zavgorodny *et al*. and later modified by Rastogi *et al*.)[14,15] The MTM ether **3** was activated with sulfuryl chloride and the transient product was coupled to the cesium salt of an *N*-FMOC-protected amino acid. The 5'/3' protecting group of **4a-d** was removed with triethylamine trihydroflouride (NEt_3-3HF) and the products **5a-d** were subjected to dimethoxytritylation and phosphitylation to yield products **7a-d**.

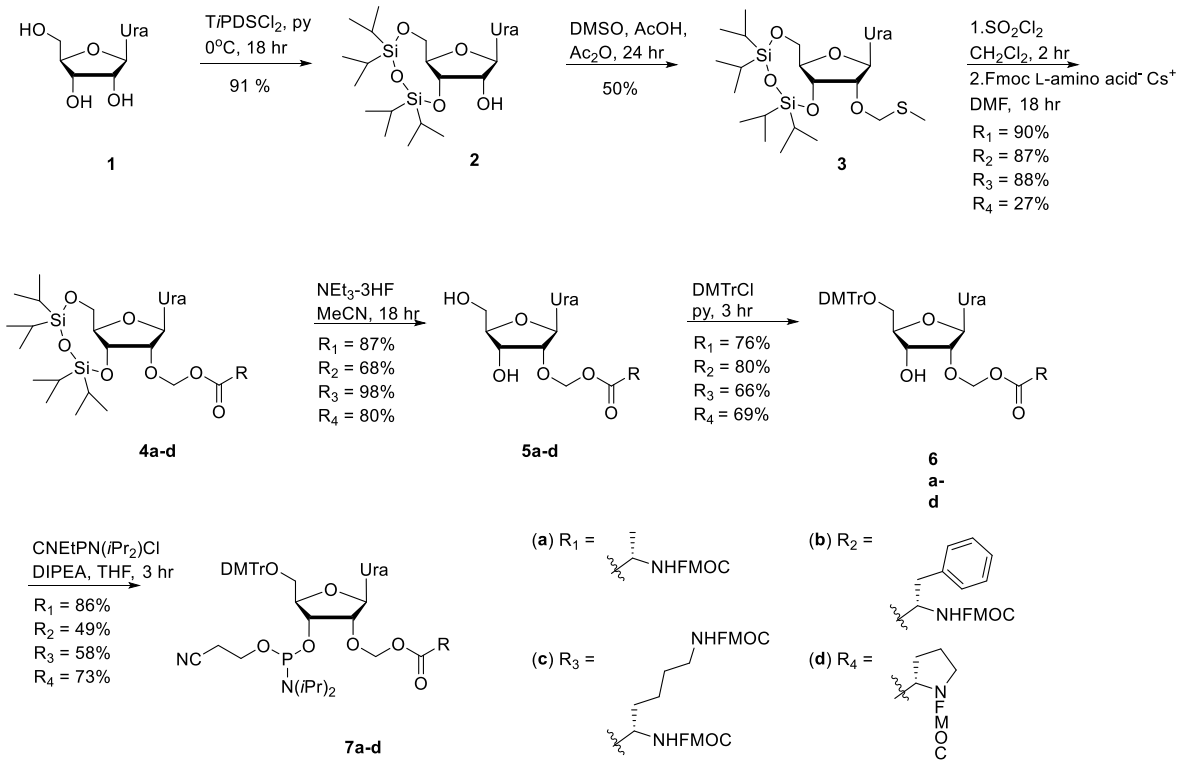

Scheme 2.5. The synthesis of phosphoramidite monomers containing 2'-*O*-AAE modifications began with uridine nucleoside.

2.2.3. Oligonucleotide Synthesis

Standard solid phase synthesis reagents were used to produce 15- and 21-nucleotide (nt)-long poly-thymidine oligonucleotides with intervening uridine 2'-*O*-AAE units (Scheme 2.6). A photocleavable linker was connected to the phosphate triester of a thymidine dimer and the oligonucleotides were grown from the 5'-end of the dimer. For those oligonucleotides containing alanine, phenylalanine, or lysine modifications, oligonucleotide synthesis was done on a dimer that had a terminal 3'-levulinyl group (Y_1 = OLev). The levulinyl group was not removed during deprotection of the oligonucleotide, thus remaining on the final product. For the oligonucleotide containing proline modifications, oligonucleotide synthesis was done on a dimer that contained a 3'-terminal dideoxythymidine (ddT; Y_2 = H). *N*-FMOC and phosphate protecting groups were removed concomitantly with triethylamine/acetonitrile (NEt_3/MeCN 2:3 v/v), thus not requiring the standard treatment of aqueous ammonia. Standard ammonia treatment would also cleave the 2'-*O*-AAE prematurely. In fact, care must be also exercised with NEt_3/MeCN reagent, as the presence of water will likely cleave the AAE groups under aqueous basic conditions. In the last

step, the oligomers were released from the solid support with ultraviolet radiation (λ_{max} = 350 nm) in acetonitrile/diisopropylamine (MeCN/DIPEA 99:1 v/v). The prepared oligomers are listed in Scheme 2.6.

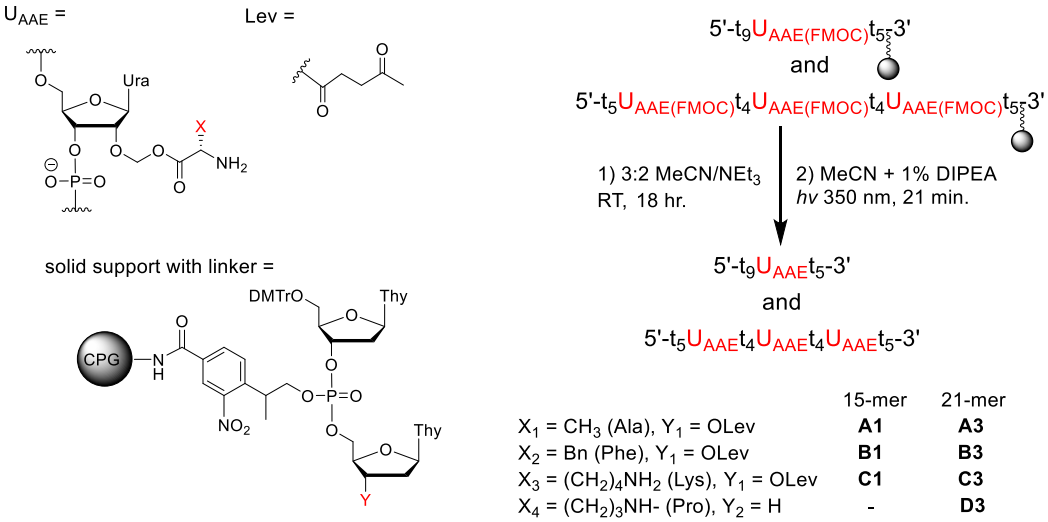

Scheme 2.6. The synthesis of 2'-*O*-AAE oligonucleotides was initiated from a photocleavable linker attached to CPG solid support.

2.3. Purification and Characterization of 2'-O-AAE Oligonucleotide Conjugates

As indicated above, all deprotection steps were conducted in a nearly anhydrous manner to avoid base-catalyzed hydrolysis of the AAE groups prior isolation and characterization of the target 2'-*O*-AAE oligonucleotides. Likewise, the use of basic buffers should be avoided during purification of oligonucleotides and handling prior to mass spectrometry analysis. Nonetheless, we found that the crude oligomers **A1**, **B1**, **C1**, and **D3** comprised a mixture of oligonucleotides that lacked one or more 2'-*O*-AAE groups.

Table 2.2 reveals that the QTOF mass analysis of the syntheses **B1** and **B3** detected oligonucleotides with all of the 2'-*O*-AAE inserts intact, while fully modified oligonucleotides were not detected from syntheses **A1**, **A3**, **C1**, **C3**, and **D3**. This suggests that the 2'-*O*-phenylalanine acetal ester (2'-*O*-Phe) modification is the most stable out of the 2'-*O*-AAEs investigated. Mass characterization of the conjugates was not utilized to quantitatively compare the degree to which the 2'-*O*-AAE modifications were retained, however; reversed-phase high-

performance liquid chromatography (RP-HPLC) was used to compare the relative amounts of hydrolysis products in each sample.

The RP-HPLC trace (Figure 2.2) of crude proline-containing oligonucleotide **D3** revealed a single major peak whose mass corresponded to the unmodified oligomer (Table 2.2 column 1). Thus, the three 2'-*O*-proline acetal ester inserts were completely hydrolyzed prior to HPLC analysis. In contrast, the chromatogram of crude 15-nt phenylalanine-containing oligonucleotide (**B1**) revealed three main products (Figure 2.3A). The most retained eluting peak **8** (ca. 30 min) was assumed to be the desired **B1** strand, and in fact confirmed to be the case from a series of MS-QTOF experiments described below.

Table 2.2. Some expected mass values of 2'-*O*-AAE-containing oligonucleotides were observed.

	1		2		3		4		5		6	
Synth	No modification		0 inserts + Lev		1 insert - Lev		1 insert		2 inserts		3 inserts	
-esis	Calc.	Found	Calc.	Found	Calc.	Found	Calc.	Found	Calc.	Found	Calc.	Found
A1[a]	4502.9	4503.0	4600.9	4601.1	4603.5	-	4701.5	-				
B1[a]	4502.9	4503.1	4600.9	4601.1	4680.0	4680.2	4778.0	4778.3				
C1[a]	4502.9	4502.8	4600.9	4601.2	4661.0	-	4759.0	-				
A3[b]	6332.1	-	6430.1	6430.3	6434.3	-	6532.3	6531.2	6632.2	6632.3	6733.3	-
B3[b]	6332.1	-	6430.1	-	6509.2	-	6607.2	6606	6784.3	6783	6961.4	6963
C3[b]	6332.1	-	6430.1	-	6490.2	-	6588.2	6586	6746.3	6747	6904.4	-
D3[b]	6313.0	6313.0					6440.0	-	6567.0	-	6694.0	-

Legend: Reported values are in atomic mass units (amu); [a] = detected as highest mass value after RP-HPLC isolation; [b] = crude sample; (-) = mass not found; grey shadow = not applicable.

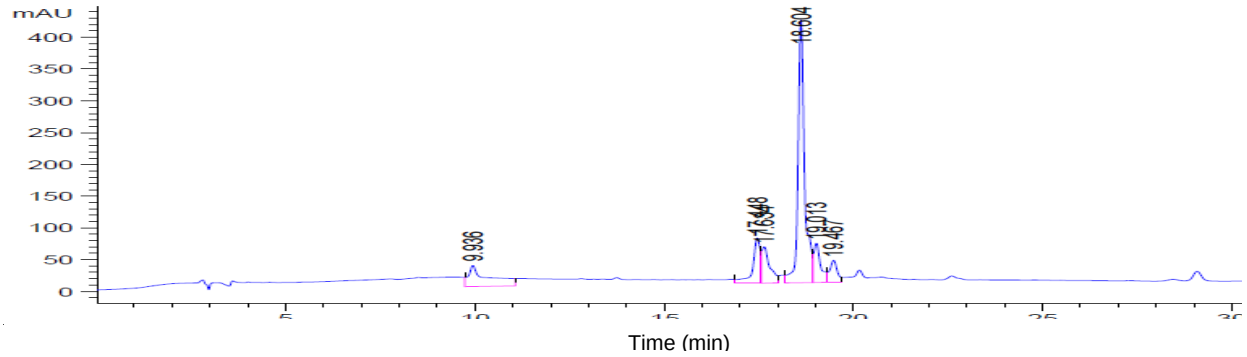

Figure 2.2. The RP-HPLC trace of **D3** reveals one main peak.

Purified product **B1** (from peak **8**) was collected in buffered HPLC water, allowed to sit at room temperature for several hours, and lyophilized for mass analysis. The three masses obtained corresponded to an oligonucleotide containing 1) one 2'-*O*-Phe insert and the 3'-*O*-Lev (Table 2.2 column 4); 2) the 3'-*O*-Lev (Table 2.2 column 2) and; 3) no modifications whatsoever (Table 2.2 column 1). Mass analysis of the lyophilized product **9** detected two oligonucleotide products – one containing a 3'-*O*-Lev group, and another oligonucleotide containing no modifications whatsoever. Mass analysis of product **10** detected only the unmodified oligomer. Therefore, the identities of products **8**, **9**, and **10** (Table 2.3) were inferred from the heaviest value obtained in their mass spectrogram. In similar fashion, isolation, lyophilization, and reinjection of **B1** (peak **8**) into the HPLC provided a mixture of **B1** (peak **8**), **9**, and **10** (Figure 2.3B). Similarly, reinjection of lyophilized product **9** appeared as a mixture **9** and **10** upon HPLC analysis. Reinjection of lyophilized **10** did not show any additional product. This is all consistent with the assigned structures shown in Table 2.3.

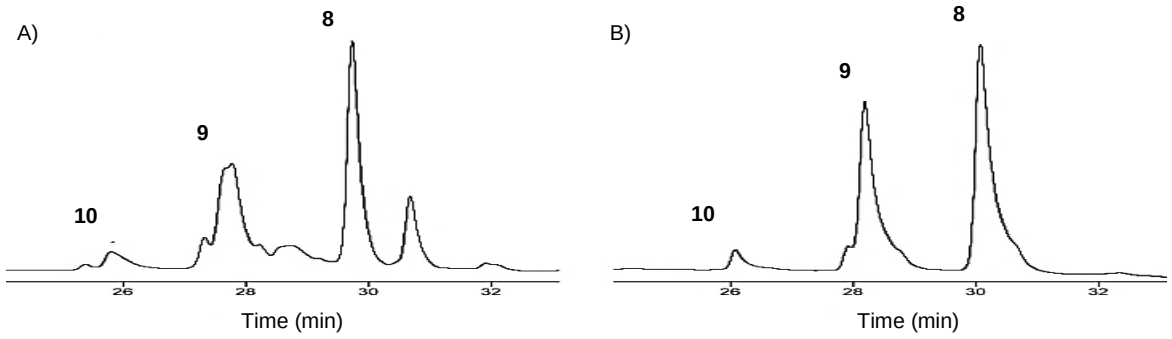

Figure 2.3. RP-HPLC analysis of A) crude **B1** consists of three main oligonucleotides (**8**, **9**, and **10**). Peak **8** corresponds to oligomer **B1**. Collection of peak **8** and reinjection produces the trace shown in panel B), suggesting that oligomers eluting as peaks **9** and **10** derive from **B2**.

Interestingly, mass analysis of crude oligomer **B1** (i.e. as isolated after cleavage from the support and before purification), detected a 15-mer oligonucleotide containing a 2'-*O*-Phe insert without the 3'-*O*-Lev ester (Table 2.2, column 3). This product did not constitute a major peak in the RP-HPLC chromatogram of the crude synthesis; however, it suggests that the rate of

Table 2.3. Three products were purified in the synthesis of **B1**.

Product	Sequence
8	5'-$t_9U_{OPhe}t_5$-3'-OLev
9	5'-$t_9U_{OH}t_5$-3'-OLev
10	5'-$t_9U_{OH}t_5$-3'-OH

hydrolysis of 2'-*O*-Phe acetal is comparable to that of the 3'-*O*-Lev group. This is in contrast to the corresponding alanine- (**A1**) and lysine-containing (**C1**) 15-mer mixtures which always contained a 3'-*O*-Lev moiety. One could infer from this that the rate of hydrolysis of lysine and alanine AAEs may be faster than that of the 3'-*O*-Phe acetals.

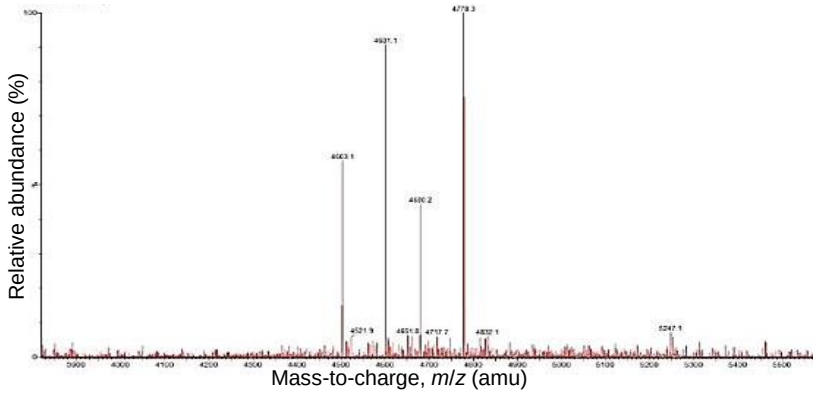

Figure 2.4. The mass spectrogram of crude **B1** reveals four compounds.

Consistent with this conclusion, fully modified alanine- and lysine-containing oligonucleotides were not detected by RP-HPLC. Both crude RP-HPLC chromatograms of the 15-mers shown in Figure 2.5 reveal two products (**9** and **10**) lacking 2'-*O*-AAEs. Furthermore, RP-HPLC reinjection of the collected and lyophilized product **9** resulted in the reappearance of product **9** in the chromatogram and a modest amount of product **10**.

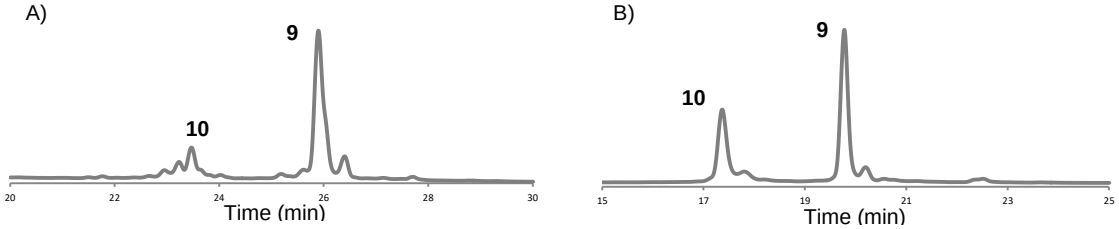

Figure 2.5. The RP-HPLC traces of crude A) **A1** and B) **C1** reveal that the 2'-*O*-Ala and 2'-*O*-Lys AAE groups are cleaved prior to purification.

Table 2.4. Two products were purified in the synthesis of **A1** and **C1**.

Product	Sequence
9	5'-$t_9U_{OH}t_5$-3'-OLev
10	5'-$t_9U_{OH}t_5$-3'-OH

The RP-HPLC chromatogram of the oligomer with three 2'-*O*-Phe AAE inserts (**B3**) was more complex, but consistent with what was previously observed for **B1**. The RP-HPLC trace of the crude oligomer consists of a mixture of five major peaks (Figure 2.6; Table 2.5). In the same fashion as described above for **B1**, isolation, lyophilization, and reinjection of major products collected (peaks **11**-**15**) revealed an oligomer with the same retention time as well as all of the lesser-retained peaks. MS analysis of these are consistent with oligonucleotides containing 1) all three 2'-*O*-Phe inserts as well as a 3'-*O*-Lev moiety (Table 2.5, **11**); 2) two 2'-*O*-Phe inserts as well as a 3'-*O*-Lev moiety (Table 2.5, **12**); 3) one 2'-*O*-Phe insert as well as a 3'-*O*-Lev moiety (Table 2.5, **13**); 4) no 2'-*O*-Phe inserts but a 3'-*O*-Lev moiety (Table 2.5, **14**); and 5) no modification whatsoever (Table 2.5, **15**). The sequences of the products listed in Table 2.5 include the possible sequence positions of 2'-*O*-Phe modifications present in products **12** and **13** (assuming that retention times of regioisomers do not vary).

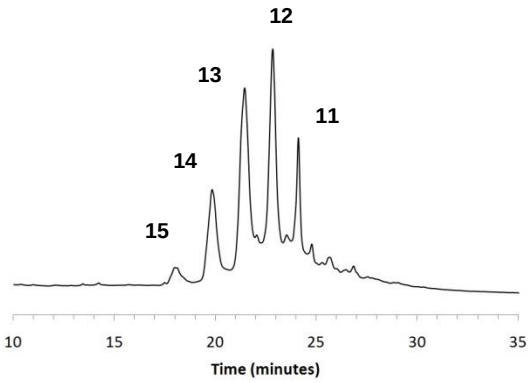

Figure 2.6. RP-HPLC trace of crude **B3** reveals five oligonucleotides.

Table 2.5. The isolation of **B3** produced several oligonucleotides with masses and HPLC profiles consistent with the oligomers listed.

Product	Sequence
11	5'-$t_5U_{OPhe}t_4U_{OPhe}t_4U_{OPhe}t_5$-3'-OLev
12	5'-$t_5U_{OPhe}t_4U_{OPhe}t_4U_{OH}t_5$-3'-OLev
	5'-$t_5U_{OPhe}t_4U_{OH}t_4U_{OPhe}t_5$-3'-OLev
	5'-$t_5U_{OH}t_4U_{OPhe}t_4U_{OPhe}t_5$-3'-OLev
13	5'-$t_5U_{OPhe}t_4U_{OH}t_4U_{OH}t_5$-3'-OLev
	5'-$t_5U_{OH}t_4U_{OPhe}t_4U_{OH}t_5$-3'-OLev
	5'-$t_5U_{OH}t_4U_{OH}t_4U_{OPhe}t_5$-3'-OLev
14	5'-$t_5U_{OH}t_4U_{OH}t_4U_{OH}t_5$-3'-OLev
15	5'-$t_5U_{OH}t_4U_{OH}t_4U_{OH}t_5$-3'-OH

2.3.1. Effect of 2'-O-Phenylalanine Acetal Ester on poly-T/poly-rA Stability

The crude samples **A1**, **B1**, and **C1** were annealed to their poly-adenosine complement in phosphate-buffered saline (PBS, pH 7.4) and thermal melting temperature (T_m) values were determined (Figure 2.7). The unmodified duplex (t_9Ut_5:A_{15}) differed from the amino acid-modified duplexes in that it contained an unmodified uridine residue in the position of the 2'-*O*-AAE uridine residue. It also did not contain a terminal 3'-*O*-Lev moiety because it was synthesized on a standard UnyLinker^{TM} support. The effect on T_m of possible levulinyl hydrolysis during data collection was assumed to be negligible since the modification was located at the terminus of the duplex.

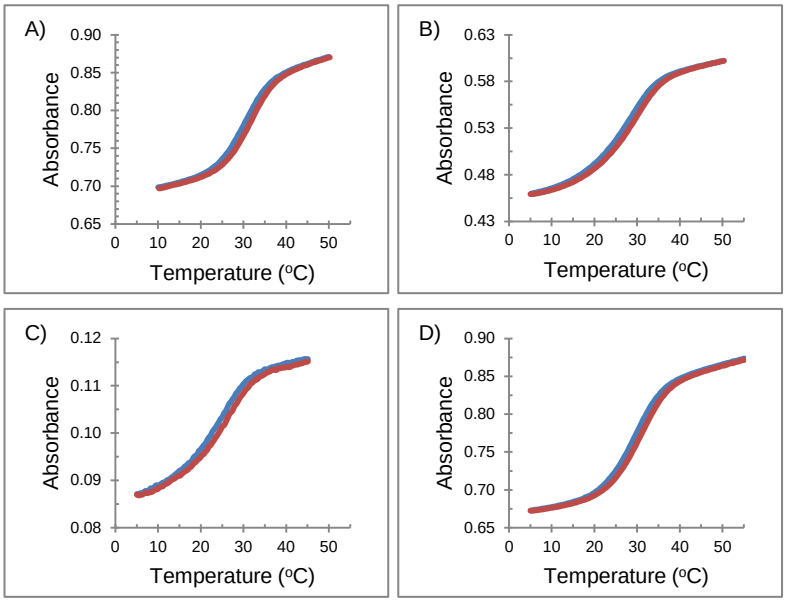

Figure 2.7. T_m curves (melting and cooling) were obtained for the duplexes of poly-adenosine annealed to A) t_9Ut_5, B) **A1**, C) **B1**, and D) **C1**.

From the HPLC and MS analyses discussed in section 2.3.1, the bulk of the oligonucleotides contained in the crude mixtures of syntheses **A1** and **C1** were expected to contain no alanine or lysine acetal esters, respectively. Any oligonucleotides in the mixture that contained 2'-*O*-AAE insertions were expected to be hydrolyzed during the 3.5-hour data collection time set for each denaturing and reannealing curve. T_m values were expected to be essentially the same as the unmodified control as a result. In reality, this was true for the duplex made from sample **C1** (ΔT_m = 0.0°C, Table 2.6). The duplex made from **A1** revealed a

destabilization of two degrees below the unmodified control (ΔT_m = -2.0°C). However, because this data was obtained from single experiments rather than triplicates, it is not possible to infer on the statistical significance of these results.

Table 2.6. T_m values were recorded for each 2'-*O*-AAE duplex containing one insert.

Duplex	T_m (°C)	ΔT_m (°C)
t_9Ut_5:A_{15}	32.0	
A1:A_{15}	30.0	-2.0
B1:A_{15}	27.0	-5.0
C1:A_{15}	32.0	0.0

The duplex made from crude sample **B1**, on the other hand, revealed a five-degree drop in T_m, suggesting again that the 2'-*O*-Phe moiety is destabilizing. This is not necessarily a disadvantage, as incorporation of the modification in a therapeutic siRNA can be placed so as to introduce a thermodynamic bias that favours the loading of the intended guide strand into the RISC complex.[16] Specifically, the manner by which Argonaute 2 selects the guide strand involves choosing the strand with the less stable 5'-end hybridization to the duplex. Consequently, the incorporation of the 2'-*O*-Phe modification nearer to the 5'-end of the guide strand or nearer to the 3'-end of the passenger strand is expected to destabilize that end of the duplex, inducing guide strand selection.[16]

2.3.2. Analysis of 2'-O-AAE Oligomers on a Denaturing Polyacrylamide Gel

To infer on the electrophoretic mobility of the conjugates, crude samples of oligonucleotides containing the smallest amino acid R group (**A6** and **A1**) were loaded onto a denaturing polyacrylamide gel and subjected to electrophoresis in parallel to unmodified strands of the same sequence (**E6** and **E1**) (Figure 2.8). Each positive charge was expected to neutralize one of the negative charges on the phosphodiester linkages, thereby lowering the mobility of the oligonucleotide one unit per 2'-*O*-alanine acetal ester. The added mass of the 2'-*O*-AAE, even if small, would also contribute to the slower electrophoretic mobility. One of the sequences tested

was a 21-nt poly-thymidine with six interspersed inserts of 2'-*O*-Ala uridine (**A6**), built using phosphoramidite **7a** in Scheme 2.5 and deprotected according to Scheme 2.6. The electrophoretic mobility of this compound was contrasted to that of a 21-mer of equivalent sequence (**E6**), synthesized on a UnyLinker^{TM} solid supoport. The other pair of sequences tested was the 15-mer comprising a single insert of 2'-*O*-Ala uridine (**A1**) and a 15-mer comprising a single insert of 2'-hydroxyl uridine (**E1**). It was predicted that the former set of oligonucleotides would display a larger difference in mobility because of the six-fold increase in positively charged inserts.

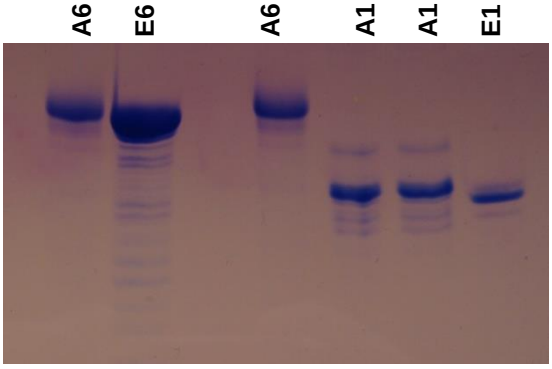

A6: 5'-ttU$_{OAla}$ ttU$_{OAla}$ ttU$_{OAla}$ ttU$_{OAla}$ ttU$_{OAla}$ ttU$_{OAla}$ ttt-3'-OLev
E6: 5'-ttU ttU ttU ttU ttU ttU ttt-3'-OH

A1: 5'-ttt ttt ttt U$_{OAla}$tt ttt-3'-OLev
E1: 5'-ttt ttt ttt Utt ttt-3'-OH

Figure 2.8. Oligonucleotides **A6** and **A1** are retained on polyacrylamide gel compared to their unmodified counterparts, **E6** and **E1**, respectively.

The modified sequences were indeed retained relative to their corresponding unmodified sequences (Figure 2.8). The slight difference in retention of the **A**-series in comparison to the corresponding **E**-series, however, was likely due to the terminal 3'-levulinyl group on the **A**-series oligonucleotides. As explored in section 2.3.1, this is a consequence of acetal ester hydrolysis in aqueous buffer. The main band of the modified 21-mer sequence (**A6**) was extracted from the gel and subjected to LC-ESI-QTOF. The deconvoluted mass peak (6373.5 amu) corresponded to the potassium adduct of the unmodified sample (6334.89 + 38.96 = 6373.85 amu); none of the six insertions of 2'-*O*-Ala AAE were detected in the crude sample. As a result of this continued inability to produce a highly modified oligonucleotide containing 2'-*O*-Ala, 2'-*O*-Lys, or 2'-*O*-Pro AAEs, the our attention was directed on the 2'-*O*-Phe AAE for further studies. Gel electrophoresis was done on a stable version of the 2'-*O*-Phe AAE in section 4.6.

Nevertheless, the gel reveals very few failure sequences (low intensity of n-1, n-2, and other truncates in the 21-mer sequence), indicating that the coupling of the 2'-*O*-Ala phosphoramidite monomers proceeds efficiently.

2.4. An Estimation of the Half-Life of the 2'-O-Phenylalanine Acetal Ester

RP-HPLC chromatograms of the purified oligomer containing one 2'-*O*-Phe insert (**B1**) shows that cleavage occurs during isolation (collection and evaporation step) and reinjection of the oligomer into the HPLC column (Figure 2.3). This comparison was done several times in order to confirm the disappearance of the most retained oligonucleotide, but it was not repeated over enough intervals to estimate a half-life of the fully modified oligonucleotide before it was completely used up. The crude mixture of oligonucleotides containing three 2'-*O*-Phe modifications (**B3**), on the other hand, was dissolved in phosphate buffered saline (PBS, pH 7.4) and incubated at 37^{o}C. Aliquots were removed after 0, 2, 5, and 20 hours, and analyzed by RP-HPLC. The resulting traces are shown in Figure 2.9. Each peak was identified as previously described (Table 2.5). As internal reference, an arrow identifies the peak corresponding to oligonucleotide intermediate **14** (5'-$t_5U_{OH}t_4U_{OH}t_4U_{OH}t_4t_{Olev}$-3'; R_t = 20 min) shown in Figure 2.6. The HPLC traces show that the relative amounts of peaks change over time with 'late' eluting peaks converting to 'early' eluting peaks, consistent with the stepwise hydrolysis of the ester moieties over time.

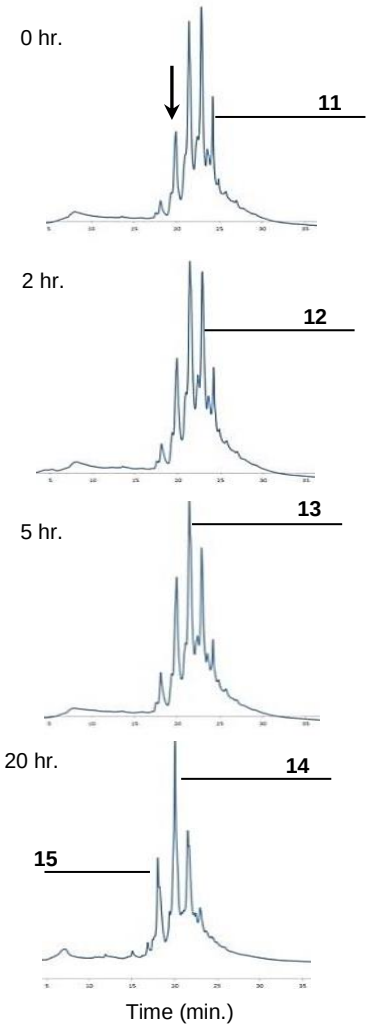

Figure 2.9. The gradual hydrolysis of **B3** in PBS occurs within hours.

At t = 0 hr, the highest peak in the sample corresponded to oligomer **12**, likely a mixture of 5'-$t_5U_{OPhe}t_4U_{OPhe}t_4U_{OH}t_4t_{Olev}$-3', 5'-$t_5U_{OPhe}t_4U_{OH}t_4U_{OPhe}t_4t_{lev}$-3', and 5'-$t_5U_{OH}t_4U_{OPhe}t_4U_{OPhe}t_4t_{Olev}$-3' (Table 2.5). After 5 hours there is only a trace of the fully modified oligomer **11** (5'-$t_5U_{OPhe}t_4U_{OPhe}t_4U_{OPhe}t_4t_{Olev}$-3'). The highest peak corresponds to the single-

modified product **13** with three possible locations of the 2'-*O*-Phe modification, specifically 5'-$t_5U_{OPhe}t_4U_{OH}t_4U_{OH}t_4t_{Olev}$-3', 5'-$t_5U_{OH}t_4U_{OPhe}t_4U_{OH}t_4t_{Olev}$-3', and 5'-$t_5U_{OH}t_4U_{OH}t_4U_{OPhe}t_4t_{Olev}$-3'. After 20 hours incubation, there is only a trace of the doubly-modified oligomer **12**. A minor peak corresponds to the singly-modified product **13** and the oligomer with only 3'-*O*-levulinyl modification (**14**) is the main peak. The fully modified oligonucleotide **11** disappeared between 5 and 20 hours. Therefore, the half-life of hydrolysis of ester groups in our oligonucleotides is roughly estimated to be on the order of several minutes to a few hours.

2.5. Exploring Different Oxidation Reagents

Another source for the premature removal of 2'-*O*-AAE groups is any synthetic step requiring an aqueous base, such as the basic iodine/water step use during oxidation of internucleotide linkages. To this end, the standard iodine oxidation reagent, which was applied in all syntheses described above, as well as alternative oxidizing reagents, were scrutinized as potential sources for removing 2'-*O*-AAE groups. We were especially curious about hydrolysis of the 2'-*O*-Phe modification in the iodine solution since it contains pyridine (a weak base) and water. ^{31}P-NMR was used to follow the reaction progress of coupling the 2'-*O*-Phe-modified uridine phosphoramidite to a dideoxythymidine (ddT) nucleoside in solution, and the *in situ* oxidation of the P(III) species to a P(V) species (Scheme 2.7).

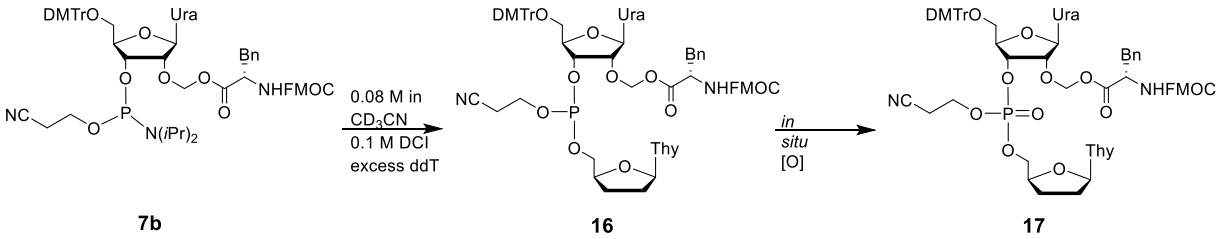

Scheme 2.7. Solution-phase synthesis of dimers containing 2'-*O*-Phe was used to assess the stability of the modification to various oxidation conditions.

With the standard iodine oxidation conditions (0.1 M I_2 in 8:16:76 py/H_2O/tetrahydrofuran (THF)), the ^{31}P-NMR revealed two peaks around -2.5 ppm corresponding to the expected diastereoisomers of the oxidized phosphorus (Figure 2.10). Application of two anhydrous oxidation solutions, 0.1 M *tert*-butylhydroperoxide (*tert*-BuOOH) in toluene[17,18] and 0.5 M (1*S*)-(+)-(10-camphorsulfonyl)-oxaziridine (CSO) in MeCN,[19] revealed

the same peaks. Application of anhydrous *N*-bromosuccinamide (NBS)/DMSO/MeCN (0.02:0.2:1 w/v/v)[20] revealed a doubling of each of the expected diastereoisomeric peaks, consistent with an additional side reaction possibly occurring in this case.

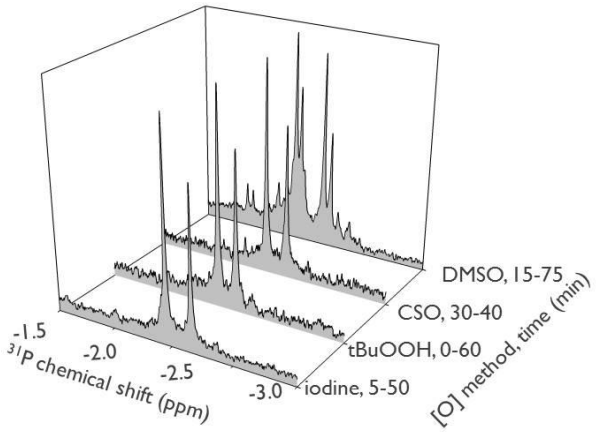

Figure 2.10. ^{31}P-NMR of the oxidation of dimer **16** by various reagents, including standard aqueous I_2 oxidation solution, *tert*-BuOOH, and CSO solutions as acceptable reagents.

ESI-MS data of the intact dimer **17** could be seen with all four oxidation conditions, including NBS/DMSO (Table 2.7). However, the latter reagent led to extra unidentified peaks of lower mass (Table 2.7). The crude reaction mixture of the dimer oxidized with CSO was then subjected to NEt_3, required for cyanoethyl and FMOC removal, and yielding the free amine with the acetal ester still intact (Table 2.7, entry 5).

The crude mixtures of the dimer oxidized with iodine, *tert*-BuOOH, and CSO were purified by RP-HPLC. The retention times of the main peaks for these three successful oxidation conditions are in agreement (Figure 2.11A-C), indicating that the desired product **17** was synthesized. As an excess of ddT nucleoside was used during synthesis of dimer **16** to consume all of the 2'-*O*-Phe phosphoramidite **7c**, the nucleoside is also visible in the HPLC traces (t = 6.9 min). The dimer oxidized by all three reagents also reveals the same retention time in the traces (t = 7.2 min), confirming that the same dimer was produced by each reagent.

Table 2.7. Crude mass values reveals that oxidations on dimer **16** was largely successful.

Entry	Reagent	Mass calc. [M + Na^+]	Mass found [M + Na^+]
1	I_2	1311.43	1309.28
2	*tert*-BuOOH		1309.25
3	CSO		1309.35
4	DMSO		1309.19, 1064.84
5	CSO; NEt_3	1036.33	1037.66

In conclusion, these experiments reveal that standard 4,5-dicyanoimidazole (DCI) coupling reagent and iodine/water oxidation reagent are suitable for the coupling of the 2'-*O*-Phe phosphoramidite and the oxidation of the resulting P(III) linkage. These reagents do not trigger the hydrolysis of the 2'-*O*-Phe groups. Therefore, the same coupling and oxidation reagents were repeated for all subsequent syntheses of pro-oligonucleotides.

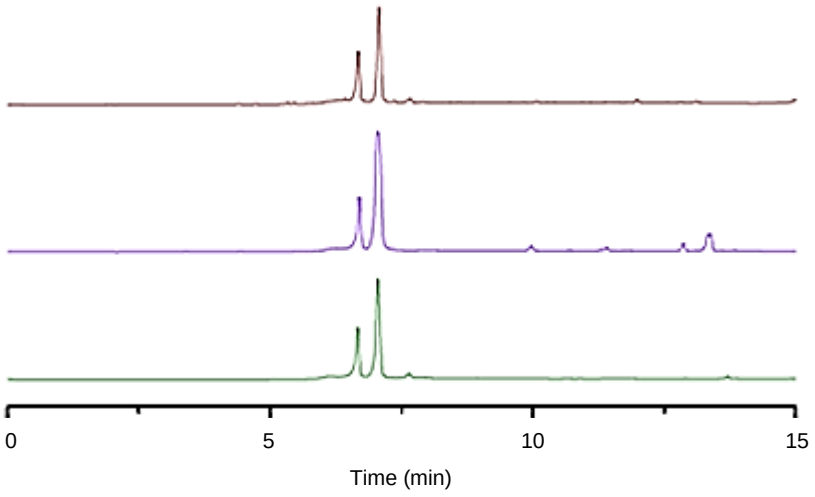

Figure 2.11. RP-HPLC traces of crude reaction mixtures after oxidation of **16** with A) I_2/water/py; B) *tert*-BuOOH; and C) CSO to produce **17**, confirmed by mass analysis.

2.6. A Plausible Hydrolysis Mechanism

The 2'-*O*-Phe AAE-modified oligonucleotides experience hydrolysis in buffered water (section 2.4). This observation, together with experiments performed on model dimers (section 2.4.2) indicates that this occurs more readily when the amino group is free (no protecting group). A plausible mechanism shown in Scheme 2.8 involves a general-acid catalyzed hydrolysis reaction. The protonated amino group serves as Brønsted acid, hence catalyzed nucleophilic addition of water at the carbonyl carbon. This predicts that an acetal ester lacking the cis alpha amino group altogether would be more resistant to hydrolysis. Hence, it was of interest to determine the stability of the ester derived from hydrocinnamic acid (HCA). The synthesis of the nucleoside 2'-*O*-HCA acetal ester is shown in Scheme 2.9. First, nucleoside intermediate **3** was activated by sulfuryl chloride and coupled *in situ* to the cesium salt of HCA. Desilylation of **4e** was done in high yield with treatment of NEt_3-3HF. Nucleoside **5e** was dimethoxytritylated and phosphitylated to give the phosphoramidite **7e**. This phosphoramidite was coupled to a poly-thymidine oligonucleotide grown on a variation of the photocleavable solid support, provided by Dr. Mathew Hassler, which left behind a terminal 3'-phosphate after cleavage (Scheme 2.10).

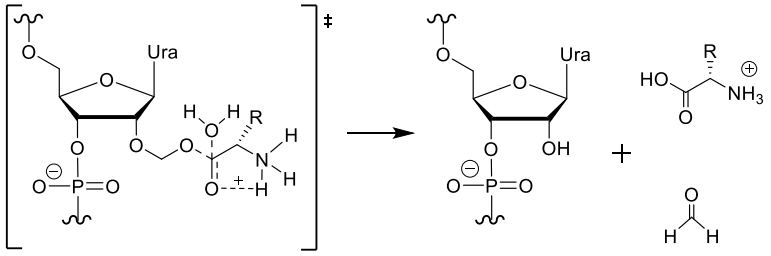

Scheme 2.8. Proposed mechanism of 2'-*O*-AAE hydrolysis. Water the nucleophile and the amino acid amino group serves as an internal general acid.

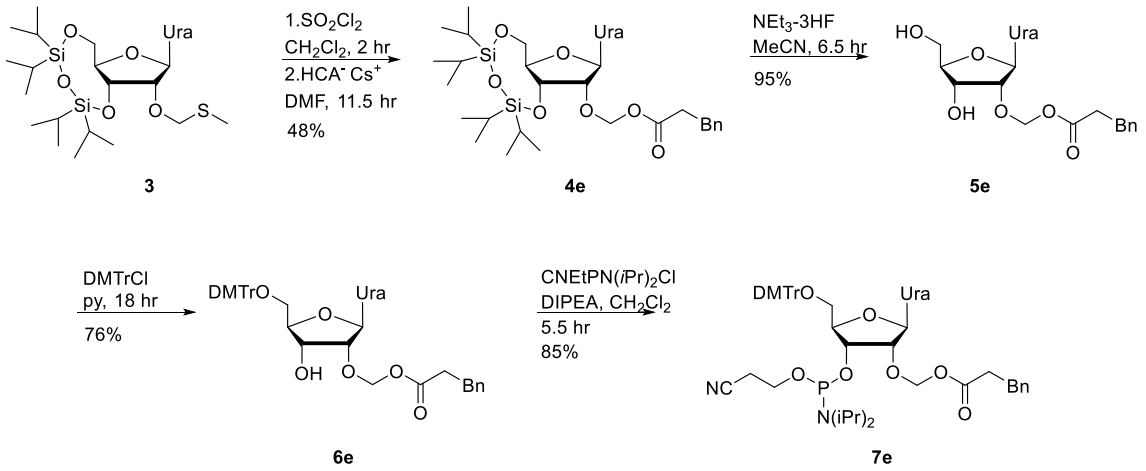

Scheme 2.9. The synthesis of phosphoramidite monomers with 2'-*O*-HCA modification was done starting from the 2'-*O*-2-methylthiomethylene ether of uridine nucleoside **3**.

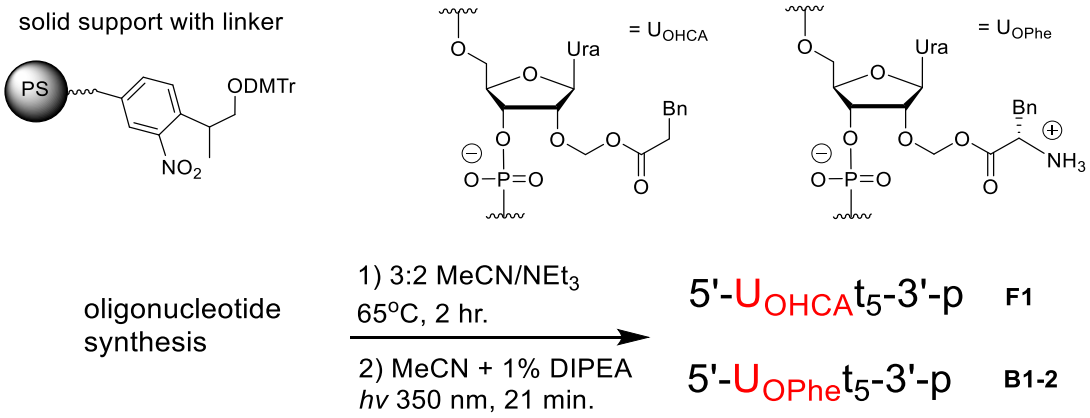

Scheme 2.10. Solid-phase synthesis of 2'-*O*-HCA- and 2'-*O*-Phe AAE-modified oligonucleotides starting from a photocleavable solid support.

Following oligonucleotide synthesis and deprotection, the resulting oligonucleotide **F1** was dissolved in PBS at 37°C and analyzed by LC-ESI-QTOF. No change in the ratio of hydrolyzed product **19** (minor component) versus HCA oligomer product **18** occurred after 32 hours (Figure 2.12, Table 2.8). This is in stark contrast to the lack of stability of the 2'-*O*-AAE-containing oligonucleotides previously observed, consistent with the notion that a neighboring (alpha) ammonium ion accelerates the hydrolysis of AAE moieties.

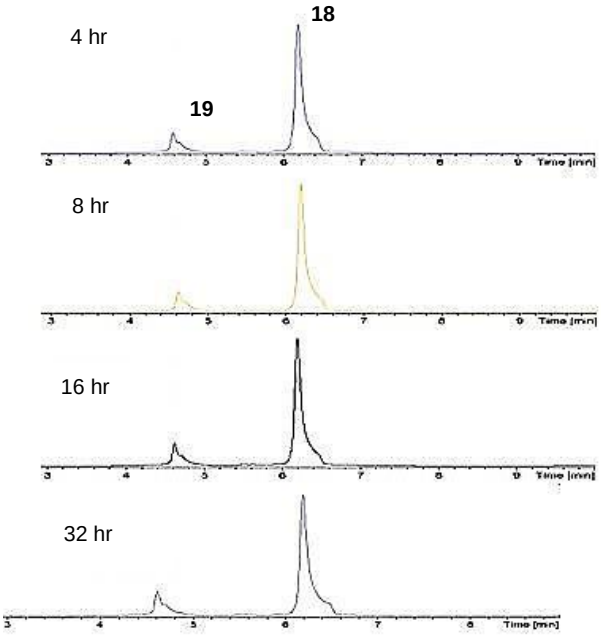

Figure 2.12. RP-HPLC indicates that the hydrolysis of **F1** does not increase over 32 hours in PBS buffer at 37°C.

Table 2.8. The mass values of the peaks seen in the RP-HPLC traces of **F1** incubated in PBS.

Peak	Oligomer	Mass calc. [M]	Mass found [M]
18	5'-$U_{OHCA}t_5$-3'-p	2006.3341	2006.3432
19	5'-$U_{OH}t_5$-3'-p	1844.2661	1844.2350

2.7. Oligonucleotides Containing 2'-O-Phenylalanine Acetal Esters Can Be Purified Intact

The studies described above revealed that while hydrolysis of 2'-*O*-Phe AAE moieties in aqueous solution is inevitable, it likely does not happen during the oligonucleotide synthesis cycle. If it did, one would likely observe shorter oligomer fragments resulting from the release of the 2'-hydroxyl which would then attack the vicinal 3',5'-phosphate triester linkage. Considering the repeatedly well-resolved, narrow peaks in RP-HPLC chromatograms of 2'-*O*-Phe conjugates indicates that hydrolysis occurs during handling of the oligomers in aqueous buffers rather than inside the HPLC column. To test this further, a poly-thymidine oligonucleotide containing a 2'-*O*-Phe AAE uridine insert was synthesized on solid support (Scheme 2.10).

This time, the FMOC and cyanoethyl eliminations were performed in a dry round bottom flask (instead of a polypropylene centrifuge tube) and dried by evaporation *in vacuo*. Photocleavage was done in a dry quartz tube with anhydrous MeCN +1% DIPEA, as was done previously. Next, the beads were washed exclusively with dry DMSO (instead of H_2O: ethanol (EtOH): MeCN 3:1:1 v/v/v) to separate crude sample **B1-2** from the solid support. Dilution of the crude sample was also performed with DMSO instead of H_2O. The DMSO-dissolved sample spent minimal time in the sample injector and was then loaded onto the RP-HPLC column (Figure 2.13). The mass of the single, clean peak **20** corresponded to the desired compound (Table 2.9) while no hydrolyzed compound was detected (indicated by the arrow in Figure 2.13).

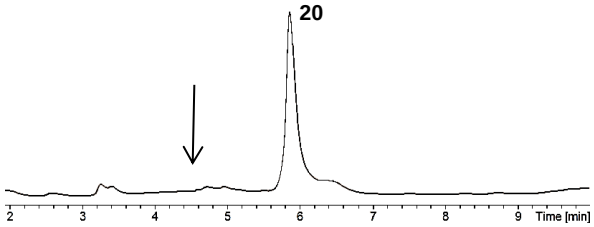

Figure 2.13. The RP-HPLC profile of **B1-2** is free of hydrolyzed product.

Next, crude **B1-2** was dissolved in PBS at 37^{o}C and RP-HPLC was performed after 4, 8, 16, and 32 hours (Figure 2.14). Mass values of peaks **20** and **19** confirm that product **20** corresponds to the intact oligonucleotide, while peak **19** corresponds to the hydrolyzed product

(Table 2.9). These results indicate that estimated half-life of hydrolysis of the 2'-*O*-Phe AAE moiety in this oligomer is about 16 hours.

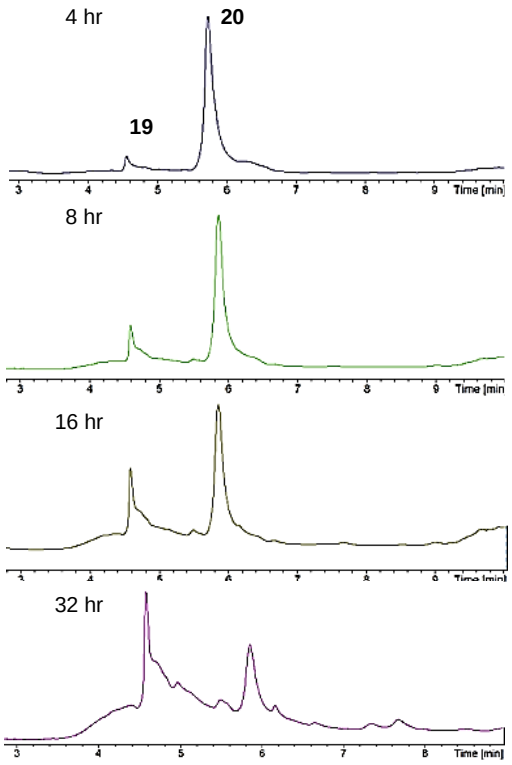

Figure 2.14. The RP-HPLC traces of **B1-2** show appreciable degradation after 32 hours in PBS buffer.

Table 2.9. The mass values of the peaks seen in the RP-HPLC traces of **B1-2** incubated in PBS.

Peak	Oligomer	Mass calc. [M]	Mass found [M]
20	5'-$U_{OPhe}t_5$-3'-p	2021.3450	2021.3134
19	5'-$U_{OH}t_5$-3'-p	1844.2661	1844.2350

2.8. Conclusion

Poly-thymidine oligonucleotides containing 2'-*O*-AAE modifications based on alanine, phenylalanine, lysine, and proline were synthesized on an orthogonal photocleavable solid

support. RP-HPLC purification of the oligonucleotides revealed that non-anhydrous deprotection conditions followed by aqueous handling of the crude reaction mixtures caused premature hydrolysis of the 2'-*O*-AAE moieties. RP-HPLC analysis suggested that the 2'-*O*-Phe AAE modification was the most stable to hydrolysis among the others studied; nevertheless, it underwent hydrolysis in RP-HPLC and gel electrophoresis buffers.

The 2'-*O*-AAE oligonucleotides are more retained on polyacrylamide gels and RP-HPLC, and hybridized with lower affinity to a target RNA strand, relative to the unmodified oligonucleotide of the same length and sequence. Finally, the slower hydrolysis observed for hydrocinnamic-based acetal esters suggests that the alpha amino group acts as a general acid catalyst in the hydrolysis of the 2'-*O*-AAE moiety. With this knowledge, a 2'-*O*-Phe AAE-containing oligonucleotide was synthesized, deprotected under anhydrous conditions, and rapidly injected into an HPLC column with minimal loss of the 3'-*O*-Phe AAE moiety. Follow up incubation in PBS buffer at 37^{o}C resulted in the slow but clean release of the 2'-hydroxyl group. These observations, together with studies reported in chapters 3–5, represent important steps towards the development of RNA prodrugs.

2.9. Experimental Methods

2.9.1. General Procedures for Monomer Synthesis

^{1}H-NMR and ^{13}C-NMR spectra were recorded at 400 MHz and 300 MHz, respectively, using the residual solvent peak as an internal standard ($CDCl_3$, CD_3CN, CD_3OD, $(CD_3)_2SO$, $(CD_3)_2CO$). ^{1}H-NMR spectra were assigned using 2D ^{1}H-NMR (COSY) spectra. ^{31}P-NMR spectra were recorded at 200 MHz using 85% H_3PO_4 as an external standard. The characterization (e.g. NMR) of known and commercially available compounds was in agreement with previously published data. Reactions were monitored by TLC on alumina plates coated with silica gel and visualized with UV light and charring with H_2SO_4. Preparative chromatography was performed with 40-60 μm, 230-400 mesh silica gel. DMF and DMSO was dried over 3Å molecular sieves for at least 48 hr. CH_2Cl_2, THF, and MeCN were dried on an mBraun SPS solvent purification system. Pyridine, NEt_3, and DIPEA were distilled from CaH_2. Where yields for monomer syntheses have been reported as an average in the previous sections, one example is described below.

2.9.2. Synthesis of Novel Monomers

3',5'-(1,1,3,3-tetraisopropyldisiloxane-1,3-diyl)-2'-*O*-[acetal-*N*-(9-fluorenyl-methyoxycarbonyl)-L-phenylalanine ester] uridine (4b): 2'-*O*-[(methylthio)methyl]-3',5'-*O*-[1,1,3,3-tetrakis(1-methylethyl)-1,3-disiloxanediyl]-uridine (**3**) (499 mg, 0.913 mmol) was dissolved in CH_2Cl_2 (10 mL) and stirred at 0^oC under N_2. SO_2Cl_2 (1 M in CH_2Cl_2, 1.0 mL) was added dropwise over 10 minutes. The solution was stirred at 0^oC for 30 min, brought to ambient temperature, and continued stirring over 1.5 hr. The solution was concentrated *in vacuo* under N_2 and dried to a white foam under high vacuum for 20 min. In a separate flask, *N*-(9-fluorenylmethoxycarbonyl)-L-phenylalanine (549 mg, 1.42 mmol) was dissolved in DMF (7 mL), and $CsHCO_3$ (265 mg, 1.37 mmol) was added. The mixture was stirred at r.t. for 2.5 h. The dried nucleoside was then redissolved in CH_2Cl_2 (3 mL) and transferred by cannula to the round bottom flask of *N*-(9-fluorenylmethoxycarbonyl)-L-phenylalanine monocesium salt in DMF. The flask was rinsed with CH_2Cl_2 (2 mL) that was transferred by cannula to the reaction mixture. The mixture was stirred at r.t. under N_2 for 18 hr and quenched by addition of saturated aqueous $NaHCO_3$. The layers were separated and the organic layer was washed twice with saturated aqueous $HaHCO_3$. The combined aqueous layers were extracted twice with CH_2Cl_2. The combined organic layers were dried with $MgSO_4$, filtered, and concentrated. The residue was purified by silica gel chromatography using a gradient ending in 7:3 hexanes/EtOAc to give **4b** (630 mg, 78%) as an amorphous while solid. ^{1}H-NMR ($CDCl_3$): δ 8.53 (s, 1H), 7.82 (d, *J* = 8.2 Hz, 1H), 7.76 (d, *J* = 7.6 Hz, 2H), 7.57 (d, *J* = 7.3 Hz, 2H), 7.38 – 7.41 (m, 2H), 7.34 – 7.17 (m, 5H), 7.14 (d, *J* = 7.2 Hz, 2H), 5.55 – 5.73 (m, 3H), 5.54 (s, 2H), 4.76 (dd, *J* = 14.5, 6.1 Hz, 1H), 4.45 (dd, *J* = 10.5, 7.1 Hz, 1H), 4.13 – 4.29 (m, 4H), 4.10 (d, *J* = 9.5 Hz, 1H), 4.06 (d, *J* = 4.0 Hz, 1H), 3.97 (dd, *J* = 13.6, 2.0 Hz, 1H), 3.17 (ddd, *J* = 20.4, 14.0, 6.0 Hz, 2H), 1.15 – 0.94 (m, 28H). ^{13}C-NMR ($CDCl_3$): δ 171.1, 162.9, 155.8, 149.5, 143.9, 143.8, 141.30, 141.29, 139.0, 136.1, 129.6, 128.4, 127.7, 127.0, 126.9, 125.2, 125.0, 119.9, 101.7, 89.3, 89.1, 81.7, 81.5, 67.8, 66.7, 59.2, 54.9, 47.2, 37.8, 29.7, 17.43, 17.36, 17.26, 17.2, 17.1, 17.0, 16.9, 16.8, 13.5, 13.0, 12.9, 12.6. ESI-QTOF calc. for $C_{46}H_{59}N_3O_{11}Si_2$ [M+Na]: 908.36; found: 908.40.

3',5'-*O*-(1,1,3,3,-tetraisopropyldisiloxane-1,3-diyl)-2'-*O*-[acetal-*N*-(9-fluorenyl-methoxycarbonyl)-L-alanine ester] uridine (4a): Same procedure as for **4b**. ^{1}H-NMR ($CDCl_3$) δ 8.21 (s, 1H), 7.85 (d, *J* = 8.2 Hz, 1H), 7.75 (d, *J* = 7.5 Hz, 2H), 7.59 – 7.62 (m, 2H), 7.39 (t, *J* =

7.5 Hz, 2H), 7.30 (t, *J* = 7.5 Hz, 2H), 5.72 (s, 1H), 5.68 (d, *J* = 8.2, 1H), 5.57 (ABq, *J* = 6.5 Hz, 1H each), 4.46 – 4.52 (m, 1H), 4.34 – 4.43 (m, 2H), 4.18 – 4.26 (m, 4H), 4.11 (d, *J* = 8.8, 1H), 3.97 (dd, *J* = 13.4, 1.6 Hz, 1H), 1.48 (d, *J* = 7.5, 3H), 1.21 – 1.28 (m, 4H), 1.02 – 1.10 (m, 24H). ^{13}C-NMR ($CDCl_3$) δ 172.6, 162.6, 155.8, 149.6, 143.92, 143.81, 141.29, 141.28, 139.1, 127.7, 127.0, 125.11, 125.08, 120.0, 101.7, 89.1, 88.7, 81.6, 67.8, 67.0, 59.2, 49.7, 47.1, 29.7, 17.44, 17.37, 17.27, 17.20, 17.1, 16.94, 16.93, 16.8, 13.4, 13.0, 12.8, 12.5. ESI-QTOF calc. for $C_{40}H_{55}N_3O_{11}Si_2$ [M+Na]: 832.33; found: 832.37.

3',5'-*O*-(1,1,3,3,-tetraisopropyldisiloxane-1,3-diyl)-2'-*O*-[acetal-*N*-(9-fluorenyl-methoxycarbonyl)-L-lysine ester] uridine (4c): Same procedure as for **4b**, except that the residue was purified by silica gel chromatography using a gradient ending with 6:4 hexanes/EtOAc. ^{1}H-NMR ($CDCl_3$) δ 9.58 (s, 1H), 7.70 – 7.78 (m, 4H), 7.56 – 7.62 (m, 4H), 7.34 – 7.42 (m, 4H), 7.26 – 7.32 (m, 4H), 5.72 (s, 1H), 5.68 (d, *J* = 4.9 Hz, 1H), 5.62 (d, *J* = 6.3 Hz, 1H), 5.49 (d, *J* = 6.5 Hz, 1H), 5.07 – 5.12 (m, 1H), 4.46 – 4.53 (m, 2H), 4.36 – 4.44 (m, 3H), 4.16 – 4.28 (m, 4H), 4.09 – 4.14 (m, 1H), 3.93 – 3.99 (m, 1H), 3.18 – 3.33 (m, 2H), 2.03 (br s, 2H), 1.75 (br s, 2H), 1.61 (s, 4H), 1.50 (bs, 2H), 0.991 – 1.127 (m, 24H). ^{13}C-NMR ($CDCl_3$) δ 172.1, 163.1, 156.7, 156.3, 150.1, 149.6, 143.9, 141.30, 141.27, 138.6, 127.7, 127.67, 127.55, 127.0, 125.1, 120.0, 119.93, 119.87, 102.0, 101.9, 88.9, 88.5, 81.6, 81.1, 75.2, 68.1, 68.0, 66.7, 59.2, 54.0, 47.3, 47.1, 40.3, 29.7, 29.2, 22.3, 17.5, 17.4, 17.3, 17.2, 17.1, 17.00, 16.95, 16.8, 13.5, 13.0, 12.8, 12.6. ESI-QTOF calc. for $C_{58}H_{72}N_4O_{13}Si_2$ [M+Na]: 1111.45; found: 1111.45.

3',5'-*O*-(1,1,3,3,-tetraisopropyldisiloxane-1,3-diyl)-2'-*O*-[acetal-*N*-(9-fluorenyl-methoxycarbonyl)-L-proline ester] uridine (4d): Same procedure as for **4c**, except that *N*-(9-fluorenylmethoxycarbonyl)-L-proline monocesium salt in DMF was added in portions to the nucleoside redissolved in CH_2Cl_2. ^{1}H-NMR ($(CD_3)_2SO$) δ 11.36 – 11.47 (m, 1H), 7.85 - 7.91 (m, 2H), 7.77 – 7.85 (m, 1H), 7.59 – 7.68 (m, 1H), 7.52 – 7.59 (m, 1H), 7.23 – 7.44 (m, 4H), 5.57 – 5.64 (m, 1H), 5.45 – 5.57 (m, 2H), 5.33 – 5.39 (m, 1H), 5.09 – 5.19 (m, 2H), 4.39 – 4.47 (m, 1H), 4.19 – 4.33 (m, 5H), 4.04 – 4.17 (m, 3H), 3.82 – 3.94 (m, 2H), 2.06 – 2.26 (m, 2H), 1.69 – 1.99 (m, 4H), 0.93 – 1.08 (m, 24H). ^{13}C-NMR ($(CD_3)_2CO$) δ 172.65, 164.12, 155.15, 150.98, 145.15, 145.06, 144.92, 142.05, 140.23, 140.07, 128.49, 127.92, 126.13, 126.05, 125.89, 120.77, 120.70, 101.94, 90.01, 88.72, 82.28, 81.61, 80.87, 69.62, 69.43, 67.93, 60.06, 47.89,

25.06, 23.96, 17.91, 17.74, 17.47, 17.38, 14.23, 14.01, 13.65, 13.70, 13.65, 13.60, 13.34, 13.30. ESI-QTOF calc. for $C_{42}H_{57}N_3O_{11}Si_2$ [M+Na]: 858.34; found: 858.21.

3',5'-(1,1,3,3-tetraisopropyldisiloxane-1,3-diyl)-2'-*O*-(acetal hydrocinnamic ester) uridine (4e): Same procedure as for **4b**, except that the residue was purified by silica gel chromatography with a gradient of 10 – 80% EtOAc in hexanes. ^{1}H-NMR ($(CD_3)_2SO$) δ 11.43 (s, 1H), 7.65 (d, *J* = 8.24 Hz, 1H), 7.27 (d, *J* = 7.32 Hz, 2H), 7.14 – 7.24 (m, 3H), 5.61 (s, 1H), 5.52 – 5.58 (m, 1H), 5.42 (q, *J* = 6.41 Hz, 2H), 4.43 (d, *J* = 4.58 Hz, 1H), 4.28 (dd, *J* = 9.16, 4.88 Hz, 1H), 4.14 (br d, *J* = 12.82 Hz, 1H), 3.88 – 4.01 (m, 2H), 2.82 – 2.91 (m, 2H), 2.57 – 2.75 (m, 2H), 0.98 – 1.09 (m, 2H). ^{13}C-NMR ($(CD_3)_2CO$) δ 172.14, 163.74, 150.52, 140.83, 140.05, 128.81, 128.65, 126.54, 101.55, 89.59, 87.99, 81.32, 80.48, 68.41, 60.14, 35.55, 30.40, 17.79, 17.57, 17.46, 17.30, 17.48, 13.15, 12.79, 12.69, 12.40. ESI-QTOF calc. for $C_{31}H_{48}N_2O_9Si_2$ [M+Na]: 671.28; found: 671.48.

2'-*O*-[acetal-*N*-(9-fluorenylmethoxycarbonyl)-L-phenylalanine ester] uridine (5b): 3',5'-(1,1,3,3-tetraisopropyldisiloxane-1,3,-diyl)-2'-[*O*-acetal-*N*-(9-fluorenyl-methyoxycarbonyl)-L-phenylalanine ester] uridine (**4b**) (247 mg, 0.28 mmol) was dissolved in MeCN (3 mL) and a solution of NEt_3-3HF (0.160 mL, 0.98 mmol) in MeCN (5 mL) was added dropwise and stirred at r.t. for 18 hr. The mixture was concentrated and the residue was purified by silica gel chromatography using isocratic elution with EtOAc to give **5b** (109 mg, 61%) as an amorphous white solid. ^{1}H-NMR (CD_3CN) δ 9.36 (s, 1H), 7.88 (d, *J* = 8.1 Hz, 1H), 7.83 (d, *J* = 7.6 Hz, 2H), 7.61 (dd, *J* = 13.3, 8.6 Hz, 2H), 7.42 (t, *J* = 7.5 Hz, 2H), 7.18 – 7.38 (m, 7H), 6.20 (d, *J* = 8.3 Hz, 1H), 5.91 (d, *J* = 3.8, 1H), 5.64 (d, *J* = 8.1 Hz, 1H), 5.46, 5.41 (ABq, *J* = 6.4 Hz, 1H each), 4.46 (tt, *J* = 11.1, 5.5 Hz, 1H), 4.15 – 4.32 (m, 5H), 3.96 – 3.97 (m, 1H), 3.77 – 3.87 (m, 1H), 3.68 – 3.72 (m, 1H), 3.51 – 3.45 (m, 1H), 3.41 – 3.35 (m, 1H), 3.20 (dd, *J* = 14.0, 4.8 Hz, 1H), 2.95 (dd, *J* = 13.9, 9.6 Hz, 1H). ^{13}C-NMR (CD_3OD) δ 171.4, 164.7, 156.9, 150.7, 143.8, 141.1, 137.0, 128.9, 128.1, 127.3, 126.7, 126.4, 124.9, 124.8, 119.5, 101.2, 89.0, 88.1, 84.4, 81.7, 68.4, 66.6, 60.1, 60.0, 55.6, 36.8, 19.5, 13.1. ESI-QTOF calc. for $C_{34}H_{33}N_3O_{10}$ [M+Na]: 666.21, found: 666.22.

2'-*O*-[acetal-*N*-(9-fluorenylmethoxycarbonyl)-L-alanine ester] uridine (5a): Same procedure as for **5b**, except that the residue was purified by silica chromatography using a gradient ending with 95:5 CH_2Cl_2/MeOH. ^{1}H-NMR (CD_3CN) δ 9.13 (s, 1H), 7.86 (d, *J* = 8.1

Hz, 3H), 7.69 (dd, *J* = 7.0, 2.5 Hz, 2H), 7.44 (t, *J* = 7.4 Hz, 2H), 7.36 (dt, *J* = 7.4, 0.9 Hz, 2H), 6.23 (d, *J* = 7.0 Hz, 1H), 5.88 (d, *J* = 4.5 Hz, 1H), 5.62 (d, *J* = 8.1 Hz, 1H), 5.46, 5.37 (ABq, *J* = 6.5 Hz, 1H each), 4.32 – 4.40 (m, 2H), 4.18 – 4.32 (m, 4H), 3.93 – 3.98 (m, 1H), 3.77 – 3.81 (m, 1H), 3.65 – 3.70 (m, 1H), 3.49 (d, *J* = 5.5 Hz, 1H), 3.36 (t, *J* = 5.0 Hz, 1H), 1.37 (d, *J* = 7.2 Hz, 3H). ^{13}C-NMR (CD_3CN) δ 172.4, 162.9, 150.6, 144.1, 141.2, 140.5, 127.7, 127.15, 127.15, 127.13, 125.2, 120.0, 101.9, 88.9, 87.4, 84.9, 81.8, 69.1, 66.5, 60.6, 49.9, 47.0, 16.4. ESI-QTOF calc. for $C_{28}H_{29}N_3O_{10}$ [M+Na]: 590.18; found: 590.21.

2'-*O*-[acetal-*N*-(9-fluorenylmethoxycarbonyl)-L-lysine ester] uridine (5c): Same procedure as for **5a**. ^{1}H-NMR (CD_3CN) δ 9.15 (s, 1H), 7.81 – 7.89 (m, 5H), 7.66 (t, *J* = 8.1 Hz, 4H), 7.39 – 7.46 (m, 4H), 7.31 – 7.37 (m, 4H), 4.27 – 4.38 (m, 5H), 4.17 – 4.27 (m, 3H), 7.10 – 4.17 (m, 1H), 3.92 – 3.97 (m, 1H), 3.77 – 3.82 (m, 1H), 3.68 (qABq, *J* = 12.1, 2.6 Hz, 1H), 3.47 (d, *J* = 5.7 Hz, 1H), 3.36 (t, *J* = 5.0 Hz, 1H), 3.08 – 3.16 (m, 1H), 1.70 (br s, 1H), 1.50 (br s, 1H), 1.40 (br s, 1H). ^{13}C-NMR (CD_3CN): δ 171.9, 162.9, 156.7, 156.3, 150.6, 144.3, 144.2, 144.1, 144.0, 141.1, 140.4, 128.3, 127.7, 127.6, 127.13, 127.11, 127.08, 125.20, 125.16, 120.00, 119.99, 119.96, 101.8, 88.9, 87.5, 84.8, 81.7, 68.99, 68.98, 66.4, 66.0, 60.5, 54.2, 48.9, 47.2, 47.0, 39.9, 30.3, 29.0, 22.4. ESI-QTOF calc. for $C_{46}H_{46}N_4O_{12}$ [M+Na]: 869.30; found: 869.38.

2'-*O*-[acetal-*N*-(9-fluorenylmethoxycarbonyl)-L-proline ester] uridine (5d): Same procedure as for **5b**. The mixture was concentrated and the residue was purified by silica gel chromatography using isocratic elution of 10% MeOH in CH_2Cl_2. ^{1}H-NMR (CD_3CN) δ 7.81 – 7.89 (m, 2H), 7.68 (dd, *J* = 7.23, 4.10 Hz, 1H), 7.57 – 7.63 (m, 1H), 7.27 – 7.50 (m, 5H), 5.89 (d, *J* = 5.08 Hz, 0.5H), 5.84 (d, *J* = 4.30 Hz, 0.5H), 5.78 (d, *J* = 2.34 Hz, 1H), 5.58 – 5.70 (m, 1H), 5.48 (d, *J* = 6.25 Hz, 0.5H), 5.39 (d, *J* = 6.25 Hz, 0.5H), 5.30 (d, *J* = 6.64 Hz, 0.5H), 5.16 (d, *J* = 6.25 Hz, 0.5H), 5.10 (d, *J* = 1.95 Hz, 0.5H), 4.75 (1H), 4.19 – 4.47 (m, 5H), 4.11 – 4.19 (m, 1H), 3.89 – 4.00 (m, 1H), 3.73 – 3.85 (m, 1H), 3.60 – 3.70 (m, 2H), 3.29 – 3.57 (m, 2.5H), 2.14 – 2.33 (m, 1H), 1.68 – 1.86 (m, 1.5H). ESI-QTOF calc. for $C_{30}H_{31}N_3O_{10}$ [M+Na]: 616.19; found: 616.20.

2'-*O*-(acetal hydrocinnamic ester) uridine (5e): Same procedure as for **5a**. ^{1}H-NMR (CD_3CN) δ 9.89 - 10.34 (m, 1 H), 8.04 (br dd, *J* = 7.82, 2.74 Hz, 1 H), 7.14 - 7.21 (m, 1 H) 7.25 (br s, 3 H), 5.99 (br d, *J* = 3.52 Hz, 1 H), 5.54 - 5.71 (m, 1 H), 5.32 - 5.48 (m, 2 H), 4.30 - 4.50

(m, 3 H), 4.16 (br s, 1 H), 4.01 (br s, 1 H), 3.75 - 3.95 (m, 2 H), 2.91 (br d, *J* = 2.74 Hz, 2 H), 2.58 - 2.75 (m, 2 H). ESI-QTOF calc. for $C_{19}H_{22}N_2O_8$ [M+Na]: 406.14; found: 406.01.

5'-*O*-(4,4'-dimethoxytrityl)-2'-*O*-[acetal-*N*-(9-fluorenylmethoxycarbonyl)-L-phenylalanine ester] uridine (6b): Nucleoside **5b** (433 mg, 673 μmol) was dissolved in pyridine (1.1 mL) and 4,4'-dimethoxytrityl chloride (250 mg, 738 μL) and $AgNO_3$ (137 mg, 806 mmol) were added. After 3 hr the reaction was diluted with CH_2Cl_2 and washed with saturated aqueous $NaHCO_3$. The aqueous layer was extracted with CH_2Cl_2 and the combined organic layers were dried over $MgSO_4$, filtered, and dried *in vacuo*. The product was purified by silica gel chromatography using a gradient ending with 2:3 hexanes/EtOAc (+1% py). ^{1}H-NMR ($CDCl_3$) δ 9.13 (s, 1H), 7.99 (d, *J* = 8.2, 1H), 7.74 (d, *J* = 7.5, 3H), 7.46 – 7.57 (m, 3H), 7.09 – 7.44 (m, 13H), 6.80 – 6.86 (m, 7H), 5.89 (s, 1H), 5.62 (d, *J* = 6.2, 1H), 5.48 (t, *J* = 7.3, 2H), 5.28 (d, *J* = 8.2 Hz, 1H), 4.63 (dd, *J* = 13.6, 7.4 Hz, 1H), 4.29 – 4.46 (m, 3H), 4.15 – 4.19 (m, 2H), 4.00 – 4.02 (m, 1H), 3.77 (s, 3H), 3.76 (s, 3H), 3.47 – 3.53 (m, 2H), 3.12 (qd, *J* = 14.0, 6.6 Hz, 2H), 2.76 (d, *J* = 8.5, 1H). ^{13}C-NMR ($CDCl_3$) δ 171.3, 163.2, 158.69, 158.66, 155.9, 150.1, 144.3, 143.7, 143.6, 141.3, 135.6, 135.2, 135.0, 130.2, 130.1, 129.3, 128.7, 128.1, 128.0, 127.7, 127.19, 127.17, 127.1, 125.1, 125.0, 120.0, 113.3, 102.1, 88.3, 87.1, 82.9, 82.6, 68.0, 67.1, 55.2, 47.1, 25.6. ESI-QTOF calc. for $C_{55}H_{51}N_3O_{12}$ [M+Na+]: 968.34; found: 968.31.

5'-*O*-(4,4'-dimethoxytrityl)-2'-*O*-[acetal-*N*-(9-fluorenylmethoxycarbonyl)-L-alanine ester] uridine (6a): Same procedure as for **6b.** ^{1}H-NMR ($CDCl_3$) δ 8.72 (s, 1H), 8.63 (s, 2H), 8.01 (d, *J* = 8.2 Hz, 1H), 7.75 (d, *J* = 7.5 Hz, 2H), 7.68 (tt, *J* = 7.6, 1.7 Hz, 1H), 7.57 (t, *J* = 6.3 Hz, 2H), 7.34 – 7.41 (m, 4H), 7.22 – 7.32 (m, 6H), 6.83 (d, *J* = 8.7 Hz, 4H), 5.91 (s, 1H), 5.66 (d, *J* = 6.2 Hz, 1H), 5.49 (d, *J* = 6.3 Hz, 1H), 5.45 (d, *J* = 7.4 Hz, 1H), 5.26 (d, *J* = 8.1 Hz, 1H), 4.50 (t, *J* = 6.9 Hz, 1H), 4.34 – 4.43 (m, 3H), 4.28 (d, *J* = 4.3 Hz, 1H), 4.20 (t, *J* = 6.9 Hz, 1H), 4.04 (d, *J* = 7.9 Hz, 1H), 3.78 (s, 3H), 3.77 (s, 3H), 3.51 – 3.55 (m, 2H), 1.44 (d, *J* = 7.2 Hz, 3H). ^{13}C-NMR ($CDCl_3$) δ 172.7, 162.9, 158.66, 158.63, 150.0, 149.7, 144.3, 141.3, 139.8, 136.0, 135.2, 135.0, 130.14, 130.08, 128.07, 128.01, 127.7, 127.1, 125.04, 125.00, 120.0, 113.28, 113.26, 102.2, 88.3, 87.11, 87.05, 82.8, 77.2, 68.3, 67.2, 55.2, 50.0, 47.0, 29.7. ESI-QTOF calc. for $C_{49}H_{47}N_3O_{12}$ [M+Na]: 892.31; found: 892.23.

5'-*O*-(4,4'-dimethoxytrityl)-2'-*O*-[acetal-*N*-(9-fluorenylmethoxycarbonyl)-L-lysine ester] uridine (6c): Same procedure as for **6b** except that the product was purified by silica gel

chromatography using a gradient ending with 9:1 CH_2Cl_2/MeOH. ^{1}H-NMR ($(CD_3)_2CO$) δ 8.58 (d, *J* = 4.0 Hz, 1H), 7.90 (d, *J* = 8.2 Hz, 1H), 7.82 – 7.87 (m, 4H), 7.64 – 7.72 (m, 4H), 7.48 (d, *J* = 4.0 Hz, 1H), 7.37 – 7.42 (m, 4H), 7.27 – 7.37 (m, 10H), 7.24 (t, *J* = 7.3 Hz, 1H), 6.95 (d, *J* = 8.1 Hz, 1H), 6.89 (d, *J* = 8.2 Hz, 4H), 6.52 (t, *J* = 5.5 Hz, 1H), 6.00 (d, *J* = 2.8 Hz, 1H), 5.57, 5.52 (ABq, *J* = 6.5 Hz, 1H each), 5.27 (d, *J* = 8.1 Hz, 1H), 4.62 (dd, *J* = 12.0, 7.0 Hz, 1H), 4.51 (dd, *J* = 4.7, 3.0 Hz, 1H), 4.18 – 4.40 (m, 8H), 4.10 – 412 (m, 1H), 3.774 (s, 3H), 3.772 (s, 3H), 3.50 (dd, *J* = 10.9, 3.6 Hz, 1H), 3.44 (dd, *J* = 10.9, 2.4 Hz, 1H), 3.18 (dd, *J* = 13.4, 7.0 Hz, 2H), 1.88 – 1.96 (m, 1H), 1.75 – 1.83 (m, 1H), 1.44 – 1.61 (m, 4H). ^{13}C-NMR ($(CD_3)_2CO$) δ 171.8, 162.5, 161.1, 158.81, 158.79, 156.5, 156.3, 150.5, 144.9, 144.3, 144.2, 144.1, 144.0, 141.2, 139.9, 135.7, 135.4, 130.2, 130.1, 128.2, 128.1, 127.8, 127.6, 127.5, 127.1, 127.02, 126.98, 126.8, 125.3, 125.22, 125.19, 119.9, 119.8, 113.11, 113.10, 101.7, 88.8, 88.0, 86.6, 82.9, 82.0, 69.1, 66.3, 65.9, 62.2, 54.62, 54.61, 54.3, 47.2, 47.1, 40.1, 29.2, 29.0, 22.7. ESI-QTOF calc. for $C_{67}H_{64}N_4O_{14}$ [M+Na]: 1171.43; found: 1171.34.

5'-*O*-(4,4'-dimethoxytrityl)-2'-*O*-[acetal-*N*-(9-fluorenylmethoxycarbonyl)-L-proline ester] uridine (6d): Same procedure as for **6b**. ^{1}H-NMR (CD_3CN) δ 7.56 - 7.91 (m, 4 H), 7.24 - 7.49 (m, 14 H), 6.83 - 6.96 (m, 4 H), 5.78 - 5.92 (m, 1 H), 5.39 - 5.55 (m, 2 H), 5.22 - 5.32 (m, 1 H), 4.20 - 4.45 (m, 5 H), 3.90 - 4.05 (m, 1 H), 3.78 (d, *J* =3.13 Hz, 6 H), 3.12 - 3.66 (m, 5 H), 2.21 - 2.35 (m, 2 H), 1.76 - 1.90 (m, 2 H). ESI-QTOF calc. for $C_{51}H_{49}N_3O_{12}$ [M+Na]: 918.32; found: 918.23.

5'-*O*-(4,4'-dimethoxytrityl)-2'-*O*-(acetal hydrocinnamic ester) uridine (6e): Same procedure as for **6b**. ^{1}H-NMR ($(CD_3)_2CO$) δ 7.79 – 7.84 (m, 1H), 7.53 – 7.60 (m, 2H), 7.25 – 7.49 (m, 12H), 7.01 (d, *J* = 8.99 Hz, 4H), 5.96 (d, *J* = 3.13 Hz, 1H), 5.55 (d, *J* = 6.64 Hz, 1H), 5.48 (s, 1H), 5.33 – 5.43 (m, 1H), 4.48 (q, *J* = 6.25 Hz, 1H), 4.38 – 4.43 (m, 1H), 4.28 – 4.32 (m, 1H), 4.09 – 4.14 (m, 1H), 3.43 – 3.54 (m, 1H), 3.40 (dd, *J* = 6.64, 3.91 Hz, 1H), 2.97 – 3.08 (m, 1H), 2.72 – 2.83 (m, 1H), 2.45 (s, 1H), 2.21 (s, 6H), 1.38 – 1.57 (m, 1H), 0.95 – 1.08 (m, 1H). ESI-TOF calc. for $C_{40}H_{40}N_2O_{10}$ [M+Na]: 731.26; found: 731.26.

5'-*O*-(4,4'-dimethoxytrityl)-2'-*O*-[acetal-*N*-(9-fluorenylmethoxycarbonyl)-L-phenylalanine ester]-3'-*O*-[(2-cyanoethyl-*N*,*N*-diisopropyl)phosphoramidite] uridine (7b): **7b** (279 mg, 0.314 mmol) was dissolved in THF (1.3 mL) and *N*,*N*-diisopropylamine (250 μL, 1.43 mmol) was added. 2-cyanoethyl *N*,*N*-diisopropylchlorophosphoramidite was added

dropwise (86 μL, 0.386 mmol) and after 3 hr the reaction mixture was diluted with CH_2Cl_2 and washed with saturated aqueous $NaCHO_3$. The aqueous layer was extracted three times and the organic layers were combined and dried over $MgSO_4$, filtered, and concentrated to dryness. The product was purified by silica gel chromatography with a gradient ending in 1:1 hexanes/EtOAc (+1% py). ^{31}P-NMR (CD_3CN) δ 151.55, 149.99. ESI-QTOF calc. for $C_{64}H_{68}N_5O_{13}P$ [M+Na]: 1168.4443; found: 1168.4444.

5'-*O*-(4,4'-dimethoxytrityl)-2'-*O*-[acetal-*N*-(9-fluorenylmethoxycarbonyl)-L-alanine ester]-3'-*O*-[(2-cyanoethyl-*N*,*N*-diisopropyl)phosphoramidite] uridine (7a): Same procedure as for **7b**. ^{31}P-NMR (CD_3CN) δ 152.20, 150.06. ESI-QTOF calc. for $C_{58}H_{64}N_5O_{13}P$ [M+Na]: 1092.41; found: 1092.41.

5'-*O*-(4,4'-dimethoxytrityl)-2'-*O*-[acetal-*N*-(9-fluorenylmethoxycarbonyl)-L-lysine ester]-3'-*O*-[(2-cyanoethyl-*N*,*N*-diisopropyl)phosphoramidite] uridine (7c): Same procedure as for **7b** except that the product was purified by silica gel chromatography with a gradient ending in 2:3 hexanes/EtOAc (+1% py). ^{31}P-NMR (CD_3CN) δ 151.57, 150.02. ESI-QTOF calc. for $C_{76}H_{81}N_6O_{15}P$ [M+Na]: 1371.54; found: 1371.54.

5'-*O*-(4,4'-dimethoxytrityl)-2'-*O*-[acetal-*N*-(9-fluorenylmethoxycarbonyl)-L-proline ester]-3'-*O*-[(2-cyanoethyl-*N*,*N*-diisopropyl)phosphoramidite] uridine (7d): Same procedure as for **7b**. ^{31}P-NMR (CD_3CN) δ 151.32, 149.98. ESI-QTOF calc. for $C_{60}H_{66}N_5O_{13}P$ [M+Na]: 1118.43; found: 1118.20.

5'-*O*-(4,4'-dimethoxytrityl)-2'-*O*-[acetal-*N*-(9-fluorenylmethoxycarbonyl)-L-hydrocinnamic ester]-3'-*O*-[(2-cyanoethyl-*N*,*N*-diisopropyl)phosphoramidite] uridine (7e): Same procedure as for **7c** except that CH_2Cl_2 was used as a solvent and the reaction was carried out for 5.5 hr. ^{31}P-NMR (CD_3CN) δ 151.65, 150.05. ESI-QTOF calc. for $C_{49}H_{57}N_4O_{11}P$ [M+Na]: 931.37; found: 931.40.

2.9.3. Solid-Supported Synthesis of Oligonucleotides

Oligonucleotides were synthesized on UnyLinker™ CPG (500 Å) or photocleavable CPG (500 Å) with an Applied Biosystems DNA/RNA 3400 Synthesizer. Standard 2'-*O*-TBDMS uridine and thymidine phosphoramidites were purchased from ChemGenes Corporation

(Wilmington, MA). Thymidine and 2'-*O*-HCA phosphoramidite was dissolved in MeCN to a concentration of 0.1 M, while uridine and 2'-*O*-AAE phosphoramidites were dissolved in MeCN to a concentration of 0.15 M. Coupling times for thymidine and uridine were 600 sec, while coupling time was 900 sec for the modified units. Activation of phorphoramidites was achieved with standard 0.25 M ETT in MeCN. Standard capping was performed with a CAP A solution of Ac_2O/py/THF (10:10:80 v/v/v) and a CAP B solution of 15% *N*-methylimidzaole in THF. The oxidation solution used was standard 0.1 M I_2 in py/H_2O/THF (8:16:76 v/v/v). Standard 3% TCA in CH_2Cl_2 was used for detritylation steps.

2.9.4. Deprotection of Oligonucleotides

UnyLinker^{TM} CPG was suspended in the standard NH_4OH/EtOH deprotection solution and put on a shaker for 48 hr at (1 mL, 3:1 v/v) at r.t. to remove the nucleobase and internucleotide protecting groups, and to cleave the support linker. After decanting and lyophilizing the supernatant, fast desilylation was performed in NEt_3-3HF/NMP/NEt_3 (0.300 mL 1.5:0.75:1 v/v/v) at 65^{o}C for 4 hr., after which NaOAc (3 M, pH 5.5, 25 μL) and cold 1-butanol (1 mL) were added to precipitate the oligonucleotide. The washed and dried oligonucleotide was dissolved in water, filtered, and purified by IE-HPLC.

A1, A3, A6, B1, B3, C1, C3, D3: CPG derivatized with a photocleavable linker attached to an internucleotide linkage was suspended in anhydrous NEt_3/MeCN (1 mL, 2:3 v/v) and shaken for 18 hr, centrifuged and decanted. Washing of the beads was done with 0.200 mL MeCN, then 0.200 mL EtOH, and 0.200 mL MeCN again. The dried beads were then suspended in 1 mL MeCN with 1% (v/v) DIPEA in a quartz tube. A Luzchem LZC-4 photoreactor was used to photocleave the oligonucleotides from the solid support beads. The beads were irradiated with fourteen 12" Luzchem LZC-UVA (UV-A, Hitachi FL8BL-B) lamps at λ_{max} = 350 nm for 21 minutes and then transferred to polypropylene tube with a 0.100-mL MeCN rinse, then a 0.100-mL EtOH rinse, and then a 0.100-mL MeCN rinse. The beads were centrifuged, decanted, and rinsed with 0.200 mL MeCN, 0.200 mL EtOH, and then 0.200 mL MeCN. The supernatant was lyophilized, dissolved in water, filtered, and purified by RP-HPLC or gel electrophoresis.

F1, B1-2: CPG derivatized with a photocleavable linker attached to the 3'-end of the first nucleotide was transferred into a 5-mL flamed round bottom flask, suspended in anhydrous NEt_3/MeCN (1 mL, 2:3 v/v) heated to 65°C, and stirred for 2 hr. The suspension was transferred to a polypropylene tube with help twice from 0.500 mL MeCN. Beads were centrifuged at 13,000 rpm for 5 min and the supernatant was decanted. The suspension was lyophilized to dryness and the beads were transferred to a flamed quartz tube, irradiated at λ_{max} = 350 nm for 21 minutes in MeCN +1% DIPEA with the same photoreactor detailed above. The beads were transferred to a polypropylene tube and lyophilized to dryness. The beads of sample **B1-2** were resuspended in anhydrous DMSO, centrifuged at 13,000 rpm for 5 min, and an aliquot of the supernatant was combined with anhydrous MeCN and injected immediately into RP-HPLC for a t = 0 hr trace. The beads were again lyophilized to dryness and beads of both samples **B1-2** and **F1** were resuspended in H_2O, centrifuged at 13,000 rpm for 5 min, and the supernatant was filtered and decanted. The supernatant was lyophilized to dryness and PBS buffer (137 mM NaCl, 2.7 mM KCl, 10 mM Na_2HPO_4, 1.8 mM KH_2PO_4) was added. The tube was incubated at 37°C and aliquots were taken at 4, 8, 16, and 32 hr for immediate injection into RP-HPLC.

2.9.5. Purification and Characterization of Oligonucleotides

Samples **A1**, **A3**, **B1**, **B3**, **C1**, **C3**, **D3**, **E1**, and **E6** were purified by RP-HPLC on an Agilent 1200 system with an Axxiom C18 ODS 5 micron, 250 x 4.6 mm column. For the purification of A_{15}, IE-HPLC was carried out on a Waters Protein PAK DEAE 5PW 7.5 mm x 7.5 cm column. After the completion of IE-HPLC the purified oligonucleotides were desalted with sephadex G-25 and lyophilized to dryness. Thermal melting analyses were performed on a Varian CARY 300 UV-VIS Spectrophotometer equipped with a peltier temperature controller. Crude **A1**, **B3**, and **C3** (2.0 nmol) were dissolved in H_2O and combined with purified A_{15} complement (2.0 nmol). The mixtures were lyophilized and then reconstituted in PBS buffer (137 mM NaCl, 2.7 mM KCl, 10 mM Na_2HPO_4, 1.8 mM KH_2PO_4). The duplexes were denatured by heating the mixtures to 95°C for 5 min and then letting them cool to r.t. slowly. Once at r.t., the samples were cooled overnight in a -20°C freezer. A denaturing and then annealing curve was then collected at a rate of 0.4°C/min. Sample **A6** was loaded onto a 24% denaturing (+ urea) polyacrylamide gel was run with tris-borate-ethylenediaminetetraacetic acid (TBE) running buffer and bromophenol blue and xylene cyanol FF marker dyes. Samples **F1**

and **B1-2** were purified using LC-ESI-QTOF using Dionex Ultimate 3000 coupled to a Bruker Maxis Impact QTOF in negative ESI mode and an Acclaim RSLC 120 C18 column (2.2 μM 120A 2.1 x 50 mm). Mobile phase A (100 mM HFIP and 5 mM NEt_3 in H_2O) was reduced from 98% to 40% in 8 min. The mobile phase B that was used was MeOH. The data was processed and deconvoluted using the Bruker DataAnalysis software version 4.1

2.9.6. Synthesis and Purification of Dimers

Phosphoramidite **7b** (57.3 mg, 0.05 mmol) was dissolved in CD_3CN (0.66 mL) and transferred into a dry NMR tube. DCI (7.7 mg, 0.10 M) and then dideoxythymidine (17.0 mg, 0.075 mmol) were added and the reaction progress was monitored by ^{31}P-NMR. When coupling was complete (marked by the complete disappearance of the diastereoisomeric peaks at 151.55 ppm and 149.99 ppm), 0.200 mL of the oxidation solution indicated was added to the NMR tube. The NMR tube was inverted three times and the reaction was monitored by ^{31}P-NMR. The dimers were purified by RP-HPLC with a gradient of 1 – 35% solvent B in 10 min (A: triethylammonium acetate (TEAA), B: MeCN).

2.10. References

1. Vig, B. S.; Huttunen, K. M.; Laine, K.; Rautio, J., Amino acids as promoieties in prodrug design and development. *Ad. Drug Delivery Rev.* **2013,** *65* (10), 1370-1385.

2. Goodman, D. W., Lisdexamfetamine Dimesylate (Vyvanse), A Prodrug Stimulant for Attention-Deficit/Hyperactivity Disorder. *Pharm. Ther.* **2010,** *35* (5), 273-287.

3. Elia, J.; Easley, C.; Kirkpatrick, P., Lisdexamfetamine dimesylate. *Nat. Rev. Drug Discov.* **2007,** *6* (5), 343-344.

4. Kawaguchi, T.; Sakairi, H.; Kimura, S.; Yamaguchi, T.; Saneyoshi, M., Synthesis and Antileukemic Activity of Chymotrypsin-Activated Derivatives of 3'-Amino-2', 3'-dideoxycytidine. *Chem. Pharm. Bull.* **1995,** *43* (3), 501-504.

5. Vig, B. S.; Lorenzi, P. J.; Mittal, S.; Landowski, C. P.; Shin, H. C.; Mosberg, H. I.; Hilfinger, J. M.; Amidon, G. L., Amino acid ester prodrugs of floxuridine: synthesis and effects of structure, stereochemistry, and site of esterification on the rate of hydrolysis. *Pharm. Res.* **2003,** *20* (9), 1381-1388.

6. Shen, W.; Kim, J.-S.; Kish, P. E.; Zhang, J.; Mitchell, S.; Gentry, B. G.; Breitenbach, J. M.; Drach, J. C.; Hilfinger, J., Design and synthesis of vidarabine prodrugs as antiviral agents. *Bioorg. Med. Chem. Lett.* **2009,** *19* (3), 792-796.

7. Fossey, C.; Huynh, N. T.; Vu, A. H.; Vidu, A.; Zarafu, I.; Laduree, D.; Schmidt, S.; Laumond, G.; Aubertin, A. M., Synthesis and anti-HIV evaluation of hybrid-type prodrugs conjugating HIV integrase inhibitors with d4t by self-cleavable spacers containing an amino acid residue. *J. Enzyme Inhib. Med. Chem.* **2007,** *22* (5), 608-619.

8. Balimane, P. V.; Tamai, I.; Guo, A.; Nakanishi, T.; Kitada, H.; Leibach, F. H.; Tsuji, A.; Sinko, P. J., Direct evidence for peptide transporter (PepT1)-mediated uptake of a nonpeptide prodrug, valacyclovir. *Biochem. Biophys. Res. Commun.* **1998,** *250* (2), 246-251.

9. Sugawara, M.; Huang, W.; Fei, Y. J.; Leibach, F. H.; Ganapathy, V.; Ganapathy, M. E., Transport of valganciclovir, a ganciclovir prodrug, via peptide transporters PEPT1 and PEPT2. *J. Pharm. Sci.* **2000,** *89* (6), 781-789.

10. Lorenzi, P. L.; Landowski, C. P.; Brancale, A.; Song, X.; Townsend, L. B.; Drach, J. C.; Amidon, G. L., N-methylpurine DNA glycosylase and 8-oxoguanine dna glycosylase metabolize the antiviral nucleoside 2-bromo-5,6-dichloro-1-(beta-D-ribofuranosyl)benzimidazole. *Drug Metab. Dispos.* **2006,** *34* (6), 1070-1077.

11. Lorenzi, P. L.; Landowski, C. P.; Song, X.; Borysko, K. Z.; Breitenbach, J. M.; Kim, J. S.; Hilfinger, J. M.; Townsend, L. B.; Drach, J. C.; Amidon, G. L., Amino acid ester prodrugs of 2-bromo-5,6-dichloro-1-(beta-D-ribofuranosyl)benzimidazole enhance metabolic stability in vitro and in vivo. *J. Pharmacol. Exp. Ther.* **2005,** *314* (2), 883-890.

12. Song, X.; Lorenzi, P. L.; Landowski, C. P.; Vig, B. S.; Hilfinger, J. M.; Amidon, G. L., Amino acid ester prodrugs of the anticancer agent gemcitabine: synthesis, bioconversion, metabolic bioevasion, and hPEPT1-mediated transport. *Mol. Pharmaceutics* **2005,** *2* (2), 157-167.

13. Dhareshwar, S. S.; Stella, V. J., Your prodrug releases formaldehyde: should you be concerned? No! *J. Pharm. Sci.* **2008,** *97* (10), 4184-4193.

14. Zavgorodny, S.; Polianski, M.; Besidsky, E.; Kriukov, V.; Sanin, A.; Pokrovskaya, M.; Gurskaya, G.; Lönnberg, H.; Azhayev, A., 1-alkylthioalkylation of nucleoside hydroxyl functions and its synthetic applications: a new versatile method in nucleoside chemistry. *Tetrahedron Lett.* **1991,** *32* (51), 7593-7596.

15. Rastogi, H.; Usher, D. A., A new 2'-hydroxyl protecting group for the automated synthesis of oligoribonucleotides. *Nucleic Acids Res.* **1995,** *23* (23), 4872-4877.

16. Deleavey, G. F.; Watts, J. K.; Alain, T.; Robert, F.; Kalota, A.; Aishwarya, V.; Pelletier, J.; Gewirtz, A. M.; Sonenberg, N.; Damha, M. J., Synergistic effects between analogs of DNA and RNA improve the potency of siRNA-mediated gene silencing. *Nucleic Acids Res.* **2010,** *38* (13), 4547-4557.

17. Hill, J. G.; Rossiter, B. E.; Sharpless, K. B., Anhydrous tert-butyl hydroperoxide in toluene: the preferred reagent for applications requiring dry TBHP. *J. Org. Chem.* **1983,** *48* (20), 3607-3608.

18. Scaringe, S. A., Advanced 5'-silyl-2'-orthoester approach to RNA oligonucleotide synthesis. *Methods Enzymol.* **2000,** *317*, 3-18.

19. Ugi, I.; Jacob, P.; Landgraf, B.; Ruppf, C.; Lemmen, P.; Verfürth, U., Phosphite Oxidation and the Preparation of Five-Membered Cyclic Phosphorylating Reagents Via the Phosphites. *Nucleosides Nucleotides* **1988,** *7* (5-6), 605-608.

20. Uzagare, M. C.; Padiya, K. J.; Salunkhe, M. M.; Sanghvi, Y. S., NBS–DMSO as a nonaqueous nonbasic oxidation reagent for the synthesis of oligonucleotides. *Bioorg. Med. Chem. Lett.* **2003,** *13* (20), 3537-3540.

Chapter 3: Fluorometric Assay for Cellular Uptake of Amino Acid-siRNA Conjugates and their Structural Analogues

3.1. The Introduction of Positive Charge to Nucleic Acids

Given the critical issue of cellular membrane penetration for the successful use of therapeutic oligonucleotides and the negatively charged nature of the membrane, the development of positively charged delivery agents and conjugates has elicited a great deal of interest.[1] Lipofectamine™ 2000, a standard delivery agent of nucleic acids for *in vitro* applications, contains lipid subunits decorated with positively-charged amines that encase the nucleic acid *via* electrostatic interactions. The nucleic acids encapsulated in this positively charged liposome are thus protected and only released into the cytoplasm upon fusion of the liposome with the cellular membrane[2] or if the cationic lipids become attracted to the cytosol-facing phospholipids after endocytosis.[3,4]

Nucleic acids carrying a net positive charge exhibit a proton sponge effect in endosomes. A large spermine group at the 5'-end of siRNA, for instance, enables this to occur. When a large number of the amino groups of the spermine moiety are protonated, it causes the pK_{aH} of the nearby non-protonated amines to decrease, which in turn allows it to buffer the solution.[5,6] The ability of modified nucleic acids in acidic endosomes or lysosomes to act as pH buffers is thought to create osmotic pressure. This causes inward movement of water, vesicle swelling, and vesicle rupture, as well as inhibition of lysosomal nuclease. Therefore, the extensive use of secondary and/or tertiary amino groups in oligonucleotide conjugates with pK_{aH}s close to endosomal and lysosomal pH is beneficial for releasing trapped therapeutic oligonucleotides into the cytoplasm. Other lipopolyamines have been explored for their delivery properties,[7,8] but cationic dendrimers such as those based on polyamidoamine (PAMAM), triazine, carbosilane, cyclodextrin, and even dendron-functionalized multiwalled carbon nanotubes (MWNTs) have also been considered.[9]

The presence of positive charges at various positions of oligonucleotides has also been explored (Figure 3.1). For instance, the presence of guanidinium groups in the backbone of oligonucleotides has been found to increase cellular uptake when comprising the entire backbone of a thymidine homopolymer.[10] Nucleic acids containing positively charged sugar analogs have

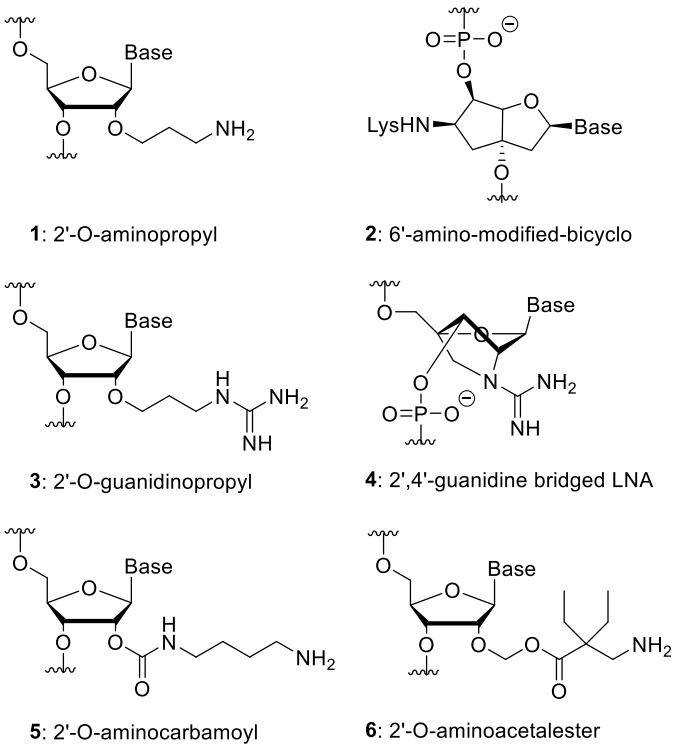

Figure 3.1. Many sugar modifications which introduce positive charge have been incorporated in ONs.

also been synthesized such as those containing 2'-*O*-aminopropyl modification (**1**),[11] 2'-*N*-acylpolyamines,[12] 6'-amino-modified-bicyclo-nucleosides (**2**),[13] 2'-*O*-guanidinopropyl inserts (**3**),[14] 2',4'-guanidine bridged nucleic acid synthons (**4**),[15] 2'-*O*-aminocarbamoyl moieties (**5**) and their derivatives,[16,17,18] and 2'-*O*-aminoacetalesters (**6**).[19,20] None of these modifications have been used in siRNA capable of unassisted cellular uptake. Indeed, an AON containing single insertions of 2'-*N*-acylpolyamines[12] and siRNAs with single inserts of 2'-*O*-guanidinopropyl modifications (**3**)[14] both achieved gene silencing, but only after lipoplex delivery, while a poly-thymidine 10-mer including five amino-modified-bicyclic residues (**2**)[13] and a poly-uridine 12-mer including ten 2'-*O*-(2-amino-methyl-2-ethyl)butyryloxymethyl residues[20] both exemplified unassisted cellular internalization, but the gene silencing potential could not be demonstrated. The 2'-*O*-2-(*N*-methylcarbamoyl)ethyl modification,[17] on the other hand, has been inserted in a splice-switching ssON which underwent successful intratumoral injection, but it has not been applied successfully to siRNA. The double-stranded nature of siRNA brings about a relatively large number of negative charges that must be counteracted while maintaining a favorable conformation and guide strand loading, and further complicates the design of sugar modifications capable of conferring unassisted siRNA delivery.

3.1.1. Amino Acids in Oligonucleotides and their Delivery Agents

The chemical diversity of amino acids has been extensively harnessed in the process of drug design. Each amino acid contains several diverse functional groups that can be exploited for their charge, lipophilic and hydrophilic properties, and as points of chemical attachment.

They are also substrates of a variety of enzymes, making them promoiety candidates in a variety of tissues (further discussed in Chapter 5). Consequently, amino acids have been used extensively in small molecule drugs and have also been considered in the development of oligonucleotide carriers and conjugates.

Poly-L-lysine (PLL) was the first polymer to be evaluated as a transfection agent owing to its adhesive property in the presence of cell surfaces.[21] Another example of a popular transfection agent are cell penetrating peptides (CPPs), also known as protein transduction domains (PTDs), which depending on their peptide sequence can bind to different cellular receptors.[22] R_9F_2, for example, a 29-residue peptide derived from rabies virus glycoprotein (RVG), binds specifically to the acetylcholine receptor (nAchR) on neuronal cells, and was fused to a polyarginine peptide to allow siRNA to form a complex with the synthetic protein.[23]

Amino acids have also been integrated into the chemical structures of ONs. For instance, the backbone of the original PNA is based on glycine condensation (Figure 1.10D), and L-arginine side chains tethered to the backbone of a polythymidine PNA have been investigated for improved binding efficiency to DNA and improved cellular uptake.[24] The Wengel lab functionalized the N2' position of homopolymers of 2'-amino-2'-deoxyuridine and locked nucleic acids (LNA) with glycine,[25] and used glycine in LNA as an attachment site for additional amino acids such as glycine, proline, or lysine.[26] The resulting LNA-amino acid conjugates were investigated for their thermal stabilities. 2'-O-acetamido modified ONs containing a peptide branch at position 2'-have also been patented.[27] A phenylalanine-alanine peptide has been conjugated to the 3'-position of a terminal riboadenosine unit on a semi-synthetic tRNA *via* an amide linkage to study resistance to hydrolysis.[28]

The use of plasmid-encasing lipids functionalized with low-branching lysine- and arginine-polymers was found to reduce cytotoxicity compared with branched polyethylenimine (PEI_{25k}) and Lipofectamine™ 2000 carriers, possibly due to differences in biodegradability.[29] These versions of cationic lipoplexes were able to distribute DNA into tumor tissue after intratumoral administration.[29] In another instance, employing gold nanoparticles functionalized with low-branching lysine resulted in increased plasmid binding efficiency and subsequent plasmid delivery into cells.[30]

3.1.2. Positively Charged Phenylalanine Sugar Modifications

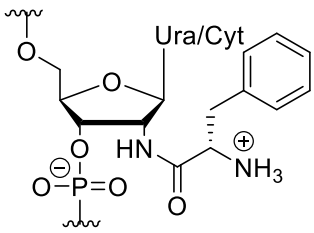

Figure 3.2. A stable 2'-*N*-acyl-L-phenylalanine modification was assayed in siRNA for cellular uptake.

We wondered if a 2'-*N*-acyl-L-phenylalanine derivative of the 2'-*O*-phenylalanine acetal ester would be both resistant to hydrolysis and enhance cellular uptake of siRNA (Figure 3.2). In fact, the 2'- or 3'-*N*-acyl-L-phenylalanine modification is a familiar feature in biologically relevant synthetic nucleosides and nucleotides, serving a diverse range of purposes. For example, it has been used on deoxycytidine monomers to form enzymatically-cleavable pro-moieties in tumor cells,[31] on deoxyuridine monomers for the well-known antibiotic activity of peptidyl nucleosides,[32] incorporated in peptide-nucleoside hybrids using unconventional nucleobase-linked solid supports,[33] and introduced into ribozymes that retained their catalytic activity.[34] To the best of our knowledge, the *N*-acyl-L-phenylalanine modification has not been employed in oligonucleotides (including siRNA) assayed for increased cellular uptake. Here we investigate these siRNA analogues and monitor their uptake *via* flow cytometric fluorescence resonance energy transfer (FCET), developed by Szöllosi and coworkers.[35]

3.2. A Method to Detect Intact siRNA using Förster Resonance Energy Transfer

The use of Förster Resonance Energy Transfer (FRET) has demonstrated that doubled-stranded (ds) siRNA is much more resistant to nuclease degradation than the single-stranded (ss) version.[36] Indeed, in duplex form, the antisense strand remains protected during translocation of the siRNA from the extracellular medium to the cytosol, where the degradation kinetics of unmodified siRNA is similar to that of nuclease-resistant siRNA.[37] Preserving the entire 19-nt-long ds stretch of canonical siRNA in our conjugates was thus important in the delivery of the intact antisense strand. Cyanine-3 (cy3) and cyanine-5 (cy5) fluorophores were conjugated to the 5'- and 3'-terminal of the sense and antisense strands, respectively, of our siRNAs (Figure 3.3A). These fluorophores were used to detect ds siRNA inside cells.

The excitation and emission spectra of the cy3 dye are centered on 550 nm, and 650 nm for cy5. The emission spectrum of cy3 overlaps, to a degree, with the excitation spectrum of cy5 (shaded area in Figure 3.3B). This overlap allows FRET to occur. On the other hand, the

excitation of cy3 only slightly overlaps with the excitation of cy5 and thus overlap is essentially avoided when cy3 is excited at 488 nm in a flow cytometer. Similarly, detection of cy5 emission at wavelengths above 650 nm by a flow cytometer detects only a small portion of the emission spectrum of cy3, thereby minimizing overestimation of the FRET intensity when cy3 is excited and cy5 is being monitored.

FRET occurs *via* the non-radiative process of long-range resonance dipole energy transfer, as illustrated by k_T, triggered when a donor fluorophore (D) such as cy3 is excited by capture of an electron, illustrated by k_{ex}, to the first excited singlet electronic state (S_1) (Figure 3.3C).[38] (The singlet electronic states are comprised of bold lines and their vibrational levels just above the bold lines.) This process is in competition with radiative decay (fluorescence) of the donor fluorophore, represented by k_f; non-radiative internal conversion, denoted by k_c; and non-radiative collisional quenching, designated as k_Q, by an external quencher.[38] After vibrational relaxation (shown as $k_{vib\ relax}$) of the electron to the lowest vibrational S_1 energy state of the excited donor (D*), the electron transfers to an S_1 vibrational level of the excited acceptor (A*) that corresponds to the energy level of the electron.[38] Fluorescence emission corresponding to the relaxation of the electron to a ground singlet state of A* can now occur.

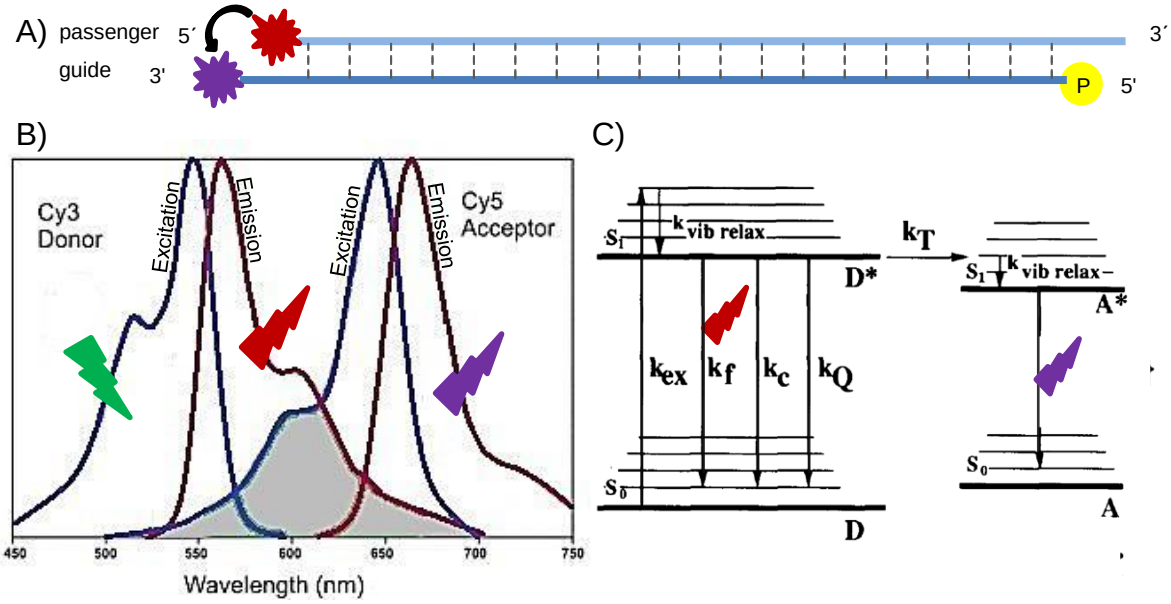

Figure 3.3. FRET-enabled siRNAs were A) modified at one terminal end of the duplex, B) excited at 488 nm, and C) monitored above 650 nm while other radiative and non-radiative processes occurred (adapted from reference 38).

FRET-based siRNA has been used to detect intact duplex inside cells and monitor siRNA localization inside cells[36,39,40,41,42] as well as monitor cellular unpacking of siRNA from quantum dot delivery vehicles derivatized with polyethylenimine cations[43] and several other delivery nanocomplexes.[44] A cy3/cy5 FRET combination has also been used to label and detect cell surface proteins,[35] but the FRET pair, or any other, has not been involved in assessing the cellular uptake of naked siRNA to the best of our knowledge.

3.3. Synthesis of Test Conjugates

3.3.1. The Monomers

The 2'-*N*-acyl-L-phenylalanine modification has not been incorporated at the 2' ribose position of siRNA to the best of our knowledge. We decided to incorporate the modification on the sense strand of an siRNA targeting the mRNA of the protein downregulated in renal cell carcinoma (DRR) and to deliver the resulting conjugates to human glial cells (primary brain cancer cells) that are over-expressing DRR.[45] These conjugates were predicted to cause an improvement in cellular uptake of the siRNA given the use of positively charged amino groups in transfection agents to improve cellular uptake of nucleic acids.

N-Fmoc protected L-phenylalanine was coupled to commercially available 2'-amino-2'-deoxyuridine **1** using *N*-ethoxycarbonyl-2-ethoxy-1,2-dihydroquinoline (EEDQ) in 80% yield, followed by standard dimethoxytritylation with DMTrCl and phosphitylation with *N*,*N*-diisopropylamino cyanoethyl phosphonamidic chloride to give the uridine phosphoramidite **4** needed for solid phase oligonucleotide synthesis (Scheme 3.1). The cytidine monomer was synthesized by Dr. Ken Yamada with benzoyl protection on the nucleobase.

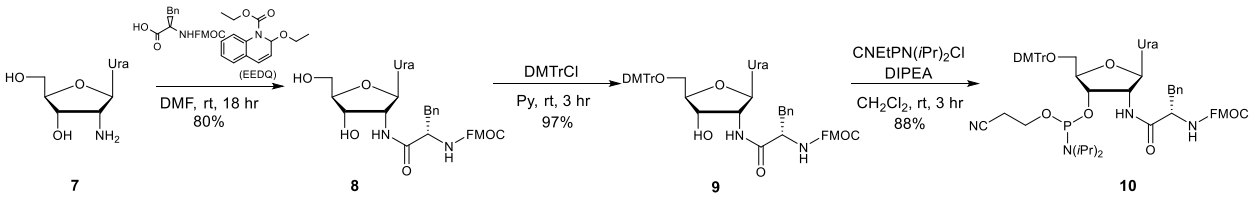

Scheme 3.1. The *N*-FMOC-protected L-phenylalanine amino acid was coupled to 2'-amino-2'-deoxyuridine using EEDQ and then prepared as a phosphoramidite for solid phase synthesis.

3.3.2. The Oligonucleotides

The sense strand of DRR siRNA was synthesized under standard solid-supported conditions with zero, three, and six 2'-*N*-acyl-L-phenylalanine inserts (Table 3.1). Since the modification was likely to introduce thermal instability, as observed with the 2'-*O*-phenylalanine acetal ester inserts in Chapter 2, it was incorporated at more positions in the strand that were near the 3'-end as opposed to the 5'-end. This was done to encourage the selective loading of the antisense strand in the silencing machinery, which partly depends on the relative thermodynamic stability at the 5'-end of siRNAs. Sense strands were then annealed to the unmodified 5'-phosphorylated antisense strand synthesized with or without cy5. The cy5 strand was

Table 3.1. Test conjugates were synthesized with cy3 and cy5 fluorophores for the assessment of cellular uptake.

siRNA	Use	Sequence
D0cy3/5	assessing duplex uptake	5'-**cy3**-GGA ACC AGC UCA UCA AGA AUU-3'
		3'-**cy5**-UU CCU UGG UCG AGU AGU UCU U-p-5'
D0cy3	Cy3 calibration, preliminary cy3 uptake	5'-**cy3**-GGA ACC AGC UCA UCA AGA AUU-3'
		3'-UU CCU UGG UCG AGU AGU UCU U-p-5'
D0cy5	Cy5 calibration	5'-GGA ACC AGC UCA UCA AGA AUU-3'
		3'-**cy5**-UU CCU UGG UCG AGU AGU UCU U-p-5'
D3cy3/5	assessing duplex uptake	5'-**cy3**-GGA ACC AGC **U**CA **U**CA AGA A**U**U-3'
		3'-**cy5**-UU CCU UGG UCG AGU AGU UCU U-p-5'
D3cy3	preliminary cy3 uptake	5'-**cy3**-GGA ACC AGC **U**CA **U**CA AGA A**U**U-3'
		3'-UU CCU UGG UCG AGU AGU UCU U-p-5'
D6cy3/5	assessing duplex uptake	5'-**cy3**-GGA AC**C** AGC **UC**A **UC**A AGA A**U**U-3'
		3'-**cy5**-UU CCU UGG UCG AGU AGU UCU U-p-5'

Legend: **U** = 2'-*N*-acyl-L-phenylalanine uridine; **C** = 2'-*N*-acyl-L-phenylalanine cytidine; p = phosphate. Sequence: sense strand on top; antisense strand on bottom.

synthesized using phosphoramidites whose nucleobase were protected with a *N*-phenoxyacetyl (PAC) group that can be cleaved after a short aqueous ammonia (NH_4OH) exposure, thus

minimizing the detrimental oxidation of cy5. The strand without cy5 fluorophore was synthesized with standard phosphoramidites and used in further silencing studies explored in Chapter 4. The 5'-phosphorylation step served as a way to encourage selective loading of the antisense strand in the silencing machinery, as with 5'-phosphorylated synthetic siRNA has been found to be more active than its non-phosporylated form.[46]

3.4. Cellular Uptake of Test Conjugates

3.4.1. Glial Cells

Glial cells overexpressing the protein downregulated in renal cell carcinoma, named DRR+, were generated and grown by the Petrecca lab at the McGill Neuorological Institute using their novel forward genetic-screening method and prepared for experiments by Dr. Phuong Le in the Petrecca lab. The cellular uptake of the conjugates in these glial cells was first assessed by staining the cells in reduced serum medium with the immunofluorescent vinculin, a specific stain of the tubulin protein, as performed by Dr. Phuong Le in the Petrecca lab. No fluorophore was detected in the cells upon incubation with naked siRNA (no transfection agent). Instead, a fraction of the standard amount of transfection agent (1/4) was used to compare the uptake of the unmodified siRNA **D0cy3** with the modified **D3cy3** (Figure 3.4). The sizes and shapes of the cells as well as their focal adhesions (FAs) increased when they were transfected with **D3cy3**, indicating that **D3cy3** was internalized and caused correct downregulation. Conversely, no phenotypic changes were seen with **D0cy3**. (The phenotypic changes associated with DRR downregulation are further discussed in Chapter 4.) On the other hand, upon inspection of the amount of internalized cy3 fluorophore, we detected more cy3 in cells transfected with **D0cy3** than in cells transfected with **D3cy3**. We surmised that the very small amount of positively charged transfection agent employed in these preliminary transfections resulted in the formation of a complex with the siRNAs, allowing them to penetrate the cellular membrane, but that complex did not necessarily develop into an encapsulating structure. Therefore, these siRNAs may have been highly susceptible to extracellular nucleases, allowing for cy3 hydrolysis. We also surmised that the modified siRNA was more nuclease resistant than the unmodified siRNA and that the incubation of **D0cy3** resulted in more hydrolyzed cy3 being released in the culture medium for uptake by the cells. (The nuclease stability of the modified siRNAs is explored in Chapter 4).

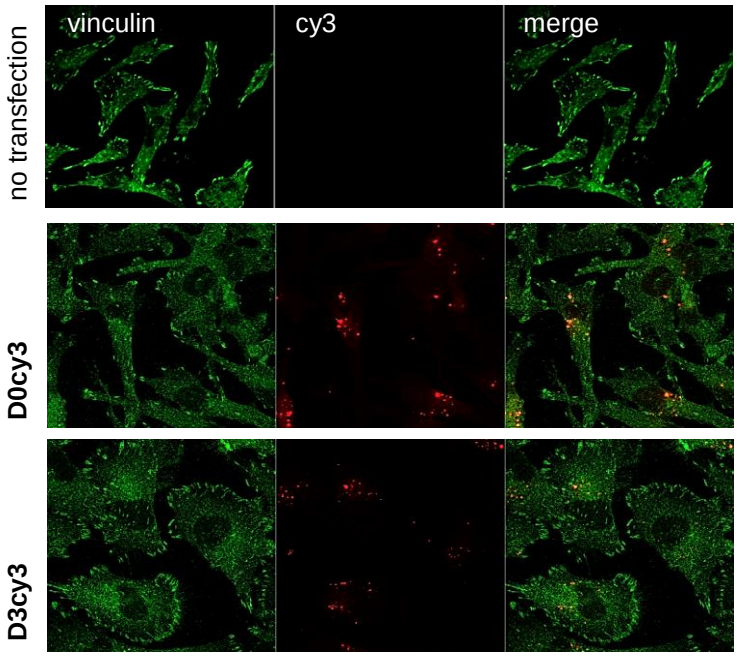

Figure 3.4. DRR+ cells were transfected with 20 nM of two different cy3-conjugated siRNAs using one quarter of the standard amount of transfection agent, incubated for 72 hours, and stained for tubulin.

In order to differentiate between duplexes and single strands or hydrolyzed fluorophore, siRNAs capable of FRET were employed. Thousands of transfected cells could be analyzed quickly by flow cytometry by exciting them at 488 nm while detecting cy5 at an emission filter of ≥650 nm. The emission filters were chosen according to an optimized procedure for detecting cell surface receptors using cy3- and cy5-labeled antibodies.[35] **D0cy3** and **D0cy5** served as compensation standards that allowed for fine tuning of the laser voltages. The use of suboptimal amounts of transfection agent (one eighth of the standard amount) was useful in showing the greater potency of the thrice-modified siRNA over the unmodified siRNA (further discussed in Chapter 4), as well as in measuring the relationship between the number of siRNA modifications and their uptake (with **D3cy3/5** serving as a measuring stick for conjugates with improved cellular uptake).

We then took on exploring the kinetics of uptake for DRR+ cells and proposed to evaluate the amount of detected duplex at several incubation times. A 4-hour evaluation time

was chosen in the event that the kinetics were similar to the uptake kinetics of HeLa cells, for example, but 8- and 18-hour test points were also considered. FRET was detected with the FL3 emission channel and is shown in Figure 3.5, above the cutoff for background FRET emission detected in untransfected cells. We found that the uptake reached a maximum after overnight incubation with an eighth of the standard amount of transfection agent and siRNAs **D0cy3/5** and **D6cy3/5**. Based on those observations, we performed the rest of our flow cytometry experiments after 18-hour incubation times.

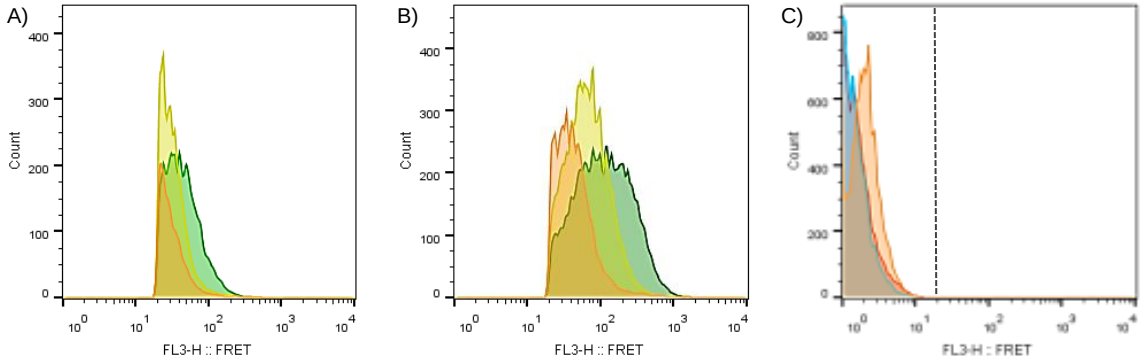

Figure 3.5. The histograms of duplexes detected in DRR+ *via* flow cytometry were transfected with A) **D0cy3/5** and B) **D6cy3/5** using 1/8th of the standard amount of transfection agent, while C) no FRET was detected above a threshold in non-transfected cells. Legend: orange = 4 hr; yellow = 8 hr; green = 18 hr.

We were then able to transfect glial cells with **D0cy3/5**, **D3cy3/5**, and **D6cy3/5** siRNAs (shaded entries in Table 3.1). The histogram shown in Figure 3.6A plots the distribution of FRET intensities detected in cell populations as a function of the number of cells detected. As the number of modifications increases, so does the median of each distribution. The transfections were repeated with these three siRNAs in three replicates and the relative median FRET intensity values were plotted in the bar graph in Figure 3.6B alongside the percentage of total cells sampled for which FRET was detected above the threshold amount. When the number of modifications is doubled from three to six, the median intensity increases but does not double; the relationship is not directly proportional. However, the percentage of cells with **D3cy3/5** and **D6cy3/5** duplexes is equal, within error, meaning that each individual cell has more **D6cy3/5**

duplex. No appreciable FRET intensity was detected in cells incubated with naked **D0cy3/5-D6cy3/5**.

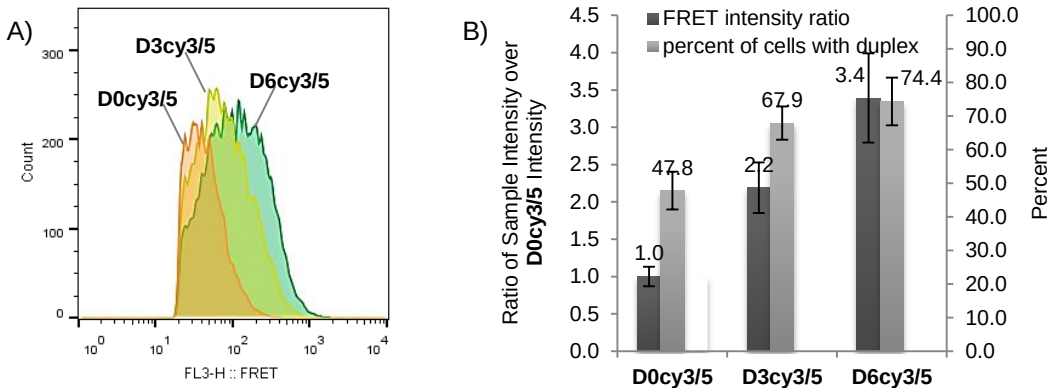

Figure 3.6. Flow cytometry was used to detect DRR+ cells transfected with one eighth of the standard amount of transfection agent and illustrated with A) histograms for three samples and B) median FRET intensity values and percentage of cells with duplex (n = 3).

The increase in cellular uptake for an siRNA duplex containing 40 negative charges and only six positively charge modifications, all the while using so little transfection agent, is substantial. Indeed, Figure 3.7 shows that the uptake of the unmodified siRNA when using half of the standard amount of transfection agent is equal to the uptake of the fully modified test conjugate **D6cy3/5** using one eighth of the standard amount of transfection agent. With half the standard amount of Lipofectamine™ 2000, FRET intensity for **D6cy3/5** increases almost 4.5 times over FRET intensity for **D6cy3/5** with an eighth of the standard amount of transfection agent, while FRET intensity of samples transfected with **D0cy3/5** increased only 3.4 times over FRET intensity for **D0cy3/5** with an eighth of the standard a mount of transfection agent, illustrating the beneficial effects of the modifications on the cellular uptake.

Figure 3.8 shows the immunofluorescent stains of DRR+ cells transfected with the test conjugates in serum-free media by Dr. Phuong Le, which confirm that the conjugates penetrate the cells and are not merely attached to the cell surface. Fluorophore intensity also increases in the order **D0cy3/5** < **D3cy3/5** < **D6cy3/5** as expected (i.e. uptake is dependent on the number of modified nucleotides within the duplex). The siRNAs seem to be localized in endosomes due to punctate localization of the cy3 fluorescence.

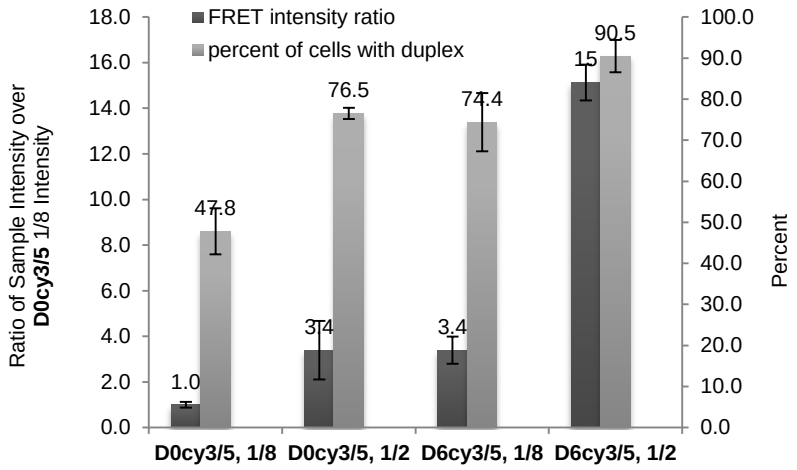

Figure 3.7. Glial cells transfected with half (1/2) and one eighth (1/8) the standard amount of transfection agent and siRNAs **D0cy3/5** and **D6cy3/5** (*n* = 3) reveals that six modifications are at least as influential as increasing the amount of transfection agent by a factor of 4.

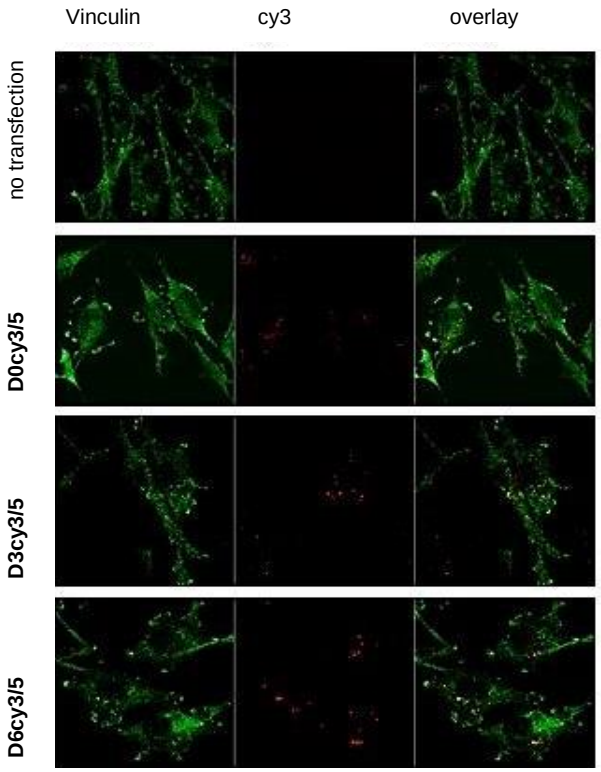

Figure 3.8. siRNAs (20 nM) were visualized in glial cells stained with vinculin for tubulin. One eighth of the standard amount of transfection agent was used for transfections.

3.4.2. Colonic and HeLa Cells

We wished to investigate the influence of the number of modifications in different cell lines and confirm that the trend in FRET intensity also applies to human colonic and HeLa cells. To do so, **D0cy3/4**, **D3cy3/5**, and **D6cy3/5** were transfected with 1/8th and 1/4th of transfection agent. The DRR-targeting siRNA sequence was used in each tissue type in order to fairly compare the uptake of these duplexes with that of human glial cells. Colonic HCT-116 cells were provided by the lab of Dr. Jean-Christophe Leroux at the ETH in Switzerland, and transfected and analyzed by flow cytometry by Elena Moroz using the same protocol as that used for the experiments performed with the glial cells. HeLa cells were provided by the Dr. Hanadi Sleiman lab at McGill University and transfected by Dr. Johans Fakhoury. Increasing the amount of transfection agent increases uptake as expected, however the response in uptake to the conjugates is essentially negligible at 1/8th transfection agent and minimal at 1/4th transfection agent regardless of the cell type used (Figure 3.9).

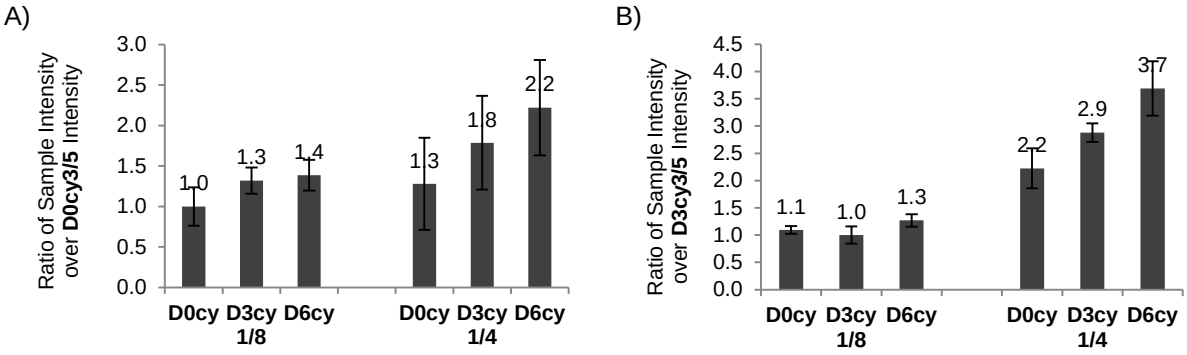

Figure 3.9. One eighth and one quarter of the standard amount of transfection agent was used to transfect A) human colonic cells and B) HeLa cells with **D0cy3**/5, **D3cy3**/5, and **D6cy3/5** siRNAs (n = 3) with no appreciable increase in uptake of conjugates using 1/8 transfection agent.

3.5. Cellular Uptake of Derivative Conjugates

3.5.1. Synthesis of Derivatives

Inspired by the strongly stimulated uptake of the test conjugates in glial cells, we wished to enquire if enhanced uptake could be maintained if the modification was altered or replaced. One modification that was investigated was a derivative of the 2'-*N*-acyl-L-phenylalanine modification in which the terminal primary amine is removed. This modification, "X", is shown

in Figure 3.10. It was incorporated into RNA by coupling hydrocinnamic acid to 2'-amino-2'-deoxy uridine **1** using EEDQ and incorporating the phosphoramide **13** (Scheme 3.2) into solid-supported synthesis of RNA. This derivative was used to investigate the effect of the amine on uptake. Another modification that was investigated, "Y", was based on glycine amino acid. The glycine-based phosphoramidite was synthesized by Dr. Ken Yamada to investigate the effect of the benzyl group on uptake.

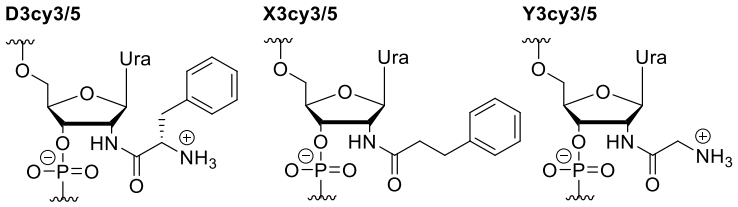

Figure 3.10. A comparison of the modifications investigated in RNA for their ability to increase cellular uptake.

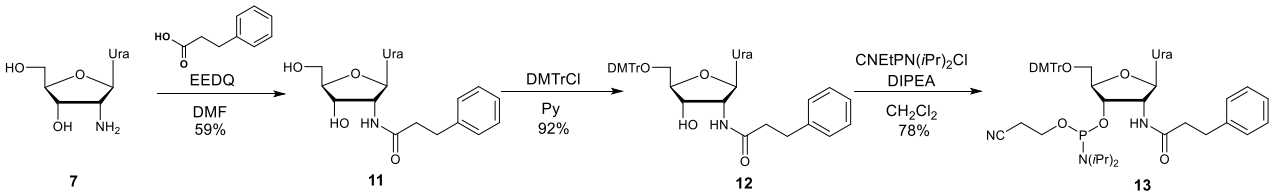

Scheme 3.2. A phosphoramidite bearing an *N*-acyl-hydrocinnamic acid modification at the 2'-position was synthesized to investigate the effect of the amino group of the phenylalanine amino acid on cellular uptake.

3.5.2. Derivative Conjugates

Phosphoramidite **13** and the glycine-based phosphoramidite were used to synthesize FRET-capable siRNAs containing modifications in the same positions as in **D3cy3/5** (Table 3.2). The FRET intensities of **Y3cy3/5** (sense strand synthesized by Dr. Ken Yamada) and **X3cy3/5** duplexes were compared to the FRET intensity of **D3cy3/5** in glial cells transfected with $1/8^{th}$ transfection agent. We found that the FRET intensities of the two novel siRNAs relative to **D3cy3/5** (relative I_{FRET}) are virtually the same as that of the phenylalanine-modified siRNA. This means that these two variations on phenylalanine increase uptake just as well as the phenylalanine does. Considering the endosomolytic properties of amine groups in

oligonucleotide therapeutics,[5,6] the phenylalanine modification was thus selected for further studies in new constructs containing a higher number of modifications (sections 3.6 and 3.7).

Table 3.2. Conjugates with variations on the phenylalanine modification were synthesized and their cellular uptake was compared to that of phenylalanine-containing conjugates.

siRNA	Sequence	Relative I_{FRET}
D3cy3/5	5'-**cy3**-GGA ACC AGC **U**CA **U**CA AGA A**U**U-3'	1.00
	3'-**cy5**-UU CCU UGG UCG AGU AGU UCU U-p-5'	
X3cy3/5	5'-**cy3**-GGA ACC AGC **X**CA **X**CA AGA A**X**U-3'	1.11
	3'-**cy5**-UU CCU UGG UCG AGU AGU UCU U-p-5'	
Y3cy3/5	5'-**cy3**-GGA ACC AGC **Y**CA **Y**CA AGA A**Y**U-3'	0.98
	3'-**cy5**-UU CCU UGG UCG AGU AGU UCU U-p-5'	

Legend: **U** = 2'-*N*-acyl-L-phenylalanine uridine; **X** = 2'-*N*-acyl-hydrocinnamic acid uridine; **Y** = 2'-*N*-acyl-glycine uridine; p = phosphate. Sequence: sense strand on top; antisense strand on bottom.

3.6. Combination of Phenylalanine and Fluorine Sugar Modifications

Given that the 2'-*N*-acyl-L-phenylalanine modification substantially decreases thermal melting temperature for every internal insert in an siRNA duplex (section 2.3.1), a maximum of five internal inserts contained in the test conjugates is allowed in order for the duplexes to remain stable above the temperature of incubation. We wanted to maintain the ds nature of the duplexes during the relatively long incubation period needed for cellular membrane penetration, in order to ensure that the antisense strand is also internalized. In our search for a homologous duplex with an improved cellular uptake over that of the duplex modified with six inserts (**D6cy3/5**), other chemical modifications have been considered in combination with phenylalanine.

The 2'-fluoro-ribo nucleic acid (2'-F-RNA) sugar derivative is an RNA mimic adopting a North sugar pucker and when introduced in oligonucleotides, yields an A-form duplex.[47] The

fluorine substitution is small, well-tolerated in the silencing machinery, and while it has not given any indication of encouraging cellular uptake, RNA modified with 2'-F-RNA units were found to be more thermally stable than the unmodified RNA (1^{o}C to 3^{o}C per 2'-F-rN insert). The origin of stabilization of 2'-F-RNA:RNA and 2'-F-RNA:2'-F-RNA duplexes has been investigated in detail by the Egli group and was found to stem from a favorable enthalpy of duplex formation, accompanied with a certain degree of preorganization of the 2'-F-RNA strand (which accounts for a more favorable entropy).[48] In addition, 2'-F-RNA causes a reduction in duplex hydration along the backbone and minor groove, an unfavorable parameter for duplex assembly,[48] but the reduced hydration sphere allows for strengthened Watson-Crick hydrogen-bonding and base-stacking.[49] The long-range inductive effects on the nucleobases are not the only factors to consider; charge polarization of C-H bonds with fluorine substituted nearby allows for FC-H2'···O4' interactions in the backbone of the duplexes, as shown by our laboratory.[50]

The 2'-F-RNA modification can be readily inserted into unmodified siRNAs since it does not lead to duplex destabilization. The choice in the pattern of 2'-F-RNA modification allowing for very similar or even improved potency compared to the unmodified duplex has a certain degree of freedom. Tracks of three inserts are tolerated anywhere in the sense or antisense strand,[51] while blunt-ended, fully modified siRNA containing equal amounts of 2'-F-RNA and 2'-*O*-Me RNA in a one-to-one alternating pattern have shown increased potency.[52] siRNA with alternating one-to-one and three-to-three tracks of 2'-F-RNA and 2'-F-ANA have been designed to improve guide strand selection, while siRNA with full 2'-F-RNA modification showed increased potency,[53] and a similar observation was made for siRNA with 2'-F-RNA modification at all pyrimidine positions, which resulted in a random pattern of single modifications and two- to four-insert-long tracks of 2'-F-RNA.[54]

New siRNAs (Table 3.3) were synthesized with 2'-*N*-acyl-L-phenylalanine modifications at the same six positions and with six 2'-F-RNA inserts at the 5'-end of the sense strand of **D6cy3/5**. The antisense strands of the new siRNAs were synthesized with zero, two, three and four 2'-*N*-acyl-L-phenylalanine uridine inserts and eight 2'-F-RNA inserts at the 3'-end. The 2'-F-RNA inserts were incorporated at the end of the duplex furthest away from the 5'-end of the antisense strand in order to encourage antisense strand loading into RISC. Most importantly, our

design was chosen in order to increase thermal stability by at least 14°C for the fourteen 2'-F-RNA inserts in the duplex, in order to offset the thermal destabilization cause by the two internal 2'-*N*-acyl-L-phenylalanine uridine modifications in the antisense strand of **F4cy5/3**.

Table 3.3. Conjugates were synthesized with eight to ten modifications that increase cellular uptake in human glial cells.

siRNA	Sequence
F0cy3/5	5'-**cy3**-gga aCC agC UCA UCA AGA AUU-3'
	3'-**cy5**-UU ccu ugg Ucg AGU AGU UCU U-p-5'
F1cy3/5	5'-**cy3**-gga aC**C** agC **UC**A **UC**A AGA A**U**U-3'
	3'-**cy5**-UU ccu ugg Ucg AGU AGU UCU U-p-5'
F2cy3/5	5'-**cy3**-gga aC**C** agC **UC**A **UC**A AGA A**U**U-3'
	3'-**cy5**-**UU** ccu ugg Ucg AGU AGU UCU U-p-5'
F3acy3/5	5'-**cy3**-gga aC**C** agC **UC**A **UC**A AGA A**U**U-3'
	3'-**UU** ccu ugg Ucg AGU AGU UCU **U**-p-5'
F3bcy3/5	5'- **cy3**-gga aC**C** agC **UC**A **UC**A AGA A**U**U-3'
	3'-**cy5**-**UU** ccu ugg **U**cg AGU AGU UCU U-p-5'
F4cy3/5	5'-**cy3**-gga aC**C** agC **UC**A **UC**A AGA A**U**U-3'
	3'-**cy5**-**UU** ccu ugg **U**cg AGU AGU UCU **U**-p-5'

Legend: Upper case letters = RNA; lower case letters = 2'-F-RNA; **U** = 2'-*N*-acyl-L-phenylalanine uridine; **C** = 2'-*N*-acyl-L-phenylalanine cytidine; p = phosphate. Sequence: Sense on top; antisense on bottom.

The siRNAs in Table 3.3 were transfected into glial cells using one eighth of the standard amount of transfection agent. The relative amounts of internalized siRNA and the percent of cells with duplex as judged by FCET reveals that siRNAs **F1cy3/5**-**F4cy3/5** containing one to four 2'-*N*-acyl-L-phenylalanine modifications in the antisense strand are internalized to about the same degree (Figure 3.11). Comparing the relative FCET values of **D6cy3/5** siRNAs transfected with one eighth of the standard amount of transfection agent to the values obtained for siRNAs **F1cy3/5** and **F4cy3/5** under the same condition reveals that the

intensity of FRET detected in about the same percentage of cells due to **D6cy3/5** is three times as great (Figure 3.12).

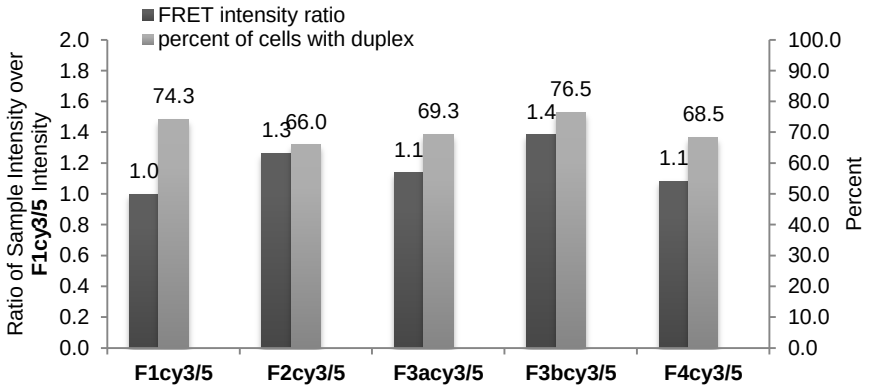

Figure 3.11. siRNAs **F1cy3/5**-**F4cy3/5** were transfected with an eighth of the standard amount of Lipofectamine^{TM} 2000 and FCET was measured.

The most interesting finding reveals that the relative intensity of FRET and the percent of cells with duplex increased over siRNAs **F1cy3/5**-**F4cy3/5** when siRNA **F0cy3/5** containing fourteen 2'-F-RNA inserts and none of the 2'-*N*-acyl-L-phenylalanine inserts was transfected (Figure 3.12). The data suggests that the 2'-F-RNA modification itself increases the uptake of siRNA in glial cells, while its combination with the 2'-*N*-acyl-L-phenylalanine modification somehow discourages uptake. Alternatively, the data may be suggesting that the combination of these modifications causes a change in the secondary structure of the oligonucleotides that distances the fluorophores from each other. A separation of the fluorophores would cause a reduction in FRET. Replicates of this experiment are needed to confirm these findings. Confirmation that duplexes did indeed form between the strands is needed *via* the measurement of thermal melting temperatures (T_ms) of each siRNA.

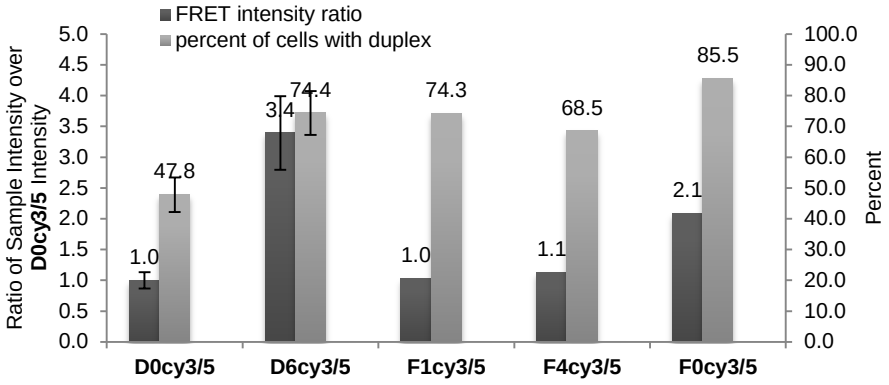

Figure 3.12. FCET of siRNAs **F0cy3/5**, **F1cy3/5**, and **F4cy3/5** was compared to siRNAs **D0cy3/5** and **D6cy3/5** transfected with an eighth of the standard amount of Lipofectamine™ 2000.

3.7. A Modified Tail Creates a Self-Delivering Asymmetric siRNA

We continued our search for a conjugate with improved uptake over the minimally modified siRNA that could deliver unmodified antisense strands by adding several of the inserts to the 5'-end of the sense strand, creating a 'tail'. A great enough improvement would allow for uptake without any transfection agent. Various functional groups have been appended to the 3'-end of the sense strand *via* the use of a solid support functionalized with lipophilic groups, such as those highlighted in section 1.4.1.1.[55] Fortunately, it has been shown that blocking of the terminal 3'-hydroxyl of the antisense strand with a functional group, as well as both termini of the sense strand, does not compromise the potency of symmetric siRNA.[56] Cholesterol and GalNAc conjugation at the 3'-end of the sense strand has been used in asymmetric shorter-duplex siRNA (asiRNA), where a 19- or 20-nt-long antisense strand is bound to a shorter sense strand, leaving behind a single-stranded 3' antisense terminus 5- to 8-nucleotides in length.[57,58] Some groups determined that a 16-nt duplex region in their asiRNA containing a 19-nt antisense strand was a minimal length requirement for potency,[59,60] while another showed that a 15-nt duplex with a 21-nt antisense efficiently silenced target genes.[61] While Tuschl and coworkers determined that 2-nt-long 3'-overhangs were the most potent in their set of symmetric siRNAs with 19-nt duplex regions,[62] those asymmetric siRNAs with variable 3'-overhang lengths are potent siRNAs presumably since the relatively long overhangs are a result of truncated sense strands, and are not due to a lengthening of the antisense strand. The terminal 5'-nucleotide on

the antisense strands was hybridized to the terminal 3'-nucleotide on the sense strands, in a blunt-ended fashion,[57,58] with the 5'-end of the antisense strand containing a phosphate group in order to bypass the need for intracellular phosphorylation[63,64] and further favour the antisense strand selection by RISC.[65]

Our design of a self-delivering asiRNA candidate with more amino acid modifications than we have previously used in one siRNA molecule, was done using the same solid supported synthetic procedure that was employed for our test conjugates. The sense strand of **D6cy3/5** was essentially extended to a 27-mer with seven 2'-*N*-acyl-L-phenylalanine uridine nucleotides connected by six PS bonds at the 5'-end, and the guanosine nucleotide at the 21st position was removed (Table 3.4). The cy3 fluorophore was moved from the 5'-position of the sense strand to the 5'-position of the antisense strand, and a cy5 fluorophore was used at the 3'-position of the sense strand. This allowed the fluorophores to communicate at the same 2-nt distance and thus yield FRET. The 7-nt tail was comprised of a phosphorothioate (PS) backbone, normally incorporated in oligonucleotides that silencing through the antisense mechanism and not the siRNA mechanism. PS modifications in the tail of the siRNA, rather than in its backbone, should avoid interfering with RISC-mediated silencing the modification. They were also expected to improve cellular uptake, as it was shown for PS-modified oligonucleotides during gymnosis.[66] The sequences and structures of the oligonucleotides are shown in Table 3.4.

Table 3.4. Asymmetric siRNAs were synthesized with up to thirteen total modifications.

siRNA	Sequence
A0cy3/5	5'-$U_sU_sU_s$ $U_sU_sU_s$ U_sGA ACC AGC UCA UCA AGA AUU-**cy5**-3'
	3'-UU CCU UGG UCG AGU AGU UCU U-**cy3**-5'
A13cy3/5	5'- **U**$_s$**U**$_s$**U**$_s$ **U**$_s$**U**$_s$**U**$_s$ **U**$_s$GA AC**C** AGC **UC**A **UC**A AGA A**U**U-**cy5**-3'
	3'-UU CCU UGG UCG AGU AGU UCU U-**cy3**-5'

Legend: **U** = 2'-*N*-acyl-L-phenylalanine uridine; **C** = 2'-*N*-acyl-L-phenylalanine cytidine; $_s$ = phosphorothioate. Sequence: sense strand on top; antisense strand on bottom.

Tuschl and coworkers studied gene silencing by symmetric duplexes with varying 3'-overhang lengths and found that 21-nt-long duplexes are the most potent silencers.[62] They also found that symmetric duplexes greater than 23-nucleotides-long had no activity; therefore, an antisense strand greater than 23-nucleotides would not be useful for silencing. In keeping with that idea, the original length of the antisense strand was not modified, but the 5'-phosphate was removed (Table 3.4). This allowed the 5'-cy3 to communicate with the 3'-cy5 of the sense strand at the same 2-nt distance as that used for the test conjugates.

Glial cells were transfected with an eighth of the standard amount of Lipofectamine™ 2000 and 20 nM of duplexes **D6cy3/5**, **A0cy3/5**, and **A13cy3/5**, the same concentration as that used in our test studies. In doing so, we wished to detect any improvement in the uptake of the asymmetric duplexes over the most modified test conjugate under the same transfection conditions used to observe an improved uptake of **D6cy3/5** over the unmodified siRNA. We reasoned that some transfection agent was still needed at this point so that any marginal improvement in uptake could be quantified even if unassisted uptake was not possible with the asymmetric conjugates. Figure 3.13 reveals that in samples transfected with **A13cy3/5**, a greater FRET intensity (normalized to the intensity of **D6cy3/5**) was detected in both replicates. The fluorescence intensity of **A13cy3/5** was greater by about half the intensity of **D6cy3/5** samples. This led us to believe that an appreciable amount of **A13cy3/5** could potentially penetrate cells without transfection agent.

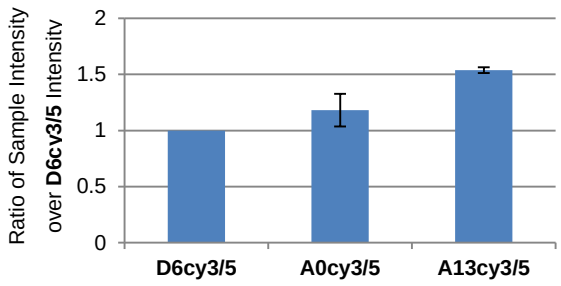

Figure 3.13. The ratio of median FRET intensity of glial cells transfected with duplex **D6cy3/5**, **A0cy3/5**, and **A13cy3/5** (n = 2) to that of **D6cy3/5** reveals that there is 50% more FRET detected from **A13cy3/5** than the test conjugate **D6cy3/5**. All duplexes were transfected with one eighth of the standard amount of transfection agent.

Glial cells were then incubated without transfection agent at a concentration of 40 nM of duplex **D0cy3/5**, **D6cy3/5**, **A0cy3/5**, and **A13cy3/5**. The histograms of the FRET intensity are shown in Figure 3.14. There is a large shift in intensity between the modified siRNA **D6cy3/5** and the amino acid-modified asymmetric **A13cy3/5**. The PS-modified asymmetric **A0cy3/5** is also detected with greater intensity than the test conjugate **D6cy3/5**. As mentioned above, without the use of transfection agent, **D6cy3/5** and **D0cy3/5** exhibit no difference in fluorophore intensity in the cells; indeed, the median intensities of their distributions as shown in Figure 3.14 are comparable. Under the microscope, this level of cellular uptake becomes negligible since the FRET intensity distributions of **D0cy3/5** and **D6cy3/5** mostly lay to the left of the line marking the upper FRET intensity of **D0cy3** in Figure 3.14 (**D0cy3** is not capable of exhibiting FRET since there is no cy5 present on the opposite strand).

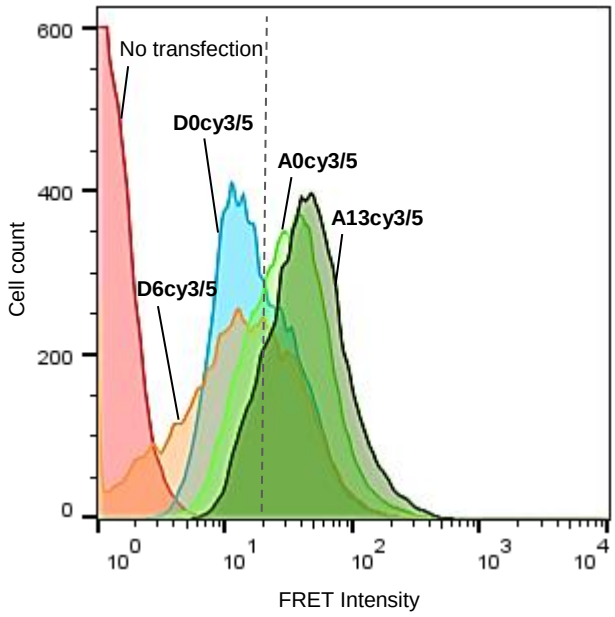

Figure 3.14. The distribution of FRET intensities in cells incubated without delivery agent reveals the improvement in uptake possible with asymmetric duplexes **A0cy3/5** and **A13cy3/5** when compared to the negligible uptake of symmetric duplexes **D0cy3/5** and **D6cy3/5**. The peaks for the asymmetric duplex peaks lie to the right of the line marking the upper FRET intensity of cy3-labeled unmodified siRNA.

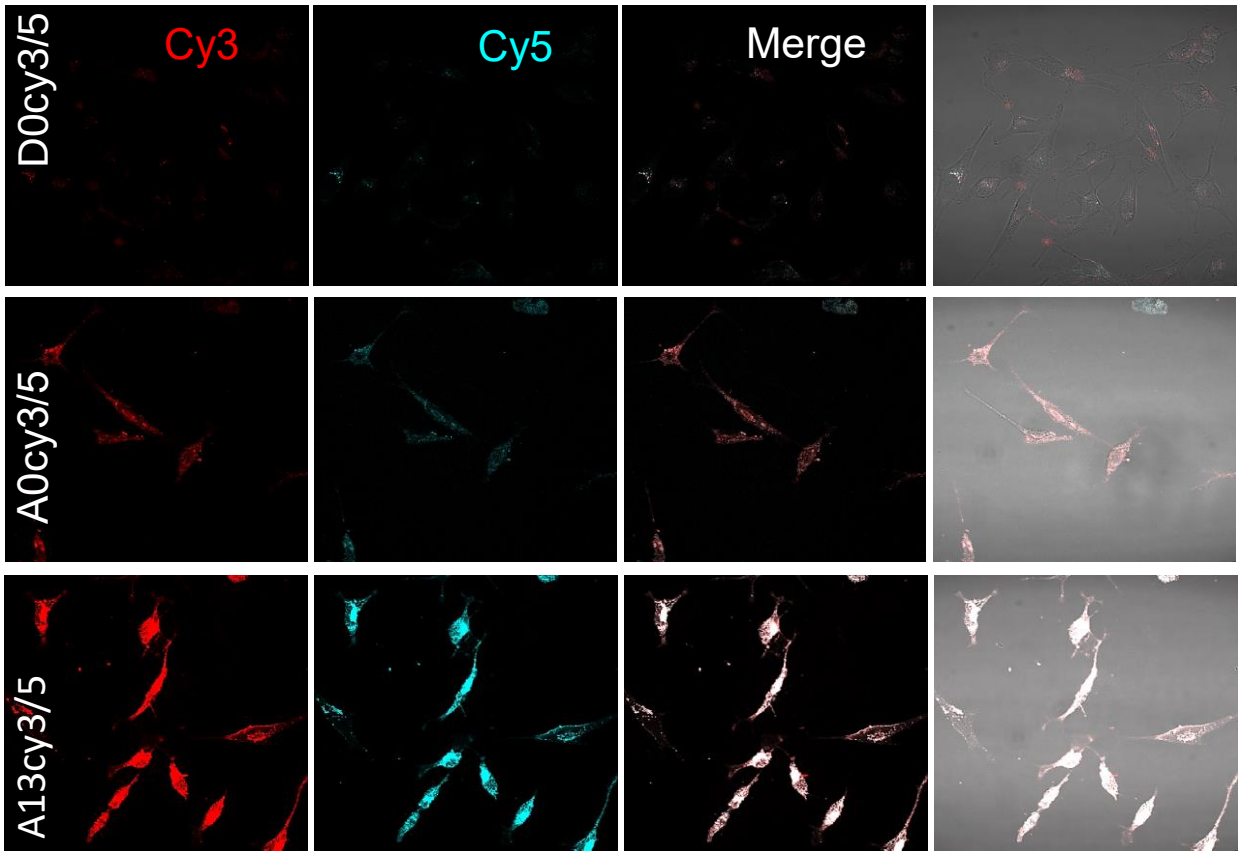

Figure 3.15. The cellular internalization of asymmetric duplex **A13cy3/5** (40 nM, without transfection agent) is much greater than the unmodified symmetric **D0cy3/5** after 18 hours incubation with glial cells.

The differences in internalization of the asymmetric duplexes over the unmodified canonical siRNA structure is shown in Figure 3.15. Dr. Phuong Le performed these immunofluorescent stains. Co-localization of the cy3 and cy5 fluorophores can be seen for the PS-modified **A0cy3/5**, indicating that the presence of the PS bonds increases the cellular uptake of the siRNA. Co-localization of the fluorophores is also seen for **A13cy3/5**, and with very high intensity for each fluorophore. In fact, the laser intensities used to capture the images for **D0cy3/5** and **A0cy3/5** were equal, however the intensities were reduced for **A13cy3/5** due to saturation of the detectors (Figure 3.16). To the best of our knowledge, this is the first demonstration of an asymmetric siRNA that is able to self-deliver to cells due to sugar modifications. In Chapter 4, the ability of unlabeled siRNA-2'-*N*-acyl-L-phenylalanine conjugates to cause protein downregulation and gene silencing with reduced amounts of

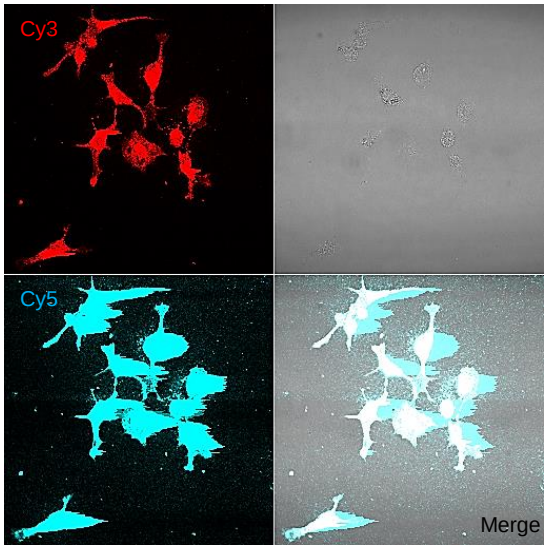

Figure 3.16. The detection of **A13cy3/5** in glial cells using the same laser intensities as those used in Figure 3.15 results in detector saturation.

transfection agent, or even none at all, is made possible by the improvement in cellular uptake demonstrated in this chapter.

3.8. Conclusion

We have employed the FCET method for detecting intact RNA duplex in cells by exploiting the ability of cyanine-3 and cyanine-5 to act as a FRET pair. We used this method in human glial cells to discover that constructs containing 2'-*N*-acyl-L-phenylalanine, 2'-*N*-acyl-hydrocinnamic acid, and 2'-*N*-acyl-glycine sugar modifications increase cellular uptake with an increasing number of modifications, and this observation applies to duplexes containing canonical 2'-hydroxyl groups but not 2'-F-RNA. This method was also used to construct duplexes with a phosphorothioate 'tail' that experience unassisted uptake in human glial cells despite an increase in the number of negatively charged internucleotide linkages. Conjugates capable of unassisted cellular uptake are attractive in the preparation of therapeutic siRNA candidates.

3.9. Experimental Methods

3.9.1. General Procedures for Monomer Synthesis

^{1}H-NMR and ^{13}C-NMR spectra were recorded at 400 MHz and 300 MHz, respectively, using the residual solvent peak as an internal standard ($(CD_3)_2CO$, CD_2Cl_2, $(CD_3)_2SO$). ^{1}H-NMR spectra were assigned using 2D ^{1}H-NMR (COSY) spectra. ^{31}P-NMR spectra were recorded at 200 MHz using 85% H_3PO_4 as an external standard. Reactions were monitored by TLC on alumina plates coated with silica gel and visualized with UV light and charring with H_2SO_4. Preparative chromatography was performed with 40-60 μm, 230-400 mesh silica gel. DMF and DMSO was dried over 3Å molecular sieves for at least 48 hr. CH_2Cl_2, THF, and MeCN were dried on an mBraun SPS solvent purification system. Pyridine, NEt_3, and DIPEA were distilled

from CaH_2. Where yields for monomer syntheses have been reported as an average in the previous sections, one example is described below.

3.9.2. Synthesis of Monomers

2'-deoxy-2'-*N*-[acyl-*N*-(9-fluorenylmethoxycarbonyl)-L-phenylalanine] uridine (8): Compound **7** (629 mg, 1.03 mmol) was dissolved in DMF (10 mL) with *N*-(9-fluorenylmethoxycarbonyl)-L-phenylalanine amino acid (597 mg, 1.54 mmol) and EEDQ (508 mg, 2.06 mmol) and stirred at 55^{o}C overnight. Upon completion, the reaction was dried *in vacuo* and purified by silica gel chromatography (CH_2Cl_2:MeOH 50:1) with 1% pyridine added to neutralize the silica to afford **8** (1.04 g, 93%). ^{1}H-NMR ($(CD_3)_2CO$) δ 7.85 (d, *J* = 7.42 Hz, 2H), 7.64 (br t, J = 7.81 Hz, 2H), 7.23 – 7.42 (m, 10H), 6.03 (d, *J* = 8.21 Hz, 1H), 5.64 (d, *J* = 8.21 Hz, 1H), 4.69 (dd, *J* = 8.50, 5.57 Hz, 1H), 4.44 (br d, *J* = 4.30 Hz, 1H), 4.09 – 4.34 (m, 4H), 3.79 (d, *J* = 2.74 Hz, 2H), 3.57 – 3.66 (m, 2H), 3.50 – 3.55 (m, 2H), 3.16 (br dd, *J* = 13.68, 5.08 Hz, 1H). ESI-QTOF calc for $C_{33}H_{32}N_4O_8$ [M+Na]: 635.21; found: 635.85.

2'-deoxy-5'-*O*-(4,4'-dimethoxytrityl)-2'-*N*-[acyl-*N*-(9-fluorenylmethoxycarbonyl)-L-phenylalanine] uridine (9): Compound **8** (350 mg, 0.57 mmol) was dissolved in pyridine (5 mL) with 4,4'-dimethoxytrityl chloride (252 mg, 0.74 mmol) and stirred at room temperature overnight. After completion, the reaction was quenched with sat. aq. $NaHCO_3$ and extracted with CH_2Cl_2. The products were dried over $MgSO_4$, filtered and dried *in vacuo*. The reaction products were purified by silica gel chromatography (hexanes:EtOAc 2:3) with 1% pyridine added to neutralize the silica to afford **9** (503 mg, 96%). #: ^{1}H-NMR ($(CD_3)_2CO$): δ 7.83 (d, *J* = 7.31 Hz, 2H), 7.75 (d, *J* = 8.20 Hz, 1H), 7.44 – 7.58 (m, 3H), 7.15 – 7.41 (m, 18H), 7.03 (br d, *J* = 8.50 Hz, 1H), 6.75 – 6.92 (m, 4H), 6.24 (d, *J* = 9.01 Hz, 1H), 5.36 (d, *J* = 8.06 Hz, 1H), 4.99 (br d, *J* = 5.42 Hz, 1H), 4.43 – 4.63 (m, 2H), 3.90 – 4.09 (m, 4H), 3.68 – 3.81 (s, 6H), 3.42 (br s, 1H), 3.14 – 3.32 (m, 2H), 2.95 – 3.10 (m, 2H). ESI-QTOF calc for $C_{54}H_{50}N_4O_{10}$ [M+Na]: 937.34; found: 937.96.

2'-deoxy-5'-*O*-(4,4'-dimethoxytrityl)-2'-*N*-[acyl-*N*-(9-fluorenylmethoxycarbonyl)-L-phenylalanine]-3'-*O*-[(2-cyanoethyl-*N*,*N*-diisopropyl)phosphoramidite] uridine (10): Compound **9** was dissolved in CH_2Cl_2 (3 mL) and stirred at room temperature. DIPEA was quickly added (940 uL, 5.40 mmol) and then 2-cyanoethyl-*N*,*N*-diisopropylphosphonamidic

chloride dropwise (361 uL, 1.62 mmol). The completed reaction after overnight stirring was quenched with sat. aq. $NaHCO_3$. The aqueous layer was extracted with CH_2Cl_2. The organic layer was dried over $MgSO_4$, filtered and dried *in vacuo*. The product was purified by silica gel chromatography (hexanes:EtOAc 3:2) with 1% pyridine added to neutralize the silica to afford **10** (775 mg, 87%). ^{31}P-NMR (CD_2Cl_2) δ 150.67, 149.19. ESI-QTOF calc for $C_{63}H_{67}N_6O_{11}P$ [M+Na]:1137.45; found: 1137.20.

2'-deoxy-2'-*N*-(acyl-*N*-hydrocinnamic acid) uridine (11): Nucleoside **7** (200 mg, 0.82 mmol) was dissolved in DMF (4 mL). At the same time, EEDQ (812 mg, 1.64 mmol) and hydrocinnamic acid (185.1 mg, 1.23 mmol) were dissolved in DMF (3 mL). After 1 hr, half (1.5 mL) of the EEDQ/hydrocinnamic acid solution was added dropwise to the nucleoside. After 24 hr, the reaction was washed with saturated aqueous $NaHCO_3$ and the aqueous layer was extracted three times with CH_2Cl_2. The organic layer was dried over $MgSO_4$, filtered, and dried *in vacuo*. The crude material was purified with silica gel with a gradient of 1 – 10% MeOH in CH_2Cl_2 to give product **11** in 67% yield. ^{1}H-NMR ($(CD_3)_2SO$): δ 11.29 (d, *J* = 1.83 Hz, 1H), 7.89 (d, *J* = 8.24 Hz, 1H), 7.85 (d, *J* = 8.85 Hz, 1H), 7.21 – 7.28 (m, 2H), 7.12 – 7.18 (m, 2H), 5.91 (d, *J* = 8.85 Hz, 1H), 5.69 (d, *J* = 4.27 Hz, 2H), 5.17 (t, *J* = 5.19 Hz, 1H), 4.53 (td, *J* = 8.70, 5.19 Hz, 1H), 4.06 (t, *J* = 5.34 Hz, 1H), 3.87 – 3.98 (m, 1H), 3.58 (br t, *J* = 4.88 Hz, 2H), 2.67 – 2.89 (m, 2H), 2.33 – 2.49 (m, 2H). ESI-QTOF calc for $C_{18}H_{21}N_3O_6$ [M+Na^+]: 398.13; found: 398.23.

2'-deoxy-5'-*O*-(4,4'-dimethoxytrityl)-2'-*N*-(acyl-*N*-hydrocinnamic acid) uridine (12): Nucleoside **7** (152 mg, 0.41 mmol) was dissolved in pyridine (4 mL) and DMTrCl (178.4 mg, 0.53 mmol) and $AgNO_3$ (89 mg, 0.53 mmol) were added. After 3 hr, the reaction was washed with saturated aqueous $NaHCO_3$ and the aqueous layer was extracted three times with CH_2Cl_2. The organic layer was dried over $MgSO_4$, filtered, and dried *in vacuo*. The crude material was was purified with silica gel to give product **12** in 91% yield with a gradient of 1 – 9% MeOH in CH_2Cl_2 with 0.5% pyridine additive. ^{1}H-NMR ($(CD_3)_2SO$): δ 11.34 (d, *J* = 2.14 Hz, 1H), 7.96 (d, *J* = 8.54 Hz, 1H), 7.65 (d, *J* = 8.24 Hz, 1H), 7.22 – 7.35 (m, 11H), 7.12 – 7.20 (m, 3H), 6.86 – 6.96 (m, 4H), 5.89 (d, *J* = 8.24 Hz, 1H), 5.40 (dd, *J* = 8.24, 2.14 1H), 4.08 – 4.20 (m, 1H), 3.95 – 4.07 (m, 1H), 3.75 (s, 6H), 3.23 – 3.39 (m, 2H), 3.18 (dd, *J* = 10.53, 3.20 Hz, 2H), 2.73 – 2.89 (m, 2H), 2.41 – 2.49 (m, 2H). ESI-QTOF calc for $C_{39}H_{39}N_3O_8$ [M+Na]: 677.27; found: 700.26.

2'-deoxy-5'-*O*-(4,4'-dimethoxytrityl)-2'-*N*-(acyl-*N*-hydrocinnamic acid)-3'-*O*-[(2-cyanoethyl-*N*,*N*-diisopropyl)phosphoramidite] uridine (13): Nucleoside **12** (240 mg, 0.35 mmol) was dissolved in CH_2Cl_2 (3 mL). DIPEA (308 μL, 1.75 mmol) and then phosphitylating reagent (119 μL, 0.9 mmol) were added. After 1.25 hr the reaction was washed with saturated aqueous $NaHCO_3$ and the aqueous layer was extracted three times with CH_2Cl_2. The organic layer was dried over $MgSO_4$, filtered, and dried *in vacuo*. The crude material was purified twice by silica gel chromatography to remove a large excess of phosphitylating reagent with 1 – 8% MeOH in CH_2Cl_2 to a yield of 78%. ^{31}P-NMR ($(CD_3)_2CO$) δ 149.82, 148.77. ESI-QTOF calc for $C_{48}H_{56}N_5O_9P$ [M+Na^+]: 900.37; found: 900.45.

3.9.3. Oligonucleotide Preparation

Oligonucleotides were synthesized on UnyLinker™ CPG (500 Å) with an Applied Biosystems DNA/RNA 3400 Synthesizer. Standard phosphoramidites were purchased from ChemGenes Corporation (Wilmington, MA) and dissolved in MeCN to a concentration of 0.15 M. Synthesized phosphoramidites were dissolved to a concentration of 0.12 M in DMSO/CH_2Cl_2/MeCN (1:5:5 v/v/v) for phosphoramidite **10** and in MeCN for phosphoramitide **13**. Coupling times for thymidine and uridine were 600 sec, while coupling time was 1200 sec for the modified units. Activation of phorphoramidites was achieved with standard 0.25 M ETT in MeCN. Standard capping was performed with a CAP A solution of Ac_2O/py/THF (10:10:80 v/v/v) and a CAP B solution of 15% *N*-methylimidazole in THF. The oxidation solution used was standard 0.1 M I_2 in py/H_2O/THF (8:16:76 v/v/v). Standard 3% TCA in CH_2Cl_2 was used for detritylation steps. Cyanine-3 was coupled to the solid support after detritylation of the last nucleotide in the sequence in the following manner. Cyanine-3 phosphoramidite was dissolved in MeCN to a concentration of 0.12 M. With argon flowing through the top of the synthesis column, a 1-mL syringe with activator solution (0.25 M ETT, 170 μL) was secured to the bottom end of the column. The line delivering argon to the top of the column was removed and the activator was immediately pushed through the column, followed by immediate attachment of another 1-mL syringe containing cyanine-3 phosphoramidite (0.12 M, 170 μL) to the top of the column. The pistons of the syringes were pushed back and forth a few times and then the column was shaken for 15 minutes. Then the support was washed with MeCN, and oxidized and then detritylated on the ABI Synthesizer. The same synthetic protocol was used for conjugate

strands with a 3'-cyanine-5, however succinyl-CPG derivatized with cyanine-5 was used with rA^{PAC}, rC^{PAC}, and $rG^{t\text{-}BuPAC}$ phosphoramidites.

The UnyLinker™ and succinyl solid supports were suspended in the standard NH_4OH/EtOH deprotection solution (1 mL, 3:1 v/v) and put on a shaker for 48 hr and 36 hr, respectively, at r.t. to remove the nucleobase and internucleotide protecting groups, and to cleave the support linker. After decanting and lyophilizing the supernatant, fast desilylation was performed in NEt_3-3HF/NMP/NEt_3 (0.300 mL 1.5:0.75:1 v/v/v) at 65°C for 4 hr., after which NaOAc (3 M, pH 5.5, 0.0025 mL) and cold 1-butanol (1 mL) were added to precipitate the oligonucleotide. The washed and dried oligonucleotide was dissolved in water, filtered, and purified by RP-HPLC. Crude oligonucleotide was suspended in autoclaved water. Because much of the modified oligonucleotides did not dissolve, 20 μL of 2 M triethylammonium acetate (TEAA) was added to dissolve the samples. A gradient of 5-40% MeCN in TEAA was used to purify the strands.

Table 3.5. Exact mass values of oligonucleotides synthesized

Oligonucleotide	Exact Mass Values			
	Sense strand		Antisense strand	
	Calculated	Found	Calculated	Found
D0cy3/5	7207.2019	7206.1563	7214.0141	7214.0469
D0cy3	7207.2019	7206.1563	6681.7709	6681.7188
D0cy5	6699.9612	6699.9612	6681.7709	6681.7188
D3cy3/5	7645.4575	7644.3359	7214.0141	7214.0469
D3cy3	7645.4575	7644.3359	6681.7709	6681.7188
D6cy3/5	8089.7569	8082.6094	7214.0141	7214.0469
X3cy3/5	7600.4233	7602.4463	7214.0141	7214.0469
Y3cy3/5	7375.3150	7377.3299	7214.0141	7214.0469
F0cy3/5	7219.1782	7219.1634	7230.0170	7230.1190
F1cy3/5	8101.7332	8101.7440	7230.0170	7230.1190
F2cy3/5	8101.7332	8101.7440	7522.1864	7522.2121
F3acy3/5	8101.7332	8101.7440	7668.2711	7668.2400

F3bcy3/5	8101.7332	8101.7440	7668.2711	7668.2400
F4cy3/5	8101.7332	8101.7440	7814.3558	7814.3693
A0cy3/5	9142.3456	9144.9141	7109.04	7110.8228
A13cy3/5	11047.4935	11049.9003	7109.04	7110.8228

3.9.4. Transfections

D0cy3/5, **D3cy3/5**, **D6cy3/5**, **X3cy3/5**, **Y3cy3/5**, **F0cy3/5-F4cy3/5**, **A0cy3/5**, and **A13cy3/5** were transfected using substandard amounts of Lipofectamine™ 2000 purchased from Invitrogen (using the manufacturer's protocol). An aliquot of siRNA (25 μM, 2 μL) in 2-[4-(2-hydroxyethyl)piperazin-1-yl]ethanesulfonic acid (HEPES)-containing buffer (0.6 M KCl, 6 μM HEPES, 1 μM $MgCl_2.6H_2O$, pH 7.4) was diluted in opti-MEM reduced serum medium (248 μL). Lipofectamine™ 2000 in opti-MEM reduced serum medium (final volume 250 μL) was added to the siRNA solutions for an siRNA concentration of 0.1 μM. Amounts of Lipofectamine™ 2000 were calculated based on ¼ and 1/8 of 5 μL per well of the 6-well plates used (final volume 2 mL). Cells plated at 100,000 cells/well were transfected and incubated with the siRNA at 37°C for 18 hours in DMEM high-glucose supplemented with 10% FBS, for a final concentration of 20 nM. **A0cy3/5** and **A13cy3/5** were also incubated at 40 nM using a 4-μL aliquot of siRNA and no Lipofectamine™ 2000.

3.9.5. Immunocytochemistry

Cells were grown on glass coverslips at a density of 50,000 cells/well, fixed with 3% PFA, permeabilized with 0.5% Triton X-100 and blocked with 0.5% BSA solution. Coverslips were incubated with primary antibody mouse anti-vinculin (1:200) for staining focal adhesions, purchased from Sigma by the Petrecca lab. This was followed by incubation with anti-mouse secondary antibody (1:1000) conjugated to Alexa 488, purchased from Invitrogen by the Petrecca lab. Fluorescently labeled cells were visualized with a Zeiss 510 confocal microscope (63 x objective) in the Petrecca lab.

3.9.6. Flow Cytometry

The cell media was removed and 10 mM EDTA in PBS (2 mL) was added to each well. Cells were incubated at 37^{o}C for 20 minutes until they all became detached from the plate. They were transferred to a tube, centrifuged for 5 minutes at 1400 rpm, decanted, and resuspended in 3% paraformaldehyde (200 μL). A BD FACSCalibur machine and CellQuest Pro software were used to analyze glial and HeLa cells. Cy3 was detected in the FL2 channel, Cy5 in FL4, autofluorescence in FL1, and FRET in FL3. **D0cy3** and **D0cy5** compensation samples were exited simultaneously with blue laser (488 nm) and red laser (635 nm) to adjust voltages. Samples were then excited with only blue laser to detect FRET-based emission of cyanine-5. On the Accuri C6 flow cytometer used for the colonic cells, the blue and red lasers were pulsed intermittently during compensation of controls and sample measurement. Red and blue laser excitations were recorded in separate files.

Cells were passed through the cytometer at a maximal rate of 200 cells/second in order to avoid issues with more than one cell passing through the interrogation. The acquisitions were stopped when 20,000 cells were measured in a large gate excluding cells lying on either forward or side scatter axes, or near the origin of the graph. The total number of cells gated and the number of cells in the FL3+/FL1- quadrant were used to calculate the percentage of cells with duplex (% cells with duplex = number of gated cells ÷ number of cells in FL3+/FL1- quadrant). The median intensity value in the FL3+/FL1- quadrant was adjusted for background excitation by subtracting the median FL3 intensity value for non-transfected cells of the sample set.

3.10. References

1. Juliano, R. L., The delivery of therapeutic oligonucleotides. *Nucleic Acids Res.* **2016**.

2. Dalby, B.; Cates, S.; Harris, A.; Ohki, E. C.; Tilkins, M. L.; Price, P. J.; Ciccarone, V. C., Advanced transfection with Lipofectamine 2000 reagent: primary neurons, siRNA, and high-throughput applications. *Methods (San Diego, Calif.)* **2004,** *33* (2), 95-103.

3. Xu, Y.; Szoka, F. C., Mechanism of DNA Release from Cationic Liposome/DNA Complexes Used in Cell Transfection. *Biochemistry* **1996,** *35* (18), 5616-5623.

4. Semple, S. C.; Akinc, A.; Chen, J.; Sandhu, A. P.; Mui, B. L.; Cho, C. K.; Sah, D. W. Y.; Stebbing, D.; Crosley, E. J.; Yaworski, E.; Hafez, I. M.; Dorkin, J. R.; Qin, J.; Lam, K.; Rajeev, K. G.; Wong, K. F.; Jeffs, L. B.; Nechev, L.; Eisenhardt, M. L.; Jayaraman, M.; Kazem, M.;

Maier, M. A.; Srinivasulu, M.; Weinstein, M. J.; Chen, Q.; Alvarez, R.; Barros, S. A.; De, S.; Klimuk, S. K.; Borland, T.; Kosovrasti, V.; Cantley, W. L.; Tam, Y. K.; Manoharan, M.; Ciufolini, M. A.; Tracy, M. A.; de Fougerolles, A.; MacLachlan, I.; Cullis, P. R.; Madden, T. D.; Hope, M. J., Rational design of cationic lipids for siRNA delivery. *Nat. Biotechnol.* **2010,** *28* (2), 172-176.

5. Merdan, T.; Kunath, K.; Fischer, D.; Kopecek, J.; Kissel, T., Intracellular Processing of Poly(Ethylene Imine)/Ribozyme Complexes Can Be Observed in Living Cells by Using Confocal Laser Scanning Microscopy and Inhibitor Experiments. *Pharm. Res.* **2002,** *19* (2), 140-146.

6. Nothisen, M.; Kotera, M.; Voirin, E.; Remy, J.-S.; Behr, J.-P., Cationic siRNAs Provide Carrier-Free Gene Silencing in Animal Cells. *J. Am. Chem. Soc.* **2009,** *131* (49), 17730-17731.

7. Remy, J.-S.; Sirlin, C.; Vierling, P.; Behr, J.-P., Gene Transfer with a Series of Lipophilic DNA-Binding Molecules. *Bioconjugate Chem.* **1994,** *5* (6), 647-654.

8. Gomes-da-Silva, L. C.; Fonseca, N. A.; Moura, V.; Pedroso de Lima, M. C.; Simões, S.; Moreira, J. N., Lipid-Based Nanoparticles for siRNA Delivery in Cancer Therapy: Paradigms and Challenges. *Acc. Chem. Res.* **2012,** *45* (7), 1163-1171.

9. Wu, J.; Huang, W.; He, Z., Dendrimers as Carriers for siRNA Delivery and Gene Silencing: A Review. *Sci. World J.* **2013,** *2013,* 630654.

10. Deglane, G.; Abes, S.; Michel, T.; Prevot, P.; Vives, E.; Debart, F.; Barvik, I.; Lebleu, B.; Vasseur, J. J., Impact of the guanidinium group on hybridization and cellular uptake of cationic oligonucleotides. *Chembiochem* **2006,** *7* (4), 684-692.

11. Teplova, M.; Wallace, S. T.; Tereshko, V.; Minasov, G.; Symons, A. M.; Cook, P. D.; Manoharan, M.; Egli, M., Structural origins of the exonuclease resistance of a zwitterionic RNA. *Proc. Natl. Acad. Sci.U.S.A.* **1999,** *96* (25), 14240-14245.

12. Winkler, J.; Saadat, K.; Diaz-Gavilan, M.; Urban, E.; Noe, C. R., Oligonucleotide-polyamine conjugates: influence of length and position of 2'-attached polyamines on duplex stability and antisense effect. *Eur. J. Med. Chem.* **2009,** *44* (2), 670-677.

13. Liétard, J.; Ittig, D.; Leumann, C. J., Synthesis, binding and cellular uptake properties of oligodeoxynucleotides containing cationic bicyclo-thymidine residues. *Bioorg. Med. Chem.* **2011,** *19* (19), 5869-5875.

14. Brzezinska, J.; D'Onofrio, J.; Buff, M. C.; Hean, J.; Ely, A.; Marimani, M.; Arbuthnot, P.; Engels, J. W., Synthesis of 2'-O-guanidinopropyl-modified nucleoside phosphoramidites and their incorporation into siRNAs targeting hepatitis B virus. *Bioorg. Med. Chem.* **2012,** *20* (4), 1594-1606.

15. Shrestha, A. R.; Kotobuki, Y.; Hari, Y.; Obika, S., Guanidine bridged nucleic acid (GuNA): an effect of a cationic bridged nucleic acid on DNA binding affinity. *Chem. Commun.* **2014,** *50* (5), 575-577.

16. Seio, K.; Tokugawa, M.; Kanamori, T.; Tsunoda, H.; Ohkubo, A.; Sekine, M., Synthesis and properties of cationic 2'-O-[N-(4-aminobutyl)carbamoyl] modified oligonucleotides. *Bioorg. Med. Chem. Lett.* **2012,** *22* (7), 2470-2473.

17. Yamada, T.; Okaniwa, N.; Saneyoshi, H.; Ohkubo, A.; Seio, K.; Nagata, T.; Aoki, Y.; Takeda, S. i.; Sekine, M., Synthesis of 2′-O-[2-(N-Methylcarbamoyl)ethyl]ribonucleosides Using Oxa-Michael Reaction and Chemical and Biological Properties of Oligonucleotide Derivatives Incorporating These Modified Ribonucleosides. *J. Org. Chem.* **2011,** *76* (9), 3042-3053.

18. Milton, S.; Ander, C.; Honcharenko, D.; Honcharenko, M.; Yeheskiely, E.; Strömberg, R., Synthesis and Stability of a 2′-O-[N-(Aminoethyl)carbamoyl]methyladenosine-Containing Dinucleotide. *Eur. J. Org. Chem.* **2013,** *2013* (31), 7184-7192.

19. Johnsson, R.; Lackey, J. G.; Bogojeski, J. J.; Damha, M. J., New light labile linker for solid phase synthesis of 2'-O-acetalester oligonucleotides and applications to siRNA prodrug development. *Bioorg. Med. Chem. Lett.* **2011,** *21* (12), 3721-3725.

20. Biscans, A.; Rouanet, S.; Bertrand, J. R.; Vasseur, J. J.; Dupouy, C.; Debart, F., Synthesis, binding, nuclease resistance and cellular uptake properties of 2'-O-acetalester-modified oligonucleotides containing cationic groups. *Bioorg. Med. Chem.* **2015,** *23* (17), 5360-5368.

21. Mazia, D. S., G.; Sale, W., Adhesion of cells to surfaces coated with polylysine. Applications to electron microscopy. *J. Cell Biol.* **1975,** *66* (1), 198-200.

22. Endoh, T.; Ohtsuki, T., Cellular siRNA delivery using cell-penetrating peptides modified for endosomal escape. *Adv. Drug Delivery Rev.* **2009,** *61* (9), 704-709.

23. Kumar, P.; Wu, H.; McBride, J. L.; Jung, K.-E.; Hee Kim, M.; Davidson, B. L.; Kyung Lee, S.; Shankar, P.; Manjunath, N., Transvascular delivery of small interfering RNA to the central nervous system. *Nature* **2007,** *448* (7149), 39-43.

24. Zhou, P.; Wang, M.; Du, L.; Fisher, G. W.; Waggoner, A.; Ly, D. H., Novel Binding and Efficient Cellular Uptake of Guanidine-Based Peptide Nucleic Acids (GPNA). *J. Am. Chem. Soc.* **2003,** *125* (23), 6878-6879.

25. Kalra, N.; Parlato, M. C.; Parmar, V. S.; Wengel, J., DNA and LNA oligonucleotides containing N2'-functionalised derivatives of 2'-amino-2'-deoxyuridine. *Bioorg. Med. Chem. Lett.* **2006,** *16* (12), 3166-3169.

26. Johannsen, M. W.; Crispino, L.; Wamberg, M. C.; Kalra, N.; Wengel, J., Amino acids attached to 2'-amino-LNA: synthesis and excellent duplex stability. *Org. Biomol. Chem.* **2011,** *9* (1), 243-252.

27. Manoharan, M.; Kawasaki, A. M.; Cook, P. D.; Fraser, A. S.; Prakash, T. P., 2'-O-acetamido modified monomers and oligomers. Google Patents: 2000.

28. Graber, D.; Moroder, H.; Steger, J.; Trappl, K.; Polacek, N.; Micura, R., Reliable semi-synthesis of hydrolysis-resistant 3′-peptidyl-tRNA conjugates containing genuine tRNA modifications. *Nucleic Acids Res.* **2010,** *38* (19), 6796-6802.

29. Jiang, Q.; Yue, D.; Nie, Y.; Xu, X.; He, Y.; Zhang, S.; Wagner, E.; Gu, Z., Specially-Made Lipid-based Assemblies for Improving Transmembrane Gene Delivery: Comparison of Basic Amino Acid Residues-Rich Periphery. *Mol. Pharmaceutics* **2016**, *13* (6), 1809-1821.

30. Ghosh, P. S.; Kim, C. K.; Han, G.; Forbes, N. S.; Rotello, V. M., Efficient gene delivery vectors by tuning the surface charge density of amino acid-functionalized gold nanoparticles. *ACS Nano* **2008,** *2* (11), 2213-2218.

31. Kawaguchi, T.; Sakairi, H.; Kimura, S.; Yamaguchi, T.; Saneyoshi, M., Synthesis and antileukemic activity of chymotrypsin-activated derivatives of 3'-amino-2',3'-dideoxycytidine. *Chem. Pharm. Bull. (Tokyo)* **1995,** *43* (3), 501-504.

32. Sharma, R. A.; Bobek, M.; Bloch, A., Preparation and biological activity of some aminoacyl and peptidyl derivatives of 2'-amino-2'-deoxyuridine. *J. Med. Chem.* **1975,** *18* (9), 955-957.

33. De Napoli, L.; Di Fabio, G.; D'Onofrio, J.; Montesarchio, D., New Nucleoside-Based Polymeric Supports for the Solid Phase Synthesis of Ribose-Modified Nucleoside Analogues. *Synlett.* **2004,** *2004* (11), 1975-1979.

34. Matulic-Adamic, J.; Beigelman, L.; Dudycz, L. W.; Gonzalez, C.; Usman, N., Synthesis and incorporation of 2′-amino acid conjugated nucleotides into ribozymes. *Bioorg. Med. Chem. Lett.* **1995,** *5* (22), 2721-2724.

35. Sebestyen, Z.; Nagy, P.; Horvath, G.; Vamosi, G.; Debets, R.; Gratama, J. W.; Alexander, D. R.; Szollosi, J., Long wavelength fluorophores and cell-by-cell correction for autofluorescence significantly improves the accuracy of flow cytometric energy transfer measurements on a dual-laser benchtop flow cytometer. *Cytometry* **2002,** *48* (3), 124-135.

36. Shin, S.; Kim, Y. S.; Kim, J.; Kwon, H. M.; Kim, D. E.; Hah, S. S., Sniffing for gene-silencing efficiency of siRNAs in HeLa cells in comparison with that in HEK293T cells: correlation between knockdown efficiency and sustainability of sirnas revealed by FRET-based probing. *Nucleic Acid Ther.* **2013,** *23* (2), 152-159.

37. Bartlett, D. W.; Davis, M. E., Effect of siRNA nuclease stability on the in vitro and in vivo kinetics of siRNA-mediated gene silencing. *Biotechnol. Bioeng.* **2007,** *97* (4), 909-921.

38. Clegg, R. M., Fluorescence resonance energy transfer and nucleic acids. *Methods Enzymol.* **1992,** *211*, 353-388.

39. Raemdonck, K.; Remaut, K.; Lucas, B.; Sanders, N. N.; Demeester, J.; De Smedt, S. C., In Situ Analysis of Single-Stranded and Duplex siRNA Integrity in Living Cells. *Biochemistry* **2006,** *45* (35), 10614-10623.

40. Järve, A.; Müller, J.; Kim, I.-H.; Rohr, K.; MacLean, C.; Fricker, G.; Massing, U.; Eberle, F.; Dalpke, A.; Fischer, R.; Trendelenburg, M. F.; Helm, M., Surveillance of siRNA integrity by FRET imaging. *Nucleic Acids Res.* **2007,** *35* (18), e124-e124.

41. Hirsch, M.; Strand, D.; Helm, M., Dye selection for live cell imaging of intact siRNA. *Biol. Chem.* **2012,** *393* (1-2), 23-35.

42. Jagannath, A.; Wood, M. J. A., Localization of Double-stranded Small Interfering RNA to Cytoplasmic Processing Bodies Is Ago2 Dependent and Results in Up-Regulation of GW182 and Argonaute-2. *Mol. Biol. Cell* **2009,** *20* (1), 521-529.

43. Lee, H.; Kim, I. K.; Park, T. G., Intracellular trafficking and unpacking of siRNA/quantum dot-PEI complexes modified with and without cell penetrating peptide: confocal and flow cytometric FRET analysis. *Bioconjug. Chem.* **2010,** *21* (2), 289-295.

44. Alabi, C. A.; Love, K. T.; Sahay, G.; Stutzman, T.; Young, W. T.; Langer, R.; Anderson, D. G., FRET-Labeled siRNA Probes for Tracking Assembly and Disassembly of siRNA Nanocomplexes. *ACS Nano* **2012,** *6* (7), 6133-6141.

45. Le, P. U.; Angers-Loustau, A.; de Oliveira, R. M.; Ajlan, A.; Brassard, C. L.; Dudley, A.; Brent, H.; Siu, V.; Trinh, G.; Molenkamp, G.; Wang, J.; Seyed Sadr, M.; Bedell, B.; Del Maestro, R. F.; Petrecca, K., DRR drives brain cancer invasion by regulating cytoskeletal-focal adhesion dynamics. *Oncogene* **2010,** *29* (33), 4636-4647.

46. Boutla, A.; Delidakis, C.; Livadaras, I.; Tsagris, M.; Tabler, M., Short 5′-phosphorylated double-stranded RNAs induce RNA interference in Drosophila. *Curr. Biol.* **2001,** *11* (22), 1776-1780.

47. Ikeda, H.; Fernandez, R.; Wilk, A.; Barchi, J. J., Jr.; Huang, X.; Marquez, V. E., The effect of two antipodal fluorine-induced sugar puckers on the conformation and stability of the Dickerson-Drew dodecamer duplex [d(CGCGAATTCGCG)]2. *Nucleic Acids Res.* **1998,** *26* (9), 2237-2244.

48. Pallan, P. S.; Greene, E. M.; Jicman, P. A.; Pandey, R. K.; Manoharan, M.; Rozners, E.; Egli, M., Unexpected origins of the enhanced pairing affinity of 2′-fluoro-modified RNA. *Nucleic Acids Res.* **2011,** *39* (8), 3482-3495.

49. Patra, A.; Paolillo, M.; Charisse, K.; Manoharan, M.; Rozners, E.; Egli, M., 2′-Fluoro RNA Shows Increased Watson-Crick H-Bonding Strength and Stacking relative to RNA: Evidence from NMR and Thermodynamic Data. *Angew. Chem. Int.Ed.* **2012,** *51* (47), 11863-11866.

50. Martin-Pintado, N.; Deleavey, G. F.; Portella, G.; Campos-Olivas, R.; Orozco, M.; Damha, M. J.; Gonzalez, C., Backbone FC-H...O hydrogen bonds in 2'F-substituted nucleic acids. *Angew. Chem. Int. Ed.* **2013,** *52* (46), 12065-12068.

51. Prakash, T. P.; Allerson, C. R.; Dande, P.; Vickers, T. A.; Sioufi, N.; Jarres, R.; Baker, B. F.; Swayze, E. E.; Griffey, R. H.; Bhat, B., Positional effect of chemical modifications on short interference RNA activity in mammalian cells. *J. Med. Chem.* **2005,** *48* (13), 4247-4253.

52. Allerson, C. R.; Sioufi, N.; Jarres, R.; Prakash, T. P.; Naik, N.; Berdeja, A.; Wanders, L.; Griffey, R. H.; Swayze, E. E.; Bhat, B., Fully 2'-modified oligonucleotide duplexes with improved in vitro potency and stability compared to unmodified small interfering RNA. *J. Med. Chem.* **2005,** *48* (4), 901-904.

53. Deleavey, G. F.; Watts, J. K.; Alain, T.; Robert, F.; Kalota, A.; Aishwarya, V.; Pelletier, J.; Gewirtz, A. M.; Sonenberg, N.; Damha, M. J., Synergistic effects between analogs of DNA and RNA improve the potency of siRNA-mediated gene silencing. *Nucleic Acids Res.* **2010,** *38* (13), 4547-4557.

54. Manoharan, M.; Akinc, A.; Pandey, R. K.; Qin, J.; Hadwiger, P.; John, M.; Mills, K.; Charisse, K.; Maier, M. A.; Nechev, L.; Greene, E. M.; Pallan, P. S.; Rozners, E.; Rajeev, K. G.; Egli, M., Unique gene-silencing and structural properties of 2'-fluoro-modified siRNAs. *Angew. Chem. Int. Ed.* **2011,** *50* (10), 2284-2288.

55. Wolfrum, C.; Shi, S.; Jayaprakash, K. N.; Jayaraman, M.; Wang, G.; Pandey, R. K.; Rajeev, K. G.; Nakayama, T.; Charrise, K.; Ndungo, E. M.; Zimmermann, T.; Koteliansky, V.; Manoharan, M.; Stoffel, M., Mechanisms and optimization of in vivo delivery of lipophilic siRNAs. *Nat. Biotechnol.* **2007,** *25* (10), 1149-1157.

56. Czauderna, F.; Fechtner, M.; Dames, S.; Aygün, H.; Klippel, A.; Pronk, G. J.; Giese, K.; Kaufmann, J., Structural variations and stabilising modifications of synthetic siRNAs in mammalian cells. *Nucleic Acids Res.* **2003,** *31* (11), 2705-2716.

57. Byrne, M.; Tzekov, R.; Wang, Y.; Rodgers, A.; Cardia, J.; Ford, G.; Holton, K.; Pandarinathan, L.; Lapierre, J.; Stanney, W.; Bulock, K.; Shaw, S.; Libertine, L.; Fettes, K.; Khvorova, A.; Kaushal, S.; Pavco, P., Novel hydrophobically modified asymmetric RNAi compounds (sd-rxRNA) demonstrate robust efficacy in the eye. *J. Ocul. Pharm. Ther.* **2013,** *29* (10), 855-864.

58. Osborn, M. F.; Alterman, J. F.; Nikan, M.; Cao, H.; Didiot, M. C.; Hassler, M. R.; Coles, A. H.; Khvorova, A., Guanabenz (Wytensin) selectively enhances uptake and efficacy of hydrophobically modified siRNAs. *Nucleic Acids Res.* **2015,** *43* (18), 8664-8672.

59. Chu, C. Y.; Rana, T. M., Potent RNAi by short RNA triggers. *RNA (New York, N.Y.)* **2008,** *14* (9), 1714-1719.

60. Chang, C. I.; Yoo, J. W.; Hong, S. W.; Lee, S. E.; Kang, H. S.; Sun, X.; Rogoff, H. A.; Ban, C.; Kim, S.; Li, C. J.; Lee, D. K., Asymmetric shorter-duplex siRNA structures trigger efficient gene silencing with reduced nonspecific effects. *Mol. Ther., J. Am. Soc.Gene Ther.* **2009,** *17* (4), 725-732.

61. Sun, X.; Rogoff, H. A.; Li, C. J., Asymmetric RNA duplexes mediate RNA interference in mammalian cells. *Nat. Biotechnol.* **2008,** *26* (12), 1379-1382.

62. Elbashir, S. M.; Martinez, J.; Patkaniowska, A.; Lendeckel, W.; Tuschl, T., Functional anatomy of siRNAs for mediating efficient RNAi in Drosophila melanogaster embryo lysate. *EMBO J.* **2001,** *20* (23), 6877-6888.

63. Nykanen, A.; Haley, B.; Zamore, P. D., ATP requirements and small interfering RNA structure in the RNA interference pathway. *Cell* **2001,** *107* (3), 309-321.

64. Chiu, Y.-L.; Rana, T. M., RNAi in Human Cells: Basic Structural and Functional Features of Small Interfering RNA. *Mol. Cell* **2002,** *10* (3), 549-561.

65. Chen, P. Y.; Weinmann, L.; Gaidatzis, D.; Pei, Y.; Zavolan, M.; Tuschl, T.; Meister, G., Strand-specific 5'-O-methylation of siRNA duplexes controls guide strand selection and targeting specificity. *RNA (New York, N.Y.)* **2008,** *14* (2), 263-274.

66. Stein, C. A.; Hansen, J. B.; Lai, J.; Wu, S.; Voskresenskiy, A.; Høg, A.; Worm, J.; Hedtjärn, M.; Souleimanian, N.; Miller, P.; Soifer, H. S.; Castanotto, D.; Benimetskaya, L.; Ørum, H.; Koch, T., Efficient gene silencing by delivery of locked nucleic acid antisense oligonucleotides, unassisted by transfection reagents. *Nucleic Acids Res.* **2010,** *38* (1), e3-e3.

Chapter 4: Gene Silencing Properties of Amino Acid-siRNA Conjugates

4.1. Positively Charged 2' Sugar Modifications in Application to RNA Interference

The mechanism of siRNA downregulation was described in Chapter 1, in which synthetic duplex RNA hijacks an endogenous process of catalytic cleavage of a target mRNA sequence. This results in fewer mRNA copies and, as a result, attenuates expression of the protein encoded by the mRNA. While the canonical siRNA duplex is comprised of 2'-hydroxyl groups, these are in fact not necessary, as activated RISC only recognizes the duplex conformation of the major groove.[1] RISC recognition also does not necessitate a perfect A-form siRNA duplex.[2] What is essential, however, is an A-form duplex between the guide strand that remains in activated RISC and the target mRNA.[2] It is also crucial that an intact guide strand of the required length is available for loading into RISC, despite the presence of extracellular and intracellular nucleases, and that the correct strand of a duplex is loaded into the complex.

There are many modifications to the ribose sugar of RNA, highlighted in section 1.3.4.2, which comprise a range of sugar conformations. They can be inserted into siRNA to confer nuclease resistance relative to the unmodified duplex, and to encourage selection of the guide strand. They can favour guide strand loading into RISC through their effect on the thermal melting temperature (T_m) - being strategically placed in the siRNA construct to guide duplex unzipping at the 5'-end of the antisense strand, allowing antisense strand loading into RISC. The modification can be used nearer the 3'-end of the intended guide strand if it is stabilizing ($+\Delta T_m$), or it can be used nearer the 5'-end of the intended guide strand if it is destabilizing ($-\Delta T_m$).[3,4] If the sugar conformation is far from A-form or unknown, the modification can be inserted into the passenger strand near the appropriate terminal, depending on its ΔT_m, since it is the A-form helical conformation between the guide strand and the mRNA target that is essential. Other modifications that are tolerated in the guide strand, such as 2'-fluoro-RNA, can be inserted near the appropriate terminal on the guide strand.

These considerations have been made in the characterization of several 2'-positively charged sugar modifications, with sparse examples of their evaluation in RNA interference. Nonetheless, positively charged 2'-positions in RNA such as single 2'-*O*-aminoethyl (2'-*O*-AE) or single 2'-*O*-guanidinoethyl (2'-*O*-GE) (pK_{aH} = 12.5) inserts in RNA retain the A-form of the

RNA duplex and increase nuclease stability.[5] In fact, these two cationic RNAs are more nuclease resistant than RNAs containing some neutral 2' modifications.[5] An analogous group to 2'-*O*-AE, 2'-*O*-3-(*N*,*N*-dimethylamino)propyl, as well as 2'-*O*-GE modification, increases T_m when modifications are spaced out in an oligonucleotide and slightly decreases T_m when they are grouped together.[6,7] A single insert of 2'-*O*-GE or 2'-*O*-AE five nucleotides away from the 3' terminus of the sense strand retains siRNA activity, while insertion of 2'-*O*-AE at the 5' terminus of the antisense strand obliterates silencing, possibly due to disfavoured loading of the antisense strand.[5] A cationic homologue to 2'-*O*-AE, 2'-*O*-aminopropyl (2'-*O*-AP) uridine (pK_{aH} = 9), interconverts between the South (60%) and North (40%) conformations when sandwiched by DNA monomers, increases nuclease stability, and alters T_m to an RNA complement in both positive and negative directions depending on its placement.[8] Used in a gapmer antisense oligonucleotide (AON), the modification inserted into the center of a phosphorothioate-AON improved gene silencing when compared to the phosphorothioate-only AON.[8] A single 2'-*O*-guanidinopropyl (2'-*O*-GP) modification, a cationic homologue to 2'-*O*-GE, is minimally thermally destabilizing and has achieved gene silencing in the antisense strand of siRNA.[9]

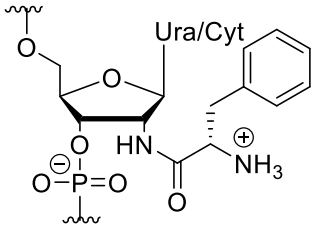

Figure 4.1. The stable 2'-*N*-acyl-L-phenylalanine modification was assayed in siRNA for compatibility with RNAi.

We sought to explore the compatibility of the 2'-*N*-acyl-L-phenylalanine modification characterized in Chapter 3 as having strong ability to increase uptake of RNA, in the RNAi pathway. Neither helix nor sugar conformation have been studied for duplexes containing this modification. Previous work studied the inhibitory effect of 2'-*N*-acyl-L-phenylalanine uridine on chitin synthesis, due to its structural similarity to UDP-*N*-acetylglucosamine,[10] as well as the protease activation of 3'-*N*-acyl-L-phenylalanine deoxycytidine prodrug.[11] The only incorporation of the modification into an oligonucleotide, to the best of our knowledge, was done in a hammerhead ribozyme, for which kinetics of substrate cleavage were measured.[12] For these reasons, T_m and nuclease resistance data have not yet been reported.

In this chapter, uridine and cytidine with 2'-*N*-acyl-L-phenylalanine modifications are incorporated into siRNAs using phosphoramidites whose syntheses were discussed in Chapter 2.

Several of the DRR-targeting sequences synthesized in this chapter are based on sequences synthesized and listed in Tables 3.1 and 3.4 in Chapter 3. Additional DRR and *bcl-2*-targeting RNAs were synthesized for this chapter. siRNAs were characterized for their ability to cause gene silencing in two endogenous systems despite the use of very little or no transfection agent. In this way, their ability to outperform their corresponding unmodified siRNAs is assessed. Their nuclease stability, polyacrylamide gel mobility, lipophilicity, and effect on thermal melting temperature are also described.

4.2. The siRNAs Synthesized Target Endogenous Genes

4.2.1. Downregulated in Renal Cell Carcinoma (DRR)

The invasion of malignant glial cells (primary brain cancer cells) into brain tissue is a multistep process. This process begins with attachment to focal adhesions (FAs) and is eventually followed by FA disassembly once the extracellular matrix in front of the cell is degraded and the cell has translocated forward.[13] The Petrecca lab at McGill University has identified a protein regulator of FA disassembly called downregulated in renal cell carcinoma (DRR).[13] It is not expressed in normal glial cells, which have a rounded cell shape and large FAs that surround the entire perimeter of the cells, yet it is highly expressed in invasive gliomas, which take on a spindle-like cell shape with a few small and spaced out FAs.[13] In this chapter, these invasive cells overexpressing DRR will be referred to as DRR+ cells.

An siRNA 19-mer duplex with 2-nucleotide (nt) 3'-overhangs was previously designed by Dr. Glen Deleavey, a former member in the Damha lab, against the mRNA sequence of the *drr* gene (NCBI accession number: NM_007177.2) from positions 786 to 805 and was used as the template for the siRNAs listed in Table 4.1.[14] The Petrecca lab generously provided me with DRR+ cells and their laboratory space for Western blots and immunofluorescent stains of DRR+ cells, which I carried out, or they performed the assays themselves, where indicated. Dr. Ken Yamada synthesized the 2'-*N*-acyl-L-phenylalanine cytidine phosphoramidite as well as sequences **D4**-**D3C** (Table 4.1). The thermally destabilizing uridine modifications were added to the sense strand nearer the 3'-end (**D1a**-**D3**), and the cytidine modification was added to the three positions closest to the 3'-end (**D4**-**D3C**), with a maximum of two consecutive 2'-*N*-acyl-L-phenylalanine modifications. This was done in an effort to encourage the loading of the desired

antisense strand for most of the conjugates. A 5'-phosphate was used on the antisense strand to further encourage the selection of the antisense strand for guide strand loading.

A scrambled duplex was synthesized in order to serve as a non-targeting negative control. It was designed by entering scrambled sequences of both the antisense and sense strand of DRR-targeting siRNA into NCBI's online BLASTn tool and searching for stretches of nucleotide matches in the human and mouse genomes and in their RNA transcripts (such as mRNAs). A scrambled sense sequence with the same number of U, rC, rG, and rA nucleotides, but with a rArA 3'-overhang instead of an rUrU 3'-overhang, was found to have an extremely low number of short complements to RNA transcripts. Its 21-mer complement with a rCrG 3'-overhang exchanges two U nucleotides in the antisense strand's overhang with an extra rC and rG as well as two more U nucleotides in its center, that were opposite the two rA nucleotides moved to the scrambled sense strand's overhang, with two extra rAs. Therefore, the scramble antisense strand contains four less U nucleotides, one more rG and rC nucleotide, and two more rA nucleotides than the targeting antisense strand, and is thus not a true "scrambled" sequence by definition. However, both the designed scrambled sense and antisense strands complement thousands of times fewer sequences in the genomes and RNA transcripts than the previously used non-targeting siRNA in DRR silencing assays,[14] thus making the designed non-targeting siRNA a much more reliable negative control. The non-targeting siRNA was also synthesized with three 2'-*N*-acyl-L-phenyalalnine uridine modifications (**D3-scr**). The use of this scramble was important in confirming that the modification itself wasn't causing downregulation by DRR-targeting siRNA conjugates (Figure 4.11 and Figure 4.18).

When the expression of DRR in DRR+ cells is silenced by siRNA, FA disassembly and reassembly is halted, reducing the malignancy of the gliomas. The phenotypic changes associated with DRR downregulation caused by siRNAs shown in Table 4.1 were observed under a microscope by the immunofluorescent staining of the cells (section 4.3.2). The potencies of these siRNAs in DRR+ cells were assessed qualitatively with immunoblots (also known as Western blots) in section 4.3.1, which measure the degree of reduction in protein expression. Quantitative assessment of DRR downregulation was measured by the invasion distance of DRR+ cells emanating from tumor spheroids transfected with the siRNAs (section 4.3.3). The

long-term objective in targeting this protein is to prevent cancer relapse after tumor removal due to leftover malignant cells.

Table 4.1. The sense strands of DRR-targeting siRNAs **D0**-**D3C** and the scramble strands **D0-scr** and **D3-scr** used for gene silencing experiments.

siRNA	Sense strand	T_m (^oC)
D0	5'-GGA ACC AGC UCA UCA AGA AUU-3'	75.9
D1a	5'-GGA ACC AGC UCA UCA AGA A**U**U-3'	75.5
D1b	5'-GGA ACC AGC UCA **U**CA AGA AUU-3'	70.3
D2	5'-GGA ACC AGC UCA **U**CA AGA A**U**U-3'	69.6
D3	5'-GGA ACC AGC **U**CA **U**CA AGA A**U**U-3'	63.8
D4	5'-GGA ACC AGC **U**CA **UC**A AGA A**U**U-3'	59.7
D5	5'-GGA ACC AGC **UC**A **UC**A AGA A**U**U-3'	-
D6	5'-GGA AC**C** AGC **UC**A **UC**A AGA A**U**U-3'	49.1
D3C	5'-GGA AC**C** AGC U**C**A U**C**A AGA AUU-3'	58.0
D0-scr	5'-UCC UUC GAC GAG AAG AAC UAA-3'	n.d.
D3-scr	5'-**U**CC U**U**C GAC GAG AAG AAC **U**AA-3'	n.d.

Legend: **U** = 2'-*N*-acyl-L-phenylalanine uridine; **C** = 2'-*N*-acyl-L-phenylalanine cytidine; antisense strand = 5'-p-UUC UUG AUG AGC UGG UUC CUU-3'; scramble antisense strand = 5'-p-AGU UCU UCU CGU CGA AGG ACG-3'; p = phosphate; (-) = single value not attainable; n.d. = not determined.

The Western blot in Figure 4.2 was performed by Dr. Phuong Le to compare the function of unmodified **D0** with modified oligonucleotides **D0cy3**, **D0cy5**, and **D0cy3/5**, described in Chapter 3. **D0** is identical in sequence to siRNAs **D0cy3**, **D0cy5**, and **D0cy3/5**, but does not contain any cyanine dye. Immunoblotting revealed that downregulation of both closely-spaced isoforms of DRR (seen as two close moving bands in Figure 4.2) is strongest for **D0**, while downregulation does not occur with the two siRNAs conjugated to a 3'-cyanine-5 on the antisense strand (**D0cy5** and **D0cy3/5**). This could be explained by the fact that a 3'-2-nt overhang on the antisense strand is instrumental in maintaining antisense strand potency,[15,16] and the conjugation of a fluorophore at that position compromises its recognition by RISC. There is

also no appreciable downregulation of DRR with siRNA **D0cy3** labeled with a cyanine-3 at the 5'-end of the sense strand. The importance of a canonical 5'-end on the sense strand of siRNA is supported in the literature by the many examples of siRNAs conjugated at the 5'-end of their sense strands with moieties whose linkers are cleavable.[17,18,19,20,21,22,23,24] In contrast, there are plenty of examples of siRNAs conjugated at the 3'-end of their sense strands with moieties whose linkers are non-cleavable.[25,26,27] Therefore, none of the sense strands of the siRNAs in Table 4.1 are conjugated to a fluorophore at their 5'-end, and none of the antisense strands of those siRNAs are conjugated to a fluorophore at their 3'- or 5'-end.

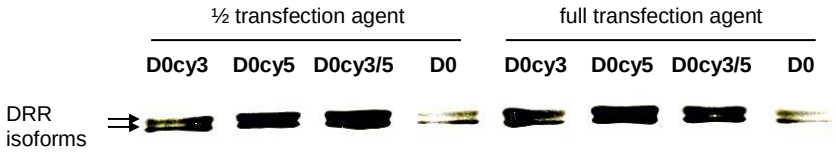

Figure 4.2. A comparison of DRR downregulation among fluorophore-labeled siRNAs and their unlabeled version **D0** reveals that the labeled siRNAs are not able to cause an appreciable amount of silencing after 72 hours. This is true when using the full standard amount of Lipofectamine™ 2000, or when using one half that amount.

4.2.2. B-Cell Lymphoma 2

The B-cell lymphoma 2 gene (*bcl-2*) plays an important role in the growth of cancerous tumors from blood cells (lymphomas) through the regulation of apoptosis. Apoptosis is the process of programmed cellular death, an essential process for the maintenance of the body's population of healthy cells. When a cell reaches the end of its life cycle or is mutated or damaged, apoptosis is triggered. Unfortunately, cancer cells with upregulated *bcl-2* transcripts are able to avoid this process through suppression of the apoptotic pathway. As a result, suppression of *bcl-2* is an attractive method for reestablishing apoptosis in cancer cells. An active siRNA against *bcl-2* has been identified to target *bcl-2* mRNA (NCBI accession number: NM_000633.2) in its open-reading frame in the 1107 to 1127 coding region,[28] whose sequence was used to synthesize siRNA conjugates **B0**-**B6** in Table 4.2. A non-targeting siRNA, **B0-scr**, was adapted from Felber *et al.*[29] The modified non-targeting siRNA **D3-scr** was also used in *bcl-2* assays in order to test whether the modification itself causes silencing in the HCT-116 cell

line overexpressing *bcl-2*. The potencies of the siRNAs were compared with quantitative polymerase chain reaction (qPCR) in section 4.5, which measures the level of *bcl-2* mRNA.

Table 4.2. The sense strands of Bcl-2-targeting siRNAs **B0**-**B6** and non-targeting **B0-scr** used for gene silencing experiments.

siRNA	Sense strand
B0	5'-GCA UGC GGC CUC UGU UUG AUU-3'
B3	5'-GCA UGC GGC C**U**C UG**U** UUG A**U**U-3'
B6	5'-GCA **U**GC GGC C**U**C **U**G**U** U**U**G A**U**U-3'
B0-scr	5'-UAG CGA CUA AAC ACA UCA AUU-3'

Legend: **U** = 2'-*N*-acyl-L-phenylalanine uridine; **C** = 2'-*N*-acyl-L-phenylalanine cytidine; antisense strand = 5'-p-UCA AAC AGA GGC CGC AUG CUU-3'; scramble antisense strand = 5'-UUG AUG UGU UUA GUC GCU AUU-3'; p = phosphate.

4.3. The Potencies of DRR-Targeting Conjugates Vary with Experimental Conditions

4.3.1. Western Blots

As our primary goal in synthesizing siRNA conjugates is to find those demonstrating improved cellular uptake, Western blots were performed with glial cells in reduced-serum medium and a non-toxic siRNA concentration of 20 nM, a slightly toxic siRNA concentration of 80 nM, and varying amounts of transfection agent Lipofectamine™ 2000. Initially, this allowed us to observe whether there was any appreciable amount of DRR downregulation possible with 20 nM of the conjugates, at any greatly reduced amount of transfection agent, before we could gauge how many more modifications were needed to produce a self-delivering functional siRNA. The Western blots in Figure 4.3 were done by Dr. Phuong Le in the Petrecca lab. They show that in order to cause appreciable silencing using 20 nM siRNA, 25% of the standard amount of Lipofectamine™ 2000 is needed, while any less transfecting agent is ineffective. The potency of **D3** is best when one quarter of the standard amount of transfection agent is used, while its potency is at its weakest level when one half is used. This is an interesting finding; cellular internalization for **D3** is expected to be high when using half of the standard amount of transfection agent, based on the findings in Chapter 2 that reveal that increased cellular

internalization is a consequence of increasing the number of 2'-*N*-acyl-L-phenyalanine modifications in RNA. In fact, relatively weak DRR downregulation is observed in comparison to unmodified siRNA for 2'-*N*-acyl-L-phenyalanine-modified siRNAs transfected with one half of the standard amount of transfection agent, in all Western blots discussed in this chapter. This may be a result of unfavorable interaction between high levels of internalized modification and the transfection agent.

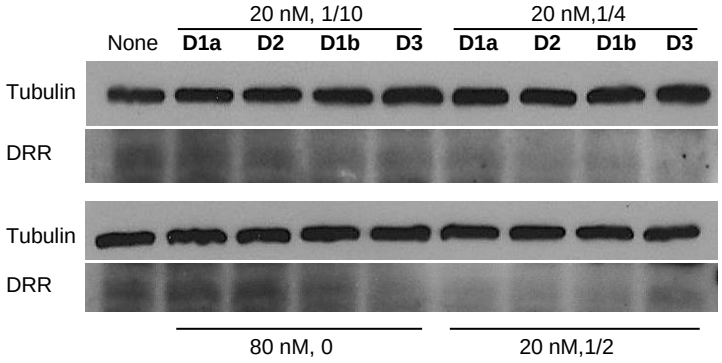

Figure 4.3. 20 nM of **D1**-**D3** requires at least 1/4 of the standard amount of Lipofectamine™ 2000 to cause appreciable downregulation, which may be a function of number and placement of modification.

Quadrupling the concentration of naked siRNA allows for some downregulation by the thrice-modified **D3**, but not for the singly-modified (**D1a**, **D1b**) or doubly-modified (**D2**) siRNAs. Thus, within a range of Lipofectamine™ 2000 that allows appreciable downregulation to occur (between one half and one quarter for this set of siRNAs), a very small amount of Lipofectamine™ 2000 is required to demonstrate a superior potency of the conjugate **D3**. A much larger amount of Lipofectamine™ 2000 is required to demonstrate a superior potency of the unmodified siRNA or the conjugates with fewer than four modifications. This is in part an obvious consequence of the data collected in Chapter 3; conjugates with few modifications have poorer cellular uptake, necessitating the use of a large amount of transfection agent. Silencing caused by **D3** was thus used as a benchmark for comparing the potencies of siRNAs with greater than three modifications at one quarter of the standard amount of Lipofectamine™ 2000 or less.

We next transfected glial cells, provided by the Petrecca lab, with siRNAs that contained up to six modifications (Figure 4.4). When a quarter of the standard amount of transfection agent was employed, the most potent siRNA was the unmodified **D0**. While all of the modified, targeting siRNAs downregulate DRR to some degree relative to the unmodified scramble and non-transfected sample, it seems that the modification causes some decrease in potency. When the siRNAs are transfected with one eighth the standard amount of transfection agent, the unmodified siRNA is no longer the most potent siRNA. Conjugates **D5**, **D6**, and **D3C** appear to exhibit a very small amount of downregulation, while conjugates **D3** and **D4** exhibit the strongest downregulation when this minimal amount of transfection agent is used. This result was expected since it was shown in Chapter 3 that increasing the number of 2'-*N*-acyl-L-phenylalanine modifications in an siRNA causes an increase in cellular uptake by glial cells. The availability of more **D3** and **D4** is likely due to a combination of increased serum stability of the conjugates (since reduced amounts of transfecting agent exposes the siRNAs to nucleases), as well as the improved ability of the conjugates to penetrate the cellular membrane. (The serum

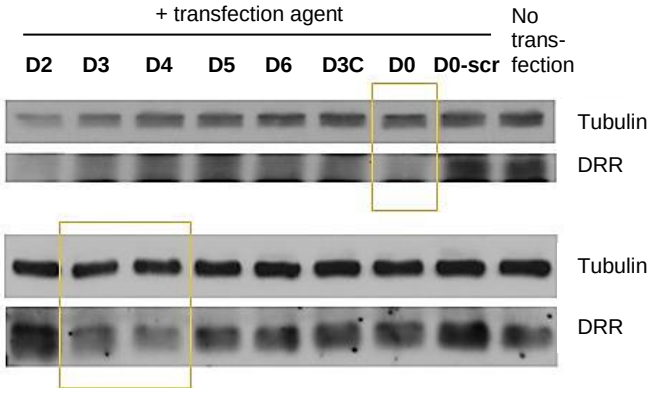

Figure 4.4. The top panel shows that potency of siRNAs transfected at 20 nM with ¼ Lipofectamine™ 2000 is strongest for the unmodified **D0**, while the bottom panel shows that potency of siRNAs transfected at 20 nM with 1/8 Lipofectamine™ 2000 is strongest for the modified **D3** and **D4** conjugates.

stability of the modified sense strands is explored in section 4.6.) Conjugate **D2** showed no detectable downregulation under this condition, which was similar to the scramble **D0-scr**. **D2** was the least-modified conjugate of those tested in Figure 4.4, thus its cellular uptake was expected to be minimal, causing no downregulation. The uptake of **D0-scr** was also expected to be minimal as it contained no modifications. **D3-D6** all contain a modification at the Argonaute

cleavage site (the tenth position from the 5'-end of the antisense strand) in common. This may have reduced their ability to downregulate DRR despite the fact that they are expected to penetrate cells to a greater degree than all of the other siRNAs tested and the fact that they have some improvement in nuclease stability (discussed in section 4.6).

4.3.2. Immunofluorescent Stains

In addition to Western blots of malignant glial cells transfected with one quarter and one eighth of the standard amount of transfection agent and siRNAs **D2-D0-scr**, we examined phenotypic changes in the transfected samples. A primary monoclonal mouse antibody to vinculin, a protein in FAs, was labeled with red fluorophore-conjugated secondary mouse antibody. A primary monoclonal rat antibody to tubulin, a protein that makes up the eukaryotic cytoskeleton, was labeled with green fluorophore-conjugated secondary rat antibody. Images were captured using a confocal microscope and processed to exchange the red and green colors for white and blue, respectively, in order to obtain higher-contrast images (Figure 4.5).

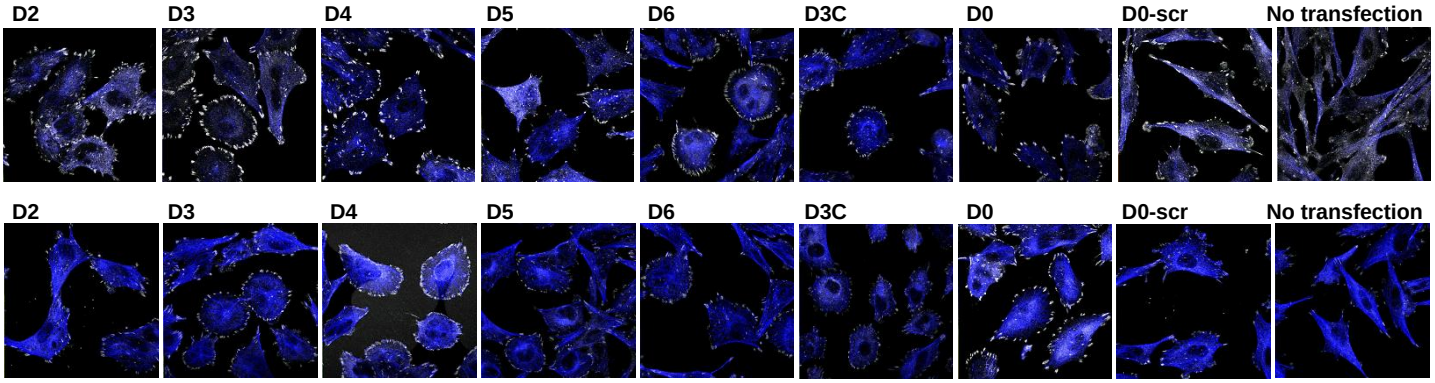

Figure 4.5. The top panel of immunofluorescent stains was taken with the siRNAs (20 nM) indicated above each image and ¼ of the standard amount of transfection agent, while the bottom panel of immunofluorescent stains was taken with the siRNAs (20 nM) indicated above each image and 1/8 of the standard amount of transfection agent. Rounded cells with strong FAs indicate DRR downregulation; spindle-like cells with small FAs indicate little DRR downregulation. 63 x objective.

Since exposure to Lipofectamine™ 2000 results in death of up to 30% of glial cells (personal communication), using less Lipofectamine™ 2000 permits examination of a larger population of cells according to their type and proportions. As expected based on the strong DRR expression shown in Figure 4.4, there was no difference in cellular morphology seen in Figure 4.5 between cells transfected with scramble RNA and cells that were not transfected. Both samples were uniformly elongated as either spindle-like or stretched cells, and neither population contained cells with more than the few FAs at the ends of anchor points. The top panel of images in Figure 4.5 reveals a few examples of perfectly round cells with strong FAs around the entire perimeter with siRNAs **D3**, **D6**, and **D3C**. However, these cells are mixed with spindle-like cells, resulting in the moderate DRR downregulation seen in Figure 4.4. The image of cells transfected with unmodified **D0** siRNA in the top panel of Figure 4.5 represents the generally uniform sample of many plumper cells with some very large FAs around the perimeter. A larger version of this image is shown in Figure 4.6 in order to illustrate the impressive size of some of the sample's FAs.

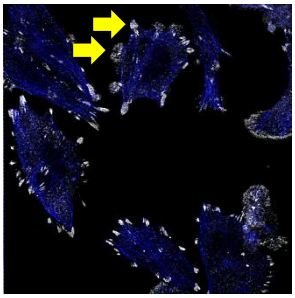

Figure 4.6. A cell transfected with 20 nM **D0** and ¼ transfection agent has very large FAs. 63 x objective.

In the images collected at 1/8 the standard amount of Lipofectamine™ 2000 (Figure 4.5, bottom panel), perfectly rounded cells with FAs around the entire perimeter are detectable in the **D3** and **D4** samples. Some nicely rounded and anchored cells are seen in the **D6** sample, but are harder to find, despite the fact that this conjugate enters cells best (Chapter 3). There were essentially no rounded cells or strong FAs observed in the **D2** sample under this condition, most likely due to low potency derived from insufficient uptake of the minimally modified conjugate. Nonetheless, **D3**, **D4**, **D6**, and **D3C** samples have provided images of cells with round shape and strong FAs around the full perimeter, while **D5** does not provide any ideal cells under either condition. This must be due to more than the fact that it is modified at the tenth position of the antisense strand. As **D3**, **D4**, and **D6** are also modified at this position, this issue with **D5** may be due to unexpected secondary structures of the antisense strand, reducing its availability for RNA interference.

4.3.3. Tumor Spheroids

McGill University researchers at the Montreal Neurological Institute developed a method for growing invasive gliomas in a spheroid suspended in growth medium, allowing a 3D reconstruction of microenvironments in the massive tumor spheroid.[30] The Petrecca lab has utilized the hanging-drop method to capture the most invasive cells that emanate from tumor spheroids to characterize their genetic profile as overexpressing *drr*.[13] These cells are deemed DRR+, while the cells remaining in the spheroid are wild-type, or non-invasive (Figure 4.7). These tumor spheroids can also be used to compare the distance DRR+ cells travel from the non-invasive tumor mass when transfected with 20 nM of our siRNA conjugates **D1**-**D3**. The invasion assays were performed by Dr. Phuong Le in the Petrecca lab.

The total diameter of the spheroids and their DRR+ invasion front (distance A in Figure 4.8) is a combination of wild-type spheroid diameter (B) and invasion distance from the wild-type spheroid (A-B). As expected, the overall diameter A of the sample increases over time due to two factors: 1) Cells are dividing and growing in the non-invasive spheroid and; 2) invasive cells are moving farther into the growth medium as time passes. Figure 4.8-1 reveals that the total spheroid diameter of the samples transfected with conjugates **D1**-**D3** and one half of the standard amount of transfection agent is much smaller than the total spheroid diameter of the untreated sample. On the other hand, the total spheroid diameter of the samples transfected with conjugates **D1**-**D3** and one quarter of the standard amount of transfection agent is smaller than the total spheroid diameter of the untreated sample to a lesser extent (Figure 4.8-2). This is expected as a reduction in the amount of transfection agent used causes an overall reduction in the amount of nucleic acid inside the cells.

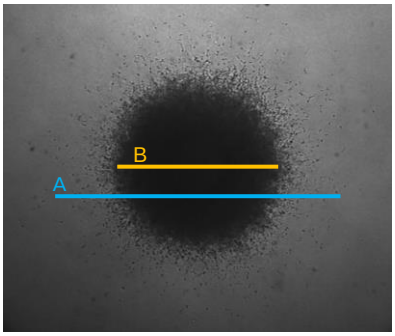

Figure 4.7. The cross-section of a tumor spheroid's DRR+ invasion front is shown by line A and that of its wild-type invasion front is shown by line B.

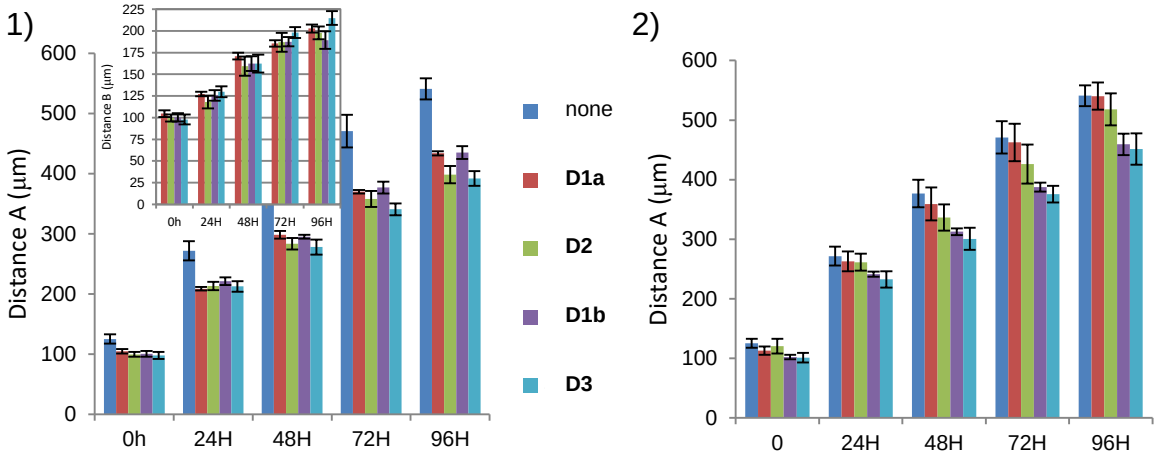

Figure 4.8. The distance traveled by DRR+ cells between transfections with 1) half of the standard amount of Lipofectamine™ 2000 and 2) one quarter of that amount reveals the simple fact that the use of more transfection agent causes a greater decrease in invasion distance over the untreated spheroid. In panel 1), non-invasive spheroid diameter B (inset) is shown for cells transfected with one half of the standard amount of Lipofectamine™ 2000. $n = 3$

Figure 4.9-1 compares the distance that invasive cells travel from an untreated spheroid with that of the spheroids transfected with the conjugates and a large amount of Lipofectamine™ 2000 (half of the standard amount). Subtraction of non-invasive spheroid diameters in Figure 4.8 (inset) from their corresponding total spheroid diameters in Figure 4.8-1, results these invasion distances (A-B). All of the tested conjugates reduced DRR+ invasion when compared with the untreated spheroid. By 72 hours the tumor spheroid transfected by **D3** exemplifies a lower DRR+ invasion distance into the surrounding medium, while the DRR+ invasion distances of the other conjugates are equal, or about equal, with **D1a**. By 96 hours, invasion distance is greatest for **D3**, smallest for **1a**, and equal for **D1b** and **D2**.

While using half of the standard amount of transfection agent showcased **D3**'s ability to reduce DRR+ invasion to a greater extent than the other three conjugates, especially **D1a**, the size of the wild-type spheroid transfected with a quarter of the standard amount of transfection agent and **D2** is larger at 92 hours than the sizes of the wild-type spheroids transfected with **D1a**

and **D1b** (Figure 4.9-2). This is an indirect measure of DRR downregulation; cells are able to divide and grow when DRR production is suppressed.

When Figure 4.9-2 distances at 96 hours are subtracted from the corresponding distances at 96 hours in Figure 4.8-2, a trend in degree of DRR downregulation resolves to **D3**>**D2**>**D1b**>**D1a**, with a much greater difference between **D3** and **D1a** than that seen in Figure 4.9-1. **D1a** may perform worse than **D1b** because, while they both penetrate glial cells to the same degree, **D1a** is modified at the second nucleotide of its overhang, potentially interfering with recognition of the 5'-end of the antisense strand, especially since it is positively charged.

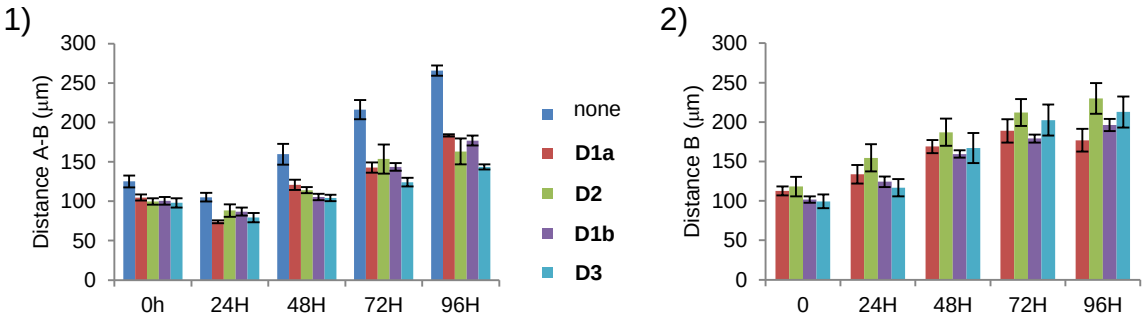

Figure 4.9. In panel 1) tumor spheroids were transfected with half of the standard amount of Lipofectamine™ 2000 and 20 nM of the conjugates, and their invasion distaces (A-B) were compared to that of a non-transfected spheroid. In panel 2) spheroids were transfected with one quarter of the standard amount of Lipofectamine™ 2000 and 20 nM of the conjugates, and the size of the non-invasive spheroid diameters (B) were compared to that of a non-transfected spheroid. $n = 3$

4.4. Structure-Activity Relationship Reveals the Necessity of the Benzyl Group for Silencing under Reduced Lipofectamine™ 2000 Amounts

We next sought to understand what features of the **D3** conjugate allow it to be highly active at very low levels of Lipofectamine™ 2000. Three siRNAs equivalent to **D3** but with the 2'-*N*-acyl-phenylalanine replaced by either a 2'-amino (**D3N**), 2'-*N*-acetyl (**D3A**), or 2'-*N*-acyl-L-glycine (**D3G**) uridine (Figure 4.10) were synthesized by Dr. Ken Yamada. It was expected that the potencies of **D3N** and **D3A** with neutral modifications would be limited by a reduction in the

amount of Lipofectamine™ 2000 due to their predicted inability to penetrate cells. The potency of **D3G**, on the other hand, was expected to be retained or possibly improve with respect to **D0** due to the cationic nature of the amino acid (and the siRNA's predicted ability to enter cells). In fact, it was expected that **D3G** would enter cells equally as well as **D3** if only charge mattered.

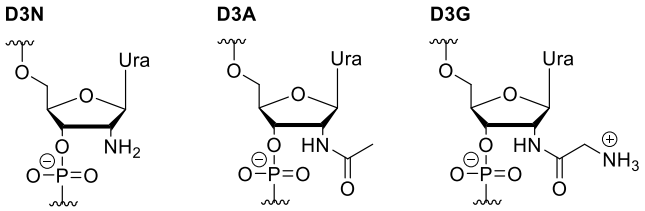

Figure 4.10. The sense strands of siRNAs **D3N**, **D3A**, and **D3G** were modified at the 2'-positions of their sugar moieties.

In actuality, using one eighth of the standard amount of transfection agent as opposed to one quarter (bottom panel as opposed to top panel of Figure 4.11) allows an improvement in potency compared to **D0**, while there is no such response when **D3G** is utilized. **D3G** may slightly downregulate DRR in the top panel, but no downregulation occurs in the bottom panel. DRR downregulation by **D3N** and **D3A** is very weak when using one quarter of the standard amount of transfection agent, but also does not occur when using one eighth of the standard amount of transfection agent.

Figure 4.11. Derivative siRNAs of **D3U** (**D3N**, **D3A**, **D3G**) vary in potency between transfection with 1/4 (top panel) and 1/8 (bottom panel) Lipofectamine™ 2000

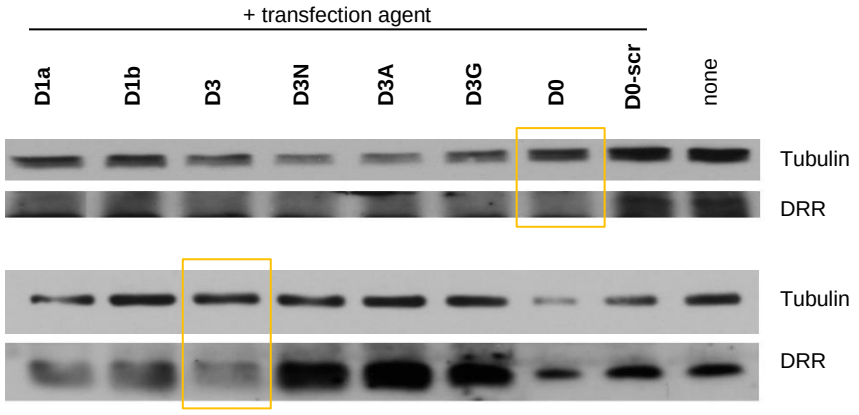

Given the increased uptake of the fluorophore-labeled **D3G** in comparison to fluorophore-labeled **D0** (Chapter 3), **D3G** should penetrate cells as well as **D3**. Therefore, the lack of observed downregulation for each of the analogues when using one eighth of the standard

amount of transfection agent could be due to different reasons. **D3N** and **D3A** may not penetrate cells well enough to cause strong DRR reduction when using either one eighth or one quarter of the standard amount of transfection agent, while **D3G** may not be a good substrate of RISC. With this knowledge, either a benzyl group or both the benzyl group and the amino group are required for RISC activity observed for **D3**. If not required for silencing, the amino group may still be required for proton-sponge-mediated endosomal rupture.

4.5. Bcl-2-Targeting Conjugates are Equally Potent

In Chapter 3 it was shown that **D3** and **D6** conjugates do not exhibit increased cellular uptake in human colonic cells when an eighth of the standard amount of Lipofectamine™ 2000 is used. There is, however, some increase in internalization of the conjugates when one quarter of the standard amount of Lipofectamine™ 2000 is used; therefore, the amounts of modified and unmodified *Bcl-2*-targeting siRNA in the cells when the full amount of Lipofectamine™ 2000 is used is not equal. It is ideal to have the same amount of siRNA inside of the cells for each sample in order to properly compare their potencies. Nonetheless, the expression of *bcl-2* mRNA was compared among colonic cells transfected with **B0**, **B3**, **B6**, **B0-scr**, and **D3-scr**, using the standard amount of transfection agent (Figure 4.12) by Elena Moroz in Dr. Jean-Christophe Leroux lab at the Swiss Federal Institute of Technology in Zurich (ETH Zurich).

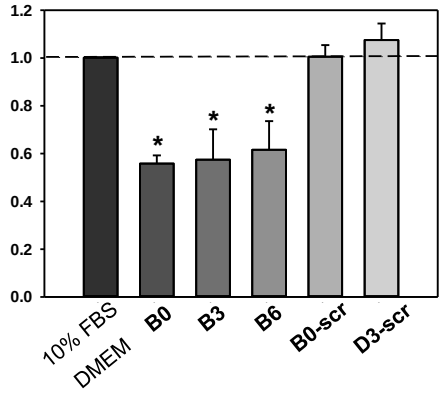

Figure 4.12. Conjugates (15 nM) were tested for silencing efficiency in human colonic cells using the standard amount of transfection agent with no statistical difference between the ones targeting *bcl-2*. ∗: $p < 0.001$ vs. medium-treated cells. $n = 3$.

It was found that there is significant downregulation by all three *bcl-2*-targeting siRNAs and that there is no statistical difference between the three of them. There is no sequence-based issue with the *bcl-2*-targeting conjugates that can interfere with silencing as there is no modification at the 10th or 11th positions of the antisense strand (the cleavage site). There is also no complication due to the presence of the modifications as the toxicity of the conjugates is not greater than that of the unmodified siRNA (Figure 4.13).

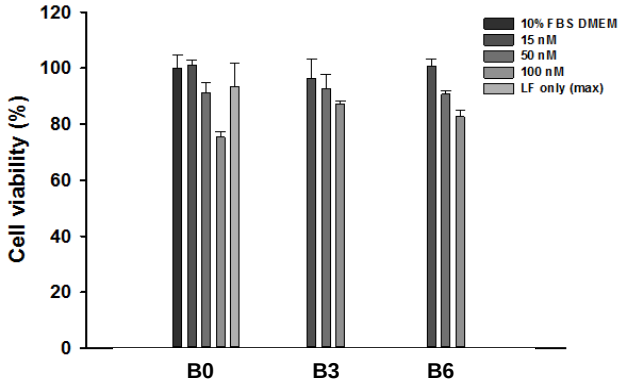

Figure 4.13. Cell viability as a consequence of siRNA concentration reveals that the *bcl-2*-targeting conjugates do not cause additional cell toxicity. $n = 3$.

4.6. The Physical Properties of the Conjugates

As stated above, the added nuclease stability of the modified siRNAs is a compulsory property. The digestion of the unmodified sense strand of the DRR-targeting siRNA in fetal bovine serum (FBS) can be followed by gel electrophoresis with ^{32}P-labeled starting material (Figure 4.14A) or gel electrophoresis and staining with Stains-All (Figure 4.14B). Five different FBS concentrations were employed in the digestion reaction with the unmodified ^{32}P-labeled sense RNA strand of the DRR-targeting siRNA (Figure 4.14A). An FBS concentration of 0.1% slowed down the digestion so that starting material was still observed after eight minutes, but did not slow it down so much that digestion was not observable after eight minutes. The amount of RNA starting material and concentration of FBS were both proportionally increased to give the stained gel in Figure 4.14B. Both the radioactive gel and the stained gel reveal that the entire full-length sample is digested by eight minutes.

The yellow arrows indicate digestion products from the same major cut in the full-length RNA. This produces one major product in the radioactive gel and two major products in the stained gel. Only one of those bands appears in the radioactive gel since one end of the strand is radioactively labeled. A light band indicated by the black arrow in Figure 4.14A may be one of the products of a pair of light bands indicated by a pair of black arrows in Figure 4.14B. This may indicate another cleavage site in the RNA. Since the radioactive gels required much less RNA for the digestion, further digestion studies were performed on radioactively labeled modified sense strands.

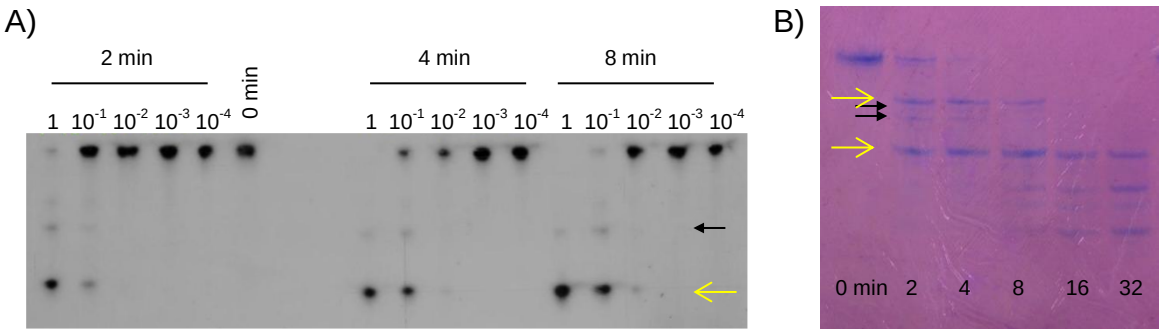

Figure 4.14. The radioactive gel A and stained gel B of the FBS-digested sense strand of **D0** is completely digested by eight minutes.

The sense strands of conjugates **D3**-**D6** and **D3C** were digested in FBS in order to illustrate any resistance to the combination of endo- and exonucleases present in the extract, and thus the rough estimate of the time required to digest the full-length oligonucleotide in comparison to the unmodified strand (Figure 4.15). Pyrimidine positions are particularly susceptible to endonuclease cleavage, and hence we expected to observe enhanced resistance of modified strands compared to the unmodified strand. Appreciable detection of full-length oligonucleotide is observed for both **D6** and **D3C** after eight minutes of incubation, while full-length **D3** is not detected at this time. These differences in resistance may be due to the position of modification in the RNA. For example, a middle spot indicated by a black arrows in Figure 4.15 is detected for the **D3**, **D4** samples, but never for the **D5**, **D6**, and **D3C** samples, which may be a result of their common modification on cytidine at position 11 (from the 5'-end). The potential cleavage site in **D3** and **D4** sense strands that is vulnerable to digestion is not a

cleavage site in the **D5**, **D6**, and **D3C** sense strands. In addition, the three cytidine modifications common to **D6** and **D3C** may be more influential for nuclease stability than any other combination of modifications.

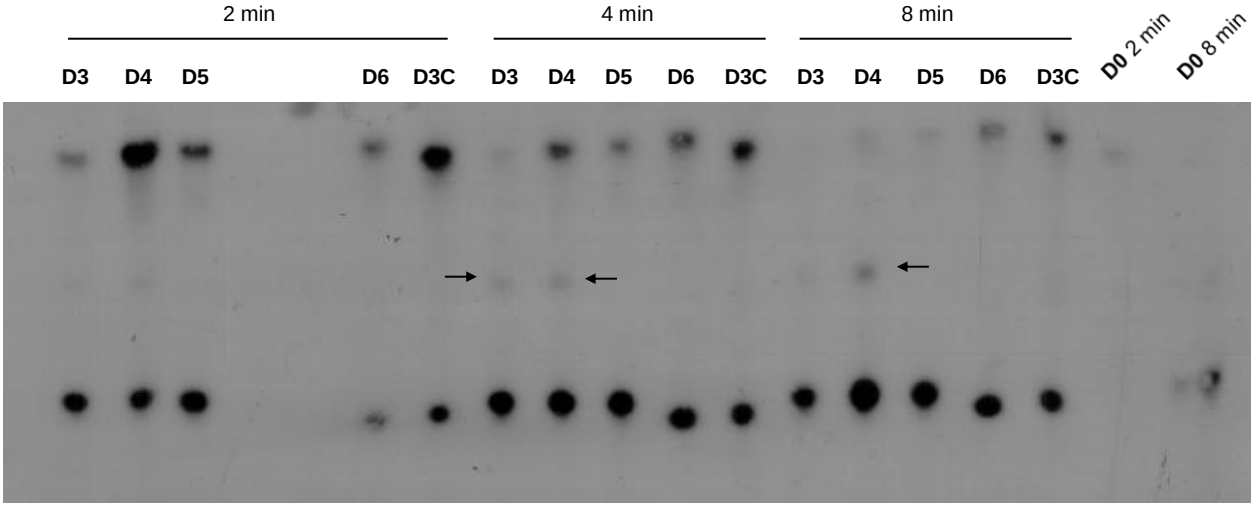

Figure 4.15. The digestion of the ^{32}P-labeled sense strands of the conjugates over eight minutes reveals the improved nuclease stability of the modified oligonucleotides.

The *bcl-2*-targeting siRNAs **B0**, **B3**, and **B6**, and scrambles **B0-scr** and **D3-scr** were run on a native 20% polyacrylamide gel by Elena Moroz (Figure 4.16). As expected, the retention of the conjugates increases proportionally to the number of modifications. It is expected that this would occurs due to the modifications reducing the overall negative character of the oligonucleotide, thus reducing its attraction to the positively-charged end of the gel. This expected effect cannot be confirmed, however, as it cannot act in isolation; the concomitant addition of greater mass to the RNAs with more modifications increases the mass-to-charge ratio, thus causing RNA retention.

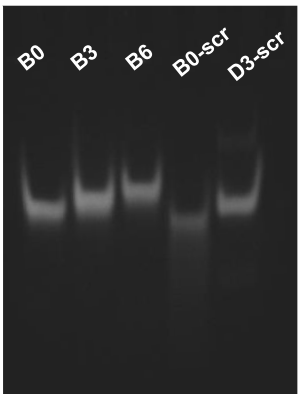

Figure 4.16. Polyacrylamide gel of siRNAs used in *bcl-2* assays.

The modifications also increase the lipophilicity of the sense strands of DRR-targeting **D1**-**D6** over the sense strands of DRR-targeting **D3N**, **D3A**, and **D3G**, as judged by the elution time of the strands during hot (65^{o}C) reverse-phase HPLC with a 0-30% MeCN gradient over 30 minutes (tabulated by Dr. Ken Yamada in Figure 4.17). As expected, the sense strands of **D3N**, **D3A**, and **D3G** are the most polar (dark grey bars) since they lack the nonpolar R group of the phenylalanine moiety. All of the phenylalanine-modified oligonucleotides (light grey bars) are more retained than **D3N**, **D3A**, and **D3G**. The retention time generally increases with the number of modifications, with **D6** being the most polar of the phenylalanine-modified oligonucleotides. In fact, the phenylalanine-modified oligonucleotides do not dissolve well in water. This is particularly true for the sense strand of **D6**. In order to load the conjugates onto the HPLC column, they were first dissolved in water spiked with 40 microliters of 2.0 M triethylammonium acetate. It is noteworthy that the sense strand of **D1a**, and by extension its siRNA duplex, is more lipophilic than the sense strand of **D1b**. While **D1a** duplex should have better cellular uptake properties than **D1b** duplex, the evidence described in this chapter indicates that **D1b** is more potent at low levels of Lipofectamine^{TM} 2000. Since the modification is thermally destabilizing in the middle of the duplex but has minimal impact in the overhang, it likely increases potency of **D1b** over **D1a** by destabilizing the 5'-end of the antisense strand.

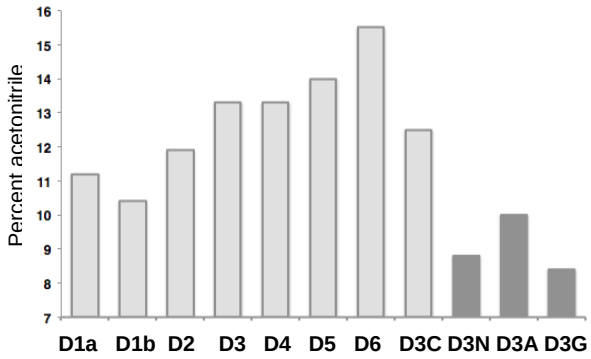

Figure 4.17. The RP-HPLC retention times of the sense strands of the indicated siRNA conjugates generally increase with increasing number of phenylalanine modifications.

The difference in thermal melting temperature (T_m) of the DRR-targeting conjugates to their corresponding siRNAs with one less modification reveals that the average change in T_m for each internal modification is -5.5^oC (Table 4.3). In the case of **D6**, this value was calculated from the T_m of **D4** and divided by two since **D5** did not produce a T_m with a single inflection point (indicating possible secondary structure). The range in ΔT_m per internal modification is considerable (-6.3 to -4.1^oC). Although a statistical method has not been applied, a closer look at $\Delta T_m/mod_{internal}$ in relation to the placement of the modifications may indicate that the difference in the change of $T_m/mod_{internal}$ ($\Delta\Delta T_m/mod_{internal}$) may be significantly less destabilizing when modifications are placed consecutively in the duplex. The change in $\Delta T_m/mod_{internal}$ in going from **D3** to **D4** is 1.7 degrees less destabilizing (+1.7 ^oC) than that of going from **D2** to **D3** (-5.8 ^oC). This may be due to the fact that the fourth modification in the sense strand occurs next to another, while all of the modifications in the sense strand of **D3** are spaced out. The calculations per modification for **D6** are averaged over the two modifications added in **D4**, however this possible trend in T_m based on modification placement may very well still hold up. The ΔT_m/mod for **D6** is the second lowest value (after that of **D4**) for the conjugates with internal modifications. That is likely due to the fact that it is a combination of the expected strong destabilization of the modification at the sixth position and the weaker-than-average destabilization of the modification next to another. The well-spaced modifications of **D3C** are strongly destabilizing (ΔT_m/mod = -6.0 ^oC), also as expected.

Table 4.3. Trends in T_m depression suggest that each 2'-*N*-acyl-L-phenylalanine modification depressed T_m to a lesser extent when it was added to DRR-targeting RNA consecutive to another 2'-*N*-acyl-L-phenylalanine modification in the sequence.

siRNA	ΔT_m/mod (^oC)	Average $\Delta T_m/mod_{internal}$ (^oC)	$\Delta\Delta T_m/mod_{internal}$ (^oC)
D1a	-0.4[a]		
D1b	-5.6[a]	-5.5	
D2	-6.3[a]		-0.7[f]
D3	-5.8[b]		+0.5[g]
D4	-4.1[c]		+1.7[h]
D6	-5.3[d]		-1.2[i]
D3C	-6.0[a]		

Legend: ΔT_m/mod calculated from the T_ms of **D0**[a], **D2**[b], **D3**[c], **D4**[d], and **D0-scr**[e]; $\Delta\Delta T_m/mod_{internal}$ calculated from the ΔT_m/mod of **D1b**[f], **D3**[g], **D3**[h], **D4**[i].

4.7. Self-Delivering Tailed siRNAs Silence DRR

Asymmetric "shorter-duplex" siRNAs, in which 19-nt-long antisense strands are hybridized to sense strands of shorter lengths, have been shown to efficiently mediate gene silencing as well as reduce sense strand-mediated off-target effects.[31,32] Our version of asymmetric siRNA retains the 19-base pair (bp) duplex region of conventional siRNA, but adds a 7-nt-long tail to the 5'-end of the sense strand. The cy3/cy5-labeled conjugates **A0cy3/5** and **A13cy3/5** (40 nM) first described in Chapter 3, were incubated by Dr. Phuong Le with stem cells and DRR expression was compared to that of samples transfected with unmodified **D0** (20 nM) and the full amount of transfection agent. The concentration of the tailed siRNAs was doubled from the standard concentration of 20 nM because it was assessed in Chapter 3 (Figure 3.14) that the uptake of 40 nM **A13cy3/5** in DRR+ cells was very strong. Regardless of its increased cellular uptake, **A13cy3/5** did not cause downregulation of DRR in Figure 4.18 following 72 hours incubation. This may be due to the presence of the 5'-cy5 fluorophore on the antisense strand. It was shown in Figure 4.2 that the presence of cy5 on the 3'-terminus of the antisense

strand of siRNA impedes the silencing of DRR. A cy5 at the 5'-position of the antisense strand may impede the phosphorylation of the 5'-terminus, which is required for guide strand selection.

On the other hand, the long sense strand is a worse guide strand for RISC-mediated RNA interference, favouring the loading of the antisense strand as the guide strand. SOX2, an important transcription factor in the maintenance of stem cell pluripotency, is not downregulated by **A13cy3/5** after both 24 hours and 72 hours, while DRR is in fact downregulated after 24 hours incubation (Figure 4.18). **D0**, on the other hand, causes strong DRR and SOX2 silencing 24 hours after transfection, and is potent enough to continue to downregulate even after 72 hours. It also may be so potent that its initial concentration in the cell is strong enough to saturate the RISC machinery and allow the leftover RNA to cause off-target effects.

In order to determine whether there is any improvement in potency of the amino acid-modified tailed siRNA when the 5'-cy3 is removed from the antisense strand, the sense strands of **A0cy3/5** and **A13cy3/5** conjugates were hybridized to the same unmodified antisense strand as that used in **D0**. As a result, the siRNAs **A0cy5** and **A13cy5** in Table 4.4 contain a 3'-cy5 fluorophore.

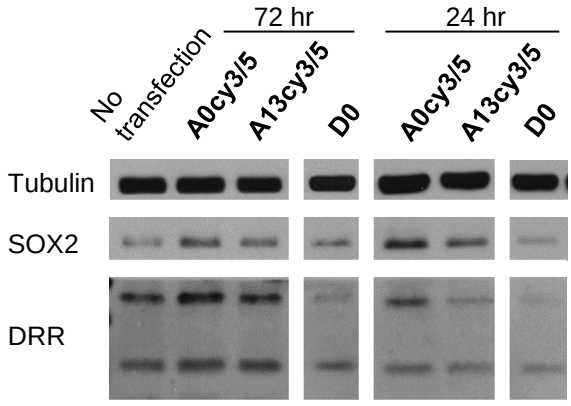

Figure 4.18. Reduction in DRR and SOX2 expression in stem cells by asymmetric siRNAs and canonical siRNA after 72 and 24 hours suggests different silencing kinetics by the two types of siRNAs.

Table 4.4. Asymmetric tailed siRNAs were employed for DRR silencing assays.

siRNA	Sequence
A0cy5	5'-$U_sU_sU_s$ $U_sU_sU_s$ U_sGA ACC AGC UCA UCA AGA AUU-**cy5**-3'
	3'-UU CCU UGG UCG AGU AGU UCU U-p-5'
A13cy5	5'- **U**$_s$**U**$_s$**U**$_s$ **U**$_s$**U**$_s$**U**$_s$ **U**$_s$GA AC**C** AGC **UC**A **UC**A AGA A**U**U-**cy5**-3'
	3'-UU CCU UGG UCG AGU AGU UCU U-p-5'

Legend: **U** = 2'-*N*-acyl-L-phenylalanine uridine; **C** = 2'-*N*-acyl-L-phenylalanine cytidine; $_s$ = phosphorothioate; p = phosphate. Sequence: sense strand on top; antisense strand on bottom.

Their ability to cause phenotypic changes in DRR+ cells after 72 hours without the aid of transfection agent was observed and compared to DRR+ cells transfected with **D0** and **D3-scr**, and the full amount of transfection agent (Figure 4.19). The immunofluorescent stain was performed by Dr. Phuong Le. These genetically engineered cells express red fluorescent DRR, therefore allowing DRR expression to be qualitatively assessed by DRR fluorescence as well as FA size and cell shape. The cells were plated on fibronectin plates, allowing the formation of FAs in serum-free medium. Judging by the round cell in the **D0** sample, DRR silencing is strongest in the sample transfected with **D0**, however all of the cells displayed in the sample incubated with **A13cy5** have a low intensity of red fluorescent DRR, indicating consistent moderate reduction in DRR levels. Some medium-sized focal adhesions were also observed in the **A13cy5** sample. In contrast, the sample incubated with **A0cy5** contains no fluorophore inside the cells, and therefore no siRNA. As a result, FAs are all small and DRR expression is strong. Modification itself does not cause downregulation, as DRR expression is strong in the sample transfected with the modified scramble **D3-scr**.

A0cy5 and **A13cy5** (40 nM) were incubated naked with DRR+ cells and their ability to downregulate DRR was assessed after 72 and 96 hours (Figure 4.20). After 72 hours, **A13cy5** causes a slight decrease in DRR, while no decrease is detected by **A0cy5**. After 92 hours, the decrease in DRR caused by **A13cy5** is drastic. Densitometry of the Western blot revealed that there is 55% and 78% less DRR expressed by cells treated with **A13cy5** compared to those treated with **A0cy5** after 72 hours and 96 hours, respectively.

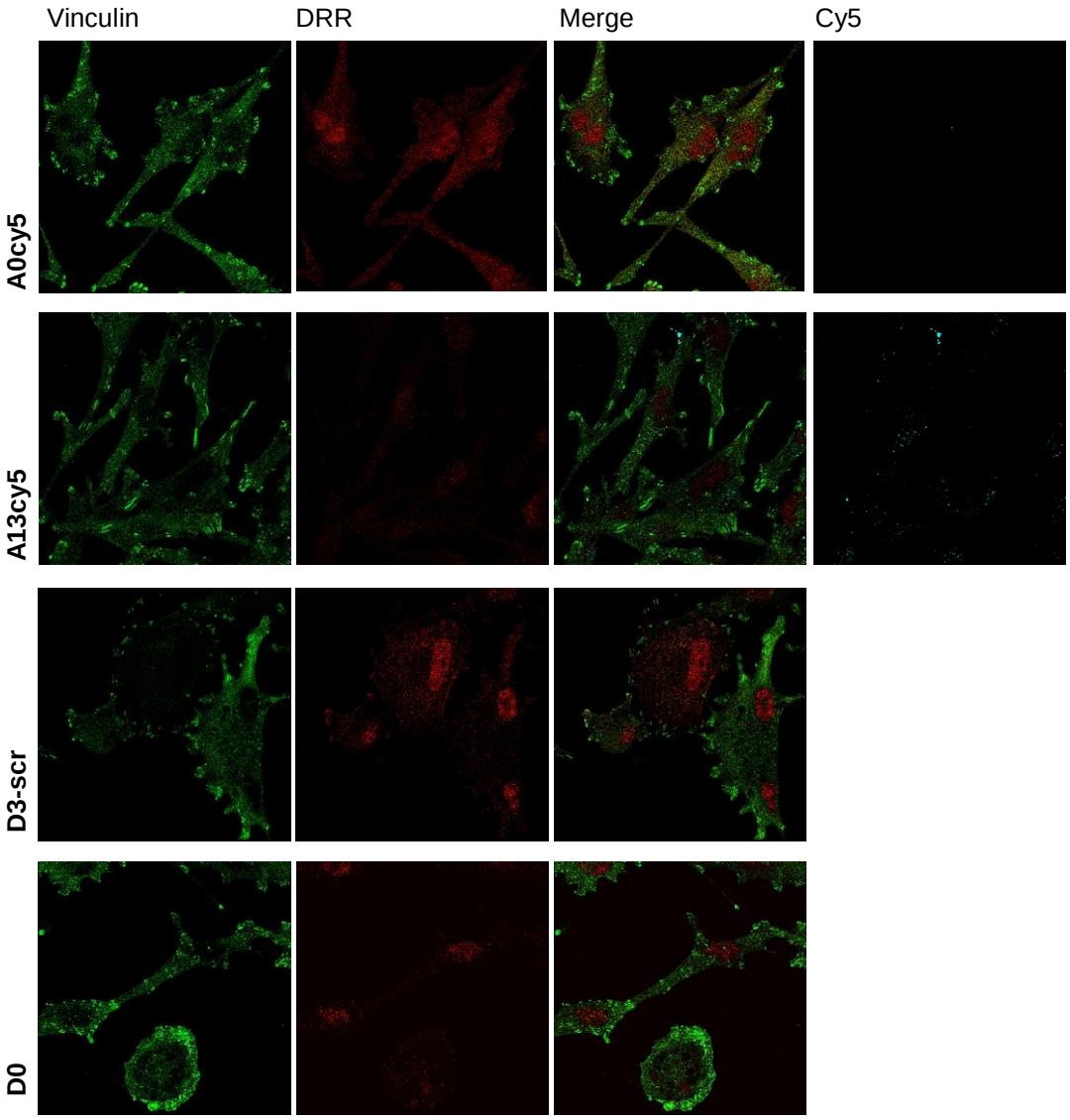

Figure 4.19. Asymmetric siRNAs **A0cy5** and **A13cy5** (40 nM) were incubated naked with DRR+ cells, while modified scramble **D3-scr** and unmodified siRNA **D0** (20 nM) were transfected into DRR+ cells. 63 x objective.

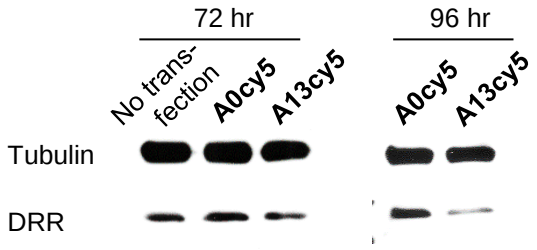

Figure 4.20. Reduction in DRR expression in glial cells by asymmetric siRNAs and canonical siRNA after 72 and 96 hours suggests slow silencing kinetics by **A13cy5**.

4.8. Conclusion

An indirect method for the development of self-delivering siRNA was utilized as a complement to the flow cytometric method employed in Chapter 2. DRR-targeting siRNAs containing one to six internal 2'-*N*-acyl-L-phenylalanine uridine and cytidine modifications were synthesized and assayed for their ability to cause gene silencing. Qualitative analysis of Western blots and immunofluorescent stains of the transfected cells revealed that when one eighth of the standard amount of transfection agent was used, siRNAs with three to four modifications were more potent than the unmodified siRNA. This was a result of the improved ability of the conjugates to enter cells (Chapter 3), and possibly due to a lack of modification at the RISC cleavage position; conjugates with five and six internal modifications, including one at the cleavage site, were not potent despite their ability to enter cells more easily than the other conjugates studied. A total of thirteen 2'-*N*-acyl-L-phenylalanine modifications were then incorporated into siRNAs containing a phosphorothioate tail at the 5'-end of the sense strand. Western blots revealed that modification of the internal positions as well as the tail with 2'-*N*-acyl-L-phenylalanine uridine and cytidine residues resulted in potent DRR downregulation without the use of transfection agent

A second endogenous target was successfully silenced: The potencies of *bcl-2*-targeting siRNAs containing three and six internal modifications were measured by qPCR after transfection with the full standard amount of transfection agent and there was no statistical difference between the siRNAs. Favorable characteristics such as increased nuclease resistance and a more lipophilic RNA as a result of incorporation of a stable version of the 2'-*O*-phenylalanine acetal ester provides great incentive to develop siRNA prodrugs based on 2'-*O*-AAEs. A reduction in potency of the conjugates when a large amount of unmodified sample is transfected provides even more incentive to develop proRNA with this biolabile feature.

4.9. Experimental Methods

4.9.1. Oligonucleotide Preparation

Oligonucleotides were synthesized on UnyLinker^{TM} CPG (500 Å) with an Applied Biosystems DNA/RNA 3400 Synthesizer. Standard phosphoramidites were purchased from ChemGenes Corporation (Wilmington, MA) and dissolved in MeCN to a concentration of 0.15

M. Synthesized phosphoramidites with 2'-*N*-acyl-L-phenylalanine modification were dissolved to a concentration of 0.12 M in DMSO/MeCN/CH_2Cl_2 (1:5:5 v/v/v). Coupling times for thymidine and uridine were 600 sec, while coupling time was 1200 sec for the modified units. Activation of phorphoramidites was achieved with standard 0.25 M ETT in MeCN. Standard capping was performed with a CAP A solution of Ac_2O/py/THF (10:10:80 v/v/v) and a CAP B solution of 15% *N*-methylimidazole in THF. The oxidation solution used was standard 0.1 M I_2 in py/H_2O/THF (8:16:76 v/v/v). Standard 3% TCA in CH_2Cl_2 was used for detritylation steps. Cyanine-3 was coupled to the solid support after detritylation of the last nucleotide in the sequence in the following manner. Cyanine-3 phosphoramidite was dissolved in MeCN to a concentration of 0.12 M. With argon flowing through the top of the synthesis column, a 1-mL syringe with activator solution (0.25 M ETT, 170 μL) was secured to the bottom end of the column. The line delivering argon to the top of the column was removed and the activator was immediately pushed through the column, followed by immediate attachment of another 1-mL syringe containing cyanine-3 phosphoramidite (0.12 M, 170 μL) to the top of the column. The pistons of the syringes were pushed back and forth a few times and then the column was shaken for 15 minutes. Then the support was washed with MeCN, and oxidized and then detritylated on the ABI Synthesizer. The same synthetic protocol was used for conjugate strands with a 3'-cyanine-5, however succinyl-CPG derivatized with cyanine-5 was used with rA^{PAC}, rC^{PAC}, and $rG^{tert\text{-}BuPAC}$ phosphoramidites. A 5'-phosphate was coupled to the antisense strands with bis-cyanoethyl-*N*,*N*-diisopropyl phosphoramidite dissolved in MeCN to a concentration of 0.12 M.

The UnyLinker™ and succinyl solid supports were suspended in the standard NH_4OH/EtOH deprotection solution (1 mL, 3:1 v/v) and put on a shaker for 48 hr and 36 hr, respectively, at r.t. to remove the nucleobase and internucleotide protecting groups, and to cleave the support linker. After decanting and lyophilizing the supernatant, fast desilylation was performed in NEt_3-3HF/NMP/NEt_3 (0.300 mL 1.5:0.75:1 v/v/v) at 65°C for 4 hr., after which NaOAc (3 M, pH 5.5, 0.0025 mL) and cold 1-butanol (1 mL) were added to precipitate the oligonucleotide. The washed and dried oligonucleotide was dissolved in water, filtered, and purified by RP-HPLC. Crude oligonucleotide was suspended in autoclaved water. Because much of the modified oligonucleotides did not dissolve, 20 uL of 2 M triethylammonium acetate (TEAA) was added to dissolve the samples. A gradient of 5-40% MeCN in TEAA was used to purify the strands.

Table 4.5. Exact mass values of oligonucleotides synthesized

Oligonucleotide	Exact Mass Values			
	Sense strand		Antisense strand	
	Calculated	Found	Calculated	Found
D0	6699.9612	6699.9063	6681.7709	6681.7188
D1a	6846.0464	6846.0552		
D1b	6846.0464	6846.2032		
D2	6992.1316	6992.1990		
D3	7138.2168	7138.0938		
D4*	7286.3177	7286.5670		
D5*	7434.4186	7434.0211		
D6*	7582.5151	7576.3750		
D3C*	7144.2639	7143.9023		
D0-scr	6699.9612	6699.9618	6765.8635	6765.8929
D3-scr	7138.2168	7137.8924		
B0	6639.8372	6639.8125	6770.9017	6773.8856
B3	7078.0928	7078.0938		
B6*	7516.3484	7516.2813		
B0-scr	6644.9452	6646.9280	6705.7537	6708.7243
A0cy5	9142.3456	9144.9141	6681.7709	6681.7188
A13cy5	11047.4935	11202.1119		

Legend: * = Oligonucleotide sense strands synthesized by Dr. Ken Yamada using 2'-*N*-acyl-L-phenylalanine cytidine phosphoramidites.

4.9.2. Thermal Melting Analysis

Thermal melting analyses were performed on a Varian CARY 300 UV-VIS Spectrophotometer equipped with a peltier temperature controller with 2 nmol of sense and antisense strands dissolved in 1 mL 2-[4-(2-hydroxyethyl)piperazin-1-yl]ethanesulfonic acid (HEPES)-containing buffer (0.6 M KCl, 6 μM HEPES, 1 μM $MgCl_2.6H_2O$, pH 7.4). The duplexes were denatured by heating the mixtures to 95^{o}C for 5 min and then letting them cool to

r.t. slowly. Once at r.t., the samples were cooled overnight in a -20^{o}C freezer. A denaturing and then annealing curve was then collected at a rate of 0.4^{o}C/min.

4.9.3. Transfections

D0cy3, **D0cy5**, **D0cy3/5**, **D0-D6**, **D3C**, **D3-scr**, **A0cy5**, and **A13cy5** were transfected using substandard amounts of Lipofectamine^{TM} 2000 purchased from Invitrogen (using the manufacturer's protocol). An aliquot of siRNA (25 μM, 2 μL) in HEPES-containing buffer was diluted in opti-MEM reduced serum medium (248 μL). Lipofectamine^{TM} 2000 in opti-MEM reduced serum medium (final volume 250 μL) was added to the siRNA solutions for an siRNA concentration of 0.1 μM. Amounts of Lipofectamine^{TM} 2000 were calculated based on ¼ and 1/8 of 5 uL per well of the 6-well plates used (final volume 2 mL). Cells plated at 100,000 cells/well were transfected and incubated with the siRNA at 37^{o}C for 18 hours in DMEM high-glucose supplemented with 10% FBS, for a final concentration of 20 nM. **A0cy5** and **A13cy5** were also incubated at 40 nM using a 4-μL aliquot of siRNA and no Lipofectamine^{TM} 2000.

4.9.4. Western Blots

Cells were lysed with 2% SDS and the lysate (30 μL) was separated on a 12% polyacrylamide gel. Proteins were electrotransferred onto a nitrocellulose membrane that was probed with rabbit anti-DRR and mouse anti-tubulin antibodies from Jackson ImmunoResearch. All washes were done with 0.05% Tween-20/PBS while a 5% milk powder blocking solution in 1% Tween-20/PBS was used. The membranes were then stained with HRP-conjugated secondary antibodies, also from Jackson ImmunoResearch, and an ECL plus reagent detection kit from Pierce was then used for protein visualization on photographic film. All reagents were supplied by the Petrecca lab.

4.9.5. Immunocytochemistry

Cells were grown on glass coverslips at a density of 50,000 cells/well, fixed with 3% PFA, permeabilized with 0.5% Triton X-100 and blocked with 0.5% BSA solution. Coverslips were incubated with primary antibody mouse anti-vinculin (1:200) for staining focal adhesions, purchased from Sigma by the Petrecca lab, and with primary antibody rat anti-microtubulin (1:300), purchased from Chemicon by the Petrecca lab. This was followed by incubation with

anti-mouse secondary antibody (1:1000) conjugated to Alexa 594, purchased from Invitrogen by the Petrecca lab, and then anti-rat secondary antibody (1:1000) conjugated to Alexa 488. Cells were visualized with a Zeiss 510 confocal microscope (63 x objective) in the Petrecca lab. LSM Image Browser software was used to change the colors of the image components.

4.9.6. Invasion Assays

The invasion assays were performed by Dr. Phuong Le at the Montreal Neurological Institute. Tumor spheroids were created using the hanging drop method and implanted in a collagen type 1 matrix according to Werbowetski-Ogilvie *et al*.[33] Images were taken after 0, 24, 48, 72, and 96 hr. The extreme diameter of the spheroids at time zero was subtracted from the extreme diameter of the spheroids at 4 different angles for each time point. The resulting calculations for invading areas were performed in triplicates and are from 3 independent experiments.

4.9.7. Autoradiography

Purified oligonucleotides **D0**, **D3**, **D4**, **D5**, **D6**, and **D3C** (200 pmol) were dissolved in autoclaved H_2O (12 μL) and reacted with γ-^{32}P-ATP (5 μL) in the presence of T4 polynucleotide kinase (PNK) (1 μL, 2000 units) and 10x PNK buffer (2 μL, 20 mM Tris-HCl, 10 mM $MgCl_2$, 5 mM DTT, pH 7.6 at 25^{o}C). After incubating at 37^{o}C for 1 hr, the reaction mixture was passed through a G-10 sephadex column (GE Healthcare) and the most radioactive fraction was diluted in H_2O. Digestions were performed in reaction mixtures incubated at 37^{o}C with ^{32}P-labeled oligonucleotide (3,000 counts per minute), 1x PBS, FBS, and non-labeled pure oligonucleotide (50 pmol) in a total volume of 10 μL. Aliquots of 3 μL were removed after 2, 4, and 8 minutes and combined with a mixture of formamide and bromophenol blue and xylene cyanol FF marker dyes (5 μL) to quench the reaction. The aliquots were frozen over dry ice until the experiment was completed, at which time they were heated to 95^{o}C for 5 minutes before performing analytical PAGE. The samples were loaded into a 16% polyacrylamide gel with 7 M urea and it was run with tris-borate-ethylenediaminetetraacetic acid (EDTA) buffer for 3 hr at 1000 V. The gel was removed from the electrophoresis apparatus and placed in a cassette with an x-ray film. The film was developed the following day.

4.9.8. Bcl-2 Silencing Efficiency

The silencing efficiencies of **B0**, **B3**, **B6**, **B0-scr**, and **D3-scr** RNAs were assessed by Elena Moroz at the ETH in Zurich. HCT-116 cells were grown in DMEM supplemented with 10% FBS. RNAs were complexed with Lipofectamine^{TM} 2000 and incubated with the cells at a concentration of 15 nM, while no RNA was incubated with the control sample. After 5 hr, fresh DMEM supplemented with 10% FBS replaced the older medium. The cells were then washed with PBS after 2.5 days of incubation. Total RNA was isolated using the RNeasy Mini kit ($Abs_{260}/Abs_{230} > 1.8$). Two-step quantitative real-time PCR (qRT-PCR) was used to compare the expression levels of *bcl-2* mRNA to that of internal control β-actin. In short, 1.2 μg total mRNA was used to synthesize cDNA using high-capacity cDNA reverse transcription kit according to the manufacturer's protocol. qRT-PCR was then performed on a 7900HT Fast Real Time PCR instrument (Applied Biosystems) according to the manufacturer's protocol using Power SYBR Green PCR Master Mix and human *bcl-2* and β-actin primers. To do this, the reaction mixtures were incubated at 50^{o}C for 2 minutes, 95^{o}C for 10 minutes, and then 40 cycles of 95^{o}C for 15 seconds and 60^{o}C for 1 minute. The delta delta Ct ($2^{-\Delta\Delta Ct}$) method was used to calculate relative gene expression levels with the fluorescence threshold set to 0.4. The change in *bcl-2* mRNA level between cells treated with siRNAs and untreated cells is displayed in the results.

4.9.9. Cell Viability

Cell viability of HCT-116 cells was assessed by Elena Moroz at the ETH in Zurich. The day before the experiment, cells were seeded at a density of 7 x 10^3 cells/well in a 96-multiwell plate. **B0**, **B3**, and **B6** siRNAs complexed in Lipofectamine^{TM} 2000 according to the manufacturer's protocol were aliquoted to cells in 50 μL DMEM supplemented with 10% FBS. The control sample was not transfected with siRNA. After 5 hr, the medium was exchanged for 100 μL DMEM supplemented with 10% FBS. Cell viability was assessed with tetrazolium-based CCK-8 reagent (Cell Counting Kit-8 from Dojindo Molecular Technologies (Rockville, MD)) after 1 day according to the manufacturer's protocol.

4.10. References

1. Chiu, Y.-L.; Rana, T. M., siRNA function in RNAi: A chemical modification analysis. *RNA (New York, N.Y.)* **2003,** *9* (9), 1034-1048.

2. Chiu, Y. L.; Rana, T. M., RNAi in human cells: basic structural and functional features of small interfering RNA. *Mol. Cell* **2002,** *10* (3), 549-561.

3. Castanotto, D.; Rossi, J. J., The promises and pitfalls of RNA-interference-based therapeutics. *Nature* **2009,** *457* (7228), 426-433.

4. Bramsen, J. B.; Laursen, M. B.; Nielsen, A. F.; Hansen, T. B.; Bus, C.; Langkjaer, N.; Babu, B. R.; Hojland, T.; Abramov, M.; Van Aerschot, A.; Odadzic, D.; Smicius, R.; Haas, J.; Andree, C.; Barman, J.; Wenska, M.; Srivastava, P.; Zhou, C.; Honcharenko, D.; Hess, S.; Muller, E.; Bobkov, G. V.; Mikhailov, S. N.; Fava, E.; Meyer, T. F.; Chattopadhyaya, J.; Zerial, M.; Engels, J. W.; Herdewijn, P.; Wengel, J.; Kjems, J., A large-scale chemical modification screen identifies design rules to generate siRNAs with high activity, high stability and low toxicity. *Nucleic Acids Res.* **2009,** *37* (9), 2867-2881.

5. Odadzic, D.; Bramsen, J. B.; Smicius, R.; Bus, C.; Kjems, J.; Engels, J. W., Synthesis of 2'-O-modified adenosine building blocks and application for RNA interference. *Bioorg. Med. Chem.* **2008,** *16* (1), 518-529.

6. Prakash, T. P.; Manoharan, M.; Fraser, A. S.; Kawasaki, A. M.; Lesnik, E. A.; Owens, S. R., Zwitterionic oligonucleotides with 2′-O-[3-(N,N-dimethylamino)propyl]-RNA modification: synthesis and properties. *Tetrahedron Lett.* **2000,** *41* (25), 4855-4859.

7. Prakash, T. P.; Puschl, A.; Lesnik, E.; Mohan, V.; Tereshko, V.; Egli, M.; Manoharan, M., 2'-O-[2-(guanidinium)ethyl]-modified oligonucleotides: stabilizing effect on duplex and triplex structures. *Org. Lett.* **2004,** *6* (12), 1971-1974.

8. Griffey, R. H.; Monia, B. P.; Cummins, L. L.; Freier, S.; Greig, M. J.; Guinosso, C. J.; Lesnik, E.; Manalili, S. M.; Mohan, V.; Owens, S.; Ross, B. R.; Sasmor, H.; Wancewicz, E.; Weiler, K.; Wheeler, P. D.; Cook, P. D., 2'-O-aminopropyl ribonucleotides: a zwitterionic modification that enhances the exonuclease resistance and biological activity of antisense oligonucleotides. *J. Med. Chem.* **1996,** *39* (26), 5100-5109.

9. Brzezinska, J.; D'Onofrio, J.; Buff, M. C.; Hean, J.; Ely, A.; Marimani, M.; Arbuthnot, P.; Engels, J. W., Synthesis of 2'-O-guanidinopropyl-modified nucleoside phosphoramidites and their incorporation into siRNAs targeting hepatitis B virus. *Bioorg. Med. Chem.* **2012,** *20* (4), 1594-1606.

10. Kawaguchi, T.; Sakairi, H.; Kimura, S.; Yamaguchi, T.; Saneyoshi, M., Synthesis and antileukemic activity of chymotrypsin-activated derivatives of 3'-amino-2',3'-dideoxycytidine. *Chem. Pharm. Bull. (Tokyo)* **1995,** *43* (3), 501-504.

11. Sharma, R. A.; Bobek, M.; Bloch, A., Preparation and biological activity of some aminoacyl and peptidyl derivatives of 2'-amino-2'-deoxyuridine. *J. Med. Chem.* **1975,** *18* (9), 955-957.

12. Matulic-Adamic, J.; Beigelman, L.; Dudycz, L. W.; Gonzalez, C.; Usman, N., Synthesis and incorporation of 2′-amino acid conjugated nucleotides into ribozymes. *Bioorg. Med. Chem. Lett.* **1995,** *5* (22), 2721-2724.

13. Le, P. U.; Angers-Loustau, A.; de Oliveira, R. M.; Ajlan, A.; Brassard, C. L.; Dudley, A.; Brent, H.; Siu, V.; Trinh, G.; Molenkamp, G.; Wang, J.; Seyed Sadr, M.; Bedell, B.; Del Maestro, R. F.; Petrecca, K., DRR drives brain cancer invasion by regulating cytoskeletal-focal adhesion dynamics. *Oncogene* **2010,** *29* (33), 4636-4647.

14. Deleavey, G. F. Modified nucleic acids for the regulation of gene expression: an investigation of synthetic 2' and 4' fluorinated oligonucleotides. McGill University, Montreal, QC, 2011.

15. Hohjoh, H., Enhancement of RNAi activity by improved siRNA duplexes. *FEBS Lett.* **2004,** *557* (1-3), 193-198.

16. Sano, M.; Sierant, M.; Miyagishi, M.; Nakanishi, M.; Takagi, Y.; Sutou, S., Effect of asymmetric terminal structures of short RNA duplexes on the RNA interference activity and strand selection. *Nucleic Acids Res.* **2008,** *36* (18), 5812-5821.

17. McNamara, J. O., 2nd; Andrechek, E. R.; Wang, Y.; Viles, K. D.; Rempel, R. E.; Gilboa, E.; Sullenger, B. A.; Giangrande, P. H., Cell type-specific delivery of siRNAs with aptamer-siRNA chimeras. *Nat. Biotechnol.* **2006,** *24* (8), 1005-1015.

18. Muratovska, A.; Eccles, M. R., Conjugate for efficient delivery of short interfering RNA (siRNA) into mammalian cells. *FEBS Lett.* **2004,** *558* (1–3), 63-68.

19. Moschos, S. A.; Jones, S. W.; Perry, M. M.; Williams, A. E.; Erjefalt, J. S.; Turner, J. J.; Barnes, P. J.; Sproat, B. S.; Gait, M. J.; Lindsay, M. A., Lung delivery studies using siRNA conjugated to TAT(48-60) and penetratin reveal peptide induced reduction in gene expression and induction of innate immunity. *Bioconjug. Chem.* **2007,** *18* (5), 1450-1459.

20. Chu, T. C.; Twu, K. Y.; Ellington, A. D.; Levy, M., Aptamer mediated siRNA delivery. *Nucleic Acids Res.* **2006,** *34* (10), e73.

21. Oishi, M.; Nagasaki, Y.; Itaka, K.; Nishiyama, N.; Kataoka, K., Lactosylated poly(ethylene glycol)-siRNA conjugate through acid-labile beta-thiopropionate linkage to construct pH-sensitive polyion complex micelles achieving enhanced gene silencing in hepatoma cells. *J. Am. Chem. Soc.* **2005,** *127* (6), 1624-1625.

22. Oishi, M.; Nagasaki, Y.; Nishiyama, N.; Itaka, K.; Takagi, M.; Shimamoto, A.; Furuichi, Y.; Kataoka, K., Enhanced growth inhibition of hepatic multicellular tumor spheroids by lactosylated poly(ethylene glycol)-siRNA conjugate formulated in PEGylated polyplexes. *ChemMedChem* **2007,** *2* (9), 1290-1297.

23. Akerman, M. E.; Chan, W. C.; Laakkonen, P.; Bhatia, S. N.; Ruoslahti, E., Nanocrystal targeting in vivo. *Proc. Natl. Acad. Sci. U.S.A.* **2002,** *99* (20), 12617-12621.

24. Kam, N. W.; Liu, Z.; Dai, H., Functionalization of carbon nanotubes via cleavable disulfide bonds for efficient intracellular delivery of siRNA and potent gene silencing. *J. Am. Chem. Soc.* **2005,** *127* (36), 12492-12493.

25. Soutschek, J.; Akinc, A.; Bramlage, B.; Charisse, K.; Constien, R.; Donoghue, M.; Elbashir, S.; Geick, A.; Hadwiger, P.; Harborth, J.; John, M.; Kesavan, V.; Lavine, G.; Pandey, R. K.; Racie, T.; Rajeev, K. G.; Rohl, I.; Toudjarska, I.; Wang, G.; Wuschko, S.; Bumcrot, D.; Koteliansky, V.; Limmer, S.; Manoharan, M.; Vornlocher, H. P., Therapeutic silencing of an endogenous gene by systemic administration of modified siRNAs. *Nature* **2004,** *432* (7014), 173-178.

26. Wolfrum, C.; Shi, S.; Jayaprakash, K. N.; Jayaraman, M.; Wang, G.; Pandey, R. K.; Rajeev, K. G.; Nakayama, T.; Charrise, K.; Ndungo, E. M.; Zimmermann, T.; Koteliansky, V.; Manoharan, M.; Stoffel, M., Mechanisms and optimization of in vivo delivery of lipophilic siRNAs. *Nat. Biotechnol.* **2007,** *25* (10), 1149-1157.

27. Hicke, B. J.; Stephens, A. W., Escort aptamers: a delivery service for diagnosis and therapy. *J. Clin. Invest.* **2000,** *106* (8), 923-928.

28. Anderson, E. M.; Miller, P.; Ilsley, D.; Marshall, W.; Khvorova, A.; Stein, C. A.; Benimetskaya, L., Gene profiling study of G3139- and Bcl-2-targeting siRNAs identifies a unique G3139 molecular signature. *Cancer Gene Ther.* **2006,** *13* (4), 406-414.

29. Felber, A. E.; Castagner, B.; Elsabahy, M.; Deleavey, G. F.; Damha, M. J.; Leroux, J. C., siRNA nanocarriers based on methacrylic acid copolymers. *J. Controlled Release* **2011,** *152* (1), 159-167.

30. Del Duca, D.; Werbowetski, T.; Del Maestro, R. F., Spheroid preparation from hanging drops: characterization of a model of brain tumor invasion. *J. Neuro-Oncol.* **2004,** *67* (3), 295-303.

31. Sun, X.; Rogoff, H. A.; Li, C. J., Asymmetric RNA duplexes mediate RNA interference in mammalian cells. *Nat. Biotechnol.* **2008,** *26* (12), 1379-1382.

32. Chang, C. I.; Yoo, J. W.; Hong, S. W.; Lee, S. E.; Kang, H. S.; Sun, X.; Rogoff, H. A.; Ban, C.; Kim, S.; Li, C. J.; Lee, D. K., Asymmetric shorter-duplex siRNA structures trigger efficient gene silencing with reduced nonspecific effects. *Mol. Ther., J. Am. Soc. Gene Ther.* **2009,** *17* (4), 725-732.

33. Werbowetski-Ogilvie, T. E.; Seyed Sadr, M.; Jabado, N.; Angers-Loustau, A.; Agar, N. Y. R.; Wu, J.; Bjerkvig, R.; Antel, J. P.; Faury, D.; Rao, Y.; Del Maestro, R. F., Inhibition of medulloblastoma cell invasion by Slit. *Oncogene* **2006,** *25* (37), 5103-5112.

Chapter 5: Towards a Method for the Synthesis of proRNA

5.1. The Utility of ProRNA with 2'-O-Phenylalanine Acetal Esters

In Chapter 2, nucleoside 3'-*O*-phosphoramidites building blocks containing novel 2'-*O*-amino acid acetal ester (2'-*O*-AAE) moieties based on L-alanine, L-phenylalanine, L-lysine, and L-proline were synthesized and incorporated into oligonucleotides. Reversed-phase-high performance liquid chromatography (RP-HPLC) purification revealed oligonucleotide products which contained a varying number of their 2'-*O*-AAE modifications intact. The 2'-*O*-phenylalanine acetal ester (2'-*O*-Phe AAE) in particular (Figure 5.1) was the only 2'-*O*-AAE of those incorporated into conjugates that could be used to prepare oligonucleotides containing all of the inserts intact, despite the presence of completely hydrolyzed product in the crude mixture. Fine-tuning of the steps used to prepare a 2'-*O*-Phe-containing conjugate for RP-HPLC revealed no hydrolyzed oligonucleotide present in the crude product, with hydrolysis taking place when the oligonucleotide was left incubating in phosphate buffered saline at 37^{o}C ($t_{1/2}$ = ca. 16 hr).

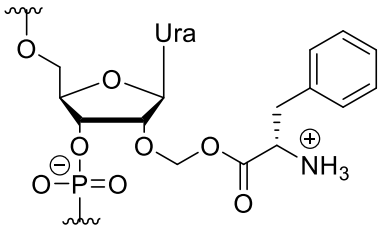

Figure 5.1. The 2'-*O*-phenylalanine acetal ester modification.

With the aim of improving cellular delivery of siRNAs in-mind, Chapter 3 described the synthesis of a stable derivative of the 2'-*O*-Phe AAE modification, namely 2'-*N*-acyl-phenylalanine, and an assessment of its ability to increase cellular uptake of siRNA. In Chapter 4 we combined this property of 2'-*N*-acyl-phenylalanine with the ability of siRNA containing 2'-*N*-acyl-phenylalanine modifications to silence endogenous genes, in a self-delivering siRNA. Replacing the 2'-*N*-acyl-phenylalanine modification of the self-delivering construct with the 2'-*O*-Phe AAE promoiety could deliver siRNAs with uncompromised potency as the modification is expected to enhance cellular penetration and then be removed in the cell prior to silencing. The most difficult part of this strategy is the release of mixed base, 2'-*O*-Phe AAE-modified oligonucleotides intact from the solid support. Towards this goal, we describe below a photocleavable solid support linker and protecting group strategies that may be useful in the synthesis and release of proRNA of mixed based composition.

5.2. Established Protocols to Synthesize ProRNA

5.2.1. ProRNA with Backbone Promoieties

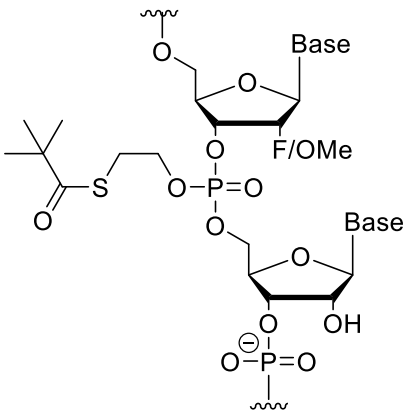

Figure 5.2. The *tert*-Bu-SATE promoiety was incorporated into siRNNs by Dowdy and coworkers.[2]

The S-acyl-2-thioethyl (SATE) biolabile internucleotide modification is the backbone promoiety that has progressed farthest in its use as a precursor to active siRNA. Its incorporation into a poly-thymidine oligonucleotide was done on photocleavable controlled pore glass (CPG) solid support and did not require nucleobase protecting groups.[1] When incorporated into a mixed-base short interfering ribonucleic neutral (siRNN, Figure 5.2), synthesis was done an orthogonal solid support not requiring a nucleophile for cleavage;[2] the hydroquinone-*O,O*'-diacetic acid ("Q-linker", Figure 5.3) is cleaved very quickly with fluoride ion in the form of triethylamine trihydrofluoride (NEt_3-3HF).[3] The nucleobases were protected with phenoxyacetyl (PAC)-based groups (Figure 1.16D), which were removed in 4 hours with 10% diisopropylamine in methanol.[2] This mild nucleobase deprotection solution, as well as the exclusive use of 2'-*O*-methyl and 2'-fluoro modifications on purine and pyrimidine phosphoramidites, respectively, were useful in preventing base-mediated phosphotriester cleavage of SATE phosphoramidites.[2] Hence, a limitation of this approach is that the 2'-hydroxyl group of ribonucleotides containing a vicinal 3'-phosphotriester, such as the SATE promoiety, must be permanently modified (2'-OMe, 2'-F) in order to avoid phosphotriester cleavage during deprotection of the oligonucleotide.

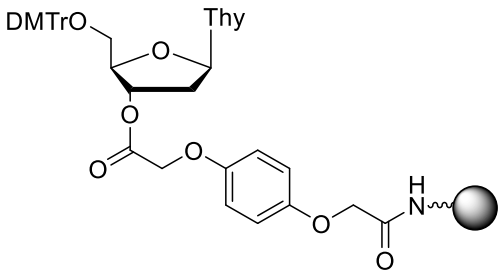

Figure 5.3. The Q-linker was developed by Pon *et al.* for rapid oligonucleotide release.[3]

Given the instability of the 2'-*O*-Phe AAE moiety in the presence of aqueous solvents, the use of fluoride ions to cleave the oligonucleotide from the solid support is not desirable for our

purposes. It requires precipitation of the crude oligonucleotide product from butanol spiked with sodium acetate buffer to remove fluoride ions. This precipitation is expected to cause cleavage of the 2'-*O*-Phe AAE moiety.

5.2.2. ProRNA with Sugar Promoieties

Solid-supported synthesis of RNA with reducible 2'-disulfide groups (Figure 1.17D) is simple, since the RNA skeleton can be grown with standard phosphoramidites and the disulfide bonds can be added after chain elongation.[4] The solid-supported synthesis of RNA with esterase-labile 2'-*O*-acetal esters, on the other hand, has employed the use of non-standard RNA synthons and deprotection conditions.

In the first demonstration of RNAi achieved by proRNA containing sugar promoieties at the 2'-position, the Debart group synthesized phosphoramidites protected at their exocyclic amines with acid-labile 4,4'-dimethoxytrityl (DMTr) for riboguanosine and a silyl-based protecting group (Figure 1.16F) for adenosine and cytosine monomers.[5] The DMTr group on guanosines was removed during the detritylation steps of oligonucleotide synthesis, however the free amine was deemed not nucleophilic enough to cause issues with oligonucleotide synthesis.[5] Each nucleotide was synthesized with 2'-*O*-pivaloyloxymethyl (pivOM) (Figure 1.17A) and 2'-*O*-*tert*-butyldimethylsilyl (TBDMS) groups.[5]

Strong base 1,8-diazabicyclo[5.4.0]undec-7-ene (DBU) was used to eliminate cyanoethyl groups on the phosphotriesters and fluoride ion was used to cleave the Q-linker of the solid support as well as the nucleobase protecting groups of adenosine and cytosine.[5] As with Dowdy's siRNNs, the final step in deprotection of these proRNAs required precipitation from butanol spiked with 3 M sodium acetate (pH 5.5). An alternative reagent for quickly cleaving the Q-linker, dry *tert*-butylamine in tetrahydrofuran (THF), has been used by the Debart lab to cleave the oligonucleotide from the solid support as well as selectively cleave all 2'-hydroxyls protected with 2'-*O*-propionyloxymethyl (prOM), leaving behind only the more stable 2'-*O*-pivOM groups.[6] This was done after deprotection of PAC-based and acetyl protecting groups on the nucleobases of ribonucleotides in the proRNA, as well as their cyanoethyl groups, with DBU in acetonitrile (MeCN).[6]

There are some details in the synthetic protocols of sugar-modified proRNA described in the literature that are not amenable to the synthesis of proRNA containing 2'-*O*-Phe AAEs. Given the instability of 2'-*O*-Phe AAE in aqueous solvent, the aqueous butanol precipitation performed in order to free the oligonucleotide from fluoride ions is not an ideal step in the deprotection of proRNA containing 2'-*O*-Phe AAEs. Precipitation can be avoided immediately after linker cleavage if instead the Q-linker is deprotected with dry *tert*-butylamine in THF. However, the 2'-*O*-TBDMS moieties would then require desilylation with NEt_3-3HF, and thus precipitation of the crude mixture to remove fluoride ion. We did not plan on using an alternative 2'-protecting group that is cleavable by orthogonal conditions for the synthesis of proRNA based on *N*-FMOC-protected phosphoramidites discussed in section 5.3, in order to avoid using a protecting group that has not yet been tested with the 2'-*O*-phenylalanine acetal ester (Chapter 1) or the 2'-*N*-acyl-L-phenylalanine modification (Chapter 3-4). The permanent 2'-fluoro and 2'-*O*-methyl modifications do not require deprotection; however, their potential to negatively affect cellular delivery when used in combination with the promoiety (suggested by the results of combining 2'-fluoro RNA with 2'-*N*-acyl-L-phenylalanine in section 3.6) also dissuaded our efforts to synthesize proRNA with 2'-*O*-Phe AAEs.

The Debart group has also utilized a phosphoramidate linker to CPG solid support (Scheme 5.1) which upon treatment with DBU in MeCN generated a monoester phosphoramidate[7] that was cleaved by aqueous acetic acid,[8] thus avoiding the use of Q-linker or UnyLinker™. The cyanoethyl deprotection with DBU, however, would also cleave the FMOC groups on the 2'-*O*-AAEs, making the moieties susceptible to hydrolysis in the aqueous acidic solution. Since the amino acetal esters are sensitive to small amounts of water, the use of strong base such as DBU is also a concern for its ability to catalyze the hydrolysis of the acetal ester in the presence of small amounts of water.

The Debart group utilized a CPG-bound photocleavable support in their synthesis of poly-uridines with 2'-*O*-acyloxymethyl and 2'-*O*-acylthiomethyl groups which required neither aqueous cleavage nor oligonucleotide precipitation when it was cleaved as a final step to oligonucleotide deprotection.[9] Cyanoethyl removal was also not required, as 2-(trimethylsilyl)ethyl (TSE) phosphate protection was removed during the standard iodine oxidation step in oligonucleotide synthesis, without any negative effect on the quality of the

product.[9] Our efforts in synthesizing proRNA also employ a photocleavable linker for the benefits of releasing deprotected oligonucleotide as a final step.

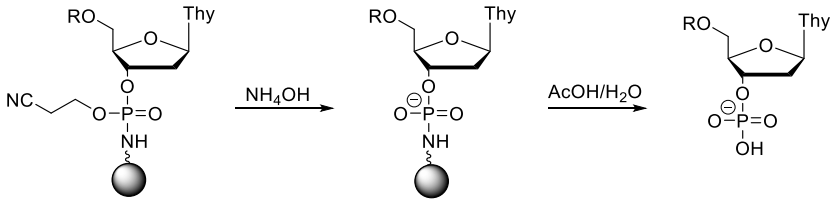

Scheme 5.1. An acid-cleavable phosphoramidate solid support linker was utilized by the Debart group to synthesize oligonucleotides containing acetal esters. Adapted from reference 7.

5.3. A Proposed Method to Prepare ProRNA with 2'-O-Phenylalanine Acetal Esters

It was previously proposed by Dr. Jeremy Lackey, a former PhD student in the Damha laboratory, that a photocleavable linker to CPG or polystyrene (PS) that branched from an internucleotide phosphotriester would be an improvement to the photocleavable solid support linkers reported in the literature. Indeed, CPG derivatized at the internucleotide phosphotriester of TpT, with 3'-*O*-levulinyl protection on the 3'-terminal thymidine monomer, reached its maximum oligonucleotide release more quickly than the conventional 3'-oligonucleotide-linked photocleavable solid supports.[10] This is most likely due to the fact that the negatively charged phosphate released by photocleavage is a better leaving group than a terminal hydroxyl group of the oligonucleotide.

Dr. Lackey's initial attempt at synthesizing proRNA on this type of photocleavable solid support was done with rA, rG, and rC phosphoramidites protected at their exocyclic amines with an *N*-fluorenylmethoxycarbonyl (FMOC) group. This mild nucleobase protecting group was employed in an intermediate step in the synthesis of phosphoramidites bearing *N*-levulinyl (*N*-Lev) or *N*-dimethylformamidine (*N*-dmf) nucleobase protecting groups, and a 2'-*O*-acetal levulinyl ester (2'-*O*-ALE) protecting group.[11] The 2'-*O*-ALE-containing phosphoramidites were initially employed as alternative synthons in solid-supported oligonucleotide synthesis, but the 2'-*O*-ALE moiety was later utilized in preliminary proRNA constructs.[11] The *N*-FMOC-protected intermediates in-hand were thus utilized to synthesize phosphoramidites containing standard 2'-*O*-TBDMS and 5'-*O*-DMTr protecting groups.

Standard solid-phase synthesis conditions were used for the oligonucleotide synthesis of preliminary RNA, including standard acetic anhydride (Ac_2O) capping reagent. Deprotection of the synthesized oligonucleotide was first done with overnight exposure to a 3:2 (v:v) solution of MeCN:NEt_3 to simultaneously remove the FMOC and cyanoethyl groups. Fast desilylation was then done with NEt_3-3HF/*N*-methyl pyrrolidinone/NEt_3 at 65°C. The last performed step was a quick photolysis in MeCN with 1% diisopropylethylamine (DIPEA) to release the oligonucleotide from the solid support. Unfortunately, the synthesis of a mixed-base 22-mer proRNA resulted in a broad peak in the RP-HPLC chromatogram and no mass corresponding to the desired prodrug was found.[11]

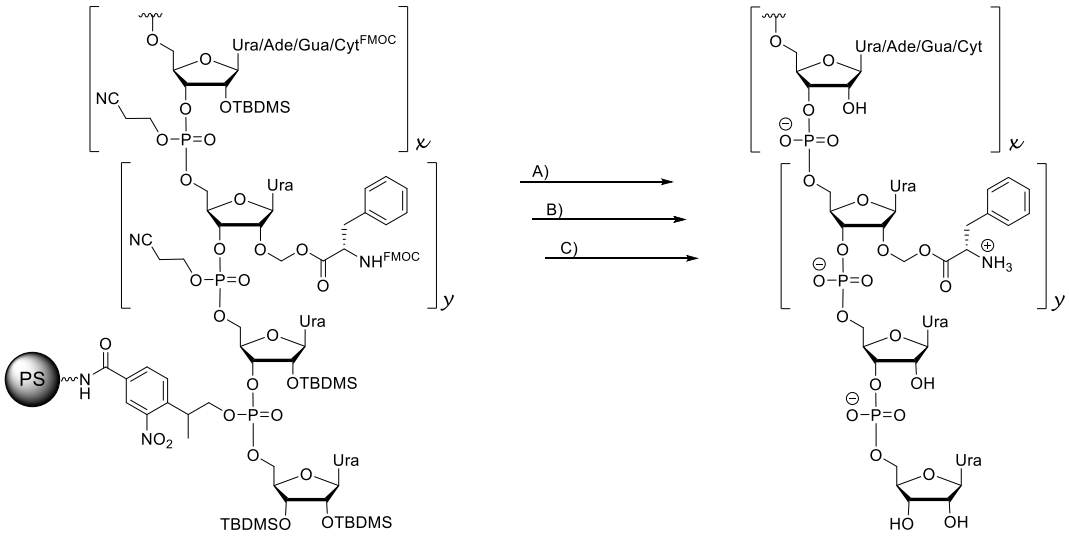

Scheme 5.2. A possible deprotection procedure for proRNA containing 2'-*O*-Phe AAEs begins with A) removal of phosphotriester and nucleobase protection with triethylamine, then includes B) desilylation with standard NEt_3-3HF desilylating solution, and ends with C) photocleavage of the phosphotriester linker to the solid support.

We used the basis of this protocol to begin our investigation into any issues that were preventing synthesis of a mass-characterized proRNA. This was necessary in order to employ an appropriate protocol to synthesize proRNA containing 2'-*O*-Phe AAEs. Scheme 5.2 illustrates the FMOC-protected nucleic acid residues that will be used in our initial attempts at RNA synthesis and the derivatized solid polymer support (PS) that will be used in order to maintain the release of a fully deprotected nucleic acid as the final step in oligonucleotide deprotection. (Note: CPG reacts with fluoride ions.) The 2'-*O*-Phe AAE uridine monomer shown in Scheme

5.2 can be incorporated in this deprotection scheme with the pictured monomers once the requirements for the use of the FMOC phosphoramidites are determined.

5.3.1. Synthesis of N-FMOC Monomers

The synthesis of the ribocytidine monomer was done using commercially available cytidine 3'-*O*-phosphoramidite with standard *N*-acetyl nucleobase protection (Scheme 5.3). The phosphoramidite **1** was dissolved in THF and a 1:1 solution of aqueous ammonia (NH_4OH) and methylamine ($MeNH_2$) in ethanol (EtOH) was added according to Ohkubo *et al*.[12] The product **2** was obtained in quantitative yield and FMOCCl was coupled to the nucleobase dissolved in THF in the presence of DIPEA,[11] yielding 60% of the product **3**.

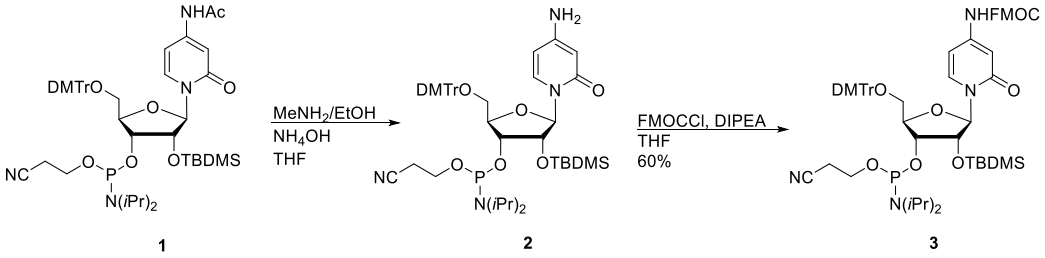

1 **2** **3**

Scheme 5.3. Cytidine *N*-FMOC-protected phosphoramidite **3** was synthesized in two steps from commercially available compound **1**.

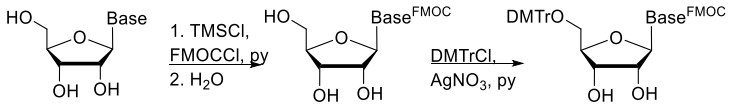

4a-b **5a-b** **6a-b**

B: (**a**) Ade, **5a** 81%, **6a** 90%; (**b**) Gua, **5b** 75%, **6b** 89%

Scheme 5.4. The synthesis of base-protected adenosine and guanosine was accomplished with the Jones method.[13]

The synthesis of the adenosine and guanosine monomers was initiated by fluorenylmethoxycarbonylation of the nucleoside transiently per-silylated by the standard Jones method (Scheme 5.4).[13] After coupling chlorotrimethylsilane (TMSCl) to the free hydroxyl groups of the nucleosides **4a** and **4b**, FMOCCl was coupled to the nucleobase. Standard cleavage of trimethylsilyl (TMS) ethers is done in a few minutes with aqueous ammonia.[13]

However, attempting to remove the TMS groups on per-silylated guanosine using an aqueous ammonia workup removed the FMOC group in addition to the TMS groups. Thus, a slower approach to one-pot FMOC installation and TMS removal was employed in which no base was needed; water was added at the end of the FMOC installation for the formation of slightly acidic pyridinium cation, causing the removal of the TMS groups.[14] Di-fluorenylmethoxycarbonylation was not observed on adenosine **5a** (nor guanosine **5b**), in contrast to di-benzoylation often observed with adenosine, likely due to the steric clash of two large FMOC groups. Standard dimethoxytritylation was accomplished with DMTrCl and pyridine to yield compounds **6a** and **6b**.

Next, a few different conditions[15] for installing the standard 2'-*O*-TBDMS group were employed on **6a** and **6b** and the yields of the products shown in Scheme 5.5 are listed in Table 5.1. Using imidazole in a 1:1 ratio with TBDMSCl in dimethylformamide (DMF) yielded 36% of the 2'-regioisomer **7a** with no 3'-regioisomer or bis-silylated product **8a**. As expected, this reaction condition caused almost complete removal of the FMOC group in the case of **6b** due to the basicity of imidazole. This discrepancy is likely due to the fact that the pK_a of the FMOC-protected exocyclic amine of guanosine is 2.1 while that of adenosine is 3.55,[16] making guanosine the better leaving group in the β-elimination reaction that leads to FMOC cleavage. An activator of TBDMSCl, silver nitrate ($AgNO_3$), was employed as an alternative to imidazole. Using THF as a solvent and a few equivalents of pyridine (py), guanosine derivative **6b** was silylated at the 2'-position to give product **7b** in slight excess of the 3'-position product **8b**, however the overall yields of both were very poor. Silylation of **6b** dissolved in py using $AgNO_3$ as an activator improved the overall yield of **7b**, in comparison to the use of THF as a solvent for **6b**, as well as its regioisomeric excess over **8b**. The yields of the adenosine derivatives **7a** and **8a** were both higher when using py as a solvent and two equivalents of $AgNO_3$ and TBDMSCl than the yield of **7a** when using DMF and imidazole. The yields of **7a** and **8a** were also equal as expected, since two equivalents of TBDMSCl were used in the reaction. The yields show that the use of $AgNO_3$ activator in py is also a suitable condition for the silylation of the adenosine nucleoside.

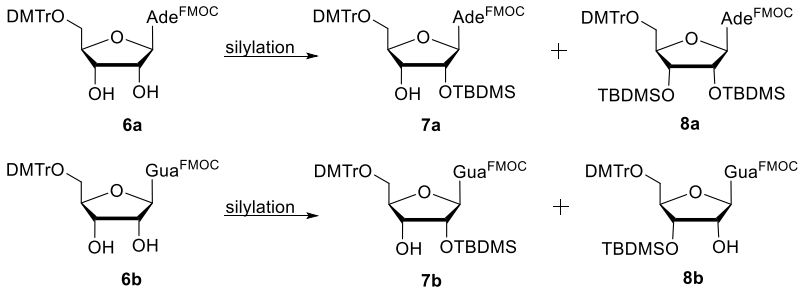

Scheme 5.5. The silylation of adenosine and guanosine nucleosides was done under different conditions.

Table 5.1. Several reaction conditions were employed for the silylation of riboadenosine and riboguanosine nucleosides.

Reaction components	Yield (%)			
	7a	**8a**	**7b**	**8b**
TBDMSCl, imidazole, DMF	36	0	4	0
TBDMSCl, $AgNO_3$, py, THF			13	9
TBDMSCl, $AgNO_3$, py	43	43	22	5

Standard phosphitylation conditions were used to obtain the phosphoramidites **9a-b** (Scheme 5.6). The adenosine *R*p and *S*p diasterioisomers were clearly resolved on TLC with various eluents such as methanol/dichloromethane (CH_2Cl_2), hexanes/ethyl acetate (EtOAc) and acetone/CH_2Cl_2.

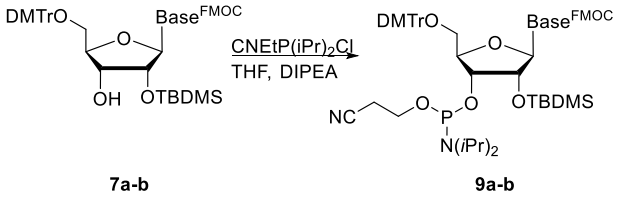

Scheme 5.6. Phosphitylation of *N*-FMOC-protected monomers proceeds by standard conditions.

5.3.2. Derivatization of Solid Support with Photocleavable Linker

Both a UpU and TpT phosphoramidite dimer were synthesized from monomers prepared with simple hydroxyl protection and deprotection chemistry and an *N*,*N*,*N*,*N*-tetraisopropyl chlorophosphite coupled to the 3'-hydroxyl of one of the monomers (Scheme 5.7). Bis-amidites **13** and **18** were coupled to monomers **15** and **19**, respectively, using different reaction conditions. Standard oligonucleotide activator 5-ethylthiotetrazole (ETT) was employed in 25-fold excess equivalents for the synthesis of dimer **16** and in a 1:1 ratio for the synthesis of dimer **20**. Solid support **21**, provided by Dr. Richard Johnsson, was then added to the solution containing dimer **16** and stirred overnight, while dimer **20** was isolated, characterized, and then manually coupled to the support in an ABI synthesizer column in 15 minutes using 1.5 equivalents of ETT. No trityl color was observed upon detritylation of the support that was reacted with **16**, while the loading of the support derivatized with **20** was 36.8 μmol/g. These supports were used to synthesize oligonucleotides in section 5.4.

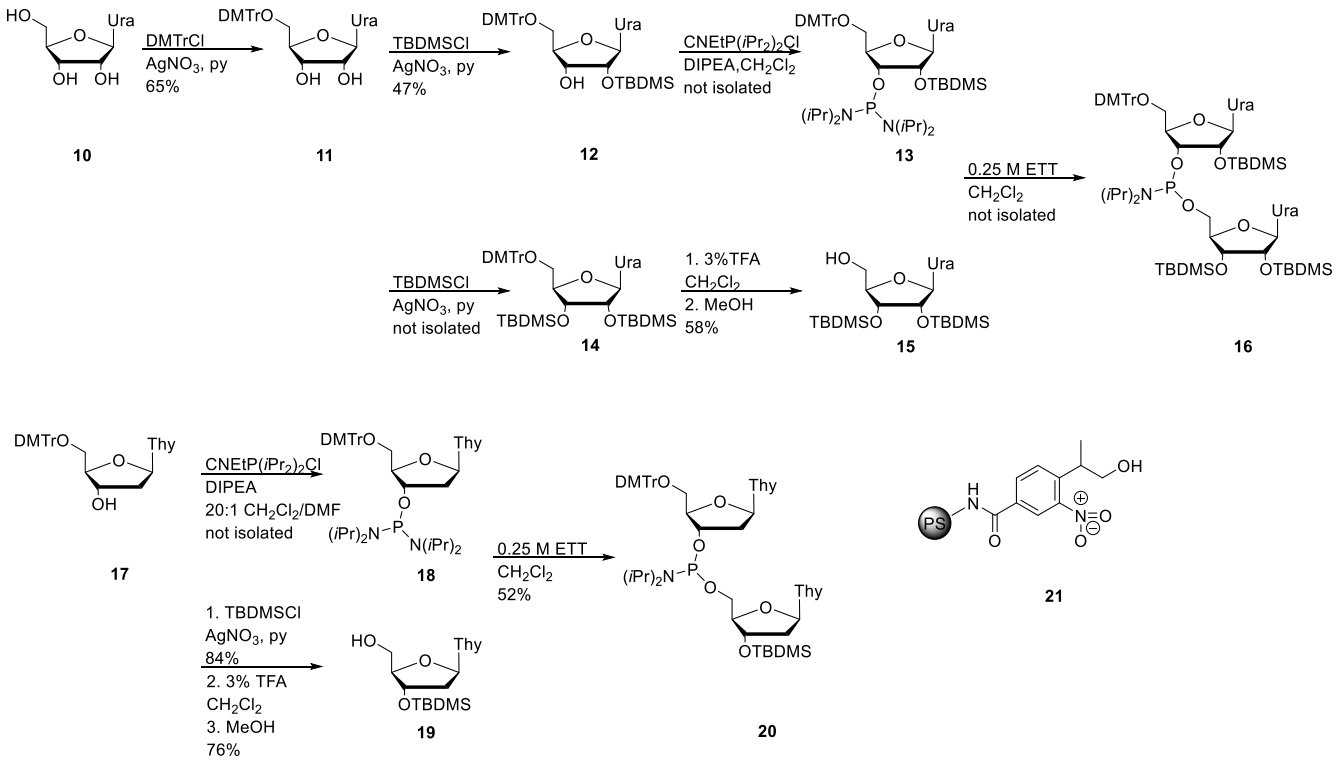

Scheme 5.7. UpU and TpT dimer phosphoramidites were synthesized and coupled to a photocleavable linker on PS solid support.

5.4. Establishing a Method to Synthesize RNA with N-FMOC-Protected Building Blocks

In order to compare the stepwise coupling yield and overall RNA yield obtainable with the synthesized phosphoramidites to that obtainable by the standard rA^{Bz}, rG^{ibu}, and rC^{Ac} phosphoramidites, a 21-mer was synthesized on UnyLinker™ CPG with the standard phosphoramidites and the *N*-FMOC-protected phosphoramidites, using standard solid-phase synthesis reagents. Fast linker cleavage was performed with aqueous $MeNH_2$. Next, fast desilylation with a solution of NEt_3-3HF:dimethylsulfoxide (DMSO) (1:1 v/v) was performed at 65°C for 90 minutes. Aqueous butanol precipitation conditions were then employed and the resulting anion exchange (IE)-HPLC chromatograms were compared in Figure 5.4. The RNA synthesized with standard phosphoramidites (inset) yielded 101.4 crude optical density units (ODs), while the non-standard phosphoramidites yielded 91.6 crude ODs of RNA. The purity of the RNA prepared with standard monomers is 90.7% (determined by the area under the HPLC peak), while that of the RNA prepared from FMOC phosphoramidites is 74.3%. The mass of the desired RNA is confirmed in entry 1 of Table 5.2 for the purified 30-minute peak.

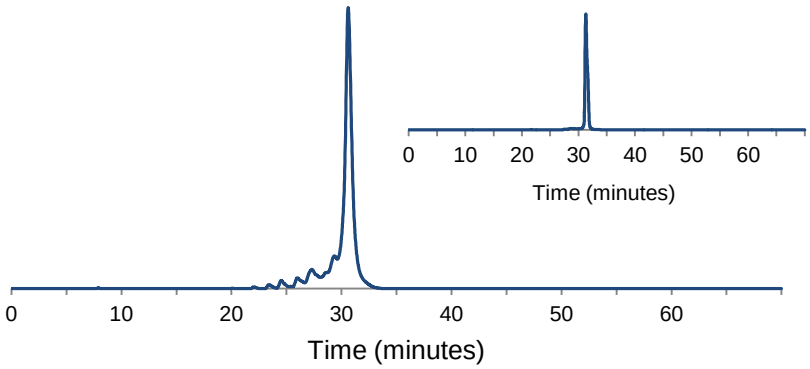

Figure 5.4. IE-HPLC chromatograms of the same oligonucleotide (5'-UUC UUG AUG AGC UGG UUC CTT-3') synthesized with standard phosphoramidites (inset) and *N*-FMOC-protected phosphoramidites.

Assuming that there was no problem with the synthesis or deprotection protocol already established, an oligonucleotide was synthesized on the UpU-derivatized photocleavable linker **16**. The cyanoethyl and FMOC groups were removed with anhydrous NEt_3/MeCN (2:3 v/v). Then fast desilylation was performed with NEt_3-3HF/DMSO (2:1 v/v), followed by photolysis in MeCN with 1% DIPEA. Crude mass peaks are shown in Figure 5.5 and identified in entry 2 of Table 5.2.

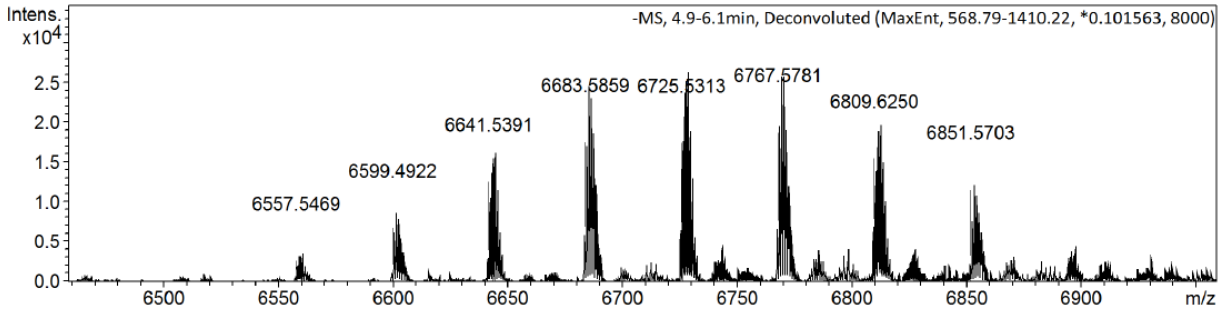

Figure 5.5. Crude mass spectrogram of oligonucleotide synthesized from photocleavable support **16**.

Two things were noticed in the observed masses: 1) An RNA without the two uridine units that should have come from the UpU-derivatized support and; 2) an envelope of peaks separated by about 42 mass units due to various degrees of acetylation of the nucleobases. The coupling of the uridine monomers to each other was done overnight with a large excess of equivalents of activator. Moisture in the peptide synthesizer column most likely caused hydrolysis of the dimer phosphoramidite. No dimer was coupled to the support, and thus the coupling of the first uridine monomer on the ABI was done directly onto **21** (Scheme 5.8). Upon photolysis, the RNA was released with a terminal 3'-phosphate. This phosphate group is not desirable in our proRNA constructs. Two additional negative charges remain in the synthesized RNA with the possibility of further repelling cellular membranes. In addition to this possible disadvantage for cellular uptake, a 3'-phosphate is not a sequence feature of the self- delivering tailed siRNA developed in Chapter 2. If this self-delivering construct is used as a template for tailed proRNA with 2'-*O*-Phe AAE insertions, a 3'-phosphate would be a slight deviation.

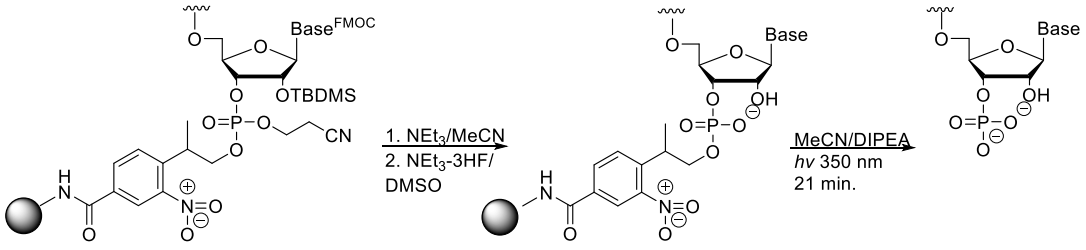

Scheme 5.8. The first nucleotide residue was coupled directly to solid support **21** in the case of entries 2 and 3 in Table 5.2.

RNA synthesis was redone starting directly from **21** in order to confirm by mass analysis that the product yielded includes an extra phosphate group. Deprotection conditions were identical to those used for the oligonucleotide listed as entry 2 in Table 5.2, except that a slightly longer time for removal of FMOCs and cyanoethyls was performed, yet the same issue with nucleobase acetylation was observed (entry 3 in Table 5.2). This mass envelope of acetylated RNA may explain the broad proRNA peak in the HPLC chromatogram of preliminary results by Dr. Lackey.[11]

Table 5.2. The synthesis of RNA with rA^{FMOC}, rG^{FMOC}, and rC^{FMOC} phosphoramidites on various solid supports was done with different capping reagents to give various results.

Entry	Support	Cap A	Base deprotection	Mass Found	Identity
1[a]	UnyLinker™	Ac_2O	40% aq. $MeNH_2$ 65 °C, 10 min	6597.6187	Desired RNA
2[b, crude]	Photocleavable (from **16**)	Ac_2O	2:3 NEt_3/MeCN 65 °C, 2 hr	6557.5469 6599.4922 6641.5391 6683.5859 6725.5313 6767.5781 6809.6250 6851.5703	RNA with 2 Ac - UU RNA with 3 Ac - UU RNA with 4 Ac - UU RNA with 5 Ac - UU RNA with 6 Ac - UU RNA with 7 Ac - UU RNA with 8 Ac - UU RNA with 9 Ac - UU
3[c, crude]	Photocleavable (**21**)	Ac_2O	2:3 NEt_3/MeCN 65 °C, 4.5 hr	6780.7668 6828.7614 6870.7896 6912.7837 6954.7918 6996.8015 7038.8065 7080.8260	RNA with 2 Ac RNA with 3 Ac RNA with 4 Ac RNA with 5 Ac RNA with 6 Ac RNA with 7 Ac RNA with 8 Ac RNA with 9 Ac
4[d, crude]	Photocleavable (from **20**)	PAC_2O	2:3:1 NEt_3/MeCN/ morpholine, 65°C, 2 hr	6695.9688	Desired RNA

Legend: CE = cyanoethyl; [a] = DRR antisense strand 5'-UUC UUG AUG AGC UGG UUC CTT-3' (calc.: 6597.8461); [b] = DRR sense strand (+ U) 5'-GGA ACC AGC UCA UCA AGA AUU U-3' (calc.:7005.9862); [c] = luciferase antisense strand 5'-UUA AUU AAA GAC UUC AAG CTT-3' (calc.:6698.8857); [d] = DRR sense strand 5'-GGA ACC AGC UCA UCA AGA ATT-3' (calc.:6696.0032).

The highly labile *N*-FMOC group, similar to the highly labile *N*-PAC group, requires a non-standard CAP A reagent. A solution of 5% phenoxyacetic anhydride (PAC_2O) in THF/pyridine must be used instead of Ac_2O. We have seen in Table 5.2 that FMOC protection on the nucleobases can exchange with acetate from Ac_2O. Once FMOC groups are exchanged for acetyl groups, they are not removed by NEt_3. This explains why acetyl groups were detected in entries 2 and 3 in Table 5.2. In entry 1 of Table 5.2, the fast deprotection performed with $MeNH_2$ was able to remove the acetylated bases before characterization was done.

With the issue of nucleobase acetylation corrected, photocleavable support made from **20** was used to make RNA (Table 5.2, entry 4). Morpholine was added to the FMOC-deprotection solution as a precaution; eliminated benzofulvene could add to the exocyclic amines of the nucleobases, forming permanent adducts in the RNA. Morpholine adds to the elimination product instead. The synthesized RNA was deprotected with NEt_3/MeCN/morpholine (2:3:1 v/v/v) and then desilylated with NEt_3-3HF/DMSO (1:1 v/v) while the oligonucleotide was still attached to the solid support. In the final deprotection step, photolysis was performed with 1% DIPEA in MeCN. No envelope of peaks was recovered in the crude mass analysis (Figure 5.6).

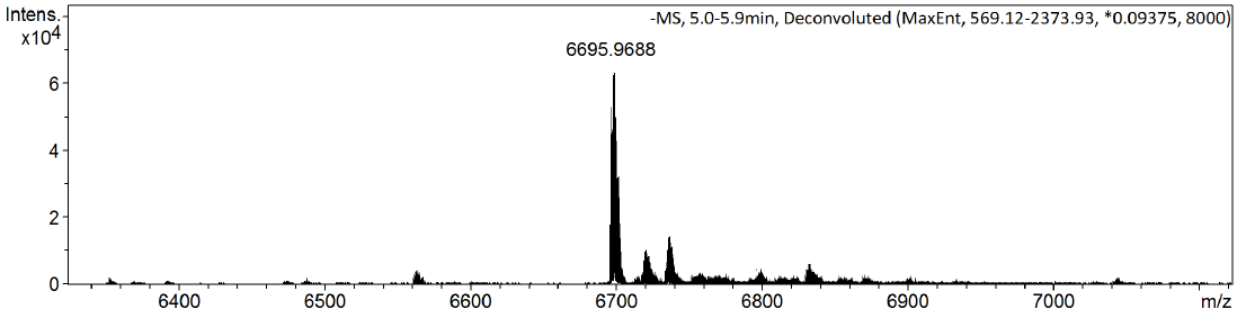

Figure 5.6. The crude mass analysis of RNA synthesized with photocleavable support **20** revealed the desired mass.

The IE-HPLC trace of the crude RNA synthesized with photocleavable support **20** is shown in Figure 5.7. The lack of short-mers in the trace indicates that the purity of desired product is very high. We believe that this orthogonal synthetic scheme and reagents can be used to synthesize proRNA containing 2'-*O*-Phe AAEs.

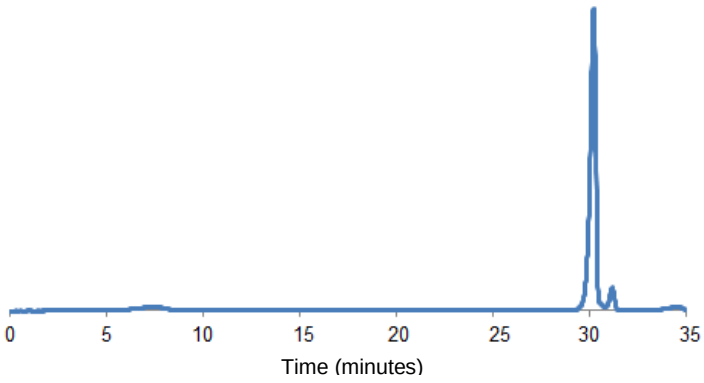

Figure 5.7. The crude IE-HPLC trace of an oligonucleotide 5'-GGA ACC AGC UCA UCA AGA ATT-3' synthesized on photocleavable linker **20** is very clean.

5.5. Stability of the 2'-O-Phenylalanine Acetal Ester to Various Deprotection Conditions

The synthesis of RNA using *N*-FMOC phosphoramidites was encouraging, as the deprotection of such RNA could be done in a way that could keep 2'-*O*-phenylalanine AAEs intact. We did notice, however, that the guanosine phosphoramidite did not fully dissolve in MeCN. Instead of adding a cosolvent, which can require an increase of the coupling time for the phosphoramidite, we first proceeded to determine if the 2'-*O*-AAE moieties could withstand the hydrazine hydrate treatment used to remove *N*-levulinyl (Lev) or *N*-dimethoxyformamidine (dmf) protecting groups from the nucleobases. These protecting groups, unlike the more commonly used protecting groups (*N*-Ac, *N*-Bz, *N*-*i*Bu), can be removed under mild conditions using a buffered hydrazine hydrate (NH_2NH_2•XH_2O)/pyridine solution.[17] To this end, 3',5'-bis silylated 2'-*O*-Phe nucleoside **22** was subjected to hydrazine treatment (Scheme 5.9A). After 1 hour the nucleoside remained completely intact by TLC and crude ESI-MS. The FMOC protection on nucleoside **22** was then removed with anhydrous NEt_3/MeCN (2:3 v/v), leaving the acetal ester intact in product **23** (Scheme 5.9B). Then the same hydrazine treatment was applied to **23**. Some of the nucleoside was converted to compound **24** within minutes (TLC, ESI-MS). Thus, *N*-Lev and *N*-dmf protection is compatible with the 2'-*O*-Phe AAE; however, their deprotection must occur prior to the removal of FMOC and cyanoethyl groups. This is in agreement with the finding that the 2'-*O*-AAE is cleaved quickly in the presence of H_2O due to the positively charged amine (section 2.6).

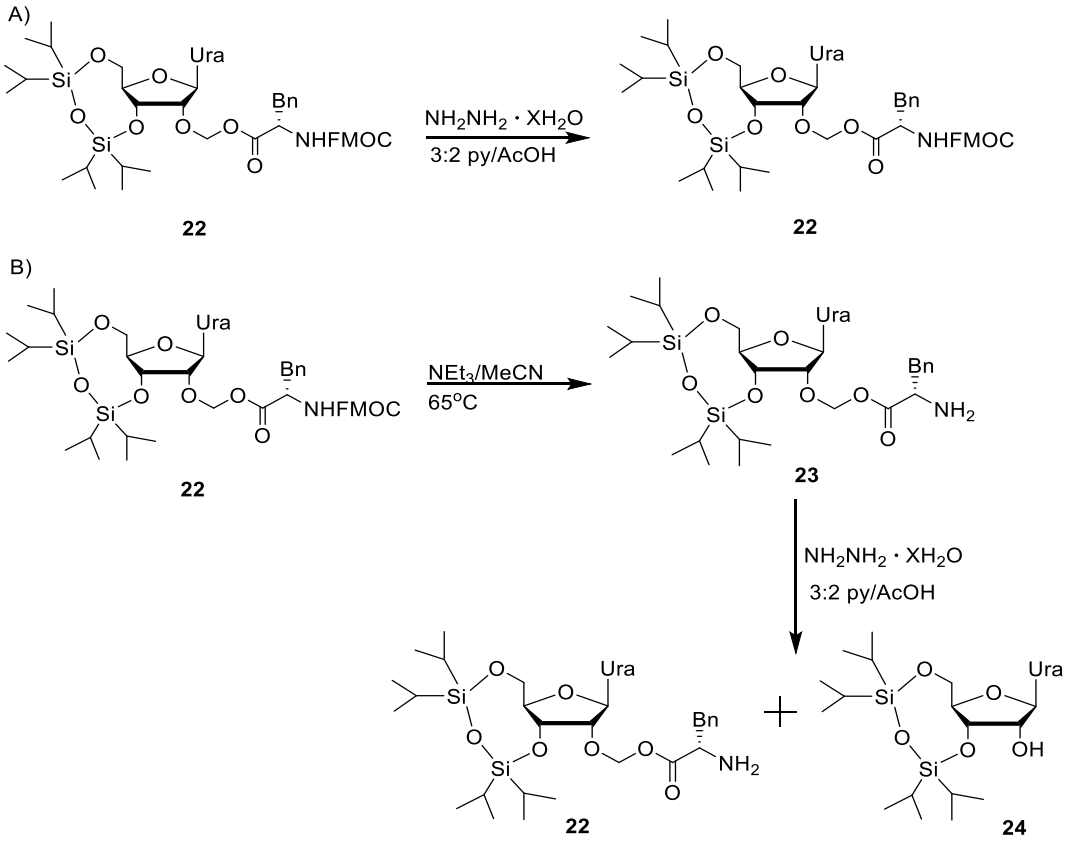

Scheme 5.9. The 2'-*O*-Phe AAE remains intact with hydrazine hydrate treatment if the FMOC protecting group is intact.

An alternative manner by which *N*-FMOC and *N*-PAC groups can be removed is by applying a solution of DIPEA in methanol (MeOH) to **22** (Scheme 5.10). This method was tested to see if it could remove FMOC groups without 2'-*O*-Phe AAE cleavage. While the benzofulvene elimination product was detected as expected, immediate cleavage of the acetal ester also occurred (TLC and ESI-MS analyses). We concluded from this data that a solution of DIPEA in MeOH is not suitable for deprotection of FMOC or PAC groups of proRNA. This is also in agreement with section 2.6, in that a protic solvent (MeOH) is likely accelerating the cleavage of the acetal ester.

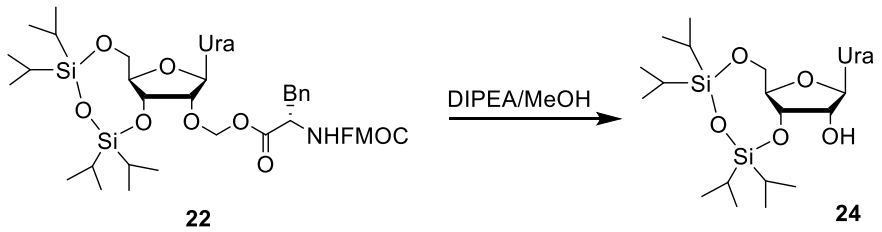

Scheme 5.10. The removal of the *N*-FMOC protection of the 2'-*O*-Phe AAE with base in methanol also causes cleavage of the acetal ester.

With these parameters in mind, the cytidine phosphoramidite **25** was synthesized with *N*-Lev protection (Scheme 5.11A) in two steps from commercial phosphoramidite, as well as a guanosine *N*-dmf phosphoramidite **26** shown in Scheme 5.11B by Undergraduate summer student Erika Steels. These phosphoramidites can be used with adenosine phosphoramidite **9a** to synthesize proRNA, as well as commercially available *N*-PAC phosphoramidites, provided that alcoholic solvent is not used to remove PAC/FMOC groups.

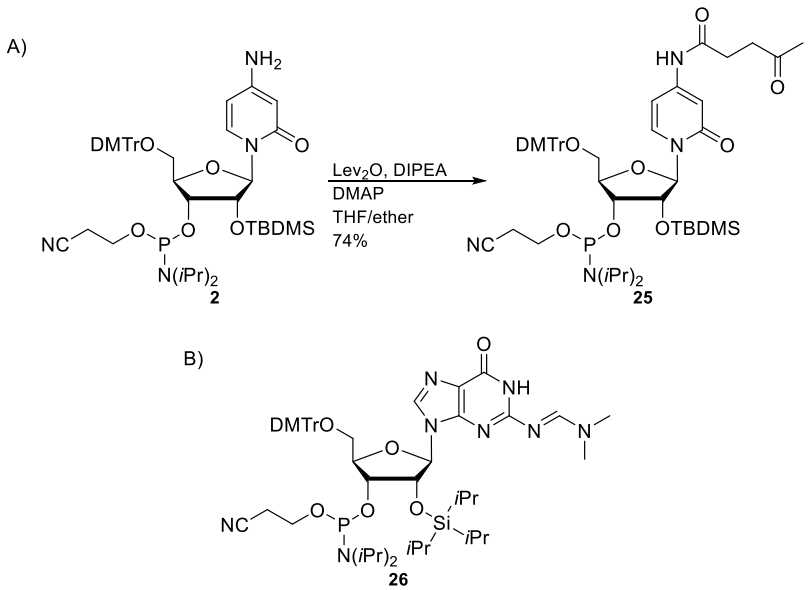

Scheme 5.11. The synthesis of A) cytidine phosphoramidite with *N*-Lev protection proceeded in two steps, and B) guanosine phosphoramidite was provided by Erika Steels.

5.6. Conclusion

RNA composed of all four bases was synthesized using *N*-FMOC-nucleobase and 2'-TBDMS protected 3'-*O*-phosphoramidites. Nucleobase and phosphate protections were removed with mild NEt_3 treatment so as to keep a potential 2'-*O*-Phe AAE insertion intact, after which desilylation and anhydrous photocleavage of the solid support linker were performed. Full-length RNA was synthesized with acetyl nucleobase adducts as a result FMOC groups exchanging with acetate of the standard acetic anhydride capping reagent. Mild capping reagent for PAC protecting groups, phenoxyacetic anhydride, was utilized to prevent exchange with acetate. Morpholine was added to the mild NEt_3/MeCN deprotection solution in order to react with the benzofulvene elimination product of FMOC cleavage, and highly pure RNA was produced. This synthesis and deprotection protocol is also amenable to nucleobase protection with PAC groups. *N*-levulinyl and *N*-dimethylformamidine nucleobase protection can also be cleaved with hydrazine hydrate while leaving the 2'-*O*-Phe AAE intact, provided that the *N*-FMOC protection on the AAE has not yet been removed. These developments signify important steps in the synthesis of proRNA containing biolabile 2'-*O*-Phe AAE moieties. Furthermore, these results have encouraged us to begin to pursue the synthesis of proRNA of mixed base composition, and study cellular uptake and potency advantages from these novel chemistries.

5.7. Experimental Methods

5.7.1. General Procedures for Monomer Characterization and Synthesis

^{1}H-NMR and ^{13}C-NMR spectra were recorded at 400 MHz and 300 MHz, respectively, using the residual solvent peak as an internal standard ($(CD_3)_2SO$, CD_3CN, $(CD_3)_2CO$). ^{1}H-NMR spectra were assigned using 2D ^{1}H-NMR (COSY) spectra. ^{31}P-NMR spectra were recorded at 200 MHz using 85% H_3PO_4 as an external standard. Reactions were monitored by TLC on alumina plates coated with silica gel and visualized with UV light and charring with H_2SO_4. Preparative chromatography was performed with 40-60 μm, 230-400 mesh silica gel. DMF and DMSO were dried over 3Å molecular sieves for at least 48 hr. CH_2Cl_2, THF, and MeCN were dried on an mBraun SPS solvent purification system. Pyridine, NEt_3, and DIPEA were distilled from CaH_2. Where yields for monomer syntheses have been reported as an average in the previous sections, one example is described below.

5.7.2. Synthesis of Oligonucleotide Monomers

5'-*O*-(4,4'-dimethoxytrityl)-2'-*O*-(*tert*-butyldimethylsilyl)-3'-*O*-[(2-cyanoethyl-*N*,*N*-diisopropyl)phosphoramidite] cytidine (2): Synthesized from phosphoramidite **1**, purchased from ChemGenes Corporation (Wilmington, MA), according to Ohkubo *et al*.[12] Product was isolated and used directly for the next reaction.

***N*^{4}-(9-fluorenylmethoxycarbonyl)-5'-*O*-(4,4'-dimethoxytrityl)-2'-*O*-(*tert*-butyldimethylsilyl)-3'-*O*-[(2-cyanoethyl-*N*,*N*-diisopropyl)phosphoramidite] cytidine (3):** Phosphoramidite **2** (916 mg, 1.1 mmol) was dissolved in THF (12 mL). DIPEA (830 μL, 4.8 mmol) was added, stirred in, and then FMOCCl (551 mg, 2.13 mmol) was added. After 5 hr, the reaction was washed with saturated aqueous $NaHCO_3$ and the aqueous layer was extracted three times with CH_2Cl_2. The organic layer was dried over $MgSO_4$, filtered and dried *in vacuo*. The crude reaction mixture was purified using silica gel chromatography and 0 to 1% MeOH in CH_2Cl_2 with a 1% pyridine additive. Product **3** was purified in 60% yield. ^{31}P-NMR $(CH_3)_2CO$) δ 149.72, 148.48. ESI-QTOF calc. for $C_{60}H_{72}N_5O_{10}PSi$ [M+H$^+$]: 1082.49; found: 1082.07. The product was also characterized by Lackey in $CDCl_3$.[11]

***N*^{6}-(9-fluorenylmethoxycarbonyl) adenosine (5a):** Nucleoside **4a** (373 mg, 1.4 mmol) purchased from ChemGenes Corporation (Wilmington, MA) was dissolved in pyridine (5.6 mL). Trimethylchlorosilane (571 mL, 4.5 mmol) was then added. After 1 hr, FMOCCl (471 mg, 1.8 mmol) was added and stirred for 17 hr. Distilled water (1.1 mL) was then added to the reaction and stirred for 3 hour. The crude material was dried *in vacuo* and the product **5a** was crystallized from toluene in 81% yield. The characterization of **5a** was in agreement with Heikkila and Chattopadhyaya.[16]

***N*^{2}-(9-fluorenylmethoxycarbonyl) guanosine (5b):** Nucleoside **4b** (400 mg, 1.4 mmol) purchased from ChemGenes Corporation (Wilmington, MA) was dissolved in pyridine (5.6 mL). Trimethylchlorosilane (584 mL, 4.6 mmol) was then added. After 1 hr, FMOCCl (430 mg, 1.7 mmol) was added and stirred for 17 hr. Distilled water (1.1 mL) was then added to the reaction and stirred for 3 hour. The crude material was dried *in vacuo* and the product **5b** was crystallized from ethanol in 75% yield. The characterization of **5b** was in agreement with Heikkila and Chattopadhyaya.[16]

***N*^{6}-(9-fluorenylmethoxycarbonyl)-5'-*O*-(4,4'-dimethoxytrityl) adenosine (6a):** Nucleoside **5a** (548 mg, 1.12 mmol) was dissolved in pyridine (11 mL), and $AgNO_3$ (221 mg, 1.3 mmol) and DMTrCl was added (455 mg, 1.3 mmol). After 5 hr the reaction was washed with saturated aqueous $NaHCO_3$ and the aqueous layer was extracted three times with CH_2Cl_2. The organic layer was dried over $MgSO_4$, filtered, and dried to a white solid *in vacuo*. The crude reaction mixture was purified using silica gel and 5 – 10% MeOH in CH_2Cl_2 with a 0.5% pyridine additive. Product **6a** was purified in 90% yield. ^{1}H-NMR ($(CD_3)_2SO$) δ 10.92 (s, 1H), 8.60 (d, *J* = 3.36 Hz, 2H), 7.91 (d, *J* = 7.32 Hz, 2H), 7.86 (d, *J* = 7.63 Hz, 2H), 7.43 (t, *J* = 7.26 Hz, 2H), 7.32 – 7.39 (m, 4H), 7.18 – 7.28 (m, 7H), 6.79 – 6.89 (m, 4H), 6.05 (d, *J* = 4.58 Hz, 1H), 5.63 (d, *J* = 5.49 Hz, 1H), 5.28 (d, *J* = 5.80 Hz, 1H), 4.77 (d, *J* = 5.19 Hz, 1H), 4.42 (d, *J* = 7.32 Hz, 2H), 4.34 (dd, *J* = 11.44, 6.26 Hz, 2H), 4.12 (d, *J* = 4.88 Hz, 1H), 3.72 (d, *J* = 2.44 Hz, 6H), 3.25 (d, *J* = 4.58 Hz, 2H). ^{13}C-NMR ($(CD_3)_2SO$) δ 158.50, 158.48, 152.53, 152.16, 152.07, 150.22, 145.28, 144.13, 143.46, 141.19, 136.03, 135.93, 130.14, 128.23, 128.20, 128.12, 127.59, 127.11, 125.99, 124.26, 120.59, 113.59, 88.69, 85.95, 83.70, 73.43, 70.79, 67.21, 64.13, 55.47, 46.81. ESI-QTOF calc. for $C_{46}H_{41}N_5O_8$ [M+H$^+$]: 792.30; found: 792.56.

***N*^{2}-(9-fluorenylmethoxycarbonyl)-5'-*O*-(4,4'-dimethoxytrityl) guanosine (6b):** The procedure was the same as that used for **6a**. **5b** (0.53 g, 1.0 mmol), pyridine (10 mL), $AgNO_3$ (204 mg, 1.2 mmol), DMTrCl (0.4 g, 1.2 mmol). The crude reaction mixture was purified using silica gel and 5 – 10% MeOH in CH_2Cl_2 with a 0.5% pyridine additive. Product **6b** was purified in 89% yield. ^{1}H-NMR ($(CD_3)_2SO$) δ 11.65 (br s, 1H), 11.35 (br s, 1H), 8.11 (s, 1H), 7.93 (d, *J* = 7.63 Hz, 2H), 7.83 (d, *J* = 7.28 Hz, 2H), 7.45 (t, *J* = 7.22 Hz, 2H), 7.32 – 7.39 (m, 4H), 7.18 – 7.29 (m, 7H), 6.75 – 6.90 (m, 4H), 5.86 (d, *J* = 4.58 Hz, 1H), 5.50 – 5.70 (m, 1H), 5.18 (br d, *J* = 5.19, 1H), 4.53 – 4.71 (m, 1H), 4.49 (d, *J* = 7.32 Hz, 2H), 4.35 (t, *J* = 7.32 Hz, 1H), 4.23 (br d, *J* = 4.58 Hz, 1H), 3.97 – 4.12 (m, 1H), 3.70 – 3.75 (m, 6H), 3.23 – 3.31 (m, 1H), 3.18 (dd, *J* = 10.38, 2.75 Hz, 1H). ^{13}C-NMR ($(CD_3)_2SO$) δ 158.49, 158.47, 145.28, 143.75, 141.23, 135.99, 135.95, 130.20, 130.16, 128.32, 128.21, 128.18, 127.64, 127.10, 125.94, 120.67, 120.51, 113.56, 113.53, 87.89, 85.97, 83.79, 73.85, 70.86, 64.55, 55.46, 46.59. ESI-QTOF calc. for $C_{46}H_{41}N_5O_9$ [M+H$^+$]: 808.30; found: 808.09.

***N*^{6}-(9-fluorenylmethoxycarbonyl)-5'-*O*-(4,4'-dimethoxytrityl)-2'-*O*-(*tert*-butyldimethylsilyl) adenosine (7a):** Nucleoside **6a** (468 mg, 0.5 mmol) was dissolved in DMF

(5 mL). TBDMSCl (107 mg, 0.71 mmol) and imidazole (48 mg, 0.71 mmol) were then added. After 5.5 hr, the reaction was washed with saturated aqueous $NaHCO_3$, extracted three times with CH_2Cl_2, dried over $MgSO_4$, filtered and dried *in vacuo* to a yellow oil. Crude mixture was purified on silica gel with a gradient of 8:2:0.1 to 6:4:0.1 petroleum ether:acetone:pyridine to give **7a** in 36% yield. ^{1}H-NMR (CD_3CN) δ 8.55 (s, 1H), 8.26 – 8.28 (m, 1H), 7.79 – 7.86 (m, 2H), 7.71 (m, 2H), 7.36 – 7.47 (m, 4H), 7.19 – 7.36 (m, 9H), 6.83 (dt, *J* = 4.30, 2.15 Hz, 4H), 6.02 (d, *J* = 4.69 Hz, 1H), 4.94 – 4.97 (m, 1H), 4.52 – 4.56 (m, 2H), 4.39 (m, 1H), 4.20 (d, *J* = 3.91 Hz, 1H), 3.73 – 3.76 (m, 6H), 3.38 (t, *J* = 4.49 Hz, 2H), 3.13 – 3.27 (m, 1H), 0.88 (s, 1H), 0.81 – 0.83 (m, 8H), -0.12 (s, 3H), -0.01 (s, 3H). ESI-QTOF calc, for $C_{52}H_{55}N_5O_8Si$ [M+Na]: 928.37; found: 928.14. Product was also characterized by Lackey in $CDCl_3$.[11]

***N*^{6}-(9-fluorenylmethoxycarbonyl)-5'-*O*-(4,4'-dimethoxytrityl)-2'-*O*-(*tert*-butyldimethylsilyl) adenosine/ *N*^{6}-(9-fluorenylmethoxycarbonyl)-5'-*O*-(4,4'-dimethoxytrityl)-3'-*O*-(*tert*-butyldimethylsilyl)-2'-*O*-(*tert*-butyldimethylsilyl) adenosine (7a/8a):** Nucleoside **6a** (4.0 g, 5.1 mmol) was dissolved in dry pyridine (25 mL). TBDMSCl (1.5 g, 10.1 mmol) and then $AgNO_3$ (1.7 g, 5.1 mmol) were added. After 3 hr, the reaction was washed with saturated aqueous $NaHCO_3$, extracted three times with CH_2Cl_2, dried over $MgSO_4$, filtered and dried *in vacuo*. The crude mixture was purified on silica gel with a gradient of 12 – 100% EtOAc in hexanes to yield **7a** and **8a** in 43% yield for each. ESI-QTOF calc, for $C_{52}H_{55}N_5O_8Si$ [M+Na]: 928.37; found: 928.14.

***N*^{2}-(9-fluorenylmethoxycarbonyl)-5'-*O*-(4,4'-dimethoxytrityl)-2'-*O*-(*tert*-butyldimethylsilyl) guanosine (7b):** Three procedures were used to synthesize **7b**. Procedure #1 was the same as that used for **7a**. **6b** (5.0 g, 6.2 mmol), DMF (30 mL), TBDMSCl (1.1g, 7.4 mmol), imidazole (504 mg, 7.2 mmol). Crude product was purified with silica gel and 3 – 30% acetone in CH_2Cl_2 with 0.5% pyridine additive to give **7b** in 4% yield. Procedure #2 dissolved nucleoside **6b** in THF (11.5 mL). Pyridine (354 μL, 4.4 mmol) and $AgNO_3$ (303 mg, 1.8 mmol) were added TBDMSCl (269 mg, 1.8 mmol) was then added. The reaction was run for 7 hr. **7b** was purified in 13% yield with silica gel and a gradient of 8:2:0.1 to 6:4:1 petroleum ether: acetone: pyridine. Procedure #3 was the same as that used for **7a/b**. **6b** (4 g, 5 mmol), pyridine (7.5 mL), $AgNO_3$ (883 mg, 5.2 mmol), TBDMSCl (784 mg, 5.2 mmol). After 3 hr product **7b** was purified with silica gel and a gradient of 0 – 1% MeOH in CH_2Cl_2 with 1% pyridine additive

in 22% yield. ^{1}H-NMR (CD_3CN) δ 7.97 (s, 1H), 7.88 – 7.97 (m, 1H), 7.69 – 7.86 (m, 1H), 7.56 – 7.69 (m, 1H), 7.10 – 7.51 (m, 14H), 6.69 – 6.93 (m, 4H), 5.82 – 6.02 (m, 1H), 4.81 – 4.93 (m, 1H), 4.54 – 4.67 (m, 2H), 4.39 – 4.53 (m, 2H), 4.21 – 4.31 (m, 2H), 3.65 – 3.76 (m, 7H), 3.50 – 3.61 (m, 1H), 3.36 – 3.45 (m, 1H), 0.79 – 1.03 (m, 9H), -0.04 – 0.19 (m, 6H). ESI-QTOF calc. for $C_{52}H_{55}N_5O_9Si$ [M+H$^+$]: 922.38; found: 922.01. The product was also characterized by Lackey in $CDCl_3$.[11]

***N*^{2}-(9-fluorenylmethoxycarbonyl)-5'-*O*-(4,4'-dimethoxytrityl)-3'-*O*-(*tert*-butyldimethylsilyl) guanosine (8b):** Procedure #2 that was used to synthesize and purify **7b** yielded 9% of **8b**. Procedure #3 that was used to synthesize and purify **7b** yielded 5% of **8b**. ^{1}H-NMR (CD_3CN) δ 7.75 – 7.88 (m, 3H), 7.66 – 7.75 (m, 2H), 7.28 – 7.47 (m, 9H), 7.15 – 7.24 (m, 4H), 6.64 – 6.82 (m, 4H), 5.81 – 5.86 (m, 1H), 4.87 – 4.90 (m, 1H), 4.48 – 4.57 (m, 4H), 4.29 – 4.36 (m, 1H), 3.61 – 3.75 (m, 7H), 3.48 – 3.56 (m, 1H), 3.09 – 3.17 (m ,1H), 0.78 – 0.99 (m, 9H), 0.05 – 0.14 (m, 3H), -0.08 – 0.03 (m, 3H). ^{13}C-NMR ($(CD_3)_2CO$) δ 158.99, 158.95, 158.66, 155.15, 154.74, 154.71, 149.68, 149.27, 147.61, 145.37, 144.70, 143.52, 141.26, 135.80, 135.76, 135.70, 135.54, 130.26, 130.10, 129.94, 128.86, 128.12, 127.89, 127.75, 127.69, 127.20, 126.82, 126.75, 125.34, 120.04, 113.20, 112.95, 112.81, 112.76, 87.26, 86.61, 86.49, 84.29, 68.05, 68.00, 54.69, 54.63, 46.58, 28.21, 25.47. ESI-QTOF calc. for $C_{52}H_{55}N_5O_9Si$ [M+H$^+$]: 922.38; found: 922.41.

***N*^{6}-(9-fluorenylmethoxycarbonyl)-5'-*O*-(4,4'-dimethoxytrityl)-2'-*O*-(*tert*-butyldimethylsilyl)-3'-*O*-[(2-cyanoethyl-*N*,*N*-diisopropyl)phosphoramidite] adenosine (9a):** Nucleoside **8a** (830 mg, 0.92 mmol) was dissolved in THF (4 mL) and DIPEA (718 μL, 4.12 mmol) and phosphitylating reagent (460 μL, 2.1 mmol) were added. After 6 hr the reaction was washed with saturated aqueous $NaHCO_3$, extracted with CH_2Cl_2, dried over $MgSO_4$, filtered, and dried *in vacuo*. The product **9a** was purified with 10 – 80% EtOAc in hexanes with 0.5% pyridine additive in 79% yield. ^{31}P-NMR ($(CD_3)_2CO$) δ 150.34 (less-retained product), 148.56 (more-retained product). ESI-QTOF calc. for $C_{61}H_{72}N_7O_9PSi$ [M+H$^+$]: 1106.50; found: 1106.91. The product was also characterized by Lackey in $CDCl_3$.[11]

***N*^{2}-(9-fluorenylmethoxycarbonyl)-5'-*O*-(4,4'-dimethoxytrityl)-2'-*O*-(*tert*-butyldimethylsilyl)-3'-*O*-[(2-cyanoethyl-*N*,*N*-diisopropyl)phosphoramidite] guanosine (9b):** The same procedure was used as for **9a**. **8b** (430 mg, 0.47 mmol), THF (2 mL), DIPEA (366 μL,

2.1 mmol), phosphitylating reagent (208 μL, 0.9 mmol). After 19 hr, product **9a** was purified with 12 – 80% EtOAc in hexanes with 0.5% pyridine additive in 55% yield. ^{31}P-NMR ($(CD_3)_2SO$) δ 149.75, 148.56. ESI-QTOF calc. for $C_{61}H_{72}N_7O_{10}PSi$ [M+H$^+$]: 1122.49; found: 1122.02. The product was also characterized by Lackey in $CDCl_3$.[11]

5'-*O*-(4,4'-dimethoxytrityl) uridine (11): The procedure was the same as that used for **6a**. **10** (1.0 g, 4.1 mmol), pyridine (30 mL), $AgNO_3$ (800 mg, 4.7 mmol), DMTrCl (1.6 g, 4.7 mmol). Product **11** was purified with silica gel and a gradient of 1 – 10% MeOH in CH2Cl2 with 0.5% pyridine additive in 65% yield. Product characterization was in agreement with Hakimelahi *et al*.[15]

5'-*O*-(4,4'-dimethoxytrityl)-2'-*O*-(*tert*-butyldimethylsilyl) uridine (12): Procedure was the same as for **7a/8a**. **11** (200 mg, 0.37 mmol), pyridine (1.5 mL), $AgNO_3$ (75 mg, 0.44 mmol), TBDMSCl (66 mg, 0.44 mmol). Product **12** was purified in 47% yield with silica gel with a gradient of 10 – 80% EtOAc in hexanes with 0.5% pyridine additive. Product characterization was in agreement with Hakimelahi *et al*.[15]

5'-*O*-(4,4'-dimethoxytrityl)-2'-O-(*tert*-butyldimethylsilyl)-3'-*O*-[(*N*,*N*,*N*,*N*-tetraisopropyl)phosphoramidite] uridine (13): Nucleoside **12** (661 mg, 0.24 mmol) was dissolved in CH_2Cl_2 (2 mL). DIPEA was added (211 μL, 1.2 mmol) and then *N*,*N*,*N*,*N*-tetraisopropyl chlorophosphite (74 mg, 0.28 mmol). The crude reaction was dried *in vacuo* after 5 hr, coevapped five times with MeCN, and used directly in the coupling with nucleoside **15** after crude ESI-QTOF calc. for $C_{48}H_{71}N_4O_8PSi$ [M+H$^+$]: 891.49; found: 891.26.

5'-*O*-(4,4'-dimethoxytrityl)-3',2'-*O*-bis(*tert*-butyldimethylsilyl) uridine (14): The procedure was the same as that used for **7a/8a**. **11** (120 mg, 0.22 mmol), pyridine (1.4 mL), $AgNO_3$ (93 mg, 0.55 mmol), TBDMSCl (83 mg, 0.55 mmol). The crude material was used for the synthesis of **15**.

3',2'-*O*-bis(*tert*-butyldimethylsilyl) uridine (15): A 3% trichloroacetic acid (TCA) solution in CH_2Cl_2 was made by dissolving TCA (402 mg, 2.46 mmol) in CH_2Cl_2 (10 mL). The TCA solution was added to nucleoside **14**. After 20 min the reaction was quenched with MeOH (10 mL). Product **15** was purified with silica gel and 17 – 85% EtOAc in hexanes in 58% yield. Characterization of the product was in agreement with Ogilvie *et al*.[18]

5'-*O*-(4,4'-dimethoxytrityl)uridin-3'-yl 3'',2''-*O*-bis(*tert*-butyldimethylsilyl)uridin-5''-yl *N*,*N*-diisopropylphosphoramidite (16) and the solid support derivatized with it: Phosphoramidite **13** (43 mg, 0.05 mmol) was dissolved in MeCN (1 mL) in a flamed fritted glass column with stopper and screw-cap. Nucleoside **15** (22 mg, 0.05 mmol) was added and 0.25 M ETT (5 mL). After 7 hr shaking, solid support **21** was added to the column and shaken for 18 hr in the dark. The support was then washed with CH_2Cl_2 three times and MeCN three times, transferred to a glass vial, and dried *in vacuo*.

5'-*O*-(4,4'-dimethoxytrityl)-3'-*O*-[(*N*,*N*,*N*,*N*-tetraisopropyl)phosphoramidite] thymidine (18): The procedure was the same as that used for **13**. **11** (611mg, 1.1 mmol), CH_2Cl_2:DMF (1:0.1 mL), DIPEA (215 μL, 1.2 mmol), *N*,*N*,*N*,*N*-tetraisopropyl chlorophosphite (329 mg, 1.2 mmol). The crude reaction was also dried *in vacuo* after 5 hr, coevapped five times with MeCN, and used directly in the coupling with nucleoside **19**.

3'-*O*-(*tert*-butyldimethylsilyl) thymidine (19): Procedure was the same as that used for **6a** and then **15**. **17** (2.0 g, 3.7 mmol), pyridine (20 mL), $AgNO_3$ (686 mg, 4.0 mmol), TBDMSCl (664 mg, 4.4 mmol). The crude material was purified in 84% yield using silica gel and a 17 – 100% EtOAc in hexanes gradient with 0.5% pyridine additive. Product of silylation (2 g, 3.1 mmol), TCA in CH_2Cl_2 (600 mg, 1.2 mmol in 12.2 mL), MeOH (10 mL). The crude material was purified in 76% yield using silica gel and a gradient of 17 – 85% EtOAc in hexanes. The characterization of product **19** was in agreement with the Ogilvie and Iwacha.[19]

5'-*O*-(4,4'-dimethoxytrityl)thymidin-3'-yl 3''-*O*-(*tert*-butyldimethylsilyl)thymidin-5''-yl *N*,*N*-diisopropylphosphoramidite (20) and the solid support derivatized with it: Phosphoramidite **18** (869 mg, 1.1 mmol) was dissolved in CH_2Cl_2 (4.2 mL) in a round bottom flask, then 0.25 M ETT (4.5 mL, 1.1 mmol) was added, and then nucleoside **19** (1.15 g, 1.1 mmol). After 1 hr stirring, the dimer was loaded directly onto silica gel run with 17 – 85% EtOAc in hexanes with 0.5% pyridine additive. A white foam was recovered, and another silica gel column was run with 17 – 100 % EtOAc in hexanes with 0.5% pyridine additive to give **20** in a white foam in 52% yield. ^{31}P-NMR ($(CD_3)_2CO$) δ 148.30, 148.39. Phosphoramidite **20** (97 mg, 0.09 mmol) was dissolved in MeCN (680 μL). Support **21** (28 mg) was weighed into an ABI column. With argon flowing through the top of the synthesis column, a 1-mL syringe with activator solution (0.25 M ETT, 300 μL) was secured to the bottom end of the column. The line

delivering argon to the top of the column was removed and the activator was immediately pushed through the column, followed by immediate attachment of another 1-mL syringe containing phosphoramidite **20** (0.15 M, 300 μL) to the top of the column. The pistons of the syringes were pushed back and forth a few times and then the column was shaken for 10 minutes. The syringe containing activator was then pushed all the way through the column and then the rest of the phosphoramidite (0.15 M, 300 μL) was immediately pushed through the other end. The pistons were pushed back and forth a few times and the column was shaken for 15 minutes. Then the support was washed with MeCN and dried with argon on the ABI Synthesizer, oxidized, and then detritylated on the ABI Synthesizer. The support was dried with argon. This derivatization of support **21** was repeated with more of phosphoramidite **20** (50 mg, 0.05 mmol) dissolved in MeCN (320 μL, 0.16 M) and 0.25 M ETT (300 μL) for one more 5-minute round of shaking. The supports were combined and a portion was used for oligonucleotide synthesis.

N^4-levulinyl-5'-*O*-(4,4'-dimethoxytrityl)-2'-*O*-(*tert*-butyldimethylsilyl)-3'-*O*-[(2-cyanoethyl-*N*,*N*-diisopropyl)phosphoramidite] cytidine (25): Levulinic acid (LevOH) was distilled under reduced pressure to a liquid at room temperature. Levulinic anhydride (Lev_2O) was prepared by dissolving LevOH (300 μL, 3.0 mmol) and DCC (619 mg, 3.0 mmol) in ether (30 mL). After 5 hr, the DCU precipitate was anhydrously filtered from the solution under N_2. Nucleoside **2** (736 mg, 0.86 mmol) was dissolved in THF (8.5 mL) and DIPEA (1 mL) and DMAP (11 mg, 0.1 mmol) were added. The Lev_2O/DCC solution (20.6 mL, 1.03 mmol) was added dropwise over 40 min to the stirring nucleotide **2**. After 17 hr the reaction was washed with saturated aqueous $NaHCO_3$. The aqueous layer was extracted three times with ether. The crude white solid was purified with silica gel and an eluent of 2.5% MeOH in CH_2Cl_2.with 0.5% of pyridine additive to give product **25** in 74% yield. ^{31}P-NMR ($(CD_3)_2CO$) δ 149.74. ESI-QTOF calc. for $C_{50}H_{68}N_5O_{10}PSi$ [M+Na]: 980.44; found: 980.56.

5.7.3. Oligonucleotide Preparation

Oligonucleotides were synthesized with an Applied Biosystems DNA/RNA 3400 Synthesizer. Standard phosphoramidites were purchased from ChemGenes Corporation (Wilmington, MA) and dissolved in MeCN to a concentration of 0.15 M. Non-standard phorphoramidites were dissolved in MeCN to a concentration of 0.12 M, while G^{FMOC}

phosphoramidite used in the synthesis of oligonucleotide on support derivatized with dimer **20** was dissolved in MeCN:CH_2Cl_2 (1:1). Coupling times for thymidine and uridine were 600 sec, while the coupling time was 900 sec for A^{FMOC} and C^{FMOC}. G^{FMOC} was coupled for 1200s. Activation of phorphoramidites was achieved with standard 0.25 M ETT in MeCN. Standard capping was performed with a CAP A solution of Ac_2O/py/THF (10:10:80 v/v/v) were indicated and a CAP B solution of 15% *N*-methylimidazole in THF. CAP A was replaced with a solution of PAC_2O/py/THF (5:10:85 v/v/v) where indicated. The oxidation solution used was standard 0.1 M I_2 in py/H_2O/THF (8:16:76 v/v/v). Standard 3% TCA in CH_2Cl_2 was used for detritylation steps.

The oligonucleotide synthesized on Unylinker^{TM} was suspended in fast 40% aq. $MeNH_2$ (1 mL) at 65 ^oC for 10 min to remove the nucleobase and internucleotide protecting groups, and to cleave the support linker. After decanting and lyophilizing the supernatant, fast desilylation was performed in NEt_3-3HF:dimethylsulfoxide (DMSO) (300 μL, 1:1 v/v) at 65^oC for 90 min, after which NaOAc (3 M, pH 5.5, 25 μL) and cold 1-butanol (1 mL) were added to precipitate the oligonucleotide. The washed and dried oligonucleotide was dissolved in water, filtered, and purified by IE-HPLC on a Waters Protein PAK DEAE 5PW 7.5 mm x 7.5 cm column. A gradient of 0 – 40% solvent B in 50 minutes (A: H_2O; B: 1 M $LiClO_4$) was used to purify the strands at a rate of 1 mL/min. The purified strands were dissolved in H_2O, desalted with sephadex G-25, and lyophilized to dryness.

The PS solid support of oligonucleotides grown from dimer **16**, **20**, or support **21** were suspended in anhydrous NEt_3/MeCN (1 mL, 2:3 v/v) or anhydrous NEt_3/MeCN/morpholine (1 mL, 2:3:1 v/v/v) at 65^oC for the time indicated in Table 5.2 to remove cyanoethyl and FMOC groups. The beads were then centrifuged at 12,000 rpm for 5 minutes, decanted, and washed twice with anhydrous DMSO. Then fast desilylation was performed on the beads with NEt_3-3HF/DMSO (150 μL: 80 μL). The beads were washed three times with DMSO and dried *in vacuo*. The beads were transferred to a quartz tube and suspended in MeCN (1 mL) with DIPEA (10 μL). A Luzchem LZC-4 photoreactor was used to photocleave the oligonucleotides from the solid support beads. The beads were irradiated with fourteen 12" Luzchem LZC-UVA (UV-A, Hitachi FL8BL-B) lamps at λ_{max} = 350 nm for 21 minutes. The beads were transferred back to a polypropylene tube and oligonucleotides made from **16** and **21** were extracted three times from

the support by resuspending the beads in autoclaved H_2O, centrifuging at 12,000 rpm, and decanting three times. Support derivatized with dimer **20** was dried *in vacuo* without decanting. The beads were instead resuspended in anhydrous DMSO, centrifuged at 12,000 rpm, and an aliquot was taken for mass spectometry. The beads were dried *in vacuo* after aliquots were taken. The beads were resuspended in H_2O and purified by IE-HPLC with a gradient of 0 – 40% solvent B in 50 minutes (A: H_2O; B: 1 M $LiClO_4$) on a Waters Protein PAK DEAE 5PW 7.5 mm x 7.5 cm column at a rate of 1 mL/minute.

5.7.4. Nucleoside Deprotection Conditions

A 0.5 M $NH_2NH_2 \bullet XH_2O$ solution was made by adding 50-60% $NH_2NH_2 \bullet XH_2O$ (1.0 mL) to a solution of pyridine/acetic acid (20.4 mL:13.6 mL, 3:2). A portion of the solution (1.73 mL) was added to either nucleoside **22** or **23**. TLC of the reaction on **22** was done using 5% MeOH in CH_2Cl_2 and revealed no change in retention of the product (R_f = 0.56) and no other products. MS(ESI) calc. [M+Na]: 908.36; found: 908.40. TLC of the reaction on **23** was done using 5% MeOH in CH_2Cl_2 and revealed many heavy spots, including product **24** (R_f = 0.23, MS(APCI) calc. [M]: 486.22; found: 486.94) and starting material **23** (R_f = 0.1, MS(ESI) calc [$M+H^+$]: 664.31; found: 664.22).

FMOC elimination of **22** (9.0 mg, 0.01 mmol) was done by dissolving the nucleoside in MeCN (1.04 mL) and adding NEt_3 (0.691 mL). The solution was stirred at 70°C for 2.75 hr, then it was further diluted with CH_2Cl_2 and washed with 5% aqueous HCl. The aqueous layer was extracted twice with CH_2Cl_2. The combined organic layers were dried over $MgSO_4$, filtered, and dried *in vacuo* to 9.9 mg of a yellow oil. TLC of the crude material was done using 3:2 EtOAc:hexanes eluent (**22** R_f = 0.8, **23** R_f = 0.1, benzofulvene R_f = 0.93). ESI-QTOF calc. of **23** [$M+H^+$]: 664.31; found: 664.27.

3',5'-(1,1,3,3-tetraisopropyldisiloxane-1,3-diyl)-2'-*O*-(acetal-L-phenylalanine ester) uridine (23): Nucleoside **22** (38.2 mg, 0.043 mmol) was dissolved in MeCN (4.41 mL) and then NEt_3 (2.93 mL) was added. The reaction was stirred at 60°C for 1 hour and then diluted with CH_2Cl_2. The solution was washed with 5% aqueous HCl and the organic layer was dried over $MgSO_4$, filtered, and dried *in vacuo*. A Pasteur pipette plugged with cotton was filled with 4 cm

of silica gel and the reaction mixture was separated with 3:2 hexanes:EtOAc → 100% EtOAc. APCI-QTOF calc. for $C_{31}H_{49}N_3O_9Si_2$ [$M+H^+$]: 664.31; found: 664.29.

3',5'-(1,1,3,3-tetraisopropyldisiloxane-1,3-diyl) uridine (24): The compound was synthesized from uridine nucleoside and characterized according to Yamashita *et al*.[20]

5.8. References

1. Tosquellas, G.; Alvarez, K.; Dell'Aquila, C.; Morvan, F.; Vasseur, J.-J.; Imbach, J.-L.; Rayner, B., The pro-oligonucleotide approach: Solid phase synthesis and preliminary evaluation of model pro-dodecathymidylates. *Nucleic Acids Res.* **1998,** *26* (9), 2069-2074.

2. Meade, B. R.; Gogoi, K.; Hamil, A. S.; Palm-Apergi, C.; Berg, A. v. d.; Hagopian, J. C.; Springer, A. D.; Eguchi, A.; Kacsinta, A. D.; Dowdy, C. F.; Presente, A.; Lonn, P.; Kaulich, M.; Yoshioka, N.; Gros, E.; Cui, X.-S.; Dowdy, S. F., Efficient delivery of RNAi prodrugs containing reversible charge-neutralizing phosphotriester backbone modifications. *Nat. Biotechnol.* **2014,** *32* (12), 1256-1261.

3. Pon, R. T.; Yu, S., Hydroquinone-O,O'-diacetic acid ('Q-linker') as a replacement for succinyl and oxalyl linker arms in solid phase oligonucleotide synthesis. *Nucleic Acids Res.* **1997,** *25* (18), 3629-3635.

4. Ochi, Y.; Imai, M.; Nakagawa, O.; Hayashi, J.; Wada, S.; Urata, H., Gene silencing by 2'-O-methyldithiomethyl-modified siRNA, a prodrug-type siRNA responsive to reducing environment. *Bioorg. Med. Chem. Lett.* **2016,** *26* (3), 845-848.

5. Lavergne, T.; Baraguey, C.; Dupouy, C.; Parey, N.; Wuensche, W.; Sczakiel, G.; Vasseur, J.-J.; Debart, F., Synthesis and Preliminary Evaluation of pro-RNA 2′-O-Masked with Biolabile Pivaloyloxymethyl Groups in an RNA Interference Assay. *J. Org. Chem.* **2011,** *76* (14), 5719-5731.

6. Biscans, A.; Bos, M.; Martin, A. R.; Ader, N.; Sczakiel, G.; Vasseur, J. J.; Dupouy, C.; Debart, F., Direct synthesis of partially modified 2'-O-pivaloyloxymethyl RNAs by a base-labile protecting group strategy and their potential for prodrug-based gene-silencing applications. *Chembiochem* **2014,** *15* (18), 2674-2679.

7. Gryaznov, S. M.; Letsinger, R. L., A new approach to synthesis of Oligonucleotides with 3′ phosphoryl groups. *Tetrahedron Lett.* **1992,** *33* (29), 4127-4128.

8. Biscans, A.; Rouanet, S.; Bertrand, J.-R.; Vasseur, J.-J.; Dupouy, C.; Debart, F., Synthesis, binding, nuclease resistance and cellular uptake properties of 2′-O-acetalester-modified oligonucleotides containing cationic groups. *Bioorg. Med. Chem.* **2015,** *23* (17), 5360-5368.

9. Parey, N.; Baraguey, C.; Vasseur, J.-J.; Debart, F., First Evaluation of Acyloxymethyl or Acylthiomethyl Groups as Biolabile 2‘-O-Protections of RNA. *Org. Lett.* **2006,** *8* (17), 3869-3872.

10. Johnsson, R.; Lackey, J. G.; Bogojeski, J. J.; Damha, M. J., New light labile linker for solid phase synthesis of 2'-O-acetalester oligonucleotides and applications to siRNA prodrug development. *Bioorg. Med. Chem. Lett.* **2011,** *21* (12), 3721-3725.

11. Lackey, J. G. New methods for the synthesis of RNA, novel RNA pro-drugs and RNA microarrays. McGill University, Montreal, QC, 2010.

12. Ohkubo, A.; Kuwayama, Y.; Kudo, T.; Tsunoda, H.; Seio, K.; Sekine, M., O-Selective Condensation Using P−N Bond Cleavage in RNA Synthesis without Base Protection. *Org. Lett.* **2008,** *10* (13), 2793-2796.

13. Ti, G. S.; Gaffney, B. L.; Jones, R. A., Transient protection: efficient one-flask syntheses of protected deoxynucleosides. *J. Am. Chem. Soc.* **1982,** *104* (5), 1316-1319.

14. Zhu, X.-F.; Williams, H. J.; Ian Scott, A., An Improved Transient Method for the Synthesis of N-Benzoylated Nucleosides. *Synth. Commun.* **2003,** *33* (7), 1233-1243.

15. Hakimelahi, G. H.; Proba, Z. A.; Ogilvie, K. K., New catalysts and procedures for the dimethoxytritylation and selective silylation of ribonucleosides. *Can. J. Chem.* **1982,** *60* (9), 1106-1113.

16. Heikkila, J. C., J., The 9-Fluorenylmethoxycarbonyl (Fmoc) Group for the Protection of Amino Functions of Cytidine, Adenosine, Guanosine and Their 2'-Deoxysugar Derivatives. *Acta Chem. Scand.* **1983,** *B37*, 263-265.

17. Lackey, J. G.; Mitra, D.; Somoza, M. M.; Cerrina, F.; Damha, M. J., Acetal levulinyl ester (ALE) groups for 2'-hydroxyl protection of ribonucleosides in the synthesis of oligoribonucleotides on glass and microarrays. *J. Am. Chem. Soc.* **2009,** *131* (24), 8496-8502.

18. Ogilvie, K. K.; Beaucage, S. L.; Schifman, A. L.; Theriault, N. Y.; Sadana, K. L., The synthesis of oligoribonucleotides. II. The use of silyl protecting groups in nucleoside and nucleotide chemistry. VII. *Can. J. Chem.* **1978,** *56* (21), 2768-2780.

19. Ogilvie, K. K.; Iwacha, D. J., Use of the tert-butyldimethylsilyl group for protecting the hydroxyl functions of nucleosides. *Tetrahedron Lett.* **1973,** *14* (4), 317-319.

20. Yamashita, J.; Takeda, S.; Matsumoto, H.; Terada, T.; Unemi, N.; Yasumoto, M., Studies on antitumor agents. VI. Syntheses and antitumor activities of acyl derivatives of 2'-deoxy-5-trifluoromethyluridine. *Chem. Pharm. Bull. (Tokyo)* **1987,** *35* (5), 2090-2094.

Chapter 6: Contributions to Knowledge

6.1. Summary of Contributions to Knowledge and Future Work

6.1.1. A Potential Sugar Promoiety for siRNA

With the long-term goal of synthesizing potent siRNA prodrugs that are able to penetrate cellular membranes, 2'-*O*- acetal ester (2'-*O*-AAE) moieties based on L-alanine, L-phenylalanine, L-lysine, and L-proline were synthesized for the first time. The positively charged amino groups of the 2'-*O*-AAEs were designed to neutralize the phosphate groups and to interact more favorably with the negatively charged cellular membrane, thus allowing increased cellular penetration. As it is required for pro-drug moieties, the 2'-*O*-AAEs investigated were cleaved in various aqueous buffers, whereas they resisted cleavage during the oxidation of phosphite triester intermediates with either iodine in water/pyridine/tetrahydrofuran, *tert*-butyl hydroperoxide, or camphorsulfonyl oxaziridine. Standard solid-supported synthesis conditions, an orthogonal linker, and a revised aprotic deprotection scheme were then used to synthesize a poly-thymidine oligonucleotide containing fully intact 2'-*O*-Phe AAE insert and no detectable product of hydrolysis. A comparison of the rate of hydrolysis of 2'-*O*-hydrocinnamic acid acetal ester versus 2'-*O*-phenylalanine (2'-*O*-Phe) AAE suggests that the positive charge of the β-amine is required for hydrolytic cleavage. In order to adjust the half-life of hydrolysis, future work will examine five structural variations of the 2'-*O*-Phe AAE moieties shown in Figure 6.1. These studies will be relevant to siRNA and particularly RNA microarray research, whereby synthesis of RNA strands necessitates fluoride-free deprotection steps.

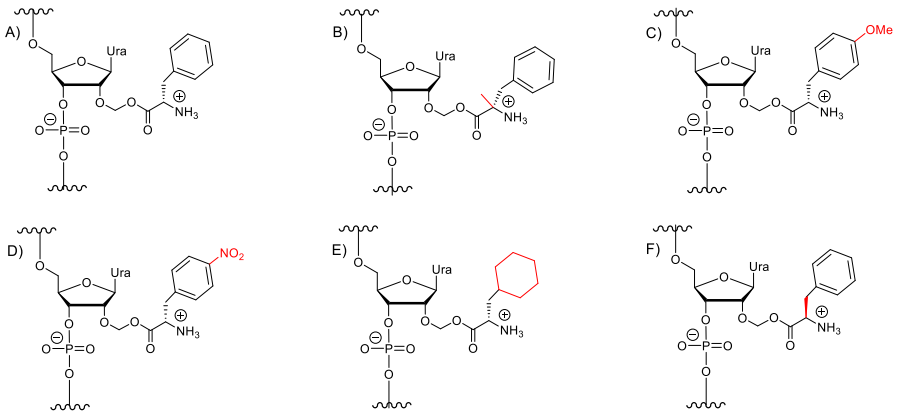

Figure 6.1. Variations on the A) 2'-*O*-phenylalanine acetal ester would test for the effect of B) a more sterically hindered carbonyl carbon; C) an electron-donating aromatic ring substituent; D) an electron-withdrawing aromatic ring substituent; E) an aliphatic ring in the place of the aromatic ring; and F) the D-phenylalanine amino acid on the stability of oligonucleotide conjugates.

6.1.2. Self-Delivering Asymmetric RNA Modified with 2'-*N*-Acyl-L-Phenylalanine

Nucleoside 3'-*O*-phosphoramidites containing stable 2'-*N*-acyl-L-phenylalanine modification were synthesized and employed to prepare fluorophore-labeled siRNA of mixed base composition. Flow cytometric fluorescence resonance energy transfer (FCET) provided a convenient method to measure the relative uptake of duplexes. In the presence of very small amounts of Lipofectamine^{TM} 2000, an siRNA duplex containing six 2'-*N*-acyl-L-phenylalanine moieties exhibited significantly better cellular uptake in human glial cells relative to the unmodified siRNA. Remarkably, when this siRNA was further conjugated to a 5'-phosphorothioated rU(2'-*N*-acyl-L-phenylalanine) 'tail' it underwent delivery without any transfection agent, despite the presence of additional negative charges. Future work will utilize FCET for probing the ability of other modifications, including 2'-*O*-Phe AAE, to improve cellular uptake of siRNAs.

6.1.3. Carrier-Free Gene Silencing by 2'-*N*-Acyl-L-Phenylalanine-Modified siRNA

2'-*N*-Acyl-L-phenylalanine modified siRNAs were effective at downregulating the *drr* and B-cell lymphoma 2 (*bcl-2*) genes. While up to six inserts of the positively charged

modification conferred a somewhat weak degree of *drr* silencing in human glial cells, siRNAs containing up to four modifications away from the Argonaute 2 cleavage site were as potent as canonical siRNA. Thus, internal 2'-*N*-acyl-L-phenylalanine modification does not necessarily attenuate potency. Without the use of a transfection agent, a self-delivering 'tailed' siRNA containing thirteen 2'-*N*-acyl-L-phenylalanine modifications was more potent in downregulating *drr* relative to the corresponding unmodified tailed RNA. While the modified tailed duplex was less potent than canonical siRNA when Lipofectamine^{TM} 2000 transfection was used, the ability to reduce the malignancy of glioblastomas *via* RNAi without the need of a delivery carrier is an exciting development. In the future, a tailed duplex modified in a new pattern will be synthesized and assayed for silencing *drr*. The sense strand will be synthesized containing thirteen 2'-*N*-acyl-L-phenylalanine modifications in order to achieve unassisted cellular uptake, but the 'tail' will be attached to the 3'-terminal instead of the 5'-terminal (Figure 6.2). This will leave a 2-nt 3' antisense overhang structure that may increase potency due to an increased preference for antisense strand loading into RISC. The duplex also contains a 'fork' at the 3'-end of the sense strand with two nucleotide mismatches, rather than a 3'-sense strand 2-nt overhang.

5'-GGA AC**C** AGC **UC**A **UC**A AG**U**$_s$ **U**$_s$**U**$_s$**U**$_s$ **U**$_s$**U**$_s$**U**$_s$ **U**-3'
3'-UU CCU UGG UCG AGU AGU UCU U-5'-p

Figure 6.2. A proposed duplex design for a potent, self-delivering siRNA. Legend: **U** = 2'-*N*-acyl-L-phenylalanine uridine; **C** = 2'-*N*-acyl-L-phenylalanine cytidine; p = phosphate; $_s$ = phosphorothioate. Sequence: sense strand on top; antisense strand on

6.1.4. Towards Methods for the Synthesis of ProRNA

Mixed-base RNA was synthesized with standard reagents on a photocleavable linker using phosphoramidites synthesized with *N*-FMOC nucleobase protection. The desired RNA sequence was deprotected with only aprotic solvent, a condition that was determined necessary during the investigation of the 2'-*O*-Phe AAE modification. The deprotection sequence was as follows: 1) triethylamine/acetonitrile/morpholine (2:3:1 v/v/v) at 65^{o}C for 2 hours; 2) triethylamine trihydrofluoride/dimethylsulfoxide (2:1 v/v) at 65^{o}C for 3.5 hours; and 3) methylamine/diisopropylamine (99:1 v/v), λ_{max} = 350 nm for 21 minutes. The ability to wash away fluoride salts from the support and the ability to avoid standard desalting of the crude oligonucleotide in butanol is also important to recover intact 2'-*O*-Phe AAE. The RNA

synthesized with *N*-FMOC monomers was purified and correctly characterized for the first time by mass spectrometry once mild capping reagent for *N*-phenoxyacetyl (PAC) nucleobase protection was used to eliminate acetylation of nucleobases. We have also found that removal of *N*-levulinyl (lev) and *N*-dimethoxyformamidine (dmf) on the nucleobases *via* hydrazine hydrate in acetic acid/pyridine is a treatment that leaves the 2'-*O*-Phe AAE intact, provided that the *N*-FMOC protection of the 2'-*O*-Phe AAE is still present. Therefore, *N*-lev and *N*-dmf protection may also be compatible with the synthesis of proRNA containing 2'-*O*-Phe AAE.

In the future, *N*-lev- and *N*-dmf-protected residues will be combined with *N*-FMOC-protected residues to produce proRNA. *N*-PAC protection will also be used to synthesize proRNA with intact 2'-*O*-Phe AAE modifications. The 2'-*O*-Phe AAE modifications will be inserted in the positions that were modified with 2'-*N*-acyl-L-phenylalanine in our self-delivering tailed siRNA. The construct will be tested for its ability to be taken up into glial cells without transfection agent and for its ability to cause a reduction in malignancy.

6.2. Manuscripts

Bogojeski, J. J.; Damha, M. J., A method to prepare 2'-O-phenylalanine acetal ester proRNA. *In preparation*.

Bogojeski, J. J.; Yamada, K.; Le, U. P.; Moroz, E.; Leroux J.-C.; Petrecca, K.; Damha, M. J., Carrier-free gene silencing by 2'-N-acyl-L-phenylalanine-modified siRNA. *In preparation*.

Bogojeski, J. J.; Yamada, K.; Le, U. P.; Moroz, E.; Fakhoury, J.; Petrecca, K.; Damha, M. J., Self-delivering asymmetric RNA modified with 2'-N-acyl-L-phenylalanine. *In preparation*.

Johnsson, R. A.; Bogojeski, J. J.; Damha, M. J., An evaluation of selective deprotection conditions for the synthesis of RNA on a light labile solid support. *Bioorg Med Chem Lett* **2014,** *24* (9), 2146-9.

Johnsson, R.; Lackey, J. G.; Bogojeski, J. J.; Damha, M. J., New light labile linker for solid phase synthesis of 2'-O-acetalester oligonucleotides and applications to siRNA prodrug development. *Bioorg Med Chem Lett* **2011,** *21* (12), 3721-5.

6.3. Conference Presentations

Bogojeski, J. J.; Le, P. U.; Yamada, K.; Moroz, E. V.; Leroux, J.-C.; Petrecca, K.; Damha, M. J., *Novel Tailed siRNA Containing 2'-N-acyl-L-phenylalanine Sugars Modifications Self-Delivers to Reduce DRR Expression in Malignant Glioblastomas*. Poster presentation at the 12th meeting of the Oligonucleotide Therapeutics Society, Montreal, Ontario, September 25 – 28, **2016**.

Bogojeski, J. J.; Liétard, J.; Steels, E.; Yamada, K.; Damha, M. J., *Synthesis of siRNA prodrugs: incorporation and evaluation of 2'-O-phenylalanine acetal esters.* Oral presentation at the 98th Canadian Chemistry Conference & Exhibition, Ottawa, Ontario, June 13 – 17, **2015**.

Bogojeski, J. J.; Yamada, K.; Le P. U.; Johnsson, R.; Petrecca, K.; Damha, M. J., *Improving siRNA delivery: novel sugar-modified siRNA increases their cellular uptake to reduce DRR expression.* Poster presentation at the 10th meeting of the Oligonucleotide Therapeutics Society, San Diego, California, October 12 – 15, **2014**.

Bogojeski, J. J.; Yamada, K.; Johnsson, R.; Le, P. U.; Petrecca, K.; Damha, M. J., *Novel sugar-modified siRNA increases their cellular uptake to reduce DRR expression.* Oral presentation at 96th Canadian Chemistry Conference & Exhibition, Quebec City, Quebec. May 26 – 30, **2013**.

Bogojeski, J. J.; Yamada, K.; Johnsson, R.; Le, P. U.; Petrecca, K.; Damha, M. J., *Novel sugar-modified siRNA increases their cellular uptake to reduce DRR expression.* Oral presentation at the 2nd McGill-CIHR Drug Development Training Program Research Retreat, Montreal, Quebec. May 31, **2013**.

Bogojeski, J. J.; Yamada, K.; Johnsson, R.; Le, P. U.; Petrecca, K.; Damha, M. J., *Novel sugar-modified siRNA increases their cellular uptake to reduce DRR expression in tumor cells.* Poster presentation at the 2nd McGill-CIHR Drug Development Training Program Research Retreat, Montreal, Quebec. May 31, **2013**.

Bogojeski, J. J.; Johnsson, R.; Yamada, K.; Le, P. U.; Petrecca, K.; Damha, M. J., *Novel siRNA-amino acid conjugates exhibit improvements in cellular uptake and reduce DRR expression in tumor cells.* Poster presentation at the 20th International Round Table on Nucleosides, Nucleotides & Nucleic Acids, Montreal, Quebec, Aug 5 – 9, **2012**.

Bogojeski, J. J.; Johnsson, R.; Le, P. U.; Petrecca, K.; Damha, M. J., *Novel siRNA-amino acid conjugates exhibit improvements in cellular uptake and reduce DRR expression in tumor cells.* Poster presentation at the 1st McGill-CIHR Drug Development Training Program Research Retreat, Montreal, Quebec, March 30, **2012**.

Bogojeski, J.J.; Johnsson, R.; Lackey, J.; Damha, M.J. *Synthesis and characterization of novel siRNA prodrugs for effective delivery.* Oral presentation at the 94th Canadian Chemistry Conference & Exhibition, Montreal, Quebec, June 5 – 9, **2011**.